Faculty of Science and Engineering
Department of Chemical Engineering

Multi-Scale Modelling and Controlled Synthesis of Titania Nanoparticles

Michael Kehinde Akindeju

This thesis is presented for the Degree of
Doctor of Philosophy
of
Curtin University

January 2013

Declaration

To the best of my knowledge and belief this thesis contains no material previously published by any other person except where due acknowledgment has been made.

This thesis contains no material which has been accepted for the award of any other degree or diploma in any university.

Signature: .....

Date: .....

Acknowledgment

I thank God, the author and perfector of all wisdom and knowledge for His favour, love and kindness and for leading me the path I have and for His enduring mercies and grace upon my life.

I herewith do acknowledge and express appreciation to my lead Supervisor Professor Moses O. Tade for his relentless efforts and assistance all through my program; to Professor Ming H. Ang, Professor Andrew Rohl, and Professor Hongwei Wu for their oversight functions at different but important points during my study; to Professor Vishnu K. Pareek for his roles that spurred me on to resolute determination to attain the highest level of success in this particular course of research.

I acknowledge and express appreciation to the Australian Federal Government for the Australian Postgraduate Award and to Curtin University Research & Development Office for the Curtin Research Scholarship Award that largely saw me through the duration of my studies financially; and to Curtin University Chemical Engineering Department for the Top-Up Scholarship in the first two years of my PhD program and for providing the laboratory equipment used for experimentally validating my results.

I like to profoundly thank Dr. Nicoleta Maynard for her enabling trust that launched my Chemical Engineering teaching contributions at Curtin University. I also want to thank Dr. Doug Myers, Dr. Euan Linday, Associate Professor Martyn Ray, Dr. Gordon Ingram, and Dr. Ewald Swinny for allowing me to contribute to various Chemical Engineering and Faculty units with them during the early years of my research, those formed good bases for my continued personal development. I like to extend appreciation to Karen Sullivan, Jann Bolton and Tammy Atkins for their administrative supports during my studies.

I like to thank my immediate family, especially my wife Susan W. Akindeju for her love, affection and care. She, though of Commerce and Accounting

background, lend me herself to bounce off my science, technology and engineering ideas with supporting smile: she continues to be a strong support. And to my children Olufunmilayo O. Akindeju “the Princess” and Oluwatobi R. Akindeju “the Prince” for their endearing love and resilience that gave me such hope to surge through all challenges that came our way during my studies.

To my family, notably my Twin Gabriel T. Akindeju with whom I can always count on for mind training arguments and troubleshooting; to my Parents Mr. Alex A. Akindeju and Mrs. Maria S. Akindeju for their prayers; and to my friends: Rawand Kader, Emmanuel Obanijesu, and Dave Mohan for their genuine interests in my progress all through the journey.

PEER REVIEWED PUBLICATIONS AND CONFERENCES

Published Book Chapter

- **Akindeju, M.K.,** and Ong, P.H.; Controlling Particle Size in the Spinning Disc Continuous Stir Tank and Settler Reactor (SDCSTR) Model for Continuous Synthesis of Titania, Materials and Molecular Systems Engineering, Computer-Aided Chemical Engineering, 29, Part B, Pg 1578, ELSEVIER, 2011.

Published Journal Article

- **Akindeju, M.K**; Pareek, V.; Rohl, A, and Tade, M.O; Spinning Disc Continuous Stir Tank and Settler Reactor (SDCSTR) Model for Continuous Synthesis of Titania, Chemical Engineering Communications, Vol 198, 73-84, 2011.

- **Akindeju, M.K**; Pareek, V.; Rohl, A, Carter, D; and Tade, M.O, 2010, Constant Pressure Molecular Modelling of six Optimised Titanium Oxide polymorphs: Metal Oxide Semiconductors, International Journal of Chemistry, Pg 26-31, Vol. 2, No. 2.

Published Conference Proceedings

- **Akindeju, M.K**; Pareek, V.; Rohl, A, and Tade, M.O; Spinning Disc Continuous Stir Tank and Settler Reactor (SDCSTR) Model for Continuous Synthesis of Titania, CHEMECA 2009, 27-30 September 2009.

- **Akindeju, M.K**; Pareek, V.; Rohl, A, Carter, D; and Tade, M.O; Constant Pressure Molecular Modelling of six Optimised Titanium Oxide polymorphs, 2009, International Conference on Nanotechnology Research and Commercialisation (ICONT2009), Malaysia, 14-18 December 2009.

- **Akindeju, M.K.,** and Ong, P.H.; Controlling Particle Size in the Spinning Disc Continuous Stir Tank and Settler Reactor (SDCSTR) Model for Continuous Synthesis of Titania, ESCAPE-21, Greece, 2011

Orally Presented Seminars/ Conference

- **Akindeju, M.K**; Pareek, V.; Rohl, A, and Tade, M.O; Spinning Disc Continuous Stir Tank and Settler Reactor (SDCSTR) Model for Continuous Synthesis of Titania, 2009, Curtin university of Technology, WA.

- **Akindeju, M.K**; Pareek, V.; Rohl, A, and Tade, M.O; Spinning Disc Continuous Stir Tank and Settler Reactor (SDCSTR) Model for Continuous Synthesis of Titania, CHEMECA 2009, 27-30 September 2009.

- **Akindeju, M.K**; Pareek, V.; Rohl, A, Carter, D; and Tade, M.O; Constant Pressure Molecular Modelling of six Optimised Titanium Oxide polymorphs, 2009, International Conference on Nanotechnology Research and Commercialisation (ICONT2009), Malaysia, 14-18 December 2009.

- **Akindeju, M.K.,** and Ong, P.H.; Controlling Particle Size Spinning Disc Continuous Stir Tank and Settler Reactor (SDCSTR) Model for Continuous Synthesis of Titania, ESCAPE-21, Greece, 2011

ABSTRACT

Considering the level of current interests in the continuous synthesis of Titania, the Chemical and Manufacturing Industry is expected to benefit from the results of this work which proposed and implemented a tailor-made scheme for the continuous synthesis of Titania nanoparticles to develop a process with improved energy efficiency, predictable particle size, narrower size distribution, polymorph selectivity, and better controllability.

This study investigated and modelled six polymorphs of Titania: Rutile, Anatase, Brookite, high-pressure Brookite, the columbite-type TiO_2-II and Corundum-like type CLT, under constant pressure using the General Utility Lattice Program (GULP) with satisfactory results when compared to the classical data on the subject. The simulated thermodynamic, mechanical and optical properties compared favourably with known references and were used to simulate stable optimized nanoparticles except for CLT due its large compressibility and electronegativity equalization correction.

The simulated properties were used as parameters to model the network reactor system comprising of a spinning disc in the aerosol reacting volume, CSTR in the "sol" volume and settling volume according to the two-step reaction chemistry for precipitating TiO_2 in a pilot scale set-up was used to validate the simulated results in Chapter 5. On one hand and using only the dominant process factors, laboratory experiments were conducted to test between 30°C and 100°C with a 10°C step change (but including 47°C being the optimum temperature predicted by simulation) to establish and verify the optimum temperature for the process while varying $TiCl_4$ molar concentration by 0.5 step change between 0.5 and 2M. On the other hand, a pilot scale was used to validate the impact of the CSTR impeller speed on the particle size and distribution varying $TiCl_4$ molar concentration by 0.5 step change between 0.5 and 2M. Further, $H_2O/TiCl_4$ was varied with step changes of 2 between 2 and 6.

From the numerical results and graphs, two conclusions were drawn that

1. In general and for all three reactor modes of operations, it is evident that the higher the spin and/or impeller speed, the smaller the particle size and the narrower the distribution for the range examined.
2. In contrast, the three modes of operations presented varied results. Whereas the SD-CSTR gave narrower distributions with mostly single peaks, the SD alone and CSTR alone produced multi-peaks and wider size distributions.

Both of the above therefore led to an overall conclusion that the SD-CSTR is a more efficient reactor mode for the continuous synthesis of TiO_2.

In addition to the above, parametric relationship between the modal particles sizes and critical operating conditions was also developed to achieve predictability of modal particle size, narrow size distribution and polymorph selectivity using the molar concentration, reaction temperature, degree of supersaturation and spinning rate as major factors by deploying Darby's (2001) Newtonian fluid relationship between shear rate and viscosity to obtain an empirical correlation comprising both molecular and reactor specific parameters. A general trend was observed when the empirical relationship was plotted for several operating conditions leading to a quick shortcut equation that can be used upon establishing initial particle size from a cooling precipitation reaction in the laboratory.

At completion, and using Rutile as base case, this work successfully investigated and developed a tailor-made process for continuously synthesizing Titania nanoparticles using molecular modelling approach to evaluate the invariable intensive properties which were used to develop models that described the process with the following significant contributions:

a) Compared to the Chemical Vapour Deposition (CVD) technology that operates at 900°C – 1100°C, this system operates between 25°C and

100°C depending on target characteristics of the desired nanoparticles. This is a significant saving in energy requirements.

b) This system produces particles within controllable and predictable narrow size distribution unlike the wide particle distribution obtainable from using the SD or CSTR alone in the Sol-Gel process.
c) While other technologies require very high super-saturation levels, typically in 20 –1000 range, our novel system only requires a maximum of 8; hence preventing material wastages.
d) By increasing the degrees of freedom, this system achieves controllability for
    i. Particle size
    ii. Particle size distribution
    iii. Polymorph selectivity
e) This system is suitable for the synthesis of temperature sensitive organic nanoparticles because the optimal operating temperature is well below the temperatures required to denature most organic particles.
f) This device is suitable for both aqua and non-aqua flow processes; adequate for developing target oriented drug delivery nanoparticles.
g) The overall process time for this system is 0.859s compared to the more than 2s for Sol-Gel processes (typically followed by calcination) and more than 5min for CVD. This translates into a gross reduction in the total time required for products to reach the target market.

Furthermore, there are indications that hydroxylated TiO_2 may present yet unknown but important applications in semiconductors.

TABLE OF CONTENT

LIST OF FIGURES

LIST OF TABLES

Chapter 1 : INTRODUCTION

1. Background

Titania exists in many different polymorphs of which the most thermodynamically stable are Rutile, Anatase and Brookite (Matsui and Akaogi, 1991; Xia et al, 1999; Swamy et al, 2001; John et al, 2004; Wang and Garrick, 2006). Several high-pressure forms have also been demonstrated to be super-hard materials, while the ambient phases are employed in many industrial processes as a white inert pigment. Its chemical stability, high resistance to deterioration in acids or alkali, strong REDOX properties, significant pollution control and medical uses have all engendered an increasing interest in the use of Titania as a metal particle support in heterogeneous catalysis, semiconductors and as a photo-catalyst for the mineralization of toxic wastes. Despite the numerous valuable applications, its synthesis is still largely highly energy intensive or with wide particle distribution due to re-crystallization and or pulverization (Mullin, 2001; Rivallin et al, 2005).

Several methods and technologies have been reported for synthesizing Titania; some of which include the Chemical Vapour Deposition: CVD (Mullin, 2001); repeated distillation of titanium tetrachloride (Kirk-Othmer, 1999-2012) both of which are effective, but quite energy intensive. Other methods involves the aqueous (sol) application for the synthesis of Titania which is well-known for about a century, but most applications require calcination to remove excess chlorides, re-crystallization for purification and pulverization with wide particle size distribution and significant equipment encrustation in continuous processes (Rivallin et al, 2005). Recent technologies includes the Aerosol reaction followed by calcination with structural dependence on ethanol dopant (Moody and Collins, 2003; John and Surender, 2005); and the Rotating Tube reactor and the Narrow Channel Reactor (Jie Fang, et. al 2010).

According to the Chemistry of Titania; the precipitation of TiO2 by hydrolyzing $TiCl_4$ is known to follow a two-stage process: (1) the generation of nuclei and (2) the subsequent growth with the nucleation step as rate controlling; the overall production rate is enhanced with heterogeneous nucleation but at the expense of introducing impurities. In this work, TiO_2 particles produced in the rate-controlled aerosol unit were used as seeding particles to achieve heterogeneous nucleation in the ‘‘SOL’’ reacting volume according to the stoichiometry presented in equation (1-1) below, at 46.27°C in a 2-stage novel reactor as shown in Figure 1-1.

$$\boldsymbol{xTiCl_4 + yH_2O \rightarrow xTiO_2 + 4HCl + (y - 2x)yH_2O} \qquad (1\text{-}1)$$

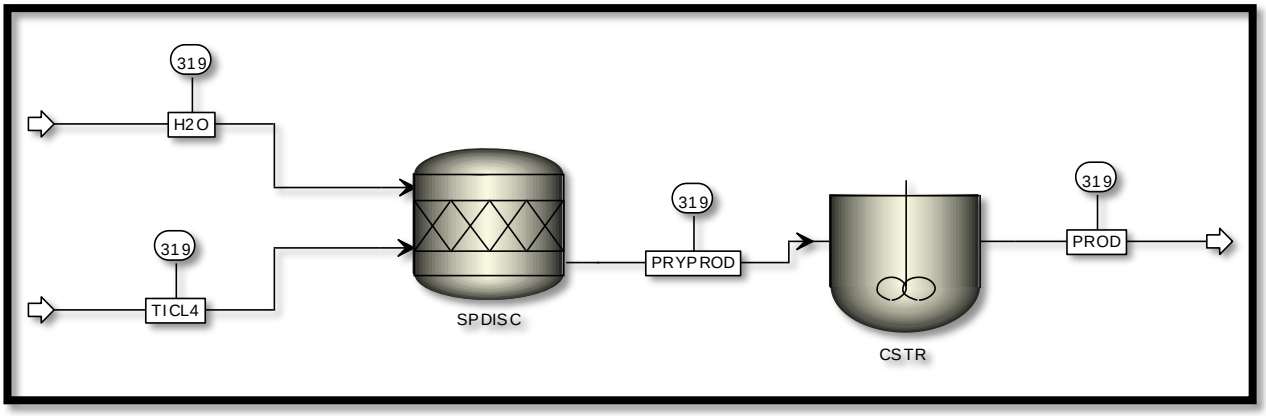

Figure 1-1: Process Flow Schematic for the Integrated Spinning Disc reactor and the CSTR

2. Aim of This Study

This research explored the fundamental chemistry of Titania to develop a tailor-made methodology for its synthesis by deploying atomistic level computations at the sub-atomic level to obtain process and molecular state variables which are otherwise obtained as lumped data for macro-systems to enhance controllability, polymorph selection, desired size and distribution. This is a cutting edge application for molecular modeling in Chemical Engineering and will lead to improved overall energy efficiency.

3. Objective of This Study

The overall aim of this work is to develop a tailor-made process for the continuous synthesis of Titania nanoparticles through Multi-scale simulation and experimental investigations. Compared to existing technologies, this work investigates and seeks to develop a better scheme with improved energy efficiency, narrow particle size distribution, polymorph selectivity and controllability; and specifically focusing on the under-listed objectives:

1. Development of a methodology for designing Titania nanoparticles of desired shape, size and morphology via a theoretical strategy that combines molecular modelling, reactor design and population balance approaches.
2. Investigate the sol-gel and aerosol processes with a view to developing a modelled reactor for the synthesis of Titania nanoparticles under a controlled hydrodynamic regime in a novel spinning disc continuous Stirred Tank Reactor.
3. Produce and characterize Titania nanoparticles through experiments and comparing them with simulation results.

4. Scope of This Study

1. Functionally compare and match the elements of the pair-wise additive coulomb, dispersion and repulsion equation used by Matsui & Akaogi (1991).
2. Obtain average intra-atomic distances and fractional occupancy data (Charlton et al, 1997; Bokhimi and Pedraza, 2004) to simulate stable non-primitive molecules.
3. Determine the least energy molecular structure using the local minimum approach.
4. Compute thermodynamic and mechanical properties for the least energy level molecular structure for the 4 known and well documented polymorphs.
5. Perform molecular dynamics to validate procedure and results using the Broyden-Fletcher-Goldfarb-Shanno: BFGS (Shanno,

1970) optimizer with a secondary switch to Rational Functional Optimization- RFO.

6. Extend the simulation to cover additional 2 polymorphs TiO2-II and CLT using The general Utility Lattice Program (GULP-V3.1) to perform the computations (Gale, 2007)

The knowledge and results from the basic, and explorative, research are to be used in the application, and descriptive research stage for

7. Obtaining a number density from Population Balance Model (PBM) for the synthesis of Titania.
8. Polymorph Selection: Each of the polymorphs has a prescriptive operating envelope boundary. These boundaries are to be investigated with a view to articulating and developing a selection mechanism.
9. Product Selectivity: Based on the kinetics, there are 2 competing plausible products—TiO_2 and $Ti(OH)_2$, but the appropriate conditions that will lead to either are defined and prescribed.
10. Particle size and distribution control.
11. Reactor design and optimisation.
12. Investigation on the effect of precursor molar concentration on nucleation, particle size and distribution
13. Case Studies & Experimentations using factorial or dominant effect experimentation design scheme (Usman et al, 2008).
14. Product characterization
15. Possible dopants and their effects on product characteristics and properties were briefly examined.

5. Significance of Study

With the level of current interests in the continuous synthesis of Titania, an enhanced energy efficient process with predictable polymorph selectivity and particle size controllability, the Chemical and Manufacturing Industry is expected to benefit from the results of this work. In addition, this work had a

potential to develop and patent a new processing reactor for large scale production as well as establishing a new academic research area.

6. Contributions of This Study

a) Compared to the Chemical Vapour Deposition (CVD) technology that operates at 900°C – 1100°C, this system operates between 25°C and 100°C depending on target characteristics of the desired nanoparticles. This is a significant saving in energy requirements.

b) This system produces particles within controllable and predictable narrow size distribution unlike the wide particle distribution obtainable from using the SD or CSTR alone in the Sol-Gel process.

c) While other technologies require very high super-saturation levels, typically in 20 –1000 range, our novel system only requires a maximum of 8; hence preventing material wastages.

d) By increasing the degrees of freedom, this system achieves controllability for
   i. Particle size
   ii. Particle size distribution
   iii. Polymorph selectivity

e) This system is suitable for the synthesis of temperature sensitive organic nanoparticles because the optimal operating temperature is well below the temperatures required to denature most organic particles.

f) This device is suitable for both aqua and non-aqua flow processes; adequate for developing target oriented drug delivery nanoparticles.

g) The overall process time for this system is 0.859s compared to the more than 2s for Sol-Gel processes (typically followed by calcination) and more than 5min for CVD. This translates into a gross reduction in the total time required for products to reach the target market.

Chapter 2 : LITERATURE REVIEW

2.1 Nanotechnology

Nanotechnology is the technical interpretation and application of knowledge generated from Nanoscience which according to the Royal Society of London (2004) is defined as the study of fundamental relationship between physical properties and material dimensions on the nano scale: time, space and shape. Nanotechnology involves the design, production, characterization and applications of nano materials which include particles, rods, wires, thin films and bulk composite materials made from nano building blocks, etc.

Industrial processes are largely scaled-up versions of successful laboratory investigations and pilot plant runs; they differ in the difficulties associated with managing the extensive thermodynamic properties of the process fluids, materials and the operations. Although the extensive properties vary with scale, the intensive (bulk) properties of all the materials involved are constant but with better predictability at nano-scales (Yu, 2009). These properties include:

- Mechanical strength
- Thermal stability
- Catalytic activities
- Electrical conductivity
- Magnetic properties
- Optical properties

According to Yu (2009), these superior predictabilities have been explored and used as parametric target variables in system designs some of which include quantum electronics, nonlinear optics, photonics, sensing, information storage and processing,

adsorbents, catalysis, solar cells, monomers and in cell biology amongst many others.

2.2 Nanoparticles Synthesis and Current Technologies

Broadly, there are two approaches for Nanoparticle synthesis, which are the top-down and bottom-up approaches (Rene, 2010).

1. Top-Down Approach: This involves mechanical and thermal cycle yields via attrition, milling and/or pulverization of bulk materials into smaller sizes. It leads to a broad size distribution (10 – 1000nm) depending on the surface characteristics of the materials with varying shapes, face geometries and co-materials as impurities introduced from the size reduction media.
2. Bottom-Up Approach: This involves the synthesis from the molecular building blocks to reach the desired composite size. Current strategies for achieving this include liquid-phase synthesis, gas-phase synthesis and vapor-phase synthesis.

2.2.1. Liquid-phase synthesis include methods such as coprecipitation, sol-gel processing, microemulsions, hydrothermal/solvothermal synthesis, microwave synthesis, sonochemical synthesis, template synthesis, micellar structured media and biomimetic synthesis.

a) Coprecipitation is a precipitation reaction where nucleation, growth, coarsening and/or agglomeration occur simultaneously and exhibit the following characteristics (Yu, 2009; Maribel et al, 2009).

i. Nucleation is the key primary step for the successful completion of the process.

ii. They form insoluble species under conditions of high supersaturations.

iii. Heterogeneous or secondary processes such as Oswald ripening and aggregation significantly influence the eventual stable size, morphology and properties of the particles formed (Rene, 2010).

iv. The supersaturation conditions represent critical operating conditions for the reaction to progress and to achieve “a” – “c” above.

Examples of co-precipitation methods include direct reduction of metal-halides to their metals from non-aqueous solutions, electrochemical reductions as used in electrowinning cells in base metal mining, and decomposition of metallurgical precursors.

b) Sol-gel processing involves the use of a wet-chemical undergoing hydrolysis and polycondensation reactions to produce a gel. Examples of this include the formation of metal oxide or hydroxide in solution (Bennajady et al, 2011; Okuyama and Lenggoro, 2004). Sol-gel processes, illustrated in Figures 2-1 and 2-2, have common characteristics which include low processing temperature and molecular-level homogeneity; and are generally useful in making complex metal oxides, temperature sensitive organic-inorganic hybrid materials and biomaterials. Rene, (2010) presented typical steps involved in a sol-gel process which includes:

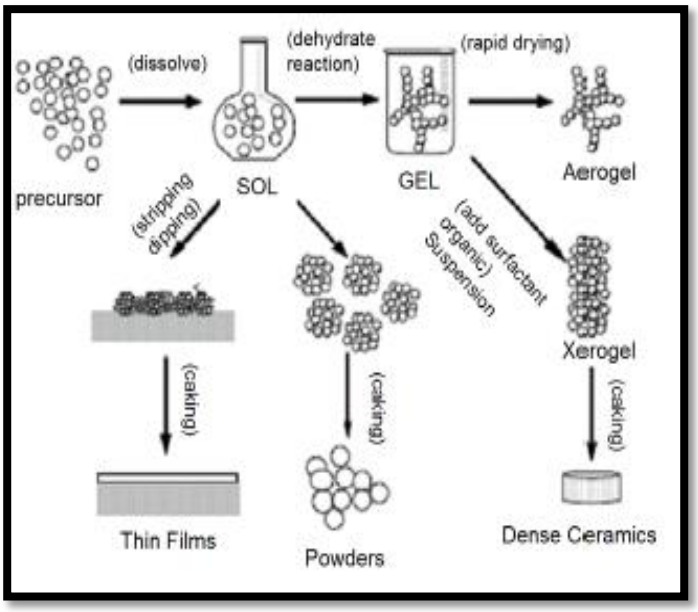

Figure 2-1: Steps involved in a typical sol-gel process (Rene, 2010)

- Formation of stable sol solution
- Gelation via a polycondensation or polyesterification reaction
- Gel aging into a solid mass, causing contraction of the gel network, also
    - phase transformations and
    - Ostwald ripening.

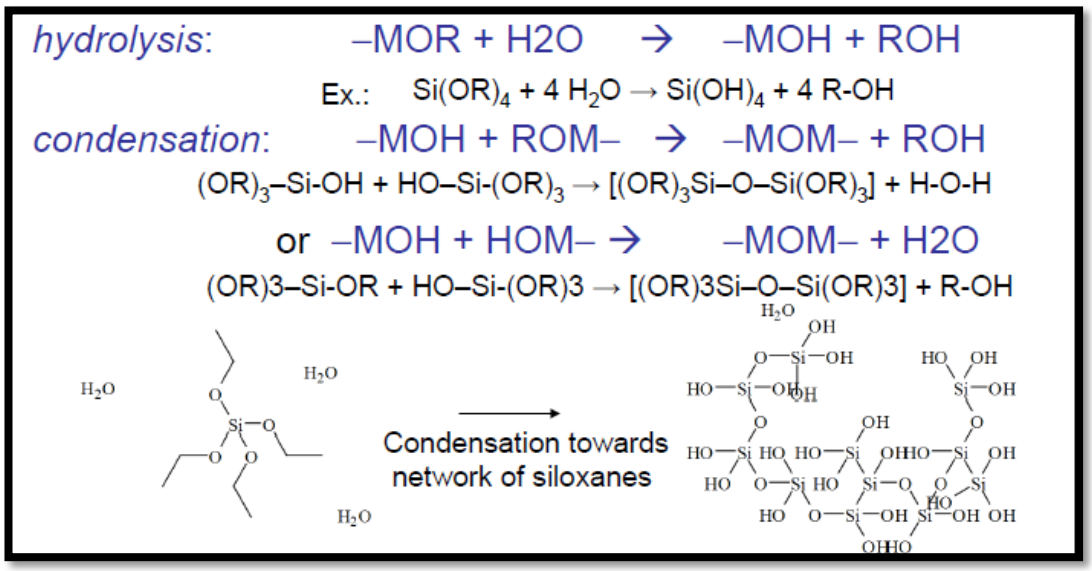

Figure 2-2: Sol-gel typical mechanism (Rene, 2010)

- Drying of the gel to remove liquid phases, and can lead to fundamental changes in the structure of the gel.
- Dehydration at temperatures as high as 8000 °C, used to remove M-OH groups for stabilizing the gel, i.e., to protect it from rehydration.
- Densification and decomposition of the gels at high temperatures (T > 8000 °C), i.e., to collapse the pores in the gel network and to drive out the remaining organic contaminants.

c) Microemulsions are clear, stable, isotropic liquid mixtures of oil, water and surfactant which may be infused with a co-surfactant for stability (Yu, 2009; Zhang et al, 2012).

d) Hydrothermal/solvothermal synthesis (illustrated in Figure 2-3) refers to chemical reactions that occur in a sealed vessel where solvents are brought to temperatures in excess of their natural occurring boiling points by increasing the local pressure (Yu, 2009; Yang et al, 2006; Somiya and Roy, 2000).

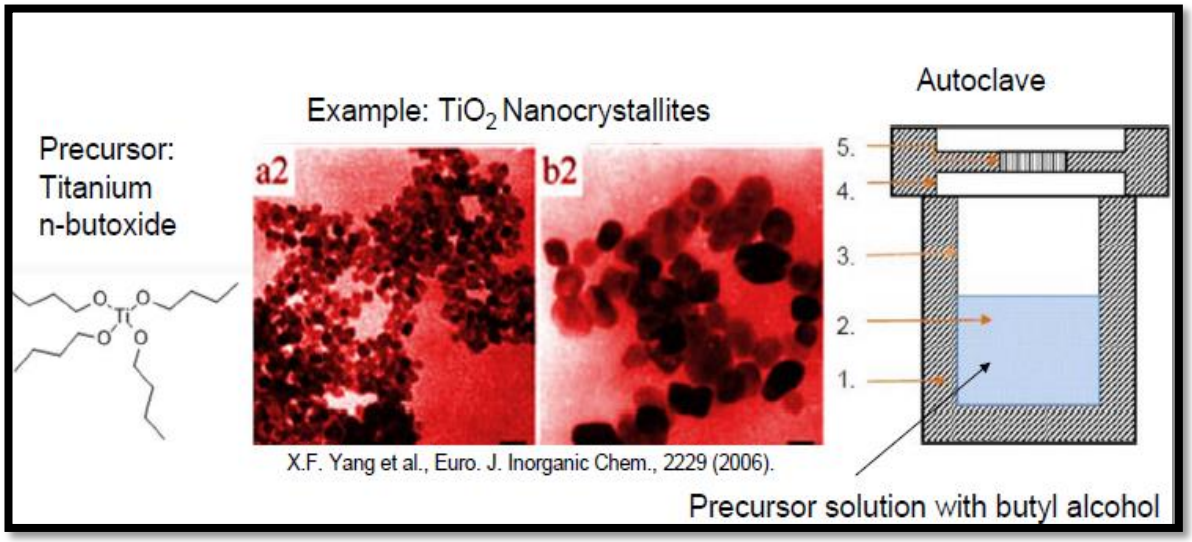

Figure 2-3: Solvothermal synthesis (Yang et al, 2006)

e) Microwave assisted synthesis are reactions enhanced by subjecting mixing reactants to a microwave field which helps

to excite the molecules, generate friction and hence help to overcome the kinetic barrier (Yu, 2009; Tsui M. et al, 2005).

f) Sonochemical synthesis deploys ultrasound irradiation to cause repetitive formation, growth and implosive collapse of bubbles in a reacting medium to generate localized hot spots of extremely high temperatures in excess of 4500K and pressures above 19Mpa. These conditions and method drive the reaction in the direction of forming instantaneous precipitates out of solutions and ideal for non-hazardous reagents (Yu, 2009).

g) Biomimetic synthesis mimics natural occurrences at mild conditions such as room temperatures, aqueous environment and neutral pH in reactions that lead to particle formations and sedimentations (Rajesh et al; 2002).

2.2.2. Gas-phase synthesis

a) Gas-phase synthesis is achieved by vaporizing the precursor material into a background gas and then cooling the gas (Yu, 2009; Gutsch et al 2002). Yu et al indicated that this strategy has two broad methods, which are;

i. Solid precursors

- Inert gas condensation as illustrated in Figure 2-4.

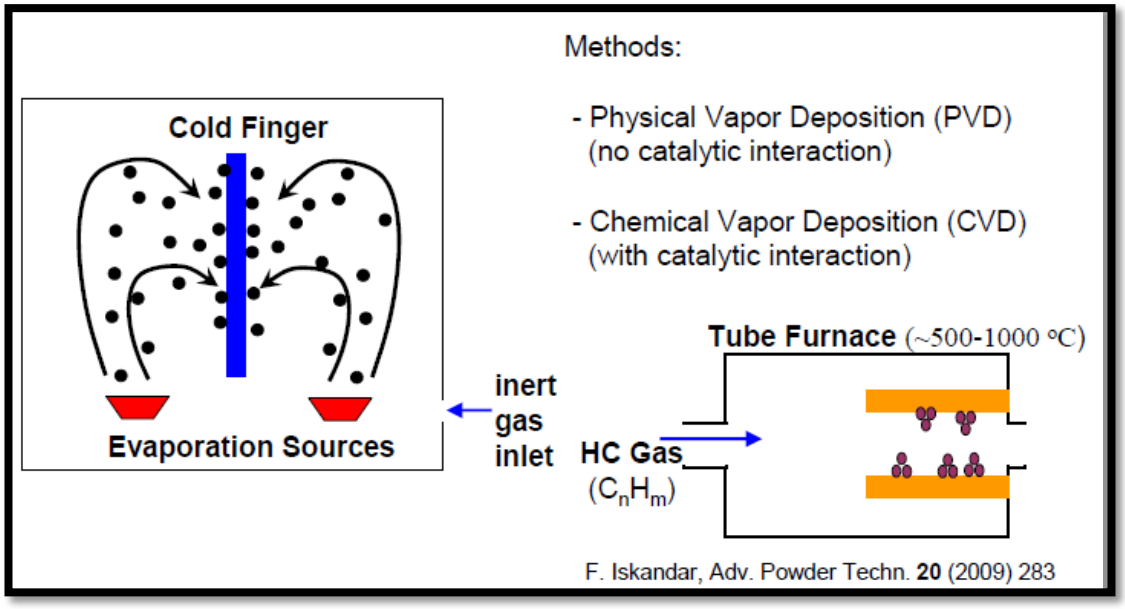

Figure 2-4: Evaporation of a course substance in an inert gas atmosphere (Iskander, 2009)

- Pulsed laser ablation
- Spark discharge generation
- Ion sputtering

ii. Liquid or vapour precursor involves:

- Chemical vapour synthesis
- Laser pyrolysis/Photochemical synthesis
- Thermal plasma synthesis
- Flame spray pyrolysis
- Spray pyrolysis as illustrated in Figure 2-5

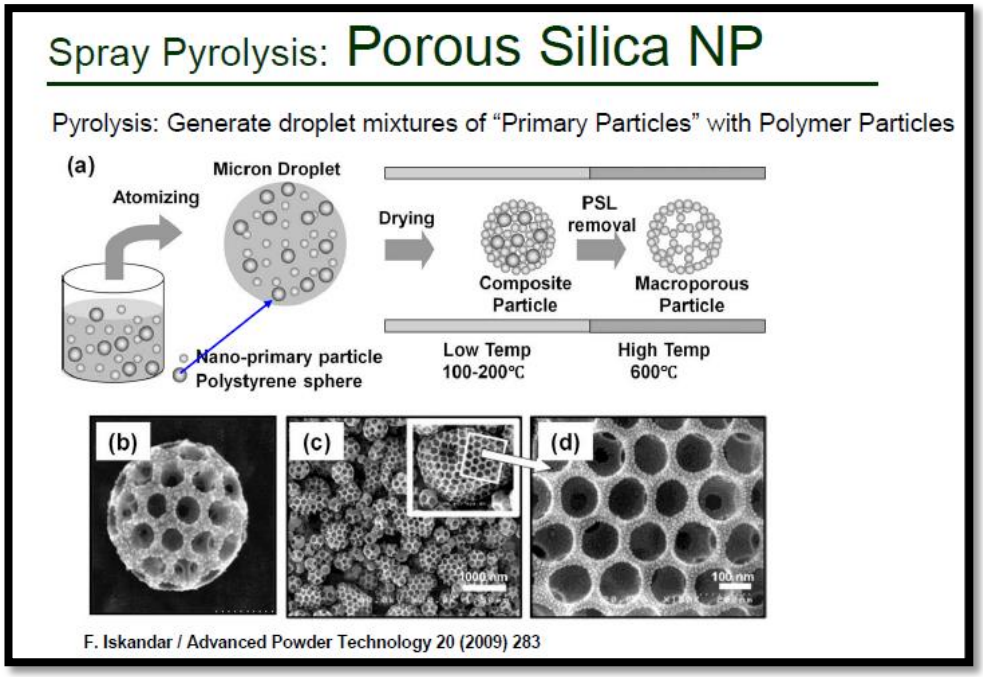

Figure 2-5: (a) Schematic diagram of experimental apparatus and the formation process of particles containing ordered pores. (b–d) Ordered pores particles (Iskander, 2009)

- Low-temperature reactive synthesis, illustrated in Figure 2-6.

$$TiCl_{4\,(g)} + O_{2\,(g)} \rightarrow TIO_{2\,(s)} + 2Cl_{2\,(g)}$$

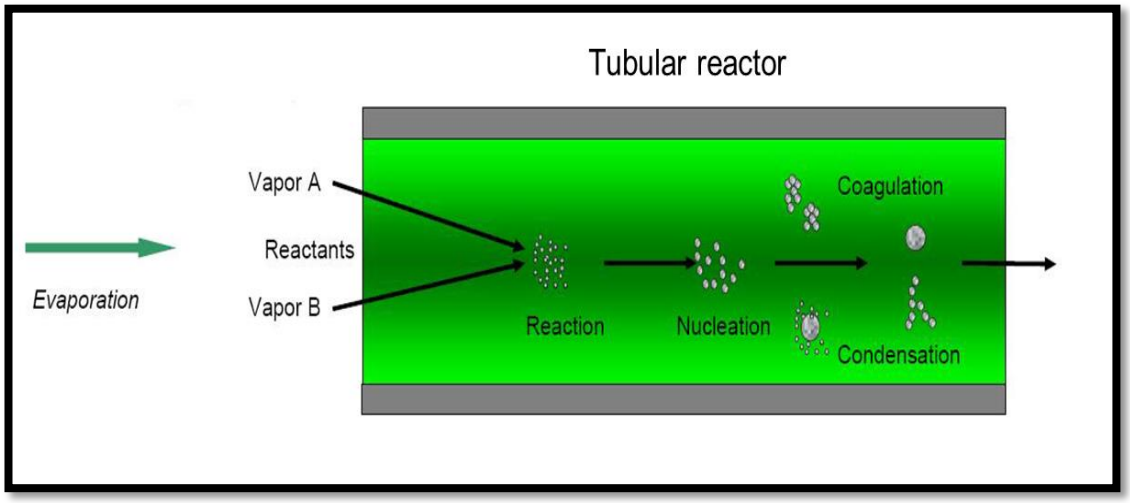

Figure 2-6: Example of gas phase chemical precipitation of TiO_2 (Yu, 2009)

2.2.3. The vapour phase synthesis follows the same route as the liquid phase reaction with elevated temperatures, typically in a vacuum or reduced pressure leading to slower particle growth. By the nature of vapour, the mixture is rendered thermodynamically unstable relative to the precipitating solid particles and hence product formation is favoured. The higher the degree of vapour supersaturation, the higher the particle formation tendency to the extent the reaction or condensation permits.

Once nucleation occurs, surface reaction becomes the driving force and growth is limited to surface attachment by condensation which causes rapid quenching. The quenching acts as a deterrent to growth as it reduces the degree of supersaturation (Yu, 2009; Davey and Garside, 2000).

2.3 Limitations of current technologies

a) As noted in section 2.1 above, the Top-Down approach (Rene, 2010 and Yu, 2009) leads to large particle size variation and introduces impurities.

b) The cooling crystallization approaches comprising of the coprecipitation, sol-gel processing, micro emulsions and gas-phase synthesis lead to polymorphic outcomes (Borissova et al, 2009; Chew et al, 2007; Medelez et al, 2006 and De Anda et al, 2005).

c) Hydrothermal/solvothermal synthesis, microwave assisted synthesis and sonochemical synthesis involve high temperatures and are hence energy intensive. Moreover, the molecular turbulence caused by raising the solvent temperature (Yu 2009) leads to local polymorphic variations.

d) The vapour phase synthesis, as reported by Yu et al (2009) and substantiated by Swaminathan et al (2004) show a slow growth rate compared to the liquid phase synthesis.

Although the current strategies for the bottom-up approach are good for nanoparticles synthesis, they are still ridded with huge energy consumption, wide particle size variation and/or lack of modal particle size predictability.

2.4 Polymorph selectivity

In general and because all the current bottom-up approaches involve temperature variations for crystallization to occur, the outcomes are polymorphic (Borissova et al, 2009; Chew et al, 2007, Medelez et al, 2006, Rohani et al, 2005, He et al, 2006:1; He et al, 2006:2). However, He et al (2006) reported some success with the crystallization of glycine with γ-glycine stable out of the 3 distinct polymorphs produced. Swaminathan et al (2007) reported the use of continuous flow in a spinning disc reactor to manipulate the size, shape, morphology, defects and phases of the nano-particles instantaneously at room temperature.

2.5 Modelling

Industrial processes are largely scaled-up versions of successful laboratory investigations and pilot plant runs; they differ in the difficulties associated with managing the extensive thermodynamic properties of the process fluids, materials and the operations. Although the extensive properties vary with scale, the intensive (bulk) properties of all the materials involved are constant. This invariability in bulk properties therefore have been used as a parametric design tool for process tuning to link micro scale processes, meso scale and large industrial scale operations. For this, computations at atomic levels otherwise known as molecular modelling are useful tool (Gale, 2007) and becomes multi-scale when combined with other modelling tools to obtain a system-wide application, obtaining input data for reactor design for example as done for this work.

Swaminathan et al (2007) reported the modelling of spinning disc processor applied for the synthesis of $AgNO_3$ nanoparticles, while Sebatstien et al (2008) reported the derivation of atomistic potential parameters based on electronic calculations for modelling electrons and hole for Titania polymorphs adopting the polarization model version of Matsui and Akaogi (1991).

Swamy et al (2000) used the fixed charge model to simulate bulk properties of TiO_2 polymorphs (including anatase, rutile, low pressure brookite, TiO_2(B), TiO_2(R), TiO_2(H), and the high pressure columbite-, baddeleyite-, cotunnite-, pyrite-, and fluorite- forms) imperative for macro system designs such as applied by Kees (2004) in their application of microscale technology in chemical process industry equipment and Zhang et al (2006) in their development and modelling of a rotating disc photo-catalytic reactor for wastewater treatment.

2.6 Surface Enhancement with Hydroxyl Doping

Partially hydrated or “wet electrons” states at the H_2O/TiO_2 interfaces represent the lowest energy pathway for electron transfer (Ken, et al. 2005) leading to improved photo-catalysis efficiency. At ~1-monolayer coverage of water on partially hydroxylated TiO_2 surfaces Ken Onda and his team that studied the photo induced electron transfer at the H_2O/TiO_2 (110) interface by means of time-resolved two-photon photoemission spectroscopy and electronic structure theory found an unoccupied electronic state 2.4 electron volts above the Fermi level”. They presented that “density functional theory showed this to be a wet-electron state analogous to that reported in water clusters and which is distinct from hydrated electrons observed on water-covered metal surfaces. The decay of electrons from the wet-electron state to the conduction band of TiO_2 occurs in about 15 femtoseconds”.

According to their study on hydroxylated TiO_2 [with only –OH remaining at above 300K, see Figure 3-19] as presented on Figures 2-7 to 2-10, it “is likely that wet-electron states perform important but yet unknown functions, for

instance, as charge-transfer promoters at transparent metal-oxide electrodes used in organic-molecule–based devices and as electron traps in conventional semiconductor devices". This was also substantiated by Mowbray (2009).

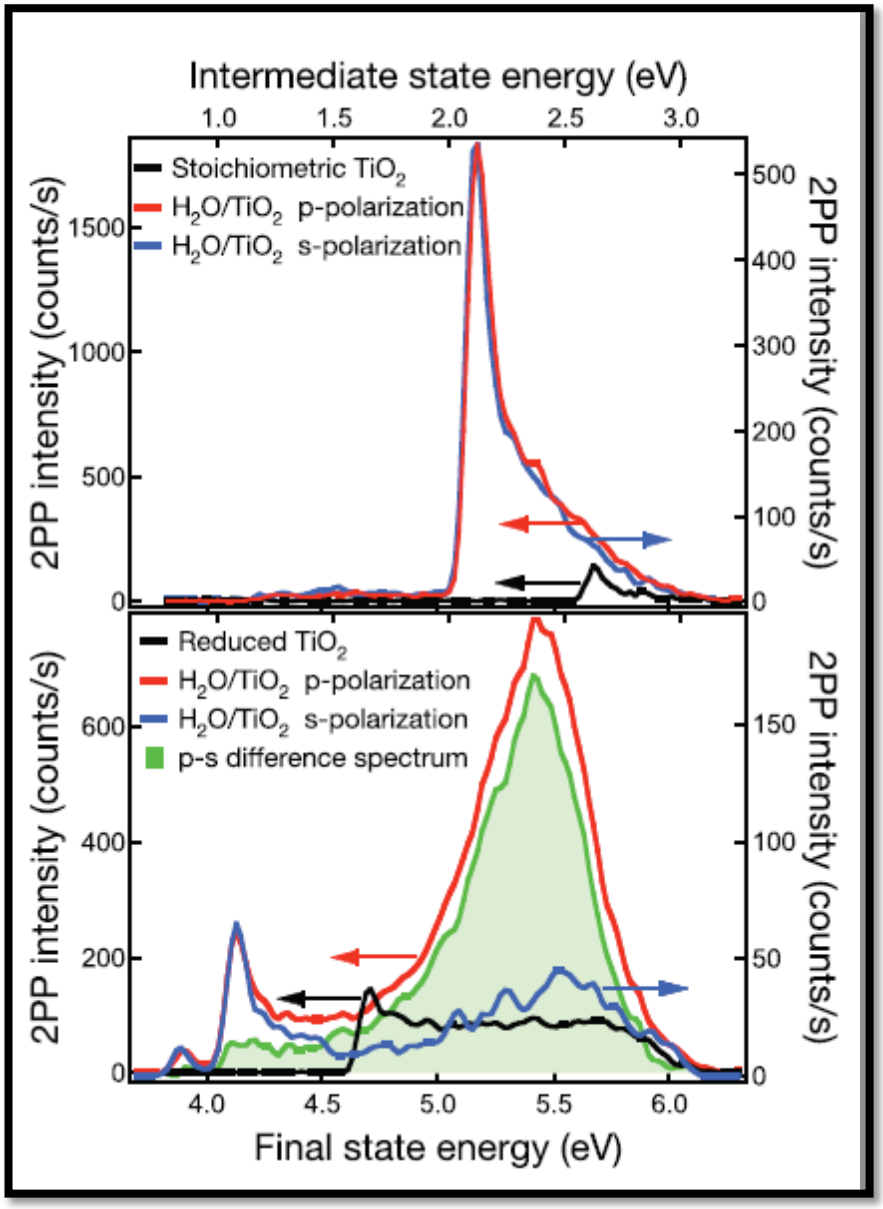

Figure 2-7: 2PP spectra of the (top) stoichiometric and (bottom) reduced TiO2 surfaces before and after deposition of ~1 ML of H2O. The H_2O/TiO_2 spectra are taken with s- and p-polarized light. The s-polarized spectra are expanded 3 x to normalize the intensities at the work-function edge (horizontal arrows indicate the appropriate axis for each spectrum). The difference between thus normalized p- and s-polarized spectra (green) for the reduced surface isolates the additional DOS of the wet-electron state. The final state energy is that measured for photoelectrons with respect to E_F, whereas the intermediate-state energy is later reduced by the 3.05-eV photon energy (Adapted from Ken, et al 2005).

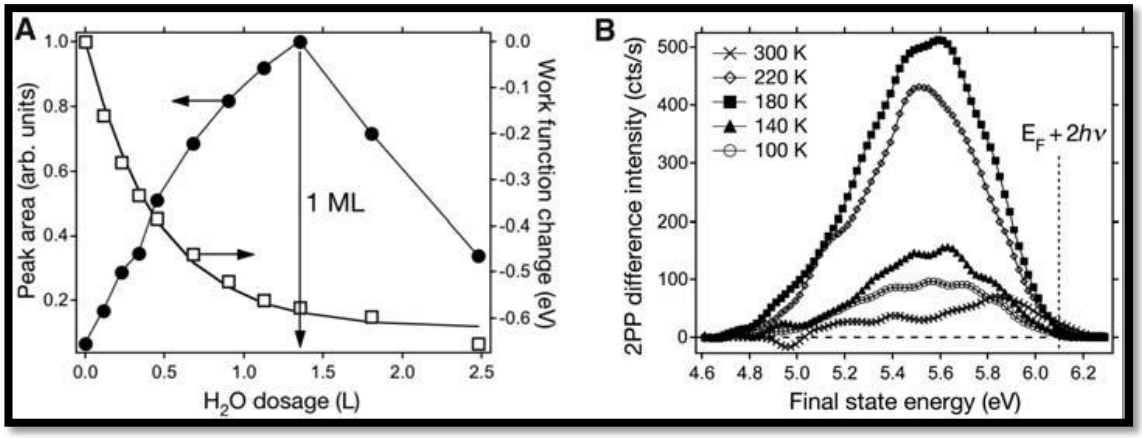

Figure 2-8: (A) Plot of the wet electron–state peak area from difference spectra such as in Fig. 2, bottom (circles), and work-function change (squares) plotted as a function of water exposure. The solid line is a fit of the work-function change as described. The coverage of 1.35 L for the intensity maximum and work-function saturation corresponds to the approximately 1-ML H2O. The horizontal arrows indicate the appropriate axis for each measurement. (B) The difference spectra recorded at different temperatures after exposing the reduced TiO2 to 3.7 L of H2O at 100 K. Based on published TPD spectra, 1-ML coverage of H2O is attained at 180 K where the wet-electron state has maximum intensity. Only OH remains above 300 K (Adapted from Ken, et al 2005).

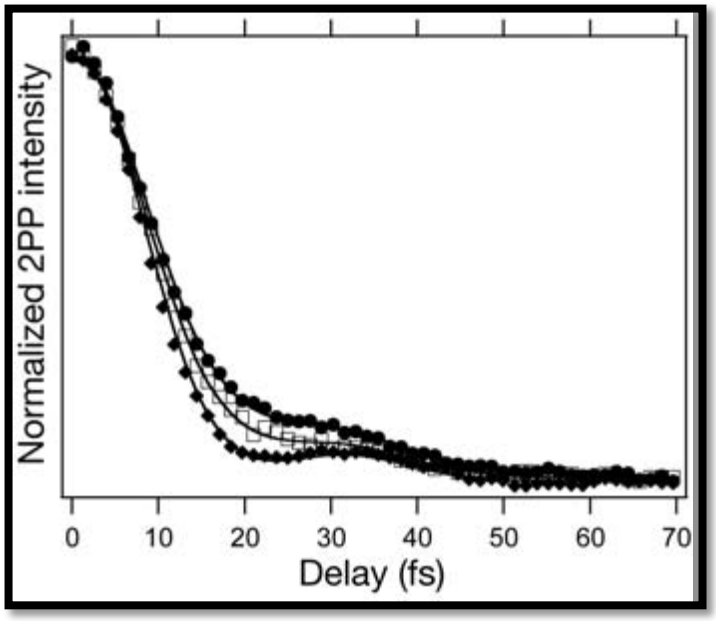

Figure 2-9: Phase-averaged I2PC scans for the reduced TiO2 (solid diamonds), and after exposure to 0.7 (open squares) and 1.6 L (solid circles) of H2O. The lines represent fits with a three-level optical Bloch equation model with the use of experimentally measured pulse autocorrelation and assuming single exponential decay kinetics for the intermediate state. The bare surface intermediate-state lifetime is too short to measure, and 10 T 1 and 14 T 1 fs for 0.7 and 1.6 L H2O/TiO2, respectively (Adapted from Ken, et al 2005).

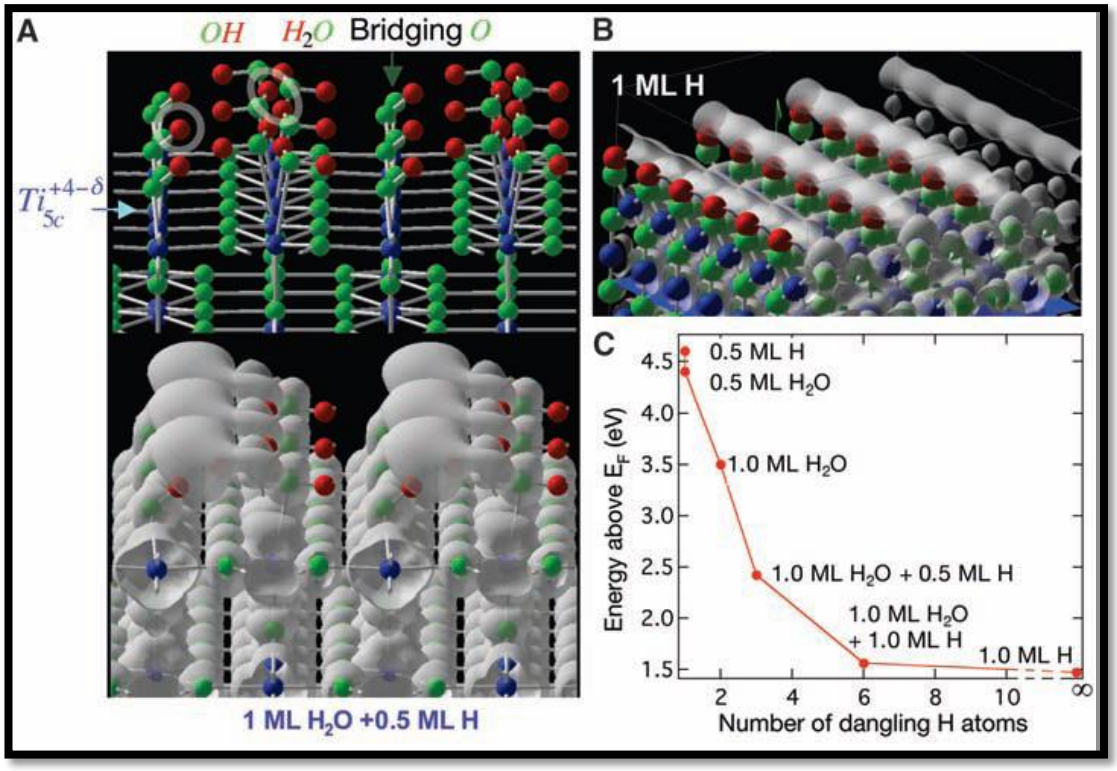

Figure 2-10: (A) The optimized geometry of a TiO2 surface covered with 1 ML H2O + 0.5 ML H. The bottom panel shows the orbital distribution for the same structure at 2.4 eV above E_F. The adsorbate orbitals are delocalized in clusters involving one OH and one H atom each contributed by two adjacent H_2O molecules, which are indicated for a single cluster by white ellipsoids. (B) The optimized geometry and orbital distributions at 1.5 eV for 1 ML H on TiO_2. The hybridization of orbitals on H atoms into 1D chain along the bridging O rows makes this the most stable wet-electron state found by theory. (C) The correlation of the wet-electron energy for different coverage of H_2O and H adsorbates with the number of dangling H atoms in each hydration cluster. The infinite limit corresponds to the structure in (B). All calculated structures in the experimentally observable energy range are associated with clusters involving both OH and H_2O (Adapted from Ken, et al 2005).

Vogtenhuber et al (1997) reported on the energetic properties of the dissociative (1 x 2) adsorption of H_2O on Rutile to enhance the photo catalytic characteristics of the polymorph by using the full potential linearized plane wave method. They found a general reduction of the bond lengths at the surface and an inwards relaxation of the surface plane. While Allegretti et al (2005) showed via scanned-energy mode photoelectron diffraction that the adsorption site of the molecular water on Ti-O (110) to be atop the under-coordinated Ti atoms' surface which they concluded confirmed their results of total energy calculations and STM imaging. They further claimed that the TiO_2 water bond length is 2:21±0.02Å, much longer those of Ti-O water and led them to conclude that this difference may be the reason for the

controversial opinions on the importance and understanding of surface reaction system.

Chapter 3 : MOLECULAR MODELLING

3.1 Introduction

Industrial processes are largely scaled-up versions of successful laboratory investigations and pilot plant runs; they differ in the difficulties associated with managing the extensive thermodynamic properties of the process fluids, materials and the operations. Although the extensive properties vary with scale, the intensive (bulk) properties of all the materials involved are constant. In this work, these invariability in bulk properties therefore have been used as a parametric design tool for process tuning to link micro scale processes, meso scale and large industrial scale operations. For this, computations at atomic levels otherwise known as molecular modelling are useful tool.

Although molecular modelling requires computational time which may range from 10 seconds to several days, its huge potential lies in its use as a process optimization tool leading to huge cost savings, better product quality and hence higher profitability. In this work, the General Utility Lattice Program (GULP [Gale, 2007]) has been used.

With no need for thermal expansivity correction, the pairwise additive Coulomb, dispersion and repulsion interaction potential used by Matsui and Akaogi (1991) was transformed to a simpler Buckingham two-body interaction potential to reproduce and predict the structural and physical properties of four polymorphs of TiO2 (Rutile, Anatase, Brookite, and the columbite-type TiO2-II) investigated by Matsui and Akaogi. The investigation was also extended to cover additional two polymorphs (high-pressure Brookite and Corundum-like type CLT) and predicted mechanical and thermodynamic properties for all six polymorphs.

Upon successfully modelling the six polymorphs, the number density of Rutile nanoparticles, as base case, was evaluated using the population balance

analytical solution developed by Randolph and Larson (1978); the results compared favourably with the experimental data (in Chapter 5).

3.2 Molecular Intra-atomic Potential Model

To obtain the variables required to compute the Buckingham intra-atomic potentials, the elements of the pairwise additive coulomb, dispersion and repulsion interaction model (equation 3-1; Table 3-1) used by Matsui and Akaogi (1991) were functionally compared and expressed in terms of intra-atomic distance rij, effective charge q, repulsive radius A, softness parameter D, Van der Waals' atomic coefficient C, and standard atomic force f (4.184kJ/Å.mol, Matsui and Akaogi, 1991); with the two-body interaction Buckingham potential model (equation 3-2) to obtain equivalent expressions presented in equations 3-3 to 3-7.

$$V_{ij} = \frac{q_i q_j}{r_{ij}} - \frac{C_i C_j}{r_{ij}^6} + f^*\left(D_i + D_j\right)^* \exp\left(\frac{A_i + A_j - r_{ij}}{D_i + D_j}\right) \quad (3\text{-}1)$$

Table 3-1: Energy Parameters from Matsui and Akaogi (1991)

	q (|e|)	A (Å)	D(Å)	C(Å^{3}kJ/mol)
Ti (Å)	2.196	1.1823	0.077	22.5
O (Å)	-1.098	1.6339	0.117	54

$$V_{ij-buck} = \left(A_{buck} e^{\frac{-r_{ij-buck}}{\varepsilon}}\right) - \left(\frac{C_{buck}}{r_{ij-buck}^6}\right) \quad (3\text{-}2)$$

$$\in = \boldsymbol{D_i + D_j} \quad (3\text{-}3)$$

$$\boldsymbol{A_{buck}} = \boldsymbol{f} \in \quad (3\text{-}4)$$

$$\boldsymbol{A_{buck}} = \boldsymbol{f}(D_i + D_j) \quad (3\text{-}5)$$

$$\frac{C_{buck}}{r_{ij-buck}^6} = \frac{C_i C_j}{r_{ij}^6} - \frac{q_i q_j r_{ij}}{r_{ij}} \quad (3\text{-}6)$$

$$r_{ij-buck} = r_{ij} - (A_i + A_j) \quad (3\text{-}7)$$

Subsequently, average intra-atomic distances (r_{ij}) and the fractional occupancy data presented as reference in Tables 3-2 and 3-3 were adopted from Meagher and Lager (1979), Bokhimi and Pedraza (2004), and Charlton et al (1997).

Table 3-2: Simulated Cell fractional coordinates of Titania using GULP

	Anatase				Rutile				TiO2-II			
	Simulated		Ref*		Simulated		Ref*		Simulated		Ref*	
	Ti	O	Ti	O	Ti	O	Ti	O	Ti	O	Ti	O
a	0.0000	0.0000	0.0000	0.0000	0.0000	0.3033	0.0000	0.30533	0.0000	0.2740	0.0000	0.2860
b	0.5000	0.5000	0.5000	0.5000	0.0000	0.3033	0.0000	0.30533	0.1625	0.3861	0.1710	0.3760
c	0.2500	0.4581	0.2500	0.4566	0.0000	0.0000	0.0000	0.0000	0.2500	0.4175	0.2500	0.41120

* Meagher and Lager (1979), Bokhimi and Pedraza (2004), and Charlton et al (1997)

Table 3-3: Simulated Cell fractional coordinates of Titania using GULP

	Brookite (10GPa)						Brookite						CLT			
	Simulated			Ref*			Simulated			Ref*			Simulated		Ref*	
	Ti	O_x	O_y	Ti	O_x	O_y	Ti	O_x	O_y	Ti	O_x	O_y	Ti	O	Ti	O
a	0.1312	0.0157	0.2382	0.1289	0.0157	0.2314	0.1307	0.0157	0.2333	0.1289	0.0095	0.2314	0.8583	0.5191	0.0000	0.3110
b	0.1011	0.1476	0.1253	0.0972	0.1483	0.1110	0.1027	0.1483	0.1198	0.0972	0.1491	0.1110	0.0081	0.8504	0.0000	0.0000
c	0.8626	0.1897	0.5347	0.8626	0.8626	0.5366	0.8597	0.183	0.5301	0.8628	0.1835	0.5366	0.3579	0.3665	0.3464	0.2500

* Meagher and Lager (1979), Bokhimi and Pedraza (2004), and Charlton et al (1997)

3.2.1 Computational Method

Adopting the computational method outlined in GULP (Gale, 2007), the main task was to “determine the structure with the minimum energy by identifying the local minimum on the global potential energy surface nearest to or in the neighbourhood of the starting cell coordinates” which is best suited for a constant pressure simulation with a continuous energy surface. However, several other approaches have been defined in literature to include simulated annealing via either Monte Carlo or Genetic algorithms (Van Laarhoven and Aarts, 1987).

Since for a given configuration at any given point, the internal energy can be expressed as

$$\boldsymbol{V}(\boldsymbol{x}+\ \boldsymbol{\delta x}) = \boldsymbol{V}(\boldsymbol{x}) + \frac{\boldsymbol{\partial V}}{\boldsymbol{\partial x}}\boldsymbol{\delta x} + \frac{\mathbf{1}}{\mathbf{2!}}\frac{\boldsymbol{\partial^2 V}}{\boldsymbol{\partial x^2}}(\boldsymbol{\delta x^2}) + \cdots \qquad (3\text{-}8)$$

which behaves harmonically; “the first term of this Taylor series expansion is collectively written as the gradient vector, g; while the matrix of the 2nd derivative is the Hessian matrix, H; and using the conjugate gradients algorithm, subsequent steps were made orthogonal to previous search vectors for which the displacement vector, x, in the current position relative to the local minimum is expressed below using Newton-Raphson procedure; where α is a scalar quantity which is determined by performing a line search along the search direction to find the one-dimensional minimum and the procedure becomes iterative as per conjugate gradients”. The accurate treatment for the displacement vector Δx is provided in Gale (2007);

$$\Delta\boldsymbol{x} = -\boldsymbol{H^{-1}g} \qquad (3\text{-}9)$$

The optimized structure (Figure 3-1) was attained at the local minimum total lattice energy with gradient vector below 0.001 thresholds. Simulated data for these simulations are presented in appendix 3b.

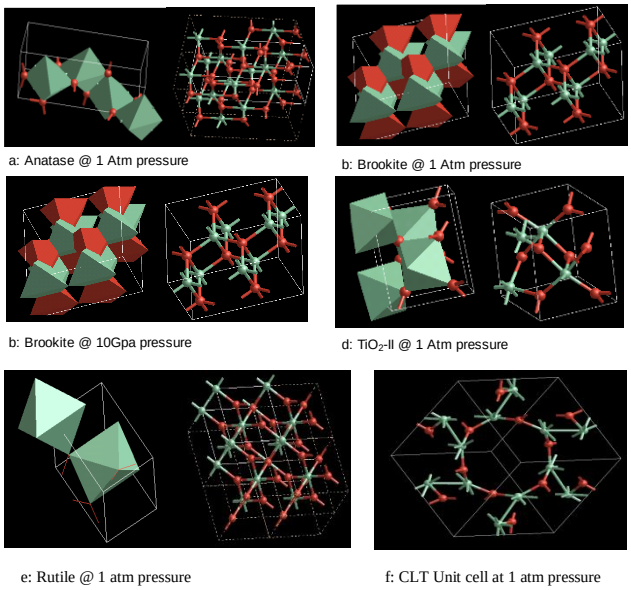

Figure 3-1: Optimized non-primitive unit cell structure of six polymorphs of Titania (Ti: green atoms; O_2: orange atoms)

3.2.2 Thermodynamic Properties

Thermodynamic quantities were calculated from the phonon density of state with accuracy dependent on the K number of mesh grid points or shrinking factor selected for the Brillouin Zone integration (Ramirez and Boehm, 1988), with focus on:

Zero Point Energy, $$ZPE = \sum_{k-points} w_K \sum_{all-nodes} \frac{1}{2} h\nu \qquad (3\text{-}10)$$

In principle, the ZPE is added to the lattice energy to obtain total internal energy for heat transfer measurements to differentiate between two structures; however it is neglected in the energy minimization calculation being a constant with zero derivatives.

Helmholtz free energy, $$A = U - TS_{vib} \qquad (3\text{-}11)$$

where $$U_{total} = U_{lattice-energy} + U_{vibrational-energy} \qquad (3\text{-}12)$$

And Heat capacity at constant pressure,

$$C_p = RT\left[2\left(\frac{\partial \ln Z_{vib}}{\partial T}\right)+\frac{\partial^2 \ln Z_{vib}}{\partial T^2}\right] \quad (3\text{-}13)$$

R is the universal gas constant, W_k is the weight associated with each k_{th} point, S_{vib} is the vibrational mode entropy (Gale 2007), h is plank's constant, v is the particle frequency and Z_{vib} is the vibrational partition function. For optimization under constant pressure calculation involving changing unit cell parameters, the specific Gibbs free energy, G, is of paramount importance as it relates the total energy required to perform a unit work with the finite cell volume in which the work is done. This is given below in terms of Helmholtz free energy, A, and the effective pressure, P.

$$G = A + PV \quad (3\text{-}14)$$

$$P_{effective} = P_{ext} - P_{\text{int}} \quad (3\text{-}15)$$

3.2.3 Mechanical Properties

Since there is no unique definition of transformation at this atomic scale for bulk defects, the Hill (Nye, 1957) definition of bulk modulus (K) and shear modulus (G*) being the average fit for Reuss and Voight determinations as given below in terms of symmetry elements C_{ij} and S_{ij} (Isaac et al, 1997) was adopted.

$$K_{Voight} = \frac{1}{9}\left[C_{11}+C_{22}+C_{33}+2\left(C_{12}+C_{13}+C_{23}\right)\right] \quad (3\text{-}16)$$

$$K_{\text{Re}uss} = \left[S_{11}+S_{22}+S_{33}+2\left(S_{12}+S_{13}+S_{23}\right)\right]^{-1} \quad (3\text{-}17)$$

$$G^*_{Voigt} = \frac{1}{15}\left[C_{11}+C_{22}+C_{33}+3(C_{44}+C_{55}+C_{66})-C_{12}-C_{13}-C_{23}\right] \quad (3\text{-}18)$$

$$G^*_{Reuss} = \frac{15}{4}[S_{11} + S_{22} + S_{33} + 3(S_{12} + S_{13} + S_{23}) - S_{12} - S_{13} - S_{23}]^{-1}$$

.... (3-19)

While the Young modulus $Y_{ά}$ is described by a unique positive resultant of vectors in the Cartesian directions defined as

$$Y_x = S_{11}^{-1} \quad (3\text{-}20)$$

$$Y_y = S_{22}^{-1} \quad (3\text{-}21)$$

$$Y_z = S_{33}^{-1} \quad (3\text{-}22)$$

In addition, the static dielectric constants, ξ computed as an imperative parameter for obtaining the response of the molecules to charge defects when placed in an electric field for which all the crystal's degree of freedom (both nuclear and electronic) respond, and are therefore able to provide screening. This (3x3) static dielectric tensor was determined from the Cartesian derivative matrix of all particles, $D_{άβ}$; and charge vector, q, containing the charges of all the particles in the same field as

$$\xi^0_{\alpha\beta} = \delta_{\alpha\beta} + \frac{4\pi}{V}\left(qD^{-1}_{\alpha\beta}q\right) \quad (3\text{-}23)$$

$\delta_{\alpha\beta}$ is the high frequency dielectric constant, while the optical refractive index, η, is directly related to the dielectric constant, ξ, by

$$\eta = \sqrt{\xi} \quad (3\text{-}24)$$

3.2.4 Results and Discussion

The simulated primitive unit cell parameters for the six polymorphs are presented in Tables 3-2 and 3-3. The results show that the two-body interaction Buckingham potential model reproduces all crystallographic

structures with unit cell to within 1% deviation for Rutile, 3% for the CLT, 4% for TiO_2-II and Brookite, and no deviation for Anatase.

The calculated structures had cell dimensions of a= 4.49 (0.02), b= 4.49 (0.02), c= 3.01 (0.01) with bond angles of 90°,90°,90° for Rutile; a=3.77 (0.01), b=3.77 (0.01), c=9.57 (0.08) with bond angles of 90°,90°,90° for Anatase; a=9.15 (-0.04), b=5.39 (-0.02), c=5.44 (-0.03) with bond angles of 90°,90°,90° for low-pressure Brookite; a=9.03 (-0.16), b=5.32 (-0.09), c=5.04 (-0.13) with bond angles of 90°,90°,90° for high pressure Brookite; a=4.52 (0.03), b=5.38 (0.02), c=4.94 (0.02) with bond angles of 90°,90°,90° for TiO2-II; and a=4.96 (0.00), b=4.96 (0.00), c=13.55 (-0.23) with bond angles of 90°,90°,90° for CLT; the parenthesized figures being deviation from reference.

The results indicated that all six polymorphs required non-primitive cells for co-ordination stability which reflected in the simulated unadjusted energy quantities as presented in Tables 3-4 and 3-5. Anatase and Rutile required two unit cells for stable co-ordination; TiO_2-II required 4, while the low and high pressure Brookite, and CLT required 8 each. The adjusted primitive cell heat capacity values are presented in Table 3-5. By comparison with Kim et al (1996), this lower heat capacity values for Anatase (-28%), Rutile (-29%) and low Pressure Brookite (-16%) are attributable to the lower level of crystal vibration within their mean-free-path and the absence on impurities at the molecular level and hence the lower total energy as depicted in equation 3-12.

The simulated mechanical properties, presented in Table 3-7, were in close agreement with the references (Bokhimi and Pedraza, 2004; Swamy et al, 2001 and Kim et al, 1996; Matsui and Akaogi, 1991) with less than 1% deviation. Input data and results for these simulations are presented in **Appendix** 3a-3d.

Table 3-4: Simulated Thermodynamic Properties of Titania using GULP @ 298K

Thermodynamic properties	**Anatase**	**Rutile**	**Brookite**	**Brookite (10GPa)**	**TiO2-II**	**CLT**
Zero Point Energy (eV)	0.48418	0.48722	2.06706	2.19799	1.03219	1.45817
Entropy (eV/K)	0.00052	0.00052	0.00274	0.00258	0.00115	0.003681
Intratomic Potentials (eV)	6.38018	6.19028	25.01190	29.74308	12.29153	13.92392
Total Lattice Energy (eV)	-78.9970	-79.6056	-316.9971	-301.5396	-159.0706	-157.4830
Helmholtz free-energy (eV)	-78.5657	-79.1732	-315.2249	-299.6193	-158.1534	-156.5177
Cp (eV/K)	0.00079	0.00078	0.00385	0.00367	0.00178	0.00377

1 eV = 96.48530891 kJ/mol

Table 3-5: Simulated Thermodynamic Properties of Titania using GULP @ 400K

Thermodynamic properties	**Anatase**	**Rutile**	**Brookite**	**Brookite (10GPa)**	**TiO2-II**	**CLT**
Zero Point Energy (eV)	0.48418	0.48722	2.06706	2.19799	1.03219	1.45817
Entropy (eV/K)	0.00078	0.00078	0.00399	0.00378	0.00173	0.004870
Intratomic Potentials (eV)	6.38018	6.19028	25.01190	29.74308	12.29153	13.92392
Total Lattice Energy (eV)	-78.9970	-79.6056	-316.9971	-301.5396	-159.0706	-157.4830
Helmholtz free-energy (eV)	-78.6320	-79.2395	-315.5691	-299.9446	-158.3007	-156.9555
C_p (eV/K)	0.00096	0.00096	0.00458	0.00444	0.00215	0.00428

1 eV **= 96.48530891** kJ/mol

Table 3-6: Simulated Heat Capacity values at 298K and 400K

	Heat Capacity values											
	Anatase		**Rutile**		**Brookite**		**Brookite-HP**		**TiO_2-II**		**CLT**	
	Simulation	***Ref****	***Simulation***	***Ref****	***Simulation***	***Ref****	***Simulation***	***Ref****	***Simulation***	***Ref****	***Simulation***	***Ref****
Cp @ 298K (J.mol/mol-K)	38.11	53.16	37.63	55.25	46.43	56.30	44.26	-	42.94	-	45.47	-
Cp @ 400K (J.mol/mol-K)	46.31	63.20	46.31	62.37	55.24	64.55	53.55	-	51.86	-	51.62	-

*Kim et al (1996), references for TiO_2-II and CLT are not available.

Table 3-7: Simulated Mechanical Properties of Titania using GULP

Mechanical Properties	Anatase		Rutile		Brookite		Brookite (10GPa)		TiO2-II		CLT	
	Simulated	Ref*	Simulated	Ref*	Simulated	Ref*	Simulated	Ref*	Simulated	Ref*	Simulated	Ref**
Cell Volume (Å3)	68.0002	68.0002	60.722	60.722	253.57	253.57	242.19	242.19	120.04	120.04	359.89	
Crystal Space group	I 41/ A M D	I 41/ A M D	P 42/M N M	P 42/M N M	P B C A	P B C A	P B C A	P B C A	P B C N	P B C N	R-3 C	R-3 C
Density (g/cm3)	3.9013	3.89▓	4.369	4.27▓	4.185	4.12▓	4.3815	-	4.42	4.33▓	2.21	-
Bulk Modulus (TPa)	0.18	0.21π	0.24	0.23π	0.20	0.22π	0.24	-	0.23	-	0.06	-
Shear Modulus (GPa)	58.78	-	116.53	-	91.96	-	89.50	-	108.91	-	6.23	-
Static Dielectric Constant	7.86	-	8.91	-	8.66	-	8.46	-	9.94	-	2.38	-
Refractive Index	1.6673	-	1.7931	-	1.7305	-	1.7208	-	1.8997	-	1.7297	-
Isothermal Compressibility (1/TPa))	6.0116	6.1	4.2175	4.3	5.0159	5.1	4.3324	-	4.4137	4.5	15.6188	-
Young Modulus (GPa)	167.35	-	365.56	-	169.64	-	135.01	-	273.24	-	97.07	-

*Matsui and Akaogi (1991); ****** Bokhimi and Pedraza (2004); ▓ Swamy et al (2001); π Kim et al (1996)

3.2.5 Optimized Nanoparticles

To further validate the procedure and results, a Molecular Dynamic optimization for all six polymorphs using the Broyden-Fletcher-Goldfarb-Shanno: BFGS (Shanno, 1970) optimizer with a secondary switch to Rational Functional Optimization- RFO (Banerjee et al, 1985) was performed. These simulations gave satisfactory results for all except CLT because of its high compressibility value and electronegativity equalization correction (Sanderson, 1951). To obtain the result images presented in Figure 3-2, the dynamic structure averages were taken for 4000 steps and time increment of 1fs was used adopting Nose-Hoover NVE (Nose, 1984; Hoover, 1985; Brode and Ahlrichs, 1986; Pearlman, 1995; Njo, 1998; and Lindan, 1993) ensemble under constant pressure. It worth noting that there are other optimizers, however this combination was found satisfactory in terms of available computing resource requirement.

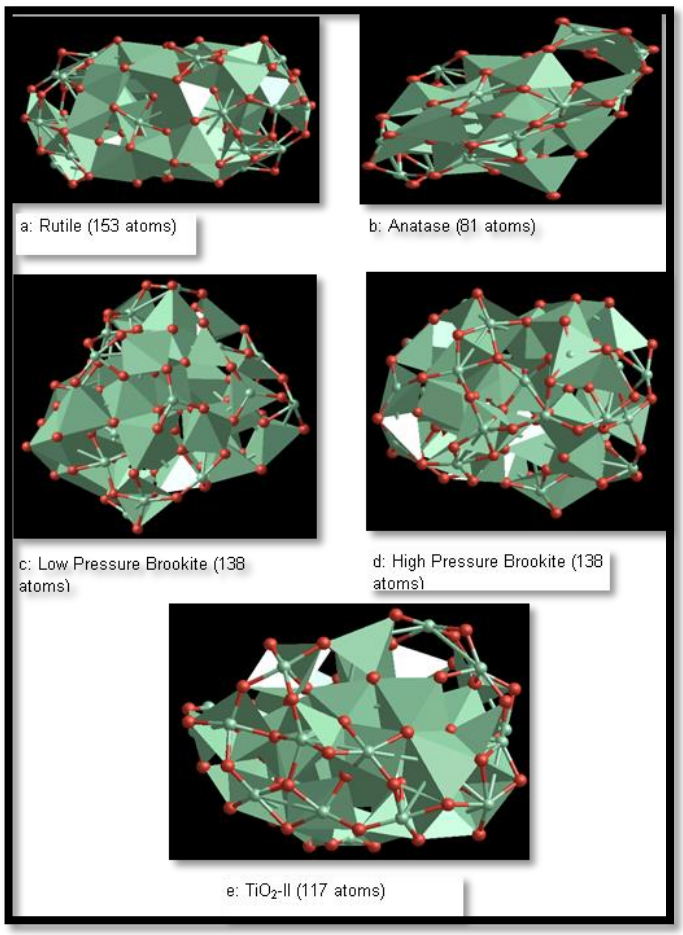

Figure 3-2: Optimized nanoparticles with 10 non-primitive unit cells (Titanium- in green, Oxygen in orange).

The BFGS-RFO algorithm maintained the local minimum and showed convergence for the root mean square gradient per variable, the maximum individual gradient component, the norm of the estimated displacement vector, and all state variables indicating continuity in the energy surface with positive dielectric frequencies. A sample input and output data for Rutile are presented in **Appendices** 3c and 3d.

The above discussed molecules represent the basic building nuclei for particle synthesis upon which nucleation and growth further occur to attain the required nanoparticles.

3.3 Nucleation and Growth

3.3.1 Nucleation

Nucleation is the onset of particle formation at the atomic scale level which can be separated into primary and secondary nucleation. Primary nucleation involves forming crystal nuclei in the saturated solution. This, typically, for sol-gel process is homogenous nucleation which occurs spontaneously at the reacting interphase between the reacting species upon contact at sufficiently high level of precursor supersaturation exceeding the metastable zone width.

Secondary nucleation is induced by the presence of nucleated surfaces or reacting surfaces in the solution which is heterogeneous in nature. The crystal nuclei in the solution perpetuates crystal growth (Mullin, 2001) reducing the degree of super-saturation. Figure 3-3 below depicts the path and progression of particle formation and crystallization from solution.

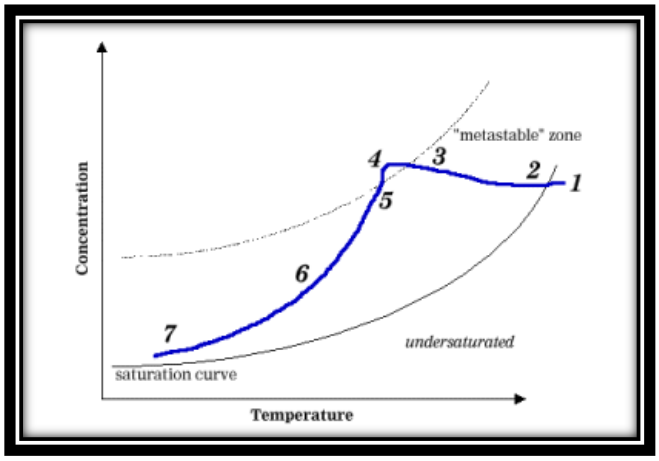

Figure 3-3 Progression of Crystallization (Crystallization, nd)

1. Feed location, under-saturated
2. Solution is saturated
3. Particle enters metastable zones, nucleation begins
4. Rapid nucleation
5. Concentration decreases with crystal growth
6. Crystal growths during main growing cycle
7. Exit location, supersaturated

In this work, $TiCl_4$ precursor solution is fed to the system and the accumulated volume on the disc became more saturated as more solution was fed into the reactor for the hydrolysis and condensation process at micro-second time-scale; that increased until the metastable zone was reached to initiate the nucleation of TiO_2. Once primary nucleation occurred at the onset with the formation of crystal nuclei, secondary nucleation began and continued at any point within the operating envelop even if the supersaturation level is below the metastable zone.

3.3.1.1 Nucleation Rate

Nucleation rate, j, is the number of nuclei formed per unit time per unit volume,

$$J = nZA \qquad (3\text{-}25)$$

n = concentration of critical nuclei (nuclei/ volume)

Z = frequency of attachment of a single molecule to a unit area of the nuclei

A = area of critical nuclei

The concentration of critical nuclei (n) was dependent on the total number of molecules in the solution, the free energy needed to create the critical nuclei and the temperature of the solution. It is given by equation 3-26 below, where the exponential factor gives the probability of critical nuclei being formed.

$$n = Ne^{(-\Delta G/kT)} \tag{3-26}$$

$$\Delta G = \frac{4}{3}\pi r^3 \Delta G_t + 4\pi r^2 \gamma \tag{3-27}$$

N = number of molecules per unit volume

ΔG = maximum free energy

k = Boltzmann constant

T = temperature of solution

γ = interfacial tension between crystal surface and supersaturated solution

The free energy per unit volume, ΔG_t, given by “equation 3-28” acts as the driving force for nucleation to occur from the supersaturated solution (Jayaraman, et al 1990) which is negative when the solution is supersaturated. Once nucleated, the process is reversible and the crystal nuclei may re-dissolve into the solution. The sustained nucleated particles initiate heterogeneous nucleation and continue to grow by surface reaction until the crystal nuclei achieve a critical radius, r_c, or stable size. The number density of molecules in critical nuclei is dependent on the operating conditions and the bigger the particle equivalent radius, the lower the free energy as depicted by Figure 3-4.

$$\Delta G_t = -kT / (\ln S) \tag{3-28}$$

k = Boltzmann constant

T = Temperature of solution

S = Supersaturation ratio

$$S = \frac{c}{c^*}$$

c = concentration of the solution

c*= equilibrium saturation of the solution at the specified temperature

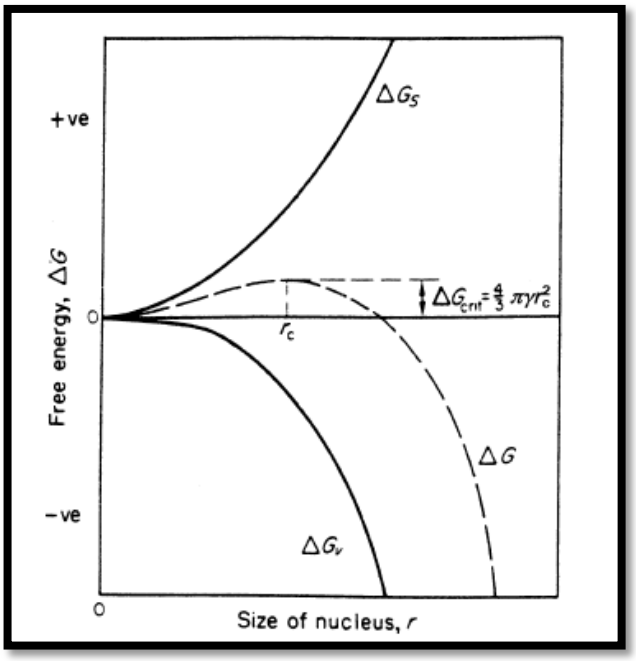

Figure 3-4 Free Energy Diagram for Nucleation
(Jayaraman et al, 1993)

The Figure shows the effect of nucleus size on maximum free energy. The surface excess free energy increases as the radius of the nucleus increase because more energy is required to form a bigger surface while the volume excess free energy will decrease with increase in size of nucleus.

$$r_c = 2\gamma / \Delta G_t \qquad (3\text{-}29)$$

$$\Delta G_{crit} = \frac{4}{3}\pi\gamma r_c^2 \qquad (3\text{-}30)$$

r_c = radius of critical nucleus

ΔG_{crit}=maximum free energy

In this work, critical radius (and hence the maximum free energy) have been used as an object parameter for determining required operating conditions for a target particle size and range. The critical radius is the smallest stable nuclei and possesses the least stable energy. Crystal nuclei will grow or dissolve in attempts to achieve this in a given system. If the crystal nucleus has a bigger radius compared to the critical radius, it will shrink or dissolve into a lower energy state. However, if the radius of the nucleus is smaller compared to the critical nucleus, it will grow to a lower free energy state. Although the energy of the solution is constant at constant temperature and pressure, there are variations in the energy levels at different parts of the liquid. When energy level in a certain region reaches the maximum free energy, nucleation will be favoured (Mullin 2001).

Usually and because both Rutile and Anatase are tetragonal, they co-exist, but at different energy levels. The prevalent stable phase is the polymorph with the lower free energy while the higher energy polymorph is known as the metastable phase. Figure 3-5 below shows the critical diameter (Dc and Dc' for Rutile and Anatase respectively) where the metastable phase changes to become stable phase.

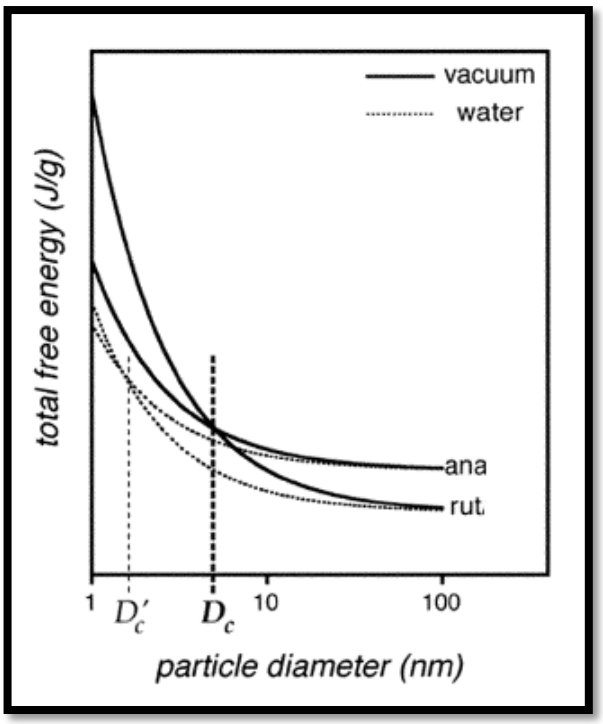

Figure 3-5 Particle Size Dependence of Free Energy
(Jayaraman et al, 1993)

At room temperature and pressure, Rutile is a more stable phase and the metastable phase is Anatase. Research has shown that the ΔG is approximately 67kJmol-1 and the Dc > 14nm. Surface energy estimation of Anatase and Rutile phase is approximately 1.3 and 1.9 J/m^2 respectively. These value shows that surface energy is a dominant function of particle size; therefore and though Rutile is more thermodynamically stable at aqueous conditions, Anatase is usually produced in the synthesis of nanoscale Titania. The smaller particle diameter allows Anatase to be the more stable phase. Pure phase Brookite is rarely available due to the low range of conditions in which Brookite is stable in. It usually forms a fraction of the Anatase polymorphs.

The Z term in “equation 3-25” is known as flux of atom impingement. It can be evaluated using the kinetic theory of gases.

$$Z = \alpha(P_v - P_s)N_a / (2\pi MRT)^{0.5} \qquad (3\text{-}31)$$

where

α = sticking coefficient

P_v = partial vapour pressure of solute

P_s = vapour pressure of solution

N_a = Avogadro’s number (6.023×10^{23})

M = molecular weight

R= Universal gas constant (8.3145 J/mol K)

The sticking coefficient is the ratio of the molecule that sticks on the surface compared to the total number of molecule that collides with the surface of the nuclei; the value is a coefficient between 0 (where none of the molecule stick on the surface) and 1 (all the molecule stick on the surface) and is a function of surface coverage, temperature and surface structure (IUPAC 1997).

3.3.1.2 Factors Affecting Nucleation Rate

Overall, nucleation rate is controlled by three main factors: the temperature, supersaturation ratio and the interfacial tension. Figures “3-6 and 3-7” below show the effect of temperature and supersaturation on nucleation rate.

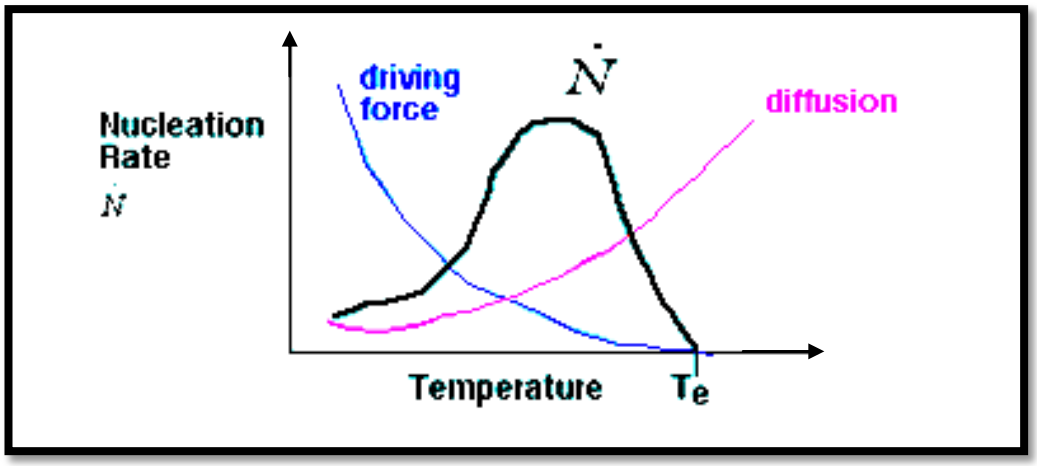

Figure 3-6 Nucleation Rate
(Thomas 2000)

Influenced by the instability of the liquid phase and the diffusion of TiO_2 towards the crystal nuclei; both act as driving forces for nucleation. The changing supersaturation along the temperature curve makes the liquid unstable, while the molecular kinetic energy enables the particles to diffuse towards the crystal nuclei. On one hand, the degree of supersaturation decreases with increases in temperature; on the other, diffusion of molecules depends on the kinetic energy and increases with temperature. Hence, optimality was achieved by independently varying both for operations in the maximum allowable level of supersaturation required for homogeneous nucleation to occur beyond which nucleation rate declines. This zone is known as the “metastable zone width” which is affected by process parameters such as saturation temperature and mixing.

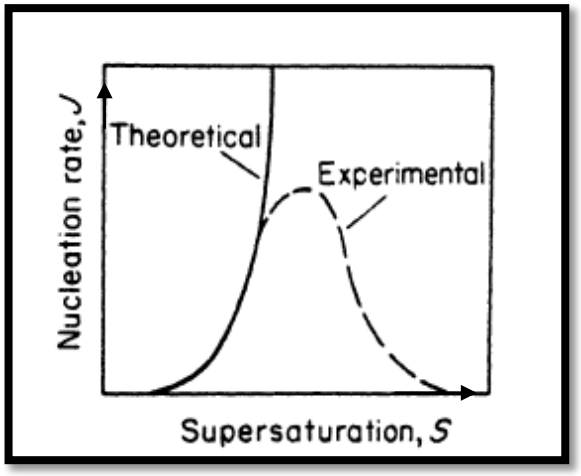

Figure 3-7 Effect of Supersaturation on Nucleation Rate (Jayaraman et al, 1993)

3.3.2 Growth and Breakages

Crystal growth begins with the emergence of crystal nuclei with critical radius and occurs in two steps. The first step involves the diffusion of titanium dioxide molecules towards the stable crystal lattice followed by the deposition of the molecule on the structure in orderly pattern (Wauqier 1998). The fixed pattern of the structure determines the properties of the crystal.

Crystal growth in nanoparticles occurs through different mechanism compared to bulk materials. This can be one of several growth mechanisms including surface precipitation of solvated atoms or few-atom clusters (diffusion based), or crystallographically-specific aggregation based growth: oriented aggregation (Gilbert et al, 2003).

Diffusion based growth, also known as Ostwald-ripening (O-R), refers to the “dissolution-precipitation” mechanism for crystal growth. The surface excess energy of the nanoparticles is proportional to the size of the particle. A bigger particle has higher chemical potential because of the higher surface energy; therefore larger particles will be preferred for further growth while the smaller particles relative solubility will increase. This growth mechanism depends on the diffusion of molecules towards a larger particle.

Aggregation based growth mechanism which is known as Oriented-attachment (O-A), is prevalent in samples of hydro-thermally treated nano-crystalline titanium dioxide. The nanoparticles act as building blocks for crystal growth aggregating and rotating so that the nanoparticles have similar orientation to each other. The oriented nanoparticles are then able to attach and eliminate the free surfaces between the particles while decreasing the neighbourhood surface excess free energy (Banfield, et al, 2000). This mechanism involves self-assembly at multiple sites. Aggregation-based growth accounts for possible collisions leading to successful coalescence. If the probability is less than 1, additional constraints such as orientation dependence and activation barrier are considered (Gilbert et al, 2003). Equations for both mechanisms are briefly discussed below. Equations “32 and 33” show the kinetics of both mechanisms.

O-R: Ostwald-ripening (Diffusion based)

$$D_{(t)} = D_0 + kt^{1/n} \tag{3-32}$$

O-A: Oriented Attachment (Aggregation based)

$$D_{(t)} = \frac{D_0\sqrt{2kt+1}}{kt+1} \tag{3-33}$$

where:

D(t) = size at time t

Do = initial particle size

k = rate constant for limiting step

n = nature of rate limiting step

There are generally three steps involved in O-R crystal growth with different rate constant possible. The rate constant selected must be from the steps with the lowest rate.

Table 3-8: Steps in Diffusion based Crystal Growth Mechanism.

Steps	**n**
Diffusion in Solution	1
Diffusion at Particle Surface	2
Interface Dissolution/ Precipitation Step	3

The crystal growth occurs in two main steps; the first step is the diffusion-convection of the molecules to the crystal lattice and the second is the integration of the ions into the lattice (Mersmann 2001). When the integration reaction occurs rapidly, the crystal growth is determined by the diffusive-convective transport of units which usually occurs when the mass flux density directed towards the crystal surface is low. Integration may be inhibited in the presence of foreign particles or impurities being adsorbed on the crystal surface. These particles must then be re-adsorbed to get rid of the impurities. In liquid, the diffusion is dependent on the volume of the diffusion species, the viscosity of the solution and on the kinetic energy.

Figure 3-8 shows a sketch of some of the main dependencies of diffusion controlled growth on operating conditions.

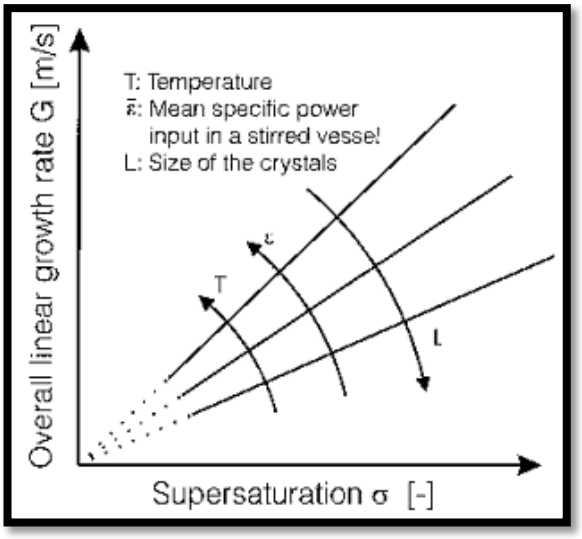

Figure 3-8: Influence of some principal operating conditions on diffusion-controlled growth (Mersmann 2001)

For this work, a two stage reactor system was adopted such that there were no foreign particles used for heterogeneous nucleation while still obtaining the advantages of the feature as discussed in Chapter 4.

3.3.2.1 Crystal Growth Rate

The growth rate of a crystal face is the incremental deposition per unit time in a direction perpendicular to the face which occurs layer by layer until a stable critical radius is reached by the transport of solute material to the face from the bulk of the solution McCabe (1929). The mass transfer of the solute A from the bulk solution of supersaturated solution can be shown as

$$\frac{N_m}{A_i} = \frac{y_A - y_{Ae}}{1/k_y + 1/k_s} = K(y_A - Y_{Ae}) \qquad (3\text{-}34)$$

Equation 3-33, where N_m is rate [Rate (kmol A/s)]; A_i is area [m^2]; Y_A is the super-saturation concentration and Y_{Ae} is the nominal saturation concentration, shows the rate of transfer per area given the mass-transfer coefficient, k_y; and surface reaction coefficient, k_s for the solution. It also shows that if the mass transfer coefficient, k_y, is very large, then growth rate is controlled by surface reaction. Conversely, when the mass-transfer coefficient is very small, growth rate is then controlled by diffusion resistance.

McCabe also showed that crystals that are geometrically similar and of the same material in the same solution will grow at the same rate. This growth can be measured as the change in length ΔL (mm) in linear direction of one crystal; this is particularly true for nanoparticles. This constant growth rate, G, can be shown as

$$\frac{\Delta L}{\Delta t} = G \qquad (3\text{-}35)$$

3.3.2.2 Factors affecting Growth Rate

According to equations “3-32 and 3-33” for O-R and O-A mechanism respectively, the computed particle size show dependence on rate constant (equation 3-34 below) which is in-turn dependent on temperature; both O-A and O-R are also dependent on diffusion and movement of molecules and particles; hence decreasing temperature will lead to reductions in the mobility of both molecules and particles, therefore decreasing the growth rate. These provide evidence that growth rate is highly dependent on the temperature of the solution as shown in Figure 3-9 for the overall transformation. The overall transformation rate evaluates the rate at which phase transformation happen and is the product of both nucleation rate and growth rate (Quigley and Rodger, 2008).

$$\ln k = \ln A - \frac{E}{RT} \qquad (3\text{-}36)$$

where:

k = rate constant

A = Arrhenius constant

E = Activation energy for crystal growth

R = Gas constant

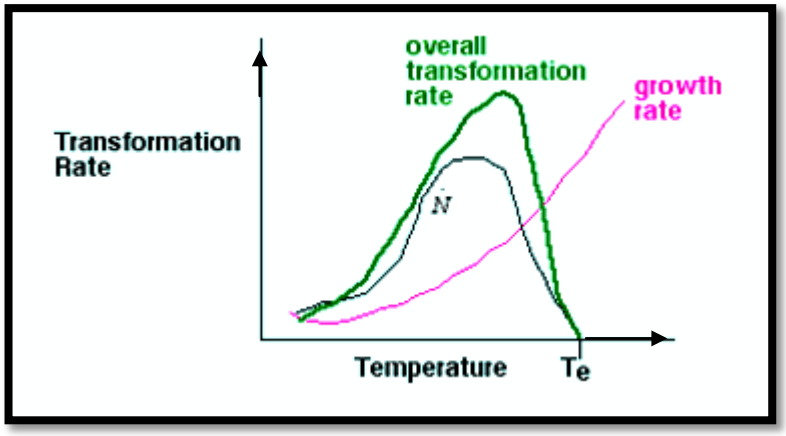

Figure 3-9: Overall Transformation Rate (Thomas, 2000)

3.4 Development of Population Balance Model Equations

3.4.1 Population Balance Model

The particle distribution and population of desired TiO_2 size was obtained from the number density, *n(v,t)* population balance equation expressed below in terms of non-zero growth, *G(v,t);* heterogeneous nucleation rate, *J(v,t);* and aggregation frequency, *q(v,t)* terms of size *v,* growing to size *v'* over time, t.

$$n(v,t) = \frac{1}{2}\int_0^v n(v-v',t)n(v',t)q(v-v',v')dv' - n(v,t)\int_0^\infty n(v',t)q(v,v')dv' - n(v,t)\frac{dG(v)}{dv} + J(v) \quad \text{....} \quad (3\text{-}37)$$

3.4.2 Population Balance Model Solution

Assuming uniform spherical shape factor and negligible breakage, the analytical solution of "equation 3-37" given in "equation 3-38" (Randolph and Larson , 1978) was adopted to obtain the number density of desired particles in the range V_0 to $V_{c,t}$ in terms of residence time τ and surface kinetics K_s [K_s= 49exp(-8993/T), Pratsinis et al., 1990] for its simplicity. Further analytical and numerical solutions abound in literature (Moody and Collins, 2003; Gilbert et al, 2003; Mersmann 2001; Quigley and Rodger 2008, Mullin and Raven 1962).

$$n(v,t) = \frac{N_0}{\tau} \exp\left(\frac{-\tau\left(v_{c,t} - v_0\right)}{G} \right) \quad (3\text{-}38)$$

where the growth rate, G_{rth} is obtained as

$$G_{rth} = 2 k_s V_m N_a C_{TiCl_4} \quad (3\text{-}39)$$

and

$$N_0 = \left(\frac{J_{(v)}}{M_{TiO_2}} + \frac{k_s V_m C_{TiCl_4}}{v_0} \right) \frac{\tau . N_a}{G_{rth}} \quad (3\text{-}40)$$

The implementation of equations 3-25 through to 3-40 using MS Excel gave results presented in Figures 3-10 to 3-15 with "E (±x)" representing "10^x". Figure 3-10 shows the rate of production of Titania to increase with increase in temperature but with practical limit at 319.27K; Figure 3-11 shows that particles growth rate is limited by the population of precursor concentration while it increases with precursor residence time in the reactor. Nonetheless, it is evident from Figure 3-12 that the number density of particles is increases with increase in the degree of supersaturation until the concentration of precursor reaches the critical supersaturation level of 6.9 for the size range examined. Figure 3-13 shows the relationship between the required spin to achieve target production rate at specified precursor molar concentrations, while Figure 3-14 shows the correlation between the required spin and the achievable particle number density; and Figure 3-15 presents the peak number density for 35 nm modal particles achieving number density of about 7×10^{29}. These results are in good agreement with literature (Collins, 2003; Gilbert et al, 2003; Mersmann 2001; Nucleation and Growth 2000, Mullin and Raven 1962). Simulated results are presented in **Appendix** 3e.

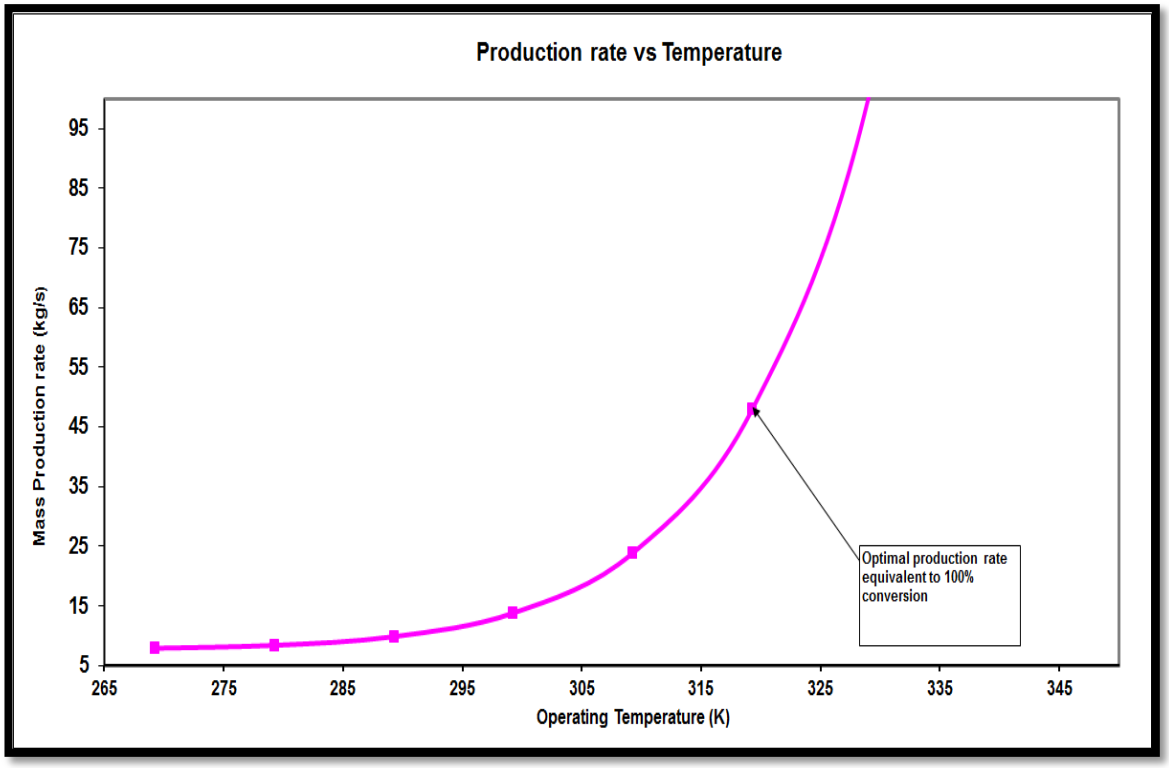

Figure 3-10: Effect of Temperature on Mass Production rate

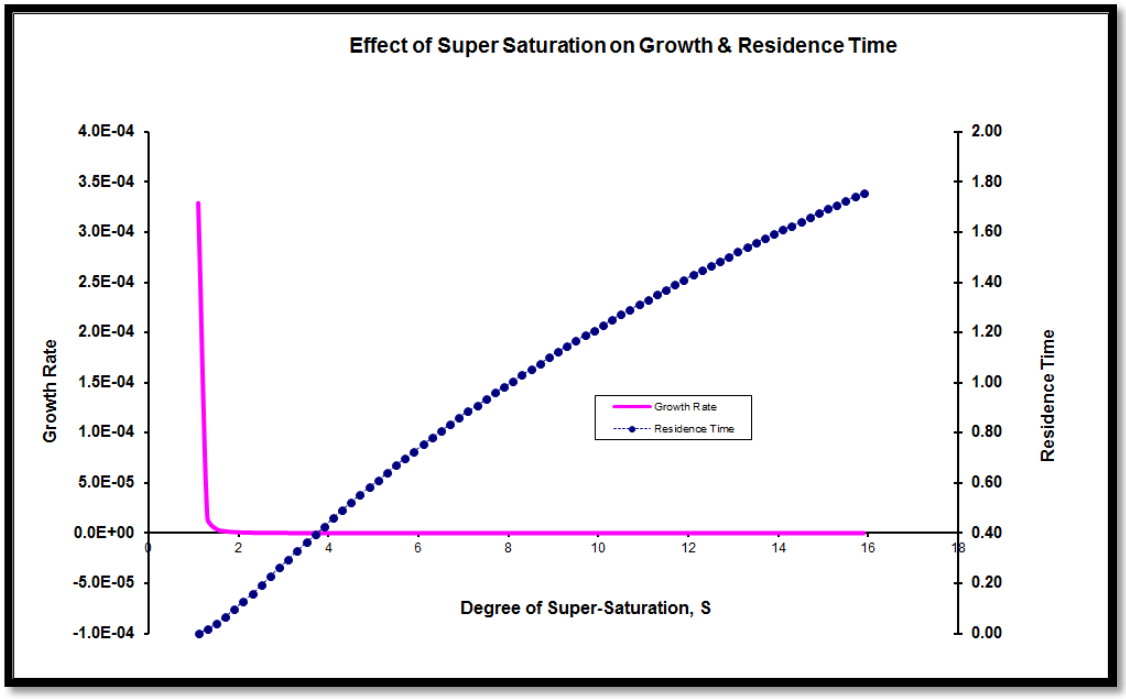

Figure 3-11: Effect of the degree on Super-Saturation on particle growth rate and required residence time

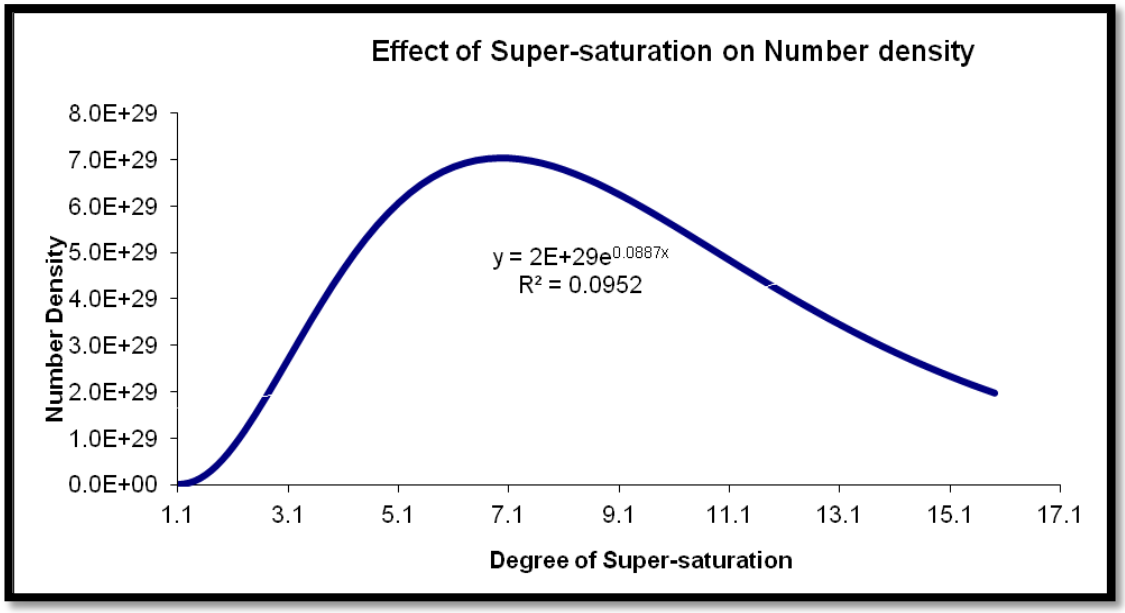

Figure 3-12: Effect of the degree on super-saturation on population number density

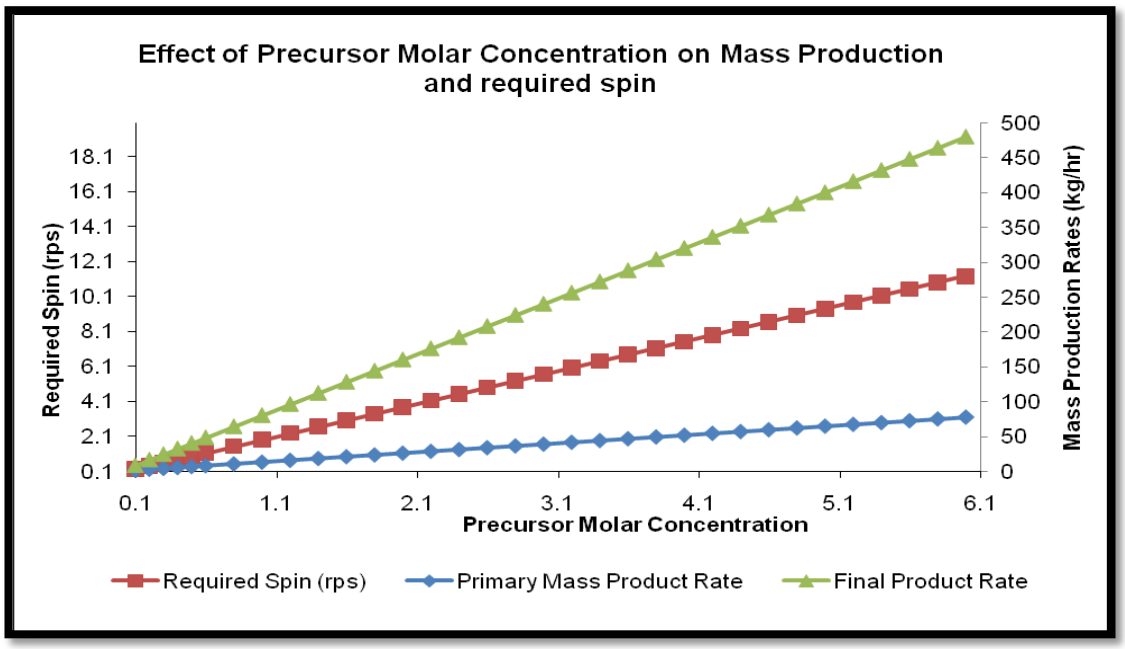

Figure 3-13: Effect of Precursor Molar Concentration on Mass Production and required spin

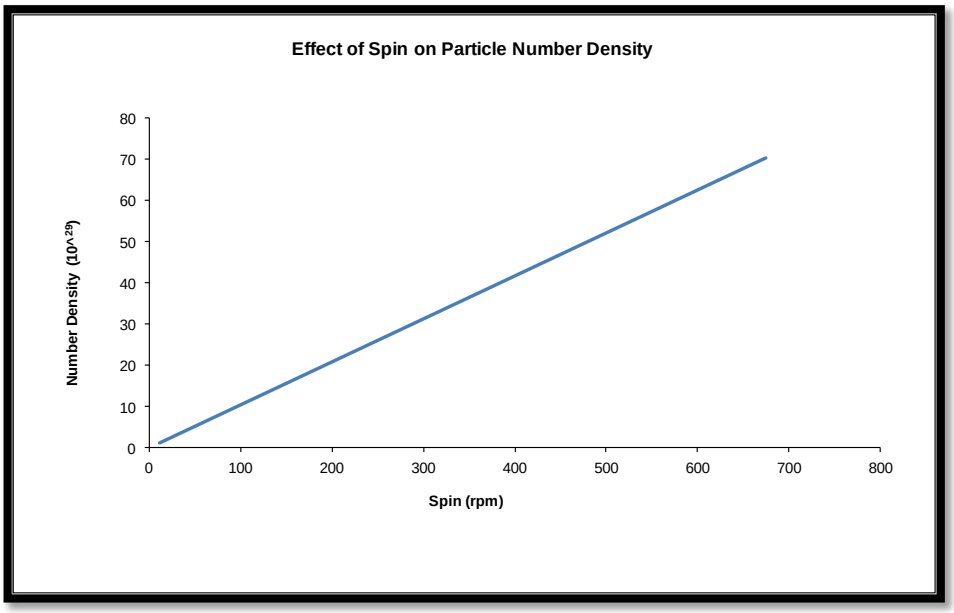

Figure 3-14: Effect of Spin on Particle Number Density

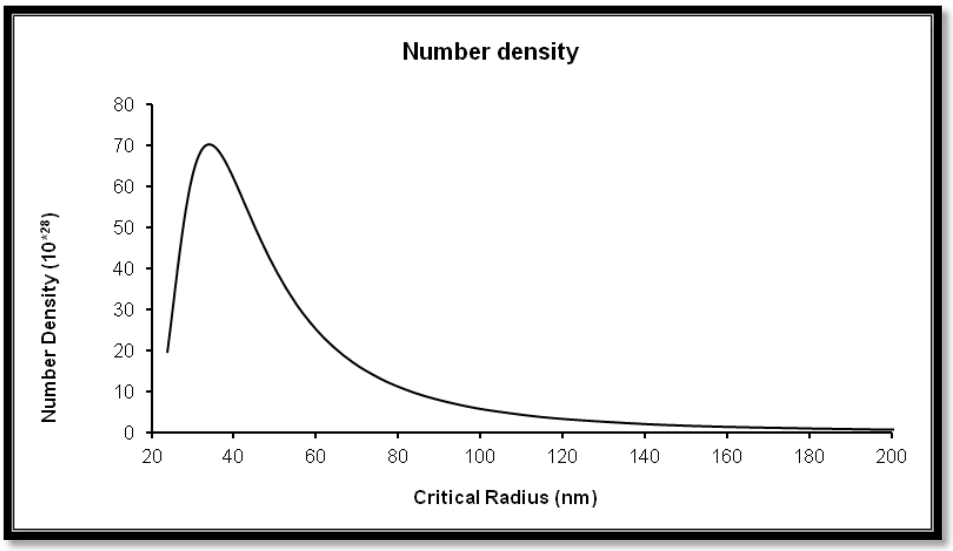

Figure 3-15: Particle Size Distribution Curve

To evaluate the validity of this model, a base case for Rutile with 0.6kmols/s (113.84kg/s) $TiCl_4$ with 34.23nm critical radius and 1.2mols/s (21.62kg/s) H_2O feed flow was used as prescribed by Figures 3-16 and 3-17 below. The results are presented in Table 3-9.

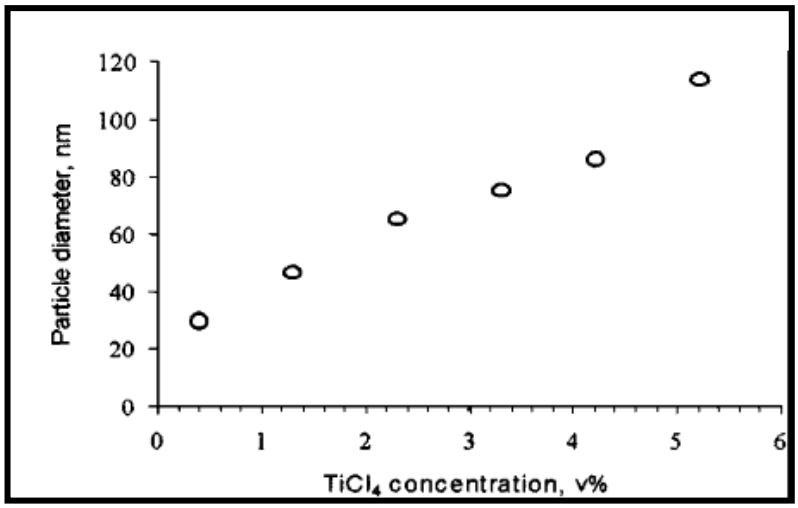

Figure 3-16 Effect of TiCl4 Concentration (Xia et al, 1999)

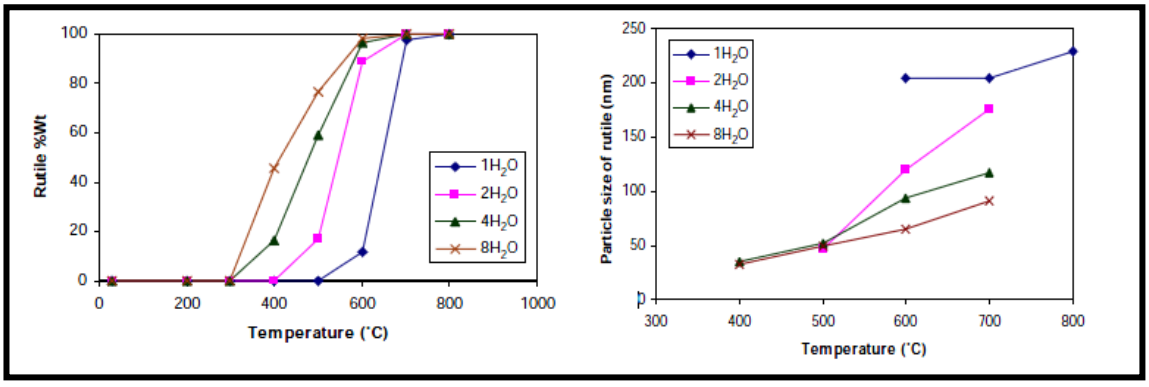

Figure 3-17 Effect of Ratio of Water to $TiCl_4$ (Xia et al 1999)

At high temperatures, this reaction will occur spontaneously in nano-second time order to yield 0.6kmols/s (47.96kg/s) TiO_2, and will continue as long as the precursor, acting as limiting reactant, is available with water in excess; however, this model predicts 0.859s as the required residence time to achieve the highest permissible conversion for a supersaturation solubility of 6.9 at 319.27K (46.27^{o}C). Table 3-9 below show the results for the base case computations.

At the optimal temperature, increase in super-saturation decreases the population (number density) of particles within the desired size range and also increases the required residence time to achieve similar conversion; particle growth follows similar trend; while increases in precursor molar

concentration requires more spin to achieve the required 16% conversion in the spinning disc unit.

Table 3-9: Results for some Base case computations

Variable	Result
Optimal Operating Temperature (K)	319.27
Precursor Feed Flow (kg/s)	113.81
Super-saturation level (s) at operating T	6.9
Spin disc radius (m)	0.05
Primary production- spin disc (kg/s)	7.22
Required Residence time (s)	0.859
Particles Critical Size (nm)	34.23
Growth rate (m/s)	3.96×10^{-8}
Number density	7.033×10^{29}
Product mass flow rate (kg/s)	47.96

It was conclusive that only temperature and degree of super-saturation have significant effects on the conversion and particle distribution for a fixed precursor molar concentration; while increases in precursor molar concentration requires more spin to achieve the same conversion and population density; and increases in spin for a fixed precursor molar concentration only leads to linearly proportional increases in number density but with no effect on residence time as shown in the following Figures 3-12 to 3-17. These results compare favourably with literature as depicted in Figures 3-6, 3-7 and 3-9.

The converse effect of agitation as depicted by Figures 3-11, 3-12 and 3-14 are in good agreement with Mullin and Raven (1962) who published [Figure 3-18 below] that agitation is often used to induce crystallization and that most agitated solutions nucleate spontaneously at lower degrees of super-cooling than quiescent ones. However, agitation's influence on nucleation is more complex than previously stated; they presented that there is a region where increased agitation can reduce the tendency to nucleate. The phenomenon was also investigated in this work through the adjustment of impeller speed during the experiment and reported in Chapter 5.

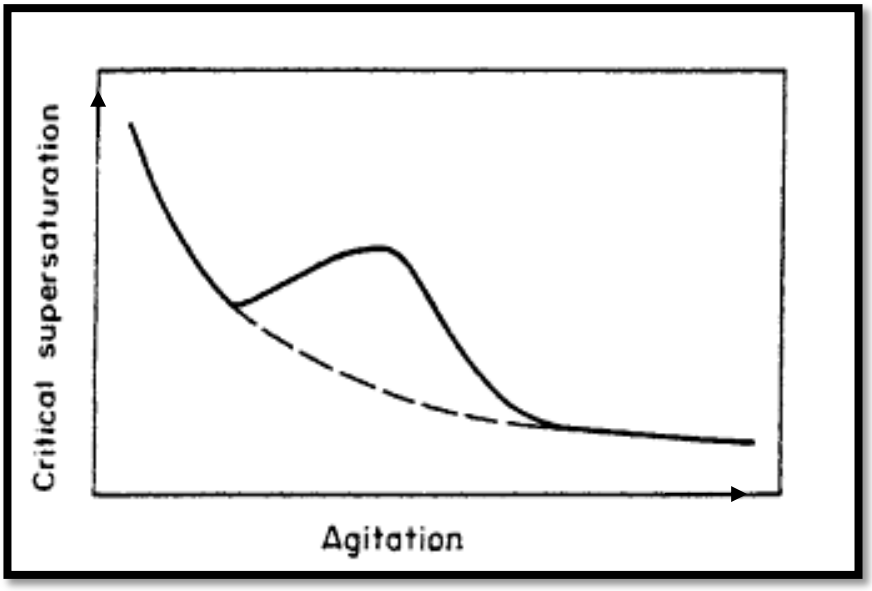

Figure 3-18: Influence of agitation on nucleation, showing a region where increased agitation can reduce the tendency to nucleate. (Mullin and Raven 1962)

3.5 Surface Enhancement with Hydroxyl Doping

For this work, optimized TiO_2 (Rutile) nanoparticles was solvated with H_2O using GROMACS (Van der Spoel, et al 2001). The result, when un-coordinated (excess) H-OH ions were deleted, showed that the Rutile particles was solvated with only one coordinated hydroxyl ion as shown on Figure 3-23; this compares favourably with Ken et al (2005) as presented Figures 2-7 to 2-10 of section 2.6.

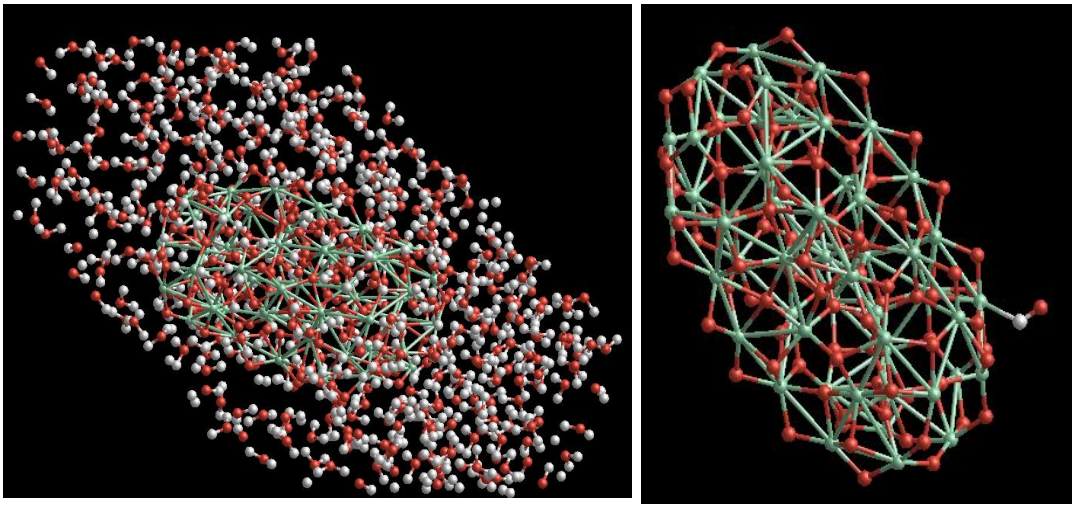

(A) (B)

Figure 3-19: A: Optimized Rutile Nanoparticles in excess H_2O molecules; B: Solvated Rutile Nanoparticles with 1 hydroxyl ion (oxygen ions in white, hydrogen in orange and titanium in green).

3.6 Conclusions

This study investigated and modelled six polymorphs of Titania: Rutile, Anatase, Brookite, high-pressure Brookite, the columbite-type TiO2-II and Corundum-like type CLT, under constant pressure using the General Utility Lattice Program (GULP) with satisfactory results compared to the Classical data on the subject. The simulated thermodynamic, mechanical and optical properties compare favourably with acceptably known references and results extended to simulate stable optimized nanoparticles except for CLT due its large compressibility and electronegativity equalization correction. The alternative Buckingham potentials are simpler to implement and the results provide a modern crystallographic compendium for Titania polymorphs. In addition, Randolph and Larson's population balance analytical solution yielded satisfactory results for the number density of Rutile nanoparticles as a base case compared to experimental data (in Chapter 5). Further, there are indications that hydroxylated TiO_2 may present yet unknown but important applications in semiconductors.

Chapter 4 : REACTOR DEVELOPMENT AND DESIGN

4. Introduction

As already established in Chapters 1 and 2, Titania exists in many different polymorphs of which the most thermodynamically stable are rutile, anatase and brookite. Several high-pressure forms have been demonstrated to be super-hard materials, while the ambient phases are employed in many industrial processes as a white inert pigment. Its chemical stability, high resistance to deterioration in acids or alkali, strong redox properties, significant pollution control and medical uses have all engendered an increasing interest in the use of Titania as a metal particle support in heterogeneous catalysis, and as a photo catalyst for the mineralization of toxic wastes. However, current schemes for the synthesis are either batch wise or energy intensive despite the numerous valuable applications of Titania.

Synthesis using microorganisms was recently reported (Jha et al 2009) but still nascent, spinning disc processor have been successfully modelled and applied for the synthesis of $AgNO_3$ nanoparticles (Swaminathan et al, 2007) but there is no known application for Titania. On the other hand, the aqueous (sol) application for the synthesis of Titania is well known for about a century. However, most applications require re-crystallization for purification, sometimes pulverization with wide particle size distribution and significant equipment encrustation for continuous processes.

4.1. This Work

From the Chemistry of formation, the precipitation of TiO_2 by hydrolyzing $TiCl_4$ is known to follow a two stage process: the generation of nuclei and the subsequent growth with the nucleation step as rate controlling. The overall production rate is enhanced with heterogeneous nucleation but at the expense of introducing impurities. In this work, TiO_2 particles produced in the rate-controlled aerosol unit are used as seeding particles to achieve

heterogeneous nucleation in the “SOL” reacting volume according to the stoichiometry below at 46.27°C (319.27K) and Xia et al demonstrated that crystallinity is dependent on the $H_2O/TiCl_4$ molar ratio (Xia et al, 1999; John and Surender, 2005; John et al, 2004; Wang and Garrick, 2006) which ensures no foreign particles are introduced.

$$^{x}T_iCl_4 + yH_2O \rightarrow {}^{x}T_iO_2 + 4xHCl + (y-2x)H_2O$$

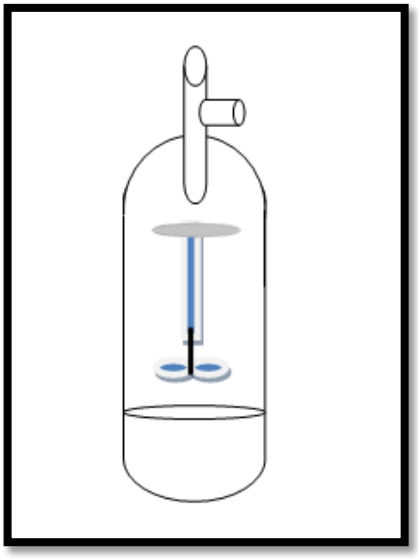

Figure 4-1: Schematic of the SDCST Reactor

Figure 4-1 shows the SDCSTSR schematic. The two inlets, inclined at 90° to each other separately inject atomized $TiCl_4$ and H_2O at 319.27K such that there is momentary imperfect pre-mix of reagent and the reaction occurs just at the surface of the disc to form products flashing on the rotating disc, this volume is denoted as the Aerosol Reacting Volume (Moody and Collins, 2003). The un-reacted $TiCl_4$, seeding TiO_2 particles formed, and H_2O, overflow from the ends of the disc into the aqueous (Sol) CSTR reacting volume to produce ionic precipitates as demonstrated by Li, et al (2004).

Both the aerosol and sol reacting volumes are within the Continuous Stir Tank maintained at 319.27K, but only the sol reacting volume is filled with reactants; the energy dissipation rate is dependent on volume homogeneity due to spinning disc, tank mixing, the heat transfer around the aqueous volume, and product withdrawal rate. The sequential process unit operating at 319.27K is depicted in Figure 4-2.

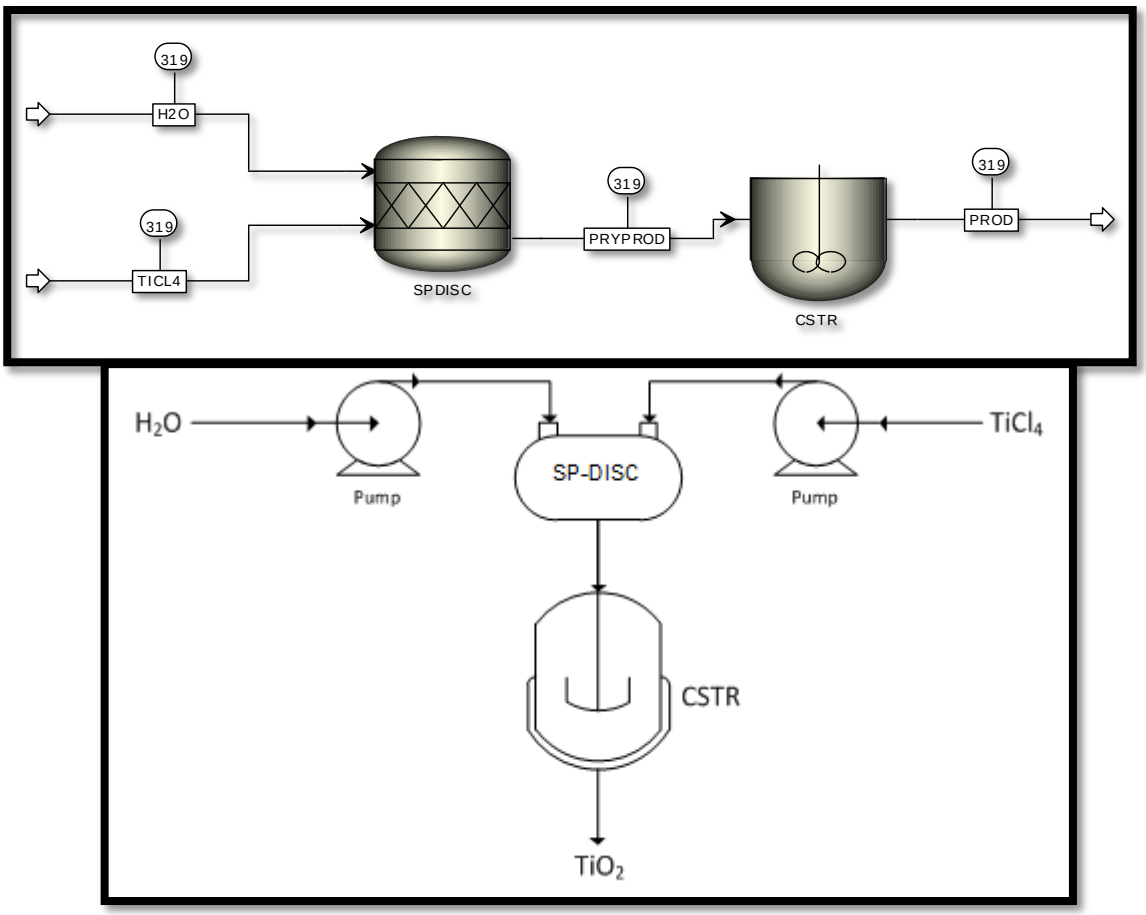

Figure 4-2: Process Flow of the unit operations in the reactor

4.2. Significance

As opposed to the high energy intensive CVD (Weiwei 2011) and the wide particle size distribution due to pulverization in the "SOL-GEL" process (Muneer, 2012, Mohammad et al 2011); this work proposed and used a new process route and reactor system for the continuous synthesis of Titania with low energy requirement (with about 80% energy savings), predictive and narrow particle size distribution and structural controllability.

4.3. The Reactor

This novel arrangement limits the number of nuclei produced in the aerosol system (~16% conversion of $TiCl_4$ to TiO_2) by controlling the concentration of reactants, impact angle and spin; while polymorph selection is achieved by selective operating conditions. The nucleated particles formed in the aerosol process are fed as seeds for heterogeneous nucleation in the metastable regime of the aqueous (sol) reacting volume after the imperfect pre-mix

induction time. The mixing (impeller rotation per second) and the degree of super-saturation provide a critical factor which limits the size and distribution of the particles formed. In accordance with section 3.2, the particles formed continue to grow by layering until a critical particle size occurs when the resultant forces acting on the bulk produce the critical breaking stress equivalent to the Young's modulus of the desired particle as described by equation 4-1 and buttressed by Motoyuki and Hidehiro (2009).

Critical breaking stress, $\Theta = \sqrt{(E\sigma)/\nu_{c,t}}$ (4-1)

$$\nu_{c,t} = 2\sigma \frac{V_m}{K_B T \ln(S)} \quad (4\text{-}2)$$

Hence $\Theta = \sqrt{(E K_B \ln S)/2\nu_m}$ (4-3)

Where V_m=Molecular volume (Å^3). Note 1 Å = 10^{-10}m

K_B = Boltzmann constant (1.3806505 x 10^{-23} J/K)

S=c/c*

c = solubility of TiO_2 of particle size $v_{c,t}$ at temperature T

c*=normal equilibrium solubility of TiO_2 at temperature T

"E" is desired particle Young's modulus; "$V_{c,t}$" the critical radius (Mullin,1993) of the desired particle size and ð is the surface energy.

To obtain the variables required to compute the critical particle radius, molecular modelling approach was adopted to simulate optimized TiO_2 nanoparticles for five different polymorphs of Titania by performing energy minimization calculations under constant pressure deploying General Utility Lattice Program: GULP (Gale, 2004) using the Buckingham intra-atomic potentials V_{ij}-buck as detailed in Chapter 3. Input cell parameters for this model were fitted from Matsui and Akaogi (1991) in terms of intra-atomic distance r_{ij}, effective charge q; repulsive radius A; softness parameter D; Van der Waals' atomic coefficient C given in Table 4-1, and standard atomic force f (4.184kJ/ Å.mol) have been used. The surface energy results are presented

in Table 4-2, while the other results are presented elsewhere (Akindeju et al, 2010).

$$V_{ij} = \frac{q_i q_j}{r_{ij}} - \frac{C_i C_j}{r_{ij}^6} + f * \left(D_i + D_j\right) * \exp\left(\frac{A_i + A_j - r_{ij}}{D_i + D_j}\right) \quad (4\text{-}4)$$

Table 4-1: Energy Parameters

	q (|e|)	A (Å)	D(Å)	C(Å^{3}kJ/mol)
Ti (Å)	2.196	1.1823	0.044	22.5
O (Å)	-1.098	1.6339	0.114	54

By re-arranging and equating the components terms, Abuck, Cbuck, $\varepsilon_{\text{buck}}$ and Rij-buck terms of the generalized Buckingham model (Vij-buck) for GULP input were derived as follows:

$$V_{ij-buck} = \left(A_{buck} e^{\frac{-r_{ij-buck}}{\varepsilon}}\right) - \left(\frac{C_{buck}}{r_{ij-buck}^6}\right) \quad (4\text{-}5)$$

$$r_{ij} = D_i + D_j \quad (4\text{-}6)$$

$$A_{buck} = f r_{ij} \quad (4\text{-}7)$$

$$\frac{C_{buck}}{r_{ij}^6} = \frac{C_i C_j - q_i q_j r_{ij}}{r_{ij}^6} \quad (4\text{-}8)$$

$$\varepsilon_{\text{buck}} = r_{ij} \quad (4\text{-}9)$$

Table 4-2: Empirical Surface Energy computation for the 5 polymorphs of Titania

	Anatase	**Rutile**	**Brookite**	**Brookite (10GPa)**	**TiO2-II**
Empirical Surface (110) energy, N/m	1.3 - 2.4	2.08 – 2.41	1.81 – 2.40	0.5 – 2.30	2.08 – 3.11

The TiO_2 nanoparticles formed are enhanced by the OH^-—H^+ chemisorbed on the surface by interacting with the cations to produce stable OH^- groups which neutralizes the electrical charge of the cations on the surface as a result of the acidic aqueous medium and layering activities. After reaching a residence time t, the settled particles are withdrawn continuously at a rate equivalent to the settling rate, given by a modified Coe and Cleavage (Perry, 1994) correlation,

$$R_s = \frac{(F - D)W}{k_{set} AS} \quad (4\text{-}10)$$

Where F = liquid: solid weight ratio at the feed interface
D = liquid: solid weight ratio for the underflow
W= F_{out}, product mass flow rate in tons/hour.
S=specific gravity of liquid in ton/cubic meter
R_S= settling rate in m/h
k_{set} = settling constant such that $1 \leq k_{set} \leq 2$; k_{set} =1 at the onset and $k_{set} \approx 2$ at steady state.

4.4. Model

The formation of the seeding particles, the growth and subsequent separation involves sequential, but alternate periods of suspension and sedimentation. This model considers the continuity and flow of particles as they go through from one phase to the other (Coltrin et al, 1991; Jone et al 2005 and Rivallin et al, 2005) and in two stages: the spinning disc and the CSTR.

4.4.1. The Spinning Disc Mixture Continuity

The seeding particle production rate from the spinning disc (depicted in Figure 4-3 below) is obtained by reducing the mixture continuity equation (4-11) using finite difference approximations and re-writing in terms of operating temperature, T; molar concentration of reactants and the spin, Ω in equation 4-12.

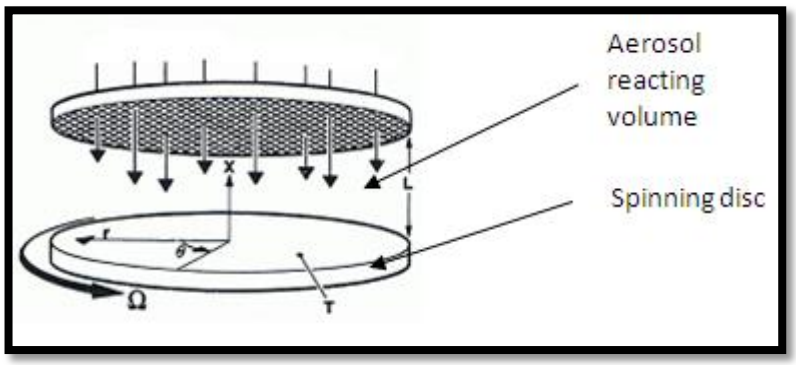

Figure 4-3: Schematic of the boundary layers across the spinning disc of the SDCST Reactor

$$\frac{1}{\rho}\frac{\partial \rho}{\partial t} = -\frac{\partial u}{\partial x} - 2\nu - \frac{u}{\rho}\frac{\partial \rho}{\partial x} \quad (4\text{-}11)$$

Where ρ = mass density (kg/m^3)
L = perpendicular distance between the inlet jet and the spinning disc
x = differential distance along L (m)
ν = scaled radial velocity, (1/s)
u = axial velocity (m/s)
t = particle residence time in the aqueous (sol) reacting volume (t)
By setting $u = MB/\rho$ and $\nu = \Omega$, where *B* = gas phase surface kinetic rate, multiplied by the surface area, the continuity equation yields equation (4-12) at steady state.

$$F_{T_iO_2} = \rho_{T_iO_2} \pi r^3 \left[C_{Ti_iCl_4} k_g \left(\Delta\bar{\rho} \left(\frac{M_{TiO_2}}{\rho^2_{TiO_2}} + \frac{M_{HCl}}{\rho^2_{HCl}} \right) + \left(\frac{M_{HCl}}{\rho_{HCl}} + \frac{M_{Ti_iCl_4}}{\rho_{Ti_iCl_4}} + \frac{M_{H2O}}{\rho_{H2OI}} \right) \right) + \frac{2\Omega\Delta x}{r} \right] \quad (4\text{-}12)$$

Δx is the stagnation height assumed to be not more than 1mm, $\Delta\bar{\rho}$ is the average density difference between the reactant and product species, and the gas kinetic rate (Pratsinis et al, 1990) kg, where kg = 8.26 x 104 exp (-10,681/T) (1/s)

4.4.2. The Continuous stir Tank

a) Overall Mass Balance

$$\frac{d(V_r \rho)}{dt} = F_{in} - F_{out} \quad (4\text{-}13)$$

where "F" denotes mass flow rate in kg/s; and V_r = Reactor Volume (m^3)

b) Specie Mass Balance

$$M_{TiO_2} V_r \frac{d\rho C_{TiO_2}}{dt} = M_{TiO_2} F_{in} C_{\underset{in}{TiO_2}} - M_{TiO_2} F_{out} C_{\underset{out}{TiO_2}} + \frac{k_s \; {}_r C_{TiCl_4}}{r_{TiCl_4}} \quad (4\text{-}14)$$

Where ks is the surface reaction rate constant for TiO_2 given by ks = 49 x exp (-8,993/T) [m/s] and rTiCl4 is the ionic radius for TiCl4.
At steady state, the specie mass balance equation yields

$$F_{\underset{out}{TiO_2}} = F_{\underset{in}{TiO_2}} + k_s \left(\frac{F_{TiCl_4} M_{TiO_2} - F_{TiO_2} M_{TiCl_4}}{M_{TiO_2} r_{TiCl_4}} \right) \quad (4\text{-}15)$$

c) Energy Balance

$$\rho C_p \frac{\partial T}{\partial t} = \frac{\partial}{\partial x}\left(\lambda \frac{\partial T}{\partial x}\right) - \rho C_p u \frac{\partial T}{\partial x} - \sum_1^i \left(C_{pi} \rho \gamma_i \forall_i \frac{\partial T}{\partial x} + k_g V_r C_{TiCl_4} \hbar_i \right) + Q \qquad (4\text{-}16)$$

Where λ = thermal conductivity (W/m.K)

C_p= specific heat (J/Kg.K)

Q = spatially distributed energy sink/source

$\hbar_i$ = specific molar enthalpy for i^{th} specie (J/mol)

$\forall_i$ =diffusion velocity of i^{th} specie (m/s)

γ_i = Mass fraction of i^{th} specie

T = operating temperature

C = inlet concentration of $TiCl_4$

At steady state operation, the overall energy difference (heat removed) between the feed and outlet streams is obtained in terms of primary nucleation (Spin disc) reaction temperature T1, feed inlet temperature T2, CSTR reaction temperature T0, the height difference between the spin disc and CSTR Δx', and height difference between feed inlet and spin disc surface Δx1 below:

$$Q = \left(\frac{T_1 - T_0}{\Delta x'}\right) \sum_1^i M_i C_{p_i} k_s C_{Ti_iCl_4} + \sum_1^i \left[C_{p_i} \rho \gamma_i \forall_i \left(\frac{T_1 - T_0}{\Delta x'}\right) + k_g C_{Ti_iCl_4} \hbar_i \right] - \sum_1^i \frac{2\lambda_i}{\Delta x'} \left[\left(\frac{T_2 - T_1}{\Delta x_1}\right) - \left(\frac{T_1 - T_0}{\Delta x'}\right) \right]$$

... (4-17)

It is immediately clear that Q = 0, for a system maintained at constant temperature. This will be of significant importance for large systems or systems operating with temperature gradients at different zones.

4.4.3. Residence Time

The residence time τ, required for the nucleated unit cell to grow by surface reaction to the required critical size is obtained from the surface reaction growth model (Pratsinis et al, 1998)

$$\tau = \frac{\left(\nu_{c,t} - \nu_0\right)}{2 k_s V_m N_a C_{TiCl_4}} \qquad (4\text{-}18)$$

Where N_a is Avogadro's number = 6.0221415 x 10^{23} /mol

and hence the feed mass flow rate (Fin = Fout) to achieve the required residence time for a given CSTR volume is obtained from

$$F_{in} = \frac{V_{cstr}}{\tau} \sum \rho_i \gamma_i \qquad (4\text{-}19)$$

4.5. Impeller Selection

Depending on application, impeller selection is imperative for proper mixing, cases keeping the particles in suspension and in this case impacting the particles walls with required shear stress to obtain desired size and range in the non-viscous aqua media to achieve crystal growth which occurs in two main steps: the first step is the diffusion-convection of the molecules to the crystal lattice and the second is the integration of the ions into the lattice (Mersmann 2001). With adequate agitation, the integration of both steps occurs rapidly and the crystal growth is determined by the diffusive-convective transport of units. This usually occurs when the mass flux density directed towards the crystal surface is low and is contingent on the volume of the diffusion species, on the viscosity of the solution and on the kinetic energy. **Error! Reference source not found.** shows a sketch of some of the main dependencies for diffusion controlled growth on the operating conditions.

There are four overlapping stages involved in the agitation provided by the impellers, they are

1) Particle induction/precipitation from solution
2) Surface wetting and growth
3) Size limitation by breaking of clusters (aggregates and agglomerates)

4) Forced settling

Stages 1 and 2 are essentially the chemical reaction and the subsequent growth discussed earlier in this chapter, while stages 3 and 4 are caused by the shear stress impacting on the particle boundaries and the centrifugal effect due to spinning in the media. However, since the expected total volume of particles formed in this process was relatively negligible compared to the volume of the aqua media leading to negligible change in viscosity from that of the media itself, the focus in this work was to appropriately select an impeller to deliver the required shear rate and to investigate the impact of the rate of agitation on particle size and distribution.

According to Devakumar (2008), who studied the design and presented comparisons for pitched, turbine and paddle impeller performances in multiphase reactors (Figure 4-4 to Figure 4-9), the paddle impeller offered the best performance at least cost at viscosity of ~0.89cP and 14rps maximum tip speed, low gas hold-up and energy consumption.

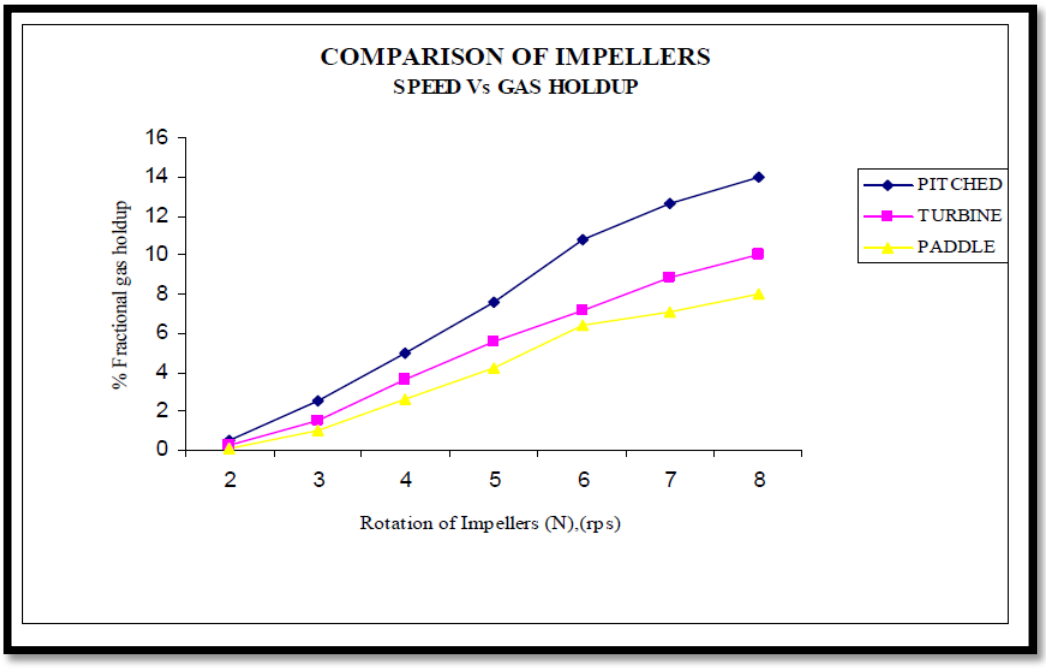

Figure 4-4: Comparison of Impellers: Speed Vs Gas Hold-up (Devakumar, 2008)

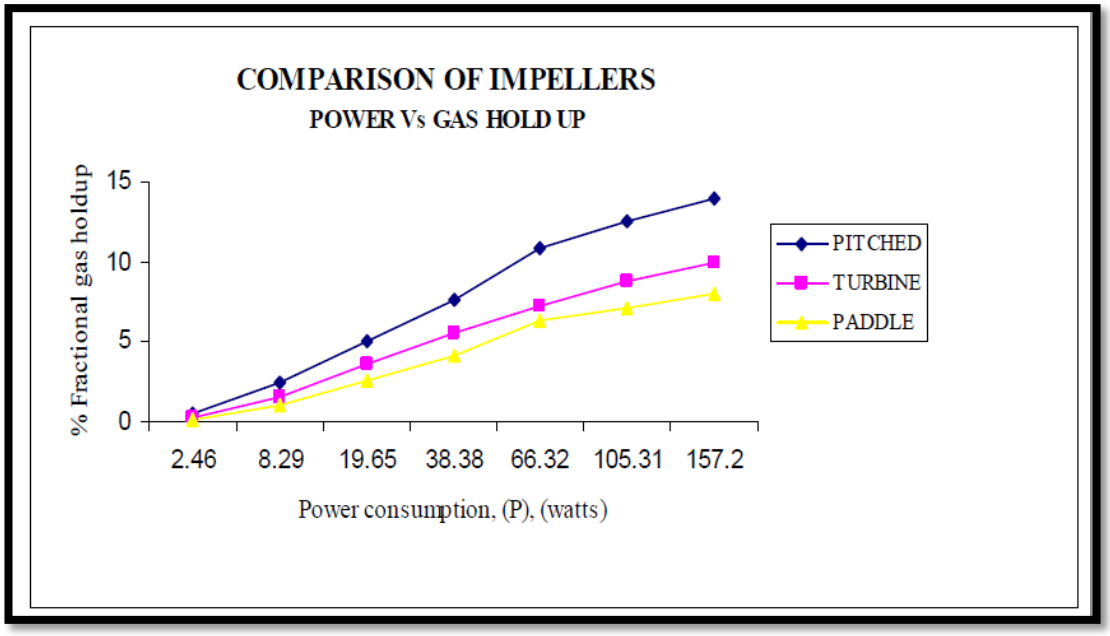

Figure 4-5: Comparison of Impellers: Power Vs Gas Hold-up (Devakumar, 2008)

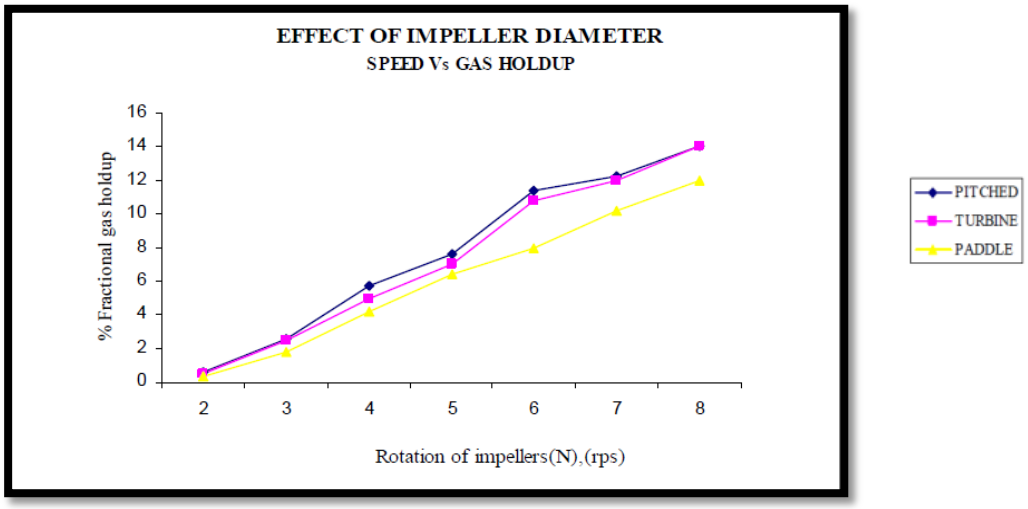

Figure 4-6: Effect of Impeller Diameters: Speed Vs Gas Hold-up (Devakumar, 2008)

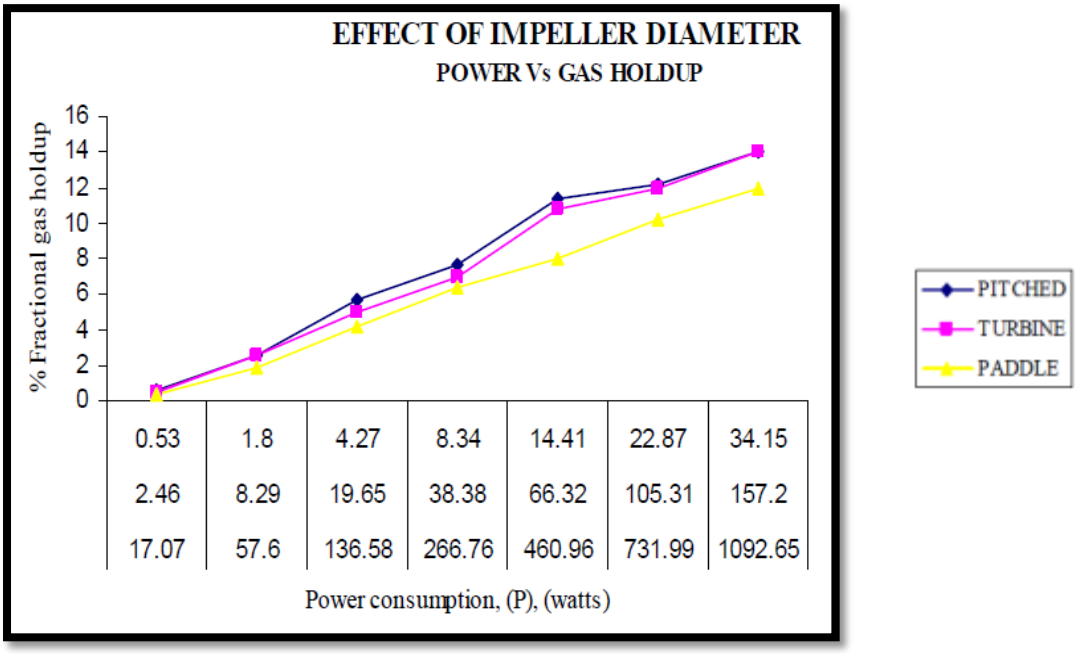

Figure 4-7: Effect of Impeller Diameters: Power Vs Gas Hold-up (Devakumar, 2008)

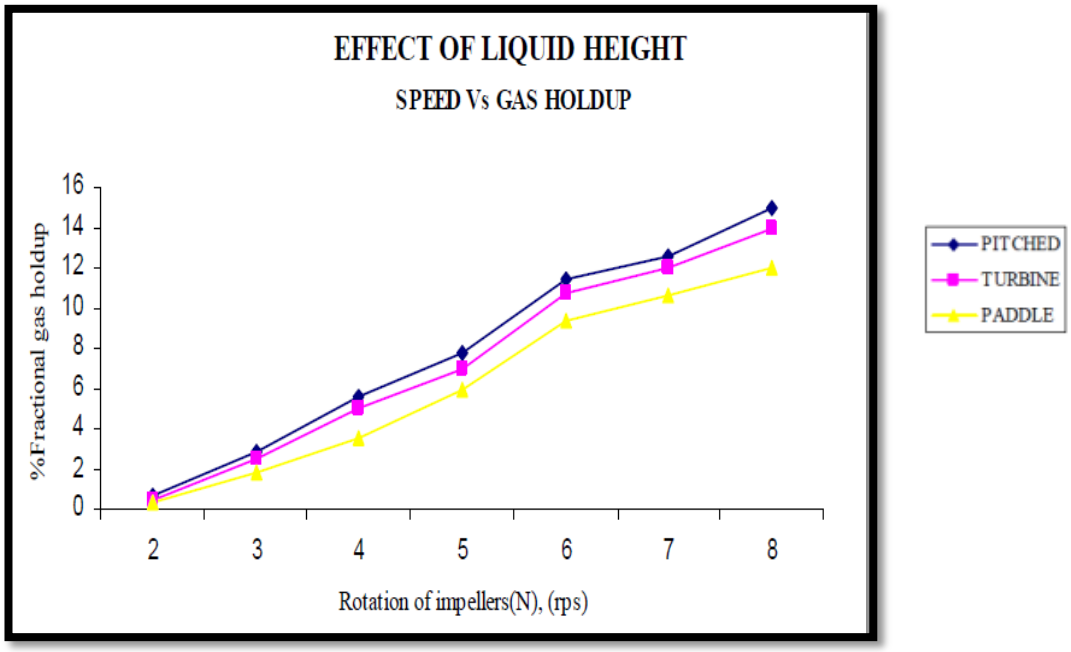

Figure 4-8: Effect of Liquid Height: Speed Vs Gas Hold-up (Devakumar, 2008)

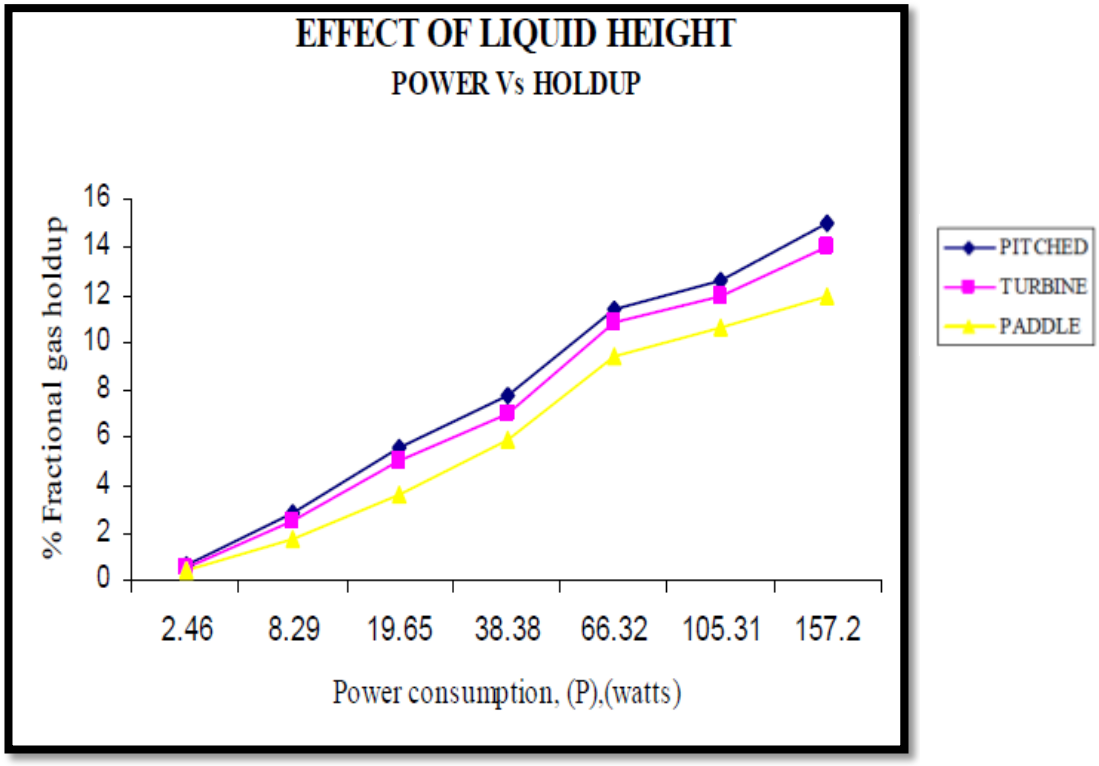

Figure 4-9: Effect of Liquid Height: Power Vs Gas Hold-up (Devakumar, 2008)

Following from the results (Figure 4-4 to Figure 4-9), a 2-blade paddle impeller with 5cm diameter being 1/3 of the tank diameter and inclined at 45° was adopted for the simulation and experiments with satisfactory results as presented in this thesis.

4.6. Inclusion of a Settler in the Continuous Stir Tank

To concentrate particles in the effluent stream, a settling volume, half the liquid height in the CSTR, was incorporated below the CSTR volume in a continuum. As particles fell out of suspension upon reaching the design critical size permitted by the shear stress which was impacted on them by the impeller spin, they are thrown tangentially downwards and towards the walls by the centrifugal force due to the spin.

Although yet to be theoretically proven, the momentary rest in the settling volume reverses the spin polarization and allows the particles not to re-agglomerate for a series of particles produced using this reactor. The same was also observed for the experimental single domain ferromagnetic nano-

composite (John et al, 2011) shown in Figure 4-10 that was also produced using this reactor.

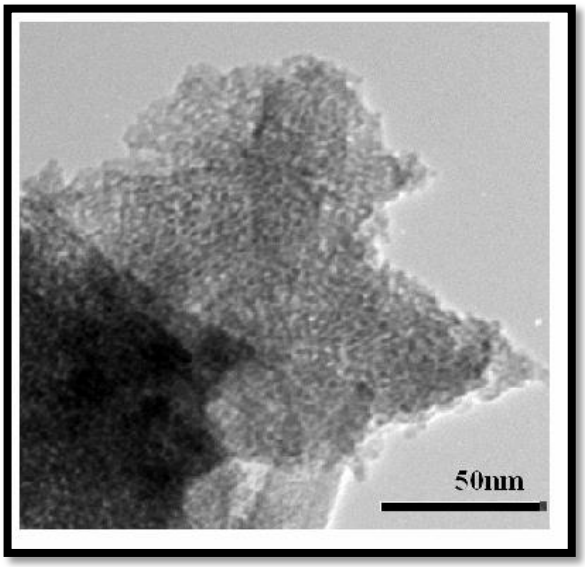

Figure 4-10: Ferromagnetic Nano-composite (John et al, 2011)

4.7. Advantages Over Existing Technologies

1) Compared to the Chemical Vapour Deposition (CVD) technology that operates at 900°C – 1100°C, this system operates between 25°C and 100°C depending on target characteristics of the desired nanoparticles. This is a significant saving of about 80% in energy requirements.
2) This system produces particles within controllable and predictable narrow size distribution unlike the wide particle distribution obtainable from using the SD or CSTR alone in the Sol-Gel process.
3) While other technologies require very high super-saturation levels, typically in 20 –1000 range, this novel system only requires a maximum of 8; hence preventing material wastages.
4) By increasing the degrees of freedom, this system achieves controllability for
5) Particle size
6) Particle size distribution
7) Polymorph selectivity
8) This system is suitable for the synthesis of temperature sensitive organic nanoparticles because the optimal operating temperature is

well below the temperatures required to denature most organic particles.

9) This device is suitable for both aqua and non-aqua flow processes; adequate for developing target oriented drug delivery nanoparticles.
10) The overall process time for this system is 0.859s compared to the more than 2s for Sol-Gel processes (typically followed by calcination) and more than 5min for CVD. This translates into a gross reduction in the total time required for products to reach the target market.

4.8. Results and Discussion

As shown in Chapter 3, a base case for Rutile with 0.6kmols/s (113.84kg/s) $TiCl_4$ with 34.233nm critical radius and 1.2mols/s (21.62kg/s) H_2O feed flow was used. At high temperatures, this reaction will occur spontaneously in nano-second time order to yield 0.6kmols/s (44.96kg/s) TiO_2, and will continue as long as the precursor, acting as limiting reactant, is available with water in excess; however, this model predicts 0.859s as the required residence time to achieve the highest permissible conversion for a supersaturation solubility of 6.9 at 319.27K (46.27 °C). Table 4-3 below show the results for some base case computations.

At the optimal temperature, increase in super-saturation decreases the population (number density) of particles within the desired size range and also increases the required residence time to achieve similar conversion; particle growth follows similar trend; while increases in precursor molar concentration requires more spin to achieve the required 16% conversion in the aerosol unit.

Table 4-3: Results for some Base case computations

Variable	**Result**
Optimal Operating Temperature (K)	319.27
Precursor Feed Flow (kg/s)	113.81
Super-saturation level (s) at operating T	6.9
Spin disc radius (m)	0.05
Primary production- spin disc (kg/s)	7.22
Required Residence time (s)	0.859
Particles Critical Size (nm)	34.23
Growth rate (m/s)	3.96×10^{-8}
Number density	7.033×10^{29}
Product mass flow rate (kg/s)	47.96

4.9. Conclusions

These results demonstrate the technical feasibility of continuously synthesizing TiO_2 nanoparticles at 46.27°C using a SDCSTR, representing a deviation from the energy intensive CVD and batch sol-gel processes. It also provides the opportunities for algorithms and software to be developed for simulations of a composite spinning-disc Continuous Stirred Tank Reactors; and provides a tool for predicting yield, residence time, and particle size distribution (population density), respectively as presented in Figures 3-10 to 3-14.

Chapter 5 : EXPERIMENTAL SYNTHESIS OF TITANIA

5.1 Introduction

Following from Chapters 3 and 4, the spinning disc continuous stirred-tank and settler reactor (SD-CSTRS) modelled for the synthesis of titanium dioxide using the major factors that affect the morphology; nucleation and growth rates as parameters. These major factors are temperature, molar concentration of titanium tetrachloride, $TiCl_4/H_2O$ molar ratio and the impeller speed in the CSTR. A pilot scale set-up was used to validate the simulation and model following successful laboratory bench experiments.

On one hand and using only the dominant process factors, the laboratory experiments were conducted to test between 30°C and 100°C with a 10°C step change (but including 47°C being the optimum temperature predicted by simulation) to establish and verify the optimum temperature for the process while varying $TiCl_4$ molar concentration by 0.5 step change between 0.5 and 2M. On the other hand, the pilot scale was used to validate the impact of the CSTR impeller speed on the particle size and distribution varying $TiCl_4$ molar concentration by 0.5 step change between 0.5 and 2M. Further, $H_2O/TiCl_4$ was varied with step changes of 2 between 2 and 6.

5.2 Experimental Validation and Characterization

5.2.1 Laboratory Scale set up

5.2.1.1 Preparation of Reactant and Safety Considerations

Titanium tetrachloride is extremely reactive with water and exothermic, especially at high concentrations and temperatures. 5M $TiCl_4$ concentrated solution from Sigma and ultra-pure de-ionized water that had been cooled down to 5°C in separate water baths were used as stocks for preparing the required molar concentrations for the experiments at 0.5M, 1M and 2M solutions.

All dilutions, preparations, storage and experiments were conducted in the fume cupboard in accordance with AS1940: The Storage and Handling of

Flammable and Combustible Liquids and AS2243.10: Guideline for the Safe storage of Chemicals.

5.2.1.2 Running the Experiment

For each $TiCl_4$ molar concentration evaluated, 25ml of stock solution was heated to 30^oC in a hot water bath and added to 50ml of ultra-pure doubly deionized water brought to 30°C on a hotplate; and the mixture was stirred for approximately 5 minutes with a magnetic stirrer. The products were held for 20min at the reaction temperature, then cooled and transferred for storage in a sample bottle.

The procedure was repeated at specified temperatures between 30°C and 100°C with a 10°C step change but including 47°C and $TiCl_4$ molar concentration between 0.5 step changes between 0.5 and 2M.

5.2.2 Result and Discussion

Figure 5-1 below shows an image of the samples produced from the laboratory experiments. All of the samples were visually examined and some were randomly selected for further analyses as presented on Table 5-1 below using the X-Ray Diffraction (XRD) and Zeiss Neon 40EsB FESEM-- (Field Emission Scattering Electron Microscope).

Figure 5-1: Images of laboratory samples produced

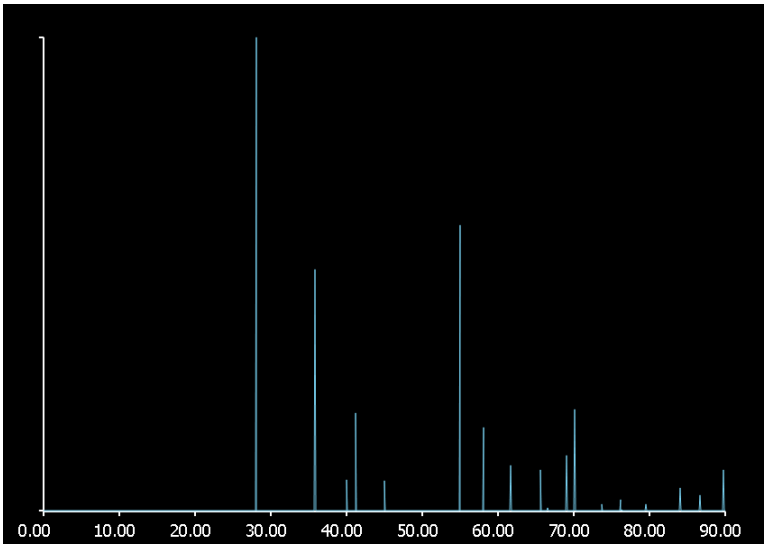

Figure 5-2: Theoretical 2 theta (degree) XRD image for TiO_2

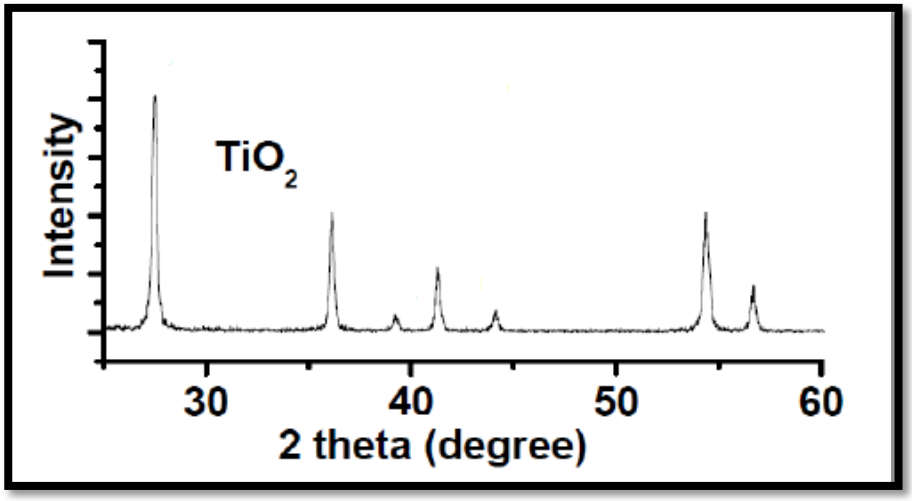

Figure 5-3: Experimental 2 theta (degree) XRD image for TiO2

The particles were confirmed to be TiO_2 using experimental XRD compared to theoretical diffraction spectrum obtained from GULP (Gale 2007). As seen the main 2-theta (degree) peaks occurred at similar locations for both the experimental and theoretical spectra at about 27°, 37°, 42° and 54°.

Zeiss Neon 40EsB FESEM was thereafter used to establish modal particle sizes as shown in Figures 5-4 to 5-6 below.

Figure 5-4: (a) - Rutile Nanoparticles with 83nm Modal Critical Particle (Sample 7); (b)- Rutile Nanoparticles with 117nm (sample 3)

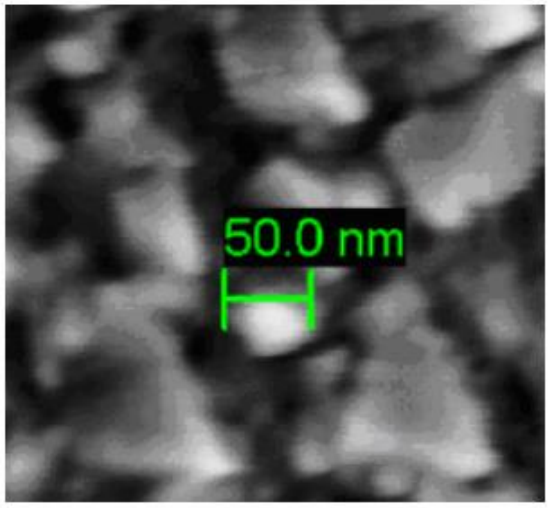

Figure 5-5: Rutile Nanoparticles with 50nm Modal Critical Particle Size with 1.29 standard deviation (Sample 8)

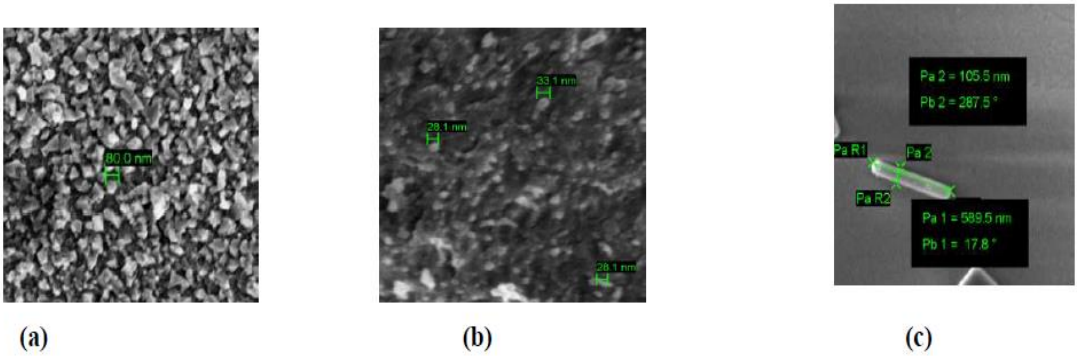

Figure 5-6: (a) Rutile Nanoparticles with 80nm Modal Critical Particle Size (sample 4); (b) Meso-Porous Rutile Nanoparticles with 28nm Modal Critical Particle Size (sample 2); and (c) Rutile Nano-tubes (sample 12)

Table 5-1: Summary of results for the randomly selected Laboratory samples

S/ No	*CSTR Impeller Speed (rpm)*	*Molarity of $TiCl_4$*	*Reaction Temperature (°C)*	*Molar Ratio ($TiCl_4/H_2O$)*	*Observation*
3	500	2.0	80	6	Crystalline formation with narrow PSD and 117nm mode
7	500	0.5	47	2	Crystalline formation with narrow PSD and 83nm mode
2	900	1.0	60	6	Meso-porous formation with narrow PSD and 28nm mode
4	900	2.0	80	6	Crystalline formation with narrow PSD and 80nm mode
8	900	0.5	47	2	Crystalline formation with narrow PSD and 50nm mode
12	900	0.5	40	2	Tubular with narrow size distribution

5.2.3 Conclusion

Figure 5-1 to Figure 5-6 and Table 5-1 above showed that TiO_2 nanoparticles were successfully produced at the set conditions with unique sizes and morphologies which provided the required impetus for a larger scale production to examine the impact of spin and impeller speed on size distribution using the 47°C to 55°C reaction temperature cases. This temperature range was chosen based on the optimal conditions predicted by the simulation and laboratory results considering the possible additional breaking-up impact of spin and high turbulence on tubular nanoparticles which may lead to biased conclusions.

5.3 Pilot Scale

5.3.1 Preparation of Reactants

As with the Laboratory experiments, 5M $TiCl_4$ concentrated solution from Sigma and ultra-pure de-ionized water that had been cooled down to 5°C in separate water baths were used as stocks for preparing the required molar concentrations for the experiments. All dilutions, preparations, storage and experiments were conducted in the fume cupboard in accordance with

AS1940: The Storage and Handling of Flammable and Combustible Liquids and AS2243.10: Guideline for the Safe storage of Chemicals.

5.3.2 Running the Experiment

For the first run, 500ml of de-ionized water was heated to 47 °C to fill the CSTR so that the impeller was submerged. The reactants, 100mL of the titanium (IV) solution and 200mL of de-ionized water were from the stocks were also heated in separate beakers in a hot water bath to a temperature of 47 ^{o} C and then pumped using peristaltic (hose) pump into the RD-CSTR. The products were then transferred to a 2L storage container where the contents were allowed to settle, decanted, sampled and stored. The procedure was repeated for the specified temperatures, and impeller speeds using the RD and CSTR separately for comparison.

5.3.3 Safety Consideration

Same as for the laboratory experiments, Titanium tetrachloride is extremely reactive with water and exothermic, especially at high concentrations and temperatures. 5M $TiCl_4$ concentrated solution from Sigma and ultra-pure de-ionized water that had been cooled down to 5°C in separate water baths were used as stocks for preparing the required molar concentrations for the experiments at 0.5M, 1M and 2M solutions.

All dilutions, preparations, storage and experiments were conducted in the fume cupboard in accordance with AS1940: The Storage and Handling of Flammable and Combustible Liquids and AS2243.10: Guideline for the Safe storage of Chemicals.

5.3.4 Test Runs

Using only the dominant influencing factors, 87 runs were conducted as per Tables 5-2 and 5-3 below.

Table 5-2 Variables to be manipulated

Factors	Range	No. of Steps	Cumulative Total
Temperature: Δ5˚C	47 – 55˚	3	3
Molar Ratio: Δ0.5M	0.5 – 2M	3	9
Impeller Speed: Δ200rpm	300 – 900rpm	4	36

Δ indicates step change used.

Table 5-3: Total number of runs

A.	**RD:**	9 experiments
B.	**CTSR:**	36 experiments
C.	**RD-CSTRS:**	36 experiments
D.	**Larger scale experiments of select samples:**	6 experiments
Total number of experiments:		**87 experiments**

5.3.5 Process Flow Diagrams

Figures 5-7 and 5-8 below present the image and schematic of the coupled pilot set up respectively, while Figures 5-9 and 5-10 show the spinning disc and CSTR decoupled.

In Figures 5-7 and 5-8, the reactants are pumped through silicon tubes into the spinning disc reactor using two separate peristaltic pumps with 20-600l/min operating range. The inlet of the ultra-pure de-ionized, been reactant in excess, was perpendicular to the flow of $TiCl_4$ been the limiting reagent. The products and un-reacted reagents were discharged via a 10cm stainless steel tube into the CSTR equipped with a paddle impeller and

settling region. Final products were withdrawn from the base of the couples rig.

In Figure 5-9, the spinning disc was de-coupled with products withdrawn directly from the stainless steel pipe, while in Figure 5-10 reagents were injected directly into the CSTR.

Figure 5-7: Image of the coupled pilot scale set up

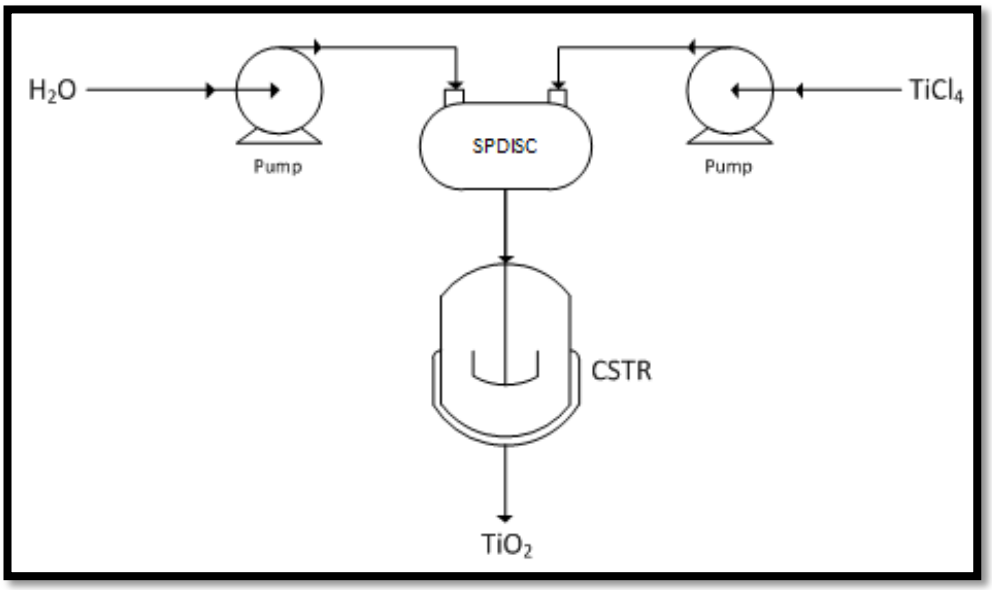

Figure 5-8: Schematic of the coupled pilot scale set up

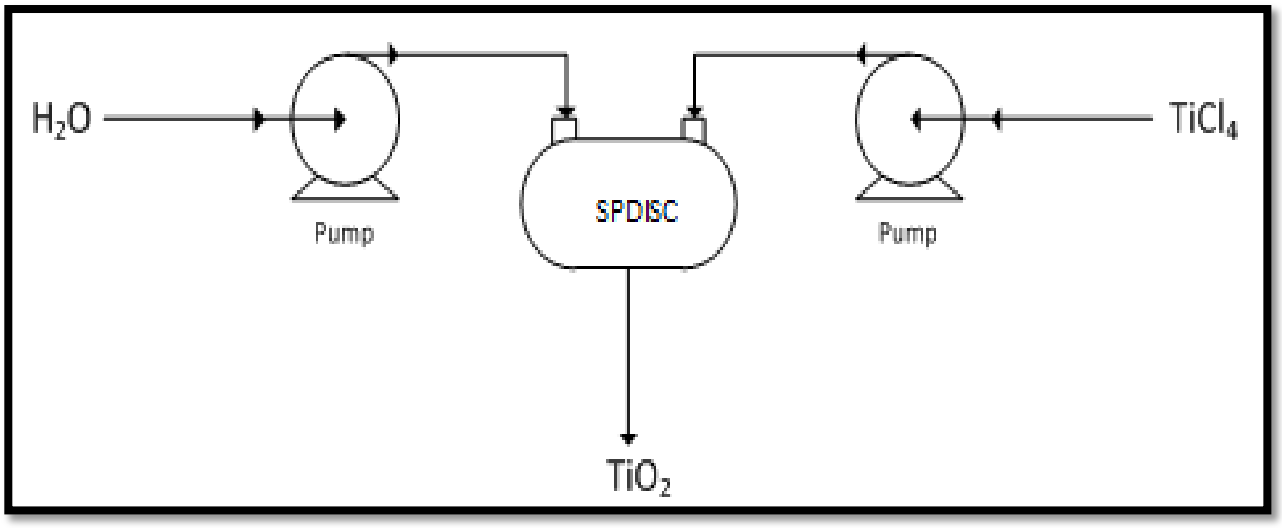

Figure 5-9 Process flow diagram of the SD reactor alone

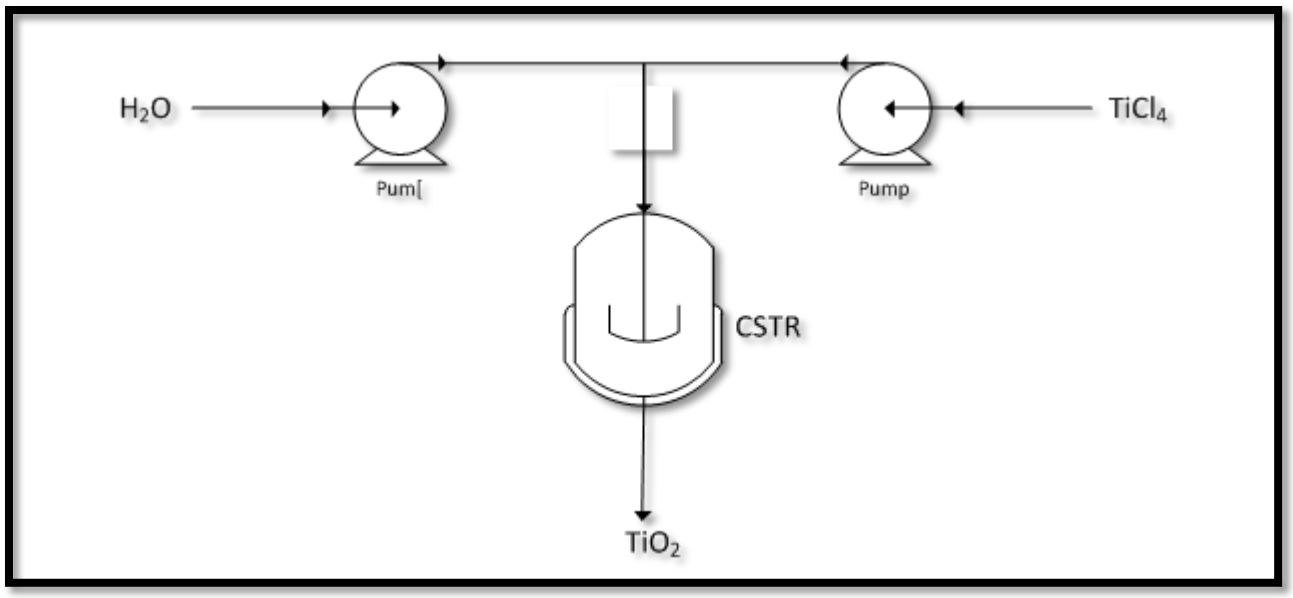

Figure 5-10 Process flow diagram of the CSTR alone

5.3.6 Results

Upon completing the test runs, samples were taken and analyzed using the "Malvern Zetasizer (DS Nanoseries)" to obtain size distribution by intensity. The Malvern Zetasizer uses light scattering intensity which is extremely sensitive to the presence of small amounts of aggregates as a function of the molecular weight and concentration to give information on the size and mass

of samples. The numerical results obtained are presented in Tables 5-4 to 5-7 below while the charts are presented in the next section.

Table 5-4: Experimental Data showing the peak size of the particles, 100ml $TiCl_4$: 200ml H_2O

Reactor Type	Temperature (C)	Concentration (M)	Speed (rpm)	Sample Name	Size (nm)		
					Peak 1	Peak 2	Peak 3
SD	47	0.5	-	A1	445		
		1	-	A2	464	50.5	5560
		2	-	A3	156	0.726	2.75
	50	0.5	-	A4	239	47	
		1	-	A5	46.6	302	4970
		2	-	A6	462	5390	0.647
	55	0.5	-	A7	71.3	318	19.8
		1	-	A8	331		
		2	-	A9	221	0.895	5210
CSTR	47	0.5	300	B1	336	5310	0.674
		0.5	500	B2	729	5020	
		0.5	700	B3	359	5450	
		0.5	900	B4	421		
		1	300	B5	278	4540	0.677
		1	500	B6	332	0.869	5180
		1	700	B7	164	4980	0.753
		1	900	B8	629	5410	
		2	300	B9	335		
		2	500	B10	337		
		2	700	B11	204		
		2	900	B12	301		
	50	0.5	300	B13	89.2	0.711	2.5
		0.5	500	B14	162		
		0.5	700	B15	554	5240	
		0.5	900	B16	339	0.67	5560
		1	300	B17	357	3.19	
		1	500	B18	211		
		1	700	B19	512		
		1	900	B20	528		
		2	300	B21	563		
		2	500	B22	282	0.68	
		2	700	B23	329	2.18	
		2	900	B24	539	11.9	
	55	0.5	300	B25	477		
		0.5	500	B26	358		
		0.5	700	B27	467	1.42	
		0.5	900	B28	332	0.675	12.7

Table 5-5: Experimental Data showing the peak size of the particles, 100ml $TiCl_4$: 200ml H_2O

Reactor Type	Temperature (C)	Concentration (M)	Speed (rpm)	Sample Name	Size (nm)		
					Peak 1	Peak 2	Peak 3
CSTR	55	1	300	B29	621	0.966	
		1	500	B30	426		
		1	700	B31	589		
		1	900	B32	122	1.47	
		2	300	B33	126	0.978	
		2	500	B34	66.6	1.12	
		2	700	B35	483	0.925	
		2	900	B36	64.4	1.27	
SD-CSTRS	47	0.5	300	C1	257		
		0.5	500	C2	195	20.2	5560
		0.5	700	C3	397		
		0.5	900	C4	176	13.5	
		1	300	C5	338		
		1	500	C6	314	65.8	
		1	700	C7	161	16.4	
		1	900	C8	147		
		2	300	C9	75.6	0.647	
		2	500	C10	291		
		2	700	C11	240		
		2	900	C12	191		
	50	0.5	300	C13	226		
		0.5	500	C14	174		
		0.5	700	C15	224	34.9	
		0.5	900	C16	187		
		1	300	C17	163	47.7	0.681
		1	500	C18	281	79	
		1	700	C19	327	65.5	
		1	900	C20	469	5210	79.5
		2	300	C21	409		
		2	500	C22	330	48.5	
		2	700	C23	296		
		2	900	C24	299	1.25	53.2
	55	0.5	300	C25	175	42.3	
		0.5	500	C26	374	97.7	5110
		0.5	700	C27	294	54.2	5560
		0.5	900	C28	419	85.6	
		1	300	C29	220	43.9	
		1	500	C30	207	5200	
		1	700	C31	350	5280	55.4
		1	900	C32	163		

Table 5-6: Experimental Data showing the peak size of the particles, 100ml $TiCl_4$: 200ml H_2O

Reactor Type	Temperature (C)	Concentration (M)	Speed (rpm)	Sample Name	Size (nm)		
					Peak 1	Peak 2	Peak 3
SD-CSTRS	55	2	300	C33	109		
		2	500	C34	98.5		
		2	700	C35	195		
		2	900	C36	111		

Table 5-7: Experimental Data showing the peak size of the particles, 750ml $TiCl_4$: 1500ml H_2O

Reactor Type	Temperature (C)	Concentration (M)	Speed (rpm)	Sample Name	Size (nm)		
					Peak 1	Peak 2	Peak 3
SD	47	0.5	-	D1	135	22.5	
		1	-	D2	383	55.4	
CSTR		0.5	500	D3	273		
		1	500	D4	411		
SD-CSTR		0.5	500	D5	174	28.3	
		1	500	D6	540	89.4	

Some samples showed single peaks indicating mono-modal particles, while others had multiple peaks indicating samples with multiple modal size range as presented on the charts.

5.3.7 Distribution comparison between similar variables

To obtain definitive conclusions, the results for similar variables using the coupled system SDCSTR, SD alone and CSTR alone were compared as presented in Figures 5-11 to 5-23.

Figure 5-11 shows the comparison between SD-CSTRS and CSTR at 0.5M, 300rpm and temperature of 47℃. At these conditions only the SD-CSTRS had a single peak for size distribution with a narrower distribution while the CSTR had multi-peaks and wider distributions.

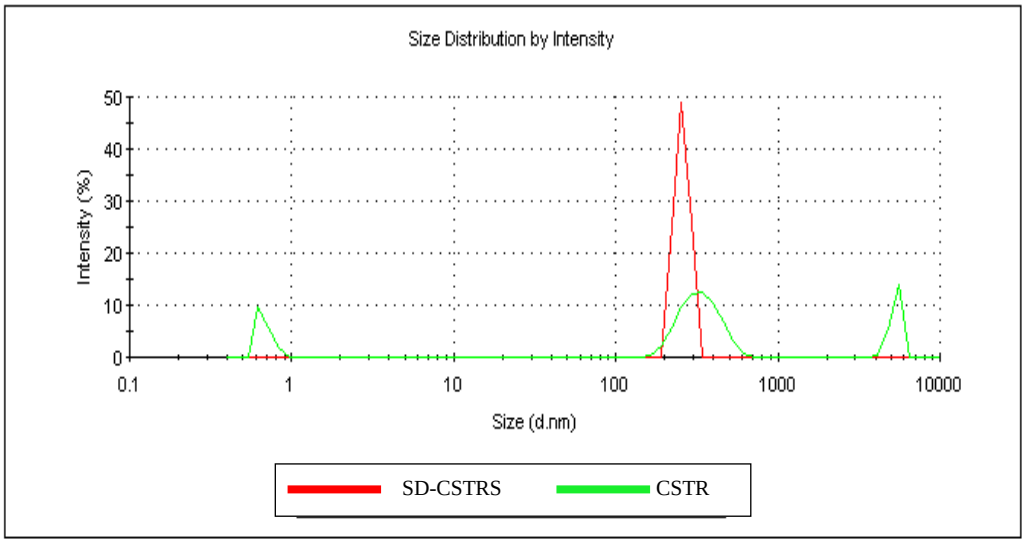

Figure 5-11: Comparison between SD-CSTRS and CSTR at 0.5M, 300rpm and 47 ℃.

Also, the CSTR at 0.5M, 700rpm and 47℃ in Figure 5-12 had two peaks size distribution while SD-CSTRS had a single peak with narrower distribution. For Figure 5-13, SD-CSTR operated at 0.5M, 900rpm and 47℃ had a main peak and narrower distribution compared to the CSTR alone. This trend is consistent all through to Figure 5-23 for all the other operating conditions.

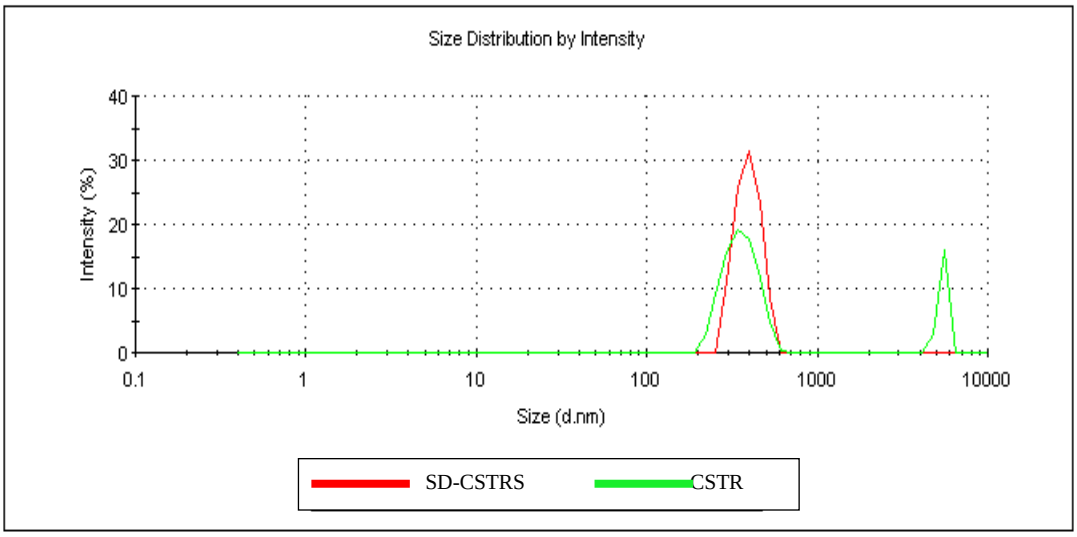

Figure 5-12: Comparison between SD-CSTRS and CSTR at 0.5M, 700rpm and 47℃.

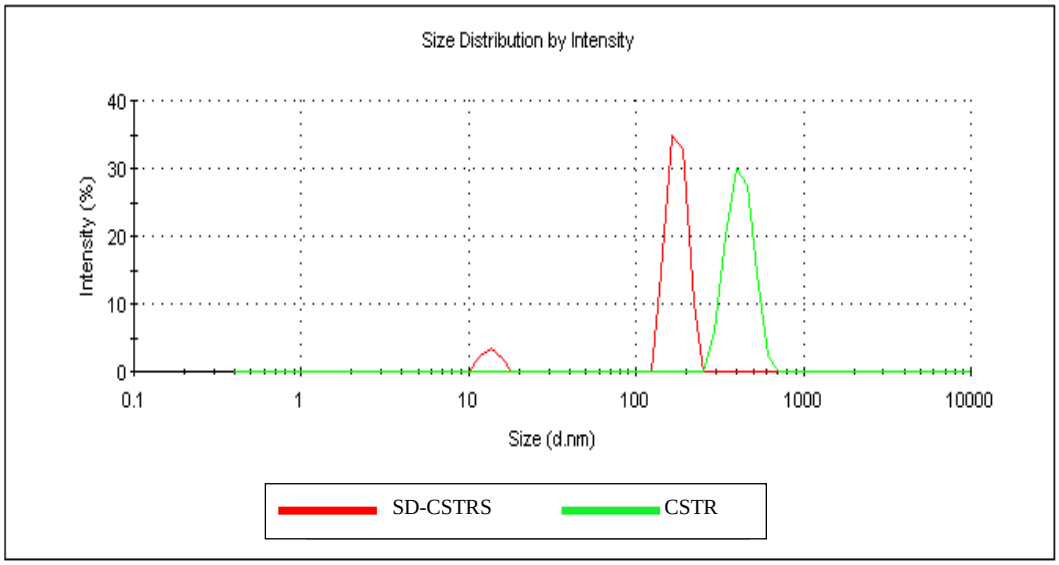

Figure 5-13: Comparison between SD-CSTRS and CSTR at 0.5M, 900rpm and 47 ℃.

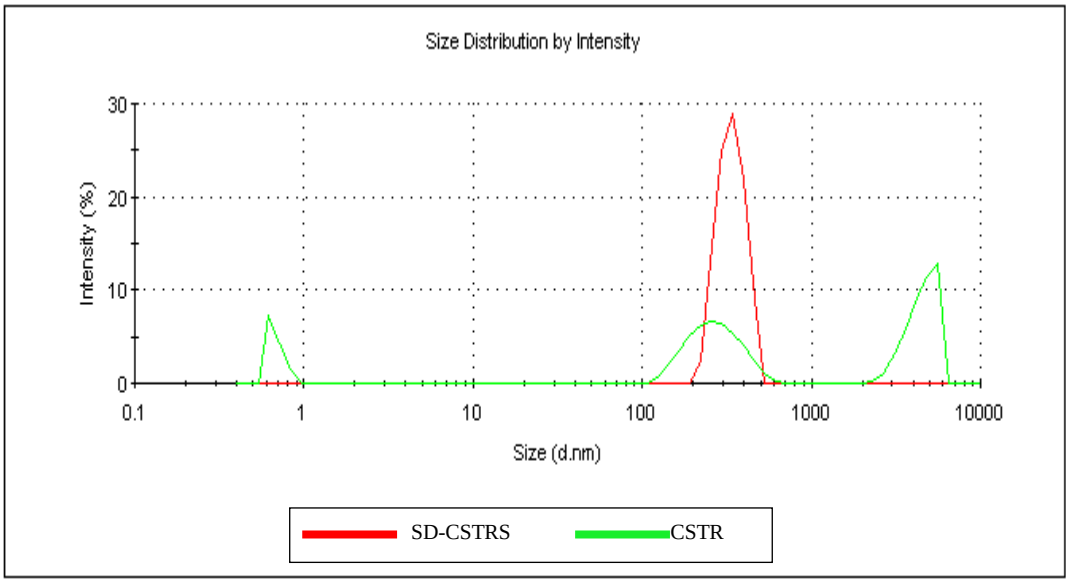

Figure 5-14: Comparison between SD-CSTRS and CSTR at 1M, 300rpm and 47 ℃.

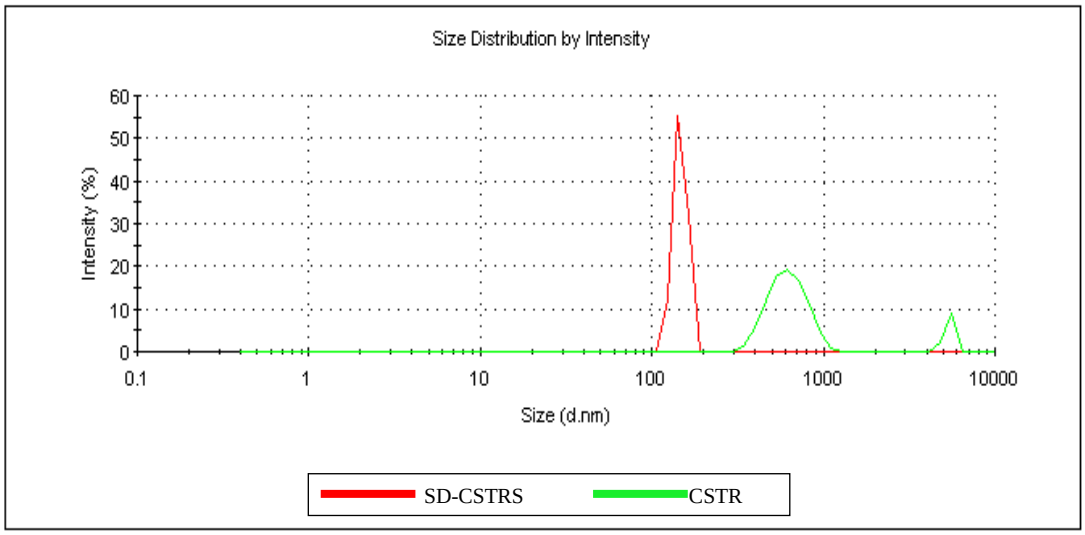

Figure 5-15: Comparison between SD-CSTRS and CSTR at 1M, 900rpm and 47 ℃.

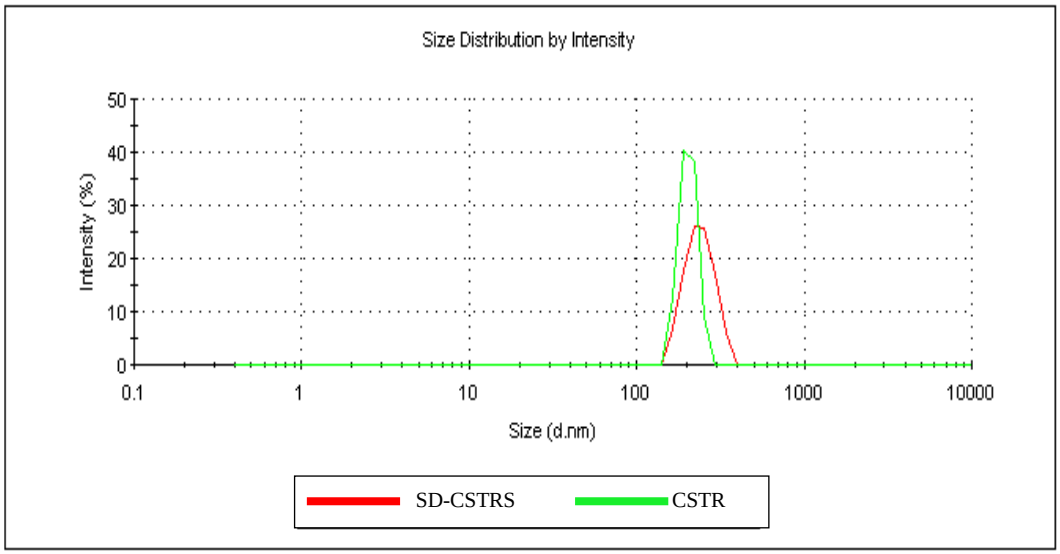

Figure 5-16: Comparison between SD-CSTRS and CSTR at 2M, 700rpm and 47 ℃.

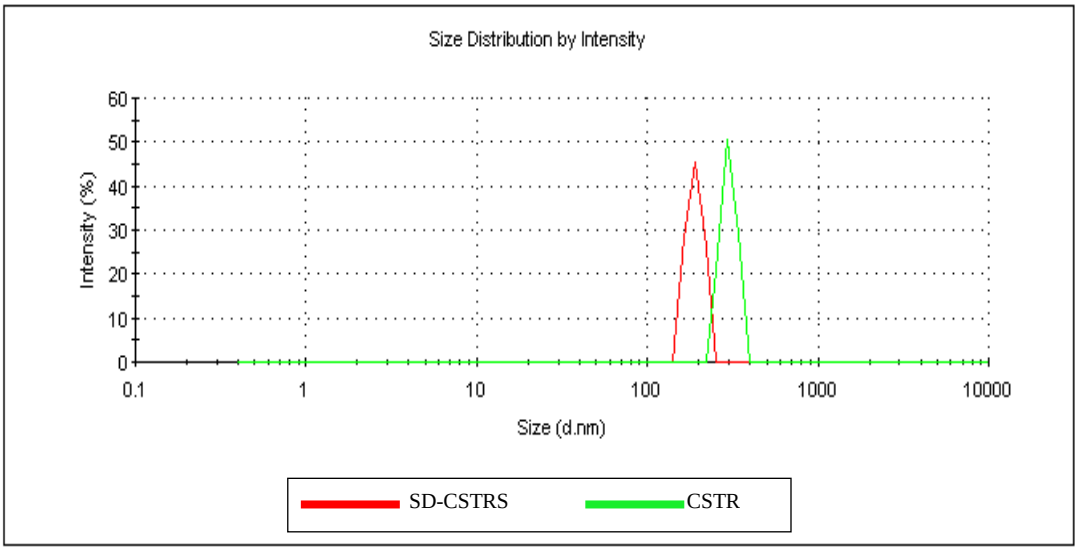

Figure 5-17: Comparison between SD-CSTRS and CSTR at 2M, 900rpm and 47 ℃.

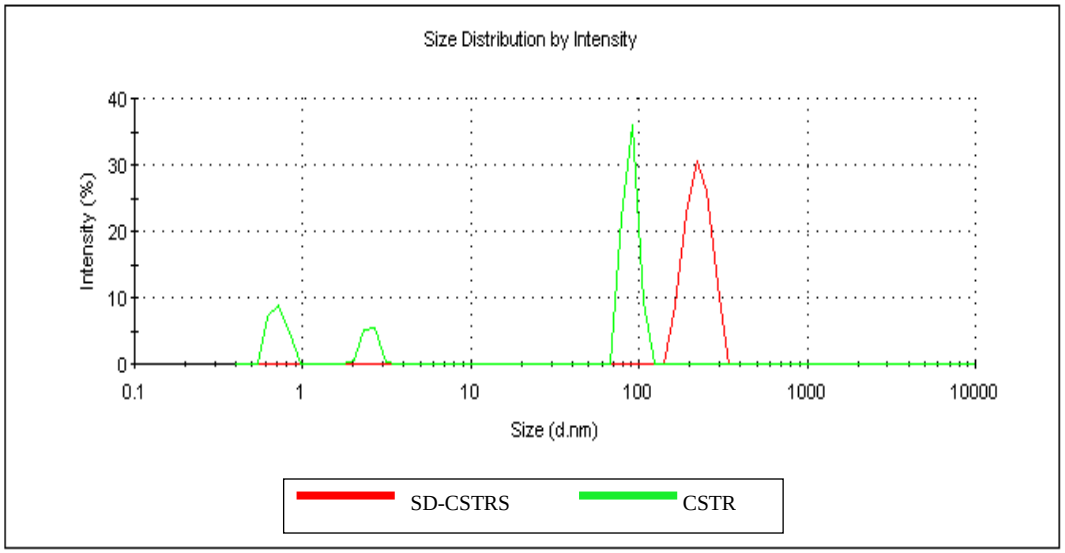

Figure 5-18: Comparison between SD-CSTRS and CSTR at 0.5M, 300rpm and 50℃.

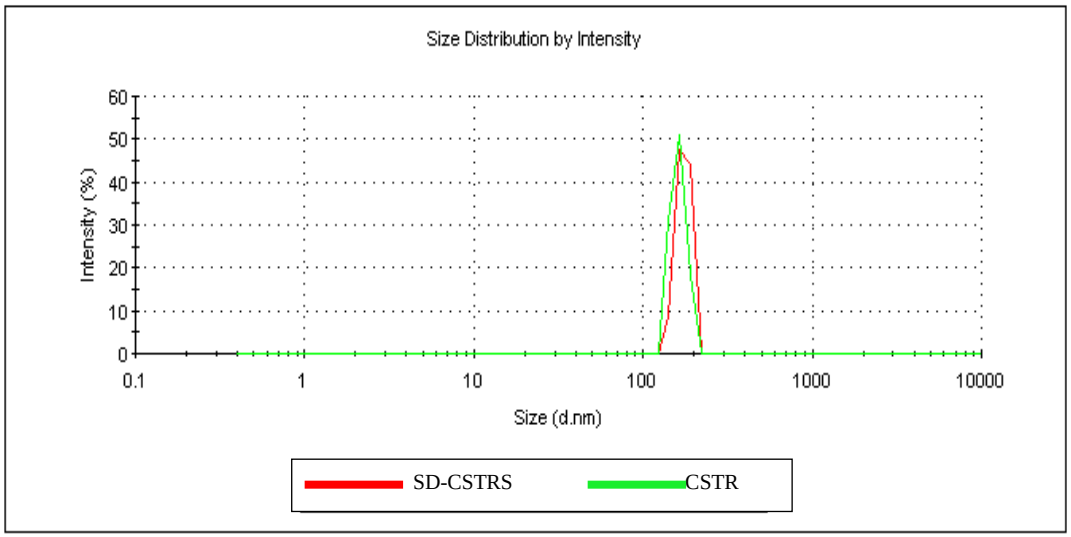

Figure 5-19: Comparison between SD-CSTRS and CSTR at 0.5M, 500rpm and 50 ℃.

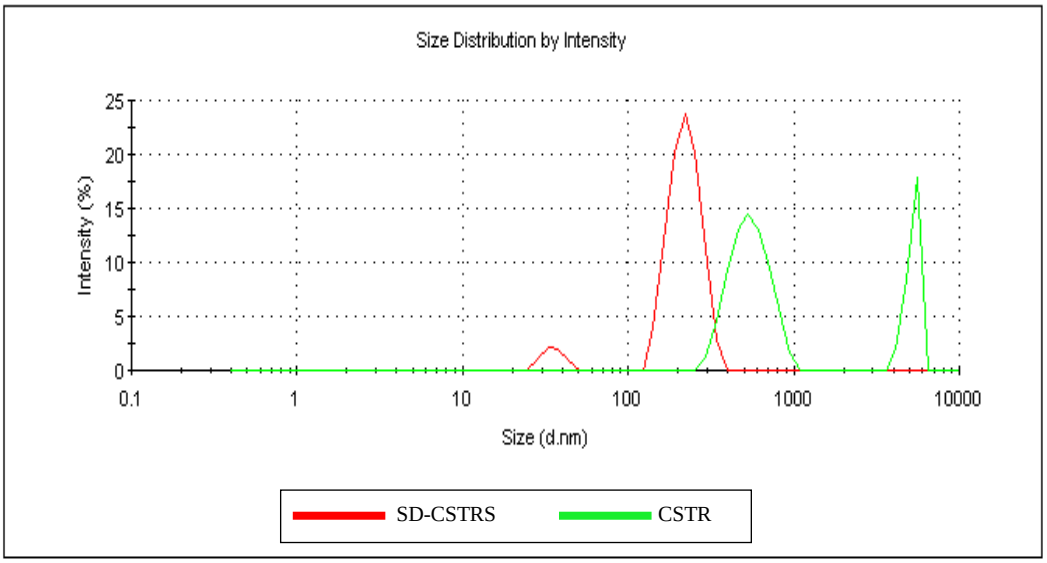

Figure 5-20: Comparison between SD-CSTRS and CSTR at 0.5M, 700rpm and 50 ℃.

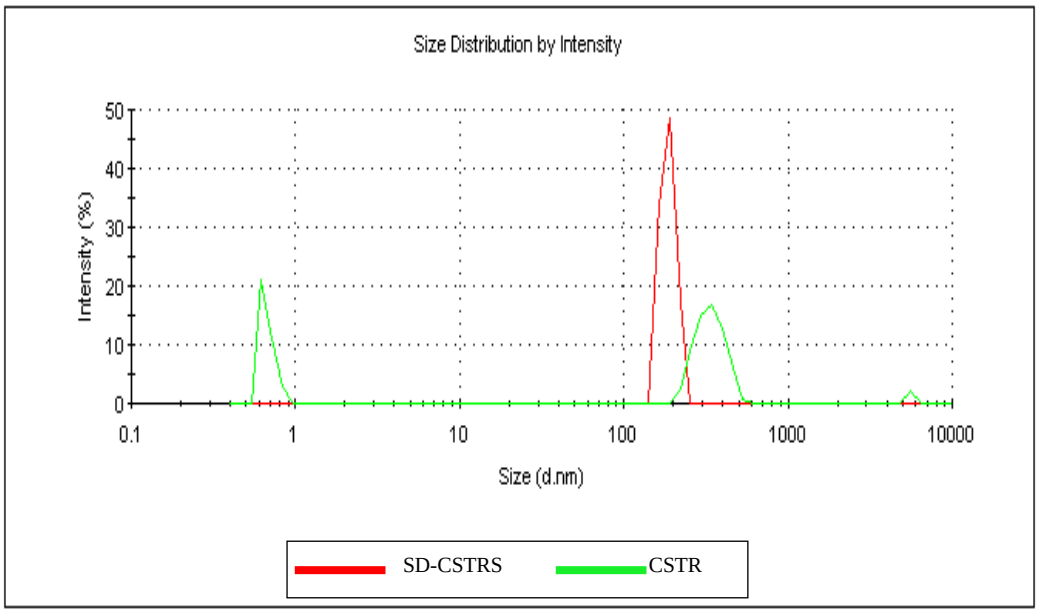

Figure 5-21: Comparison between SD-CSTRS and CSTR at 0.5M, 900rpm and 50 ℃.

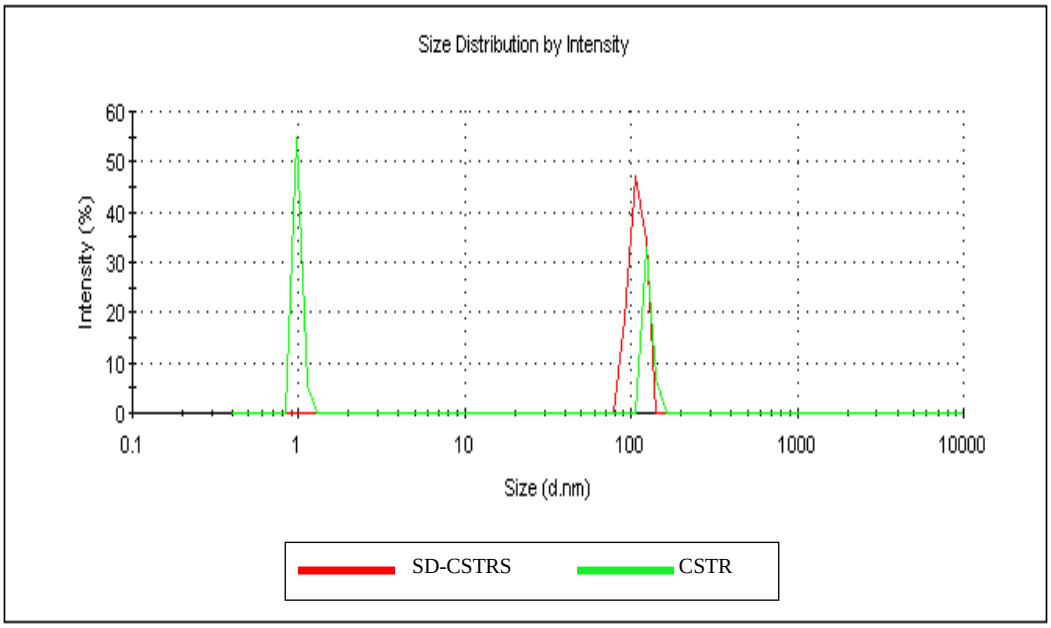

Figure 5-22: Comparison between SD-CSTRS and CSTR at 2M, 300rpm and 55 ℃.

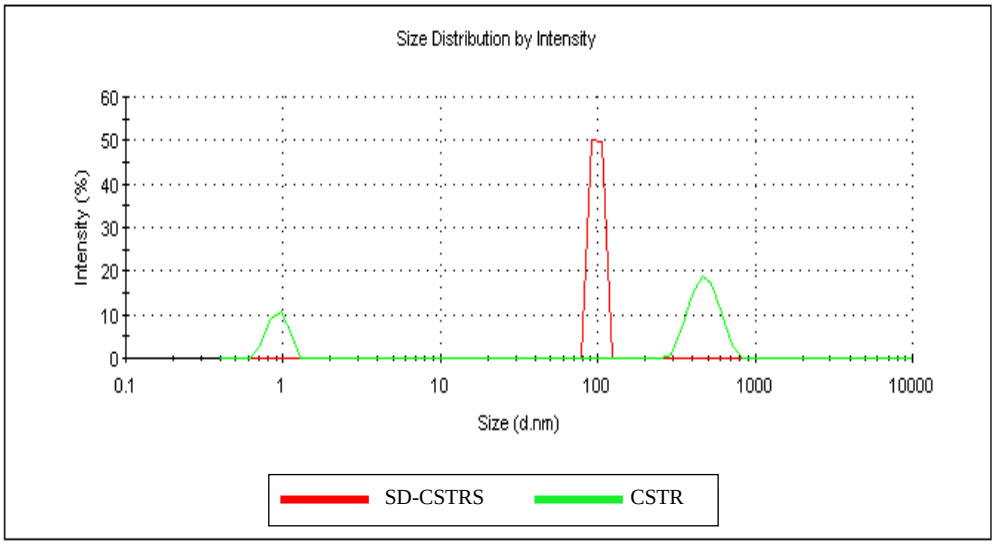

Figure 5-23: Comparison between SD-CSTRS and CSTR at 2M, 500rpm and 55 ℃.

5.4 Discussion

5.4.1 Overall Size Distribution

The titanium dioxide crystals synthesized using the Spinning-Disc reactor (SD) only had a wide size distribution. As shown in Figure 5-24, the size distribution of the main peaks for all 9 samples on SD only ranged from 15nm to 900nm with wide spread individual peaks. The low intensity and wide distribution suggest that it is difficult to predict or control particle size distribution using SD alone.

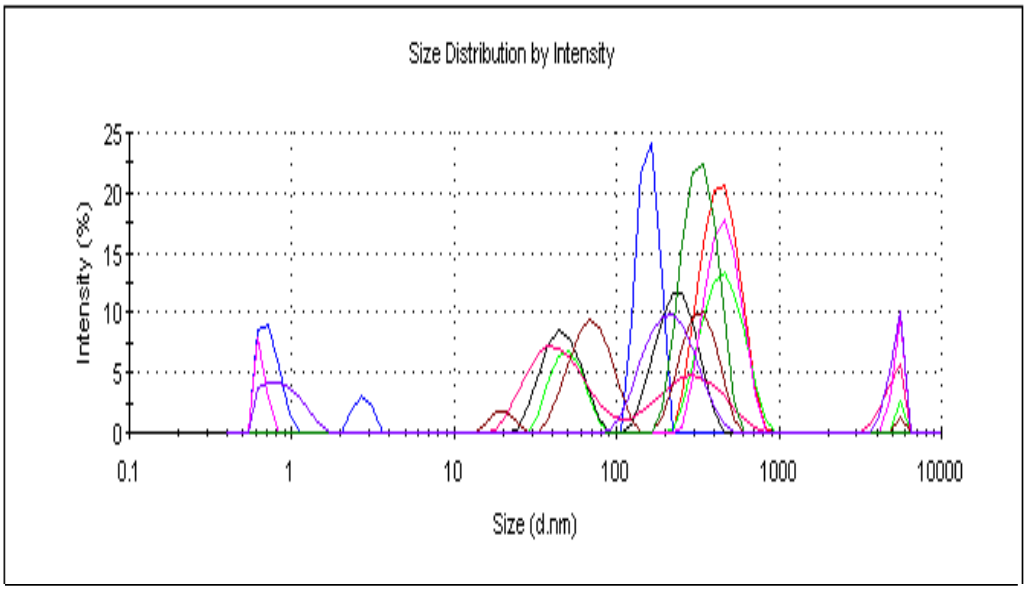

Figure 5-24: Size distribution of all the SD experiments

The results from the 36 runs on the Continuous Stirred-Tank Reactor (CSTR) alone presented in Figure 5-25 shows multi-peaks with main size distribution ranging from 40nm to 1500nm; and two other peaks at 0.9nm and 5000nm. The two other peaks were considered as anomalies caused by dust for example, or agglomerates of foreign particles and can be ignored for this comparison. The high intensity and wide distribution suggest relative ease for control and predictability compared to the SD alone.

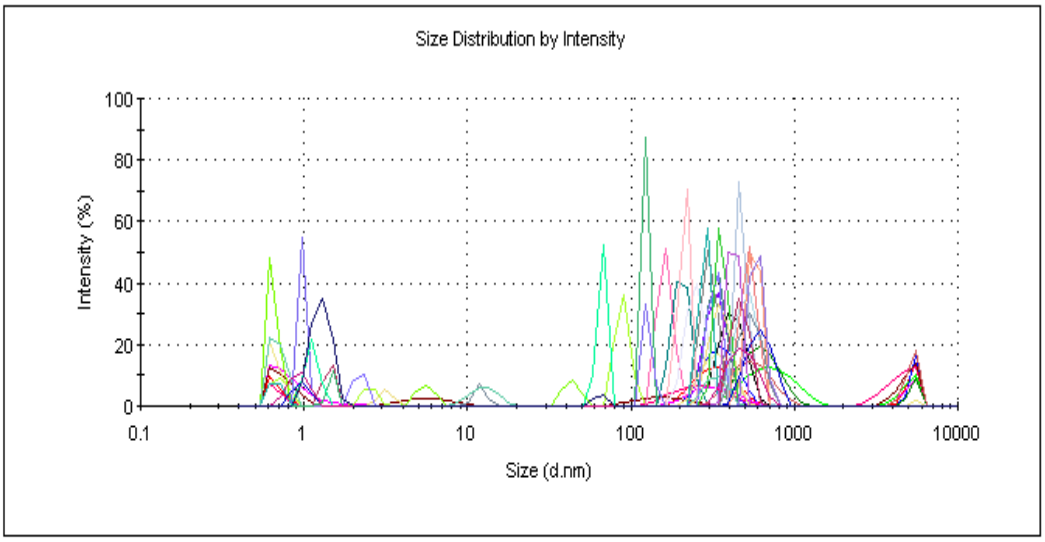

Figure 5-25: Size distribution of all the CSTR experiments

Figure 5-26 shows the experimental results from 36 runs of the Rotating-Disc Continuous Stirred-Tank Reactor and Settler (SD-CSTRS). With the narrowest range and high intensity reading, this graph suggests that predictability is best achievable with the SD-CSTRS. The main conglomeration of size distribution peaks are in the range of 60nm to 1000nm.

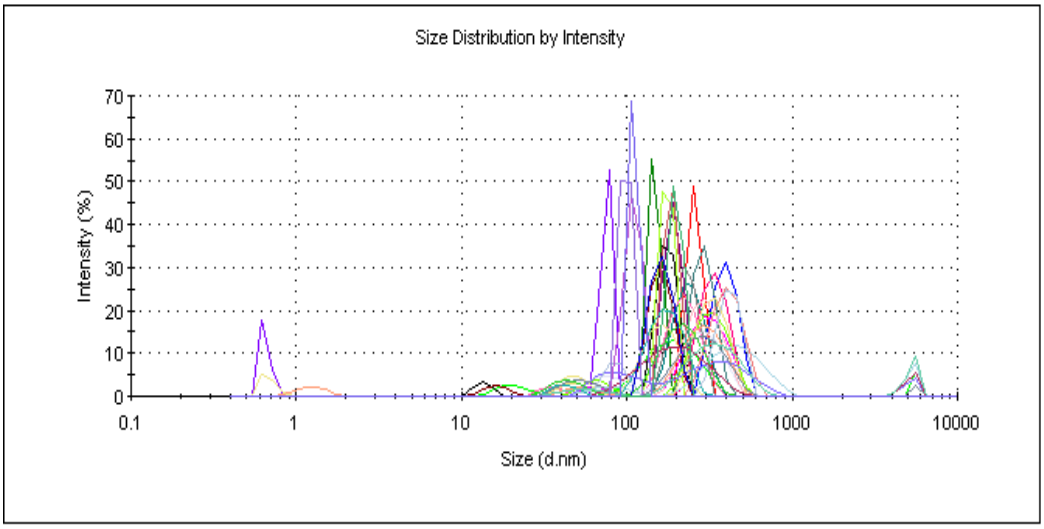

Figure 5-26: Size distribution of all the SD-CSTRS experiments

5.5 Overall Conclusions

From the numerical results and graphs, two conclusions have been drawn that

3. In general and for all three reactor modes of operations, it is evident that the higher the spin and/or impeller speed the smaller the particle size and the narrower the distribution for the range examined.

4. In contrast, the three modes of operations presented varied results. Whereas the SD-CSTR gave narrower distributions with mostly single peaks, the SD alone and CSTR alone produced multi-peaks and wider size distributions.

Both of the above therefore led to an overall conclusion that the SD-CSTR is a more efficient reactor mode for the continuous synthesis of TiO_2.

Chapter 6 : PARTICLE SIZE CONTROL

6.1 Introduction

After the success of the associated simulations, both laboratory bench and pilot scale experiments, the products were characterized and analyzed to establish useful trends based on the dominant factors that were varied for both type of experiments in order to deduce optimal conditions for synthesizing Titania using the spinning disc continuous stirred-tank and settler reactor (SD-CSTRS).

6.2 Particle Size Control

From Chapters 4 and 5, the novel arrangement limits the number of nuclei produced in the aerosol system (16% conversion of $TiCl_4$ to TiO_2) by controlling the concentration of reactants, impact angle and spin; while polymorph selection is achieved by selective operating conditions. The nucleated particles formed in the aerosol process are fed as seeds for heterogeneous nucleation in the metastable regime of the aqueous (sol) reacting volume after the induction time. The mixing (impeller rotation per second) and the degree of super-saturation provide a critical factor which limits the size and distribution of the particles formed. The particles continue to grow by layering until a critical particle size occurs when the resultant forces acting on the bulk produce the critical breaking stress equivalent to the Young's modulus of the desired particle as described by equations 4-1 to 4-3.

Where V_m=Molecular volume ($Å^3$)

K_B = Boltzmann constant ($1.3806505 \times 10^{-23}$ J/K)

S=c/c*

c = solubility of TiO_2 of particle size $v_{c,t}$ at temperature T

c*=normal equilibrium solubility of TiO_2 at temperature T

"E" is desired particle Young's modulus and "$V_{c,t}$" the critical radius (Mullin, 1993) of the desired particle size and σ is the surface energy.

Molecular modelling was adopted to obtain the variables required to compute the critical particle radius as reported in Chapter 3 to simulate optimized TiO_2 nanoparticles for the five different polymorphs of Titania investigated by performing energy minimization calculations under constant pressure deploying General Utility Lattice Program: GULP (Gale J. D., 2007) using the Buckingham intreatomic potentials $V_{ij\text{-}buck}$. Input cell parameters for the model were fitted from Matsui & Akaogi (1991) in terms of intreatomic distance r_{ij}, effective charge *q*; repulsive radius *A*; softness parameter *D*; Van der Waals' atomic coefficient C, and standard atomic force *f* (4.184kJ/ Å.mol) have been used. The methodology and results are presented elsewhere (Akindeju et al, 2010).

6.3 The Model

For Newtonian fluid (Darby Ronald, 2001); $\Theta = \gamma\mu$; where the shear rate is γ, and μ is the viscosity of resulting system; and expressed in terms of the equipment

$$\gamma = \frac{\mu\pi D_{imp}}{60L_{imp}} \quad (6\text{-}1)$$

And hence

$$\Theta = \frac{\mu^2\pi D_{imp}}{60L_{imp}} \quad (6\text{-}2)$$

In terms of required spin, Ω; the impeller diameter D_{imp}; and the effective spin channel depth, L_{imp} which is the perpendicular distance from the impeller shaft to the to the impeller boundary.

By combining equations (4-3) and (6-2), the required spin to predict particles size in terms of the operating conditions is obtained as

$$\Omega = \frac{60L_{imp}}{\mu^2 \pi D_{imp}} \left(\frac{EK_B In(S)}{2V_m}\right)^{\frac{1}{2}} \quad (6\text{-}3)$$

Equation 6-3 was modified with a Viscosity Power Correction Factor (VPCF), Ψ to obtain a good fit to experimental data, where Ψ= -0.17.

$$\Omega = \frac{60\mathrm{L_{imp}}}{\mu^{2\Psi} \pi \mathrm{D_{imp}}} \left(\frac{\mathrm{EK_B In(S)}}{2\mathrm{V_m}}\right)^{\frac{1}{2}} \quad (6\text{-}4)$$

The LHS of equation 6-4 has two components; the molecular component in parenthesis and the other half being the reactor component, hence both the reactor and molecular components have impact on the achievable particle size and distribution.

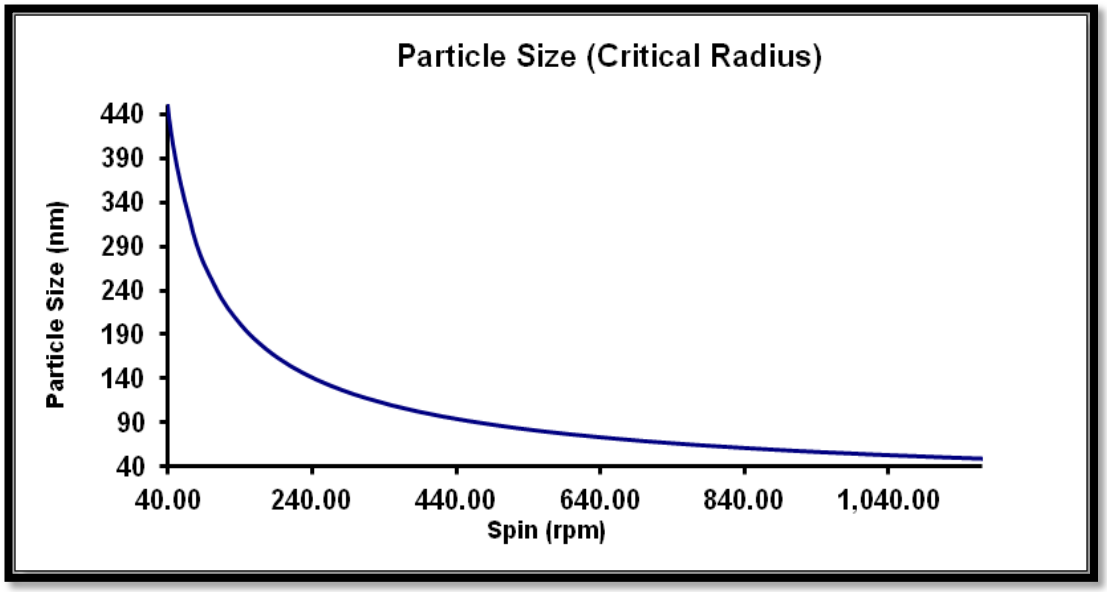

Figure 6-1: Effect of CSTR spin on modal (critical) particle size

6.4 Particle Size Distribution

The particle distribution and population of desired TiO_2 size is obtained from the number density, *n(v,t)* population balance equation expressed below in terms of non-zero growth, *G(v,t);* heterogeneous nucleation rate, *J(v,t);* and aggregation frequency, *q(v,t)* terms of size *v,* growing to size *v'* over time t.

$$n(v,t) = \frac{1}{2}\int_0^v n(v-v',t)n(v',t)q(v-v',v')dv' - n(v,t)\int_0^\infty n(v',t)q(v,v')dv' - n(v,t)\frac{dG(v)}{dv} + J(v) \quad (6\text{-}5)$$

Assuming uniform shape factor and negligible breakage, the analytical solution (Randolph and Larson, 1978) of the above equation is applied to obtain the number density (Figures 3-14 and 3-15) of desired particles in the range V_0 to $V_{c,t}$. However, the derivations of several numerical solutions are also available in literature (Artelt et al, 2004; McCoy, 2002 and Hounslow, 1990). Those derivations and their applications in this context have been discussed in Chapter 4.

These results are in agreement and consistent with those presented in Table 3-9.

6.5 Effect of Degree of Supersaturation and Temperature on Particle Size

Temperature and the degree of supersaturation affect the mean particle sizes in the same direction; the higher the temperature, the higher the solubility of $TiCl_4$. Figures 6-2 to 6-9 below show the effect of increasing degree of supersaturation, S, on the modal particle size using equation 6-4.

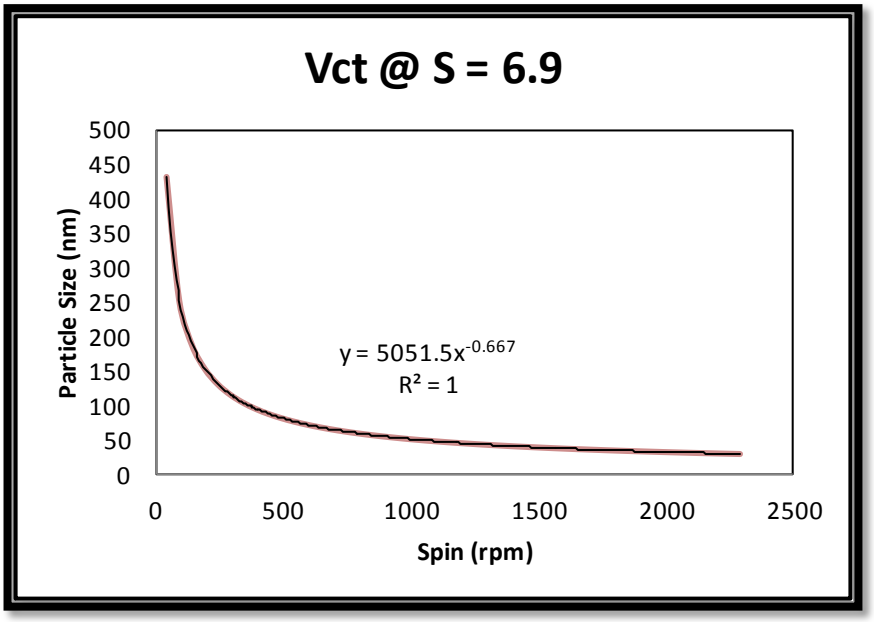

Figure 6-2: Effect of Spin on Particle Size at Degree at Supersaturation of 6.9

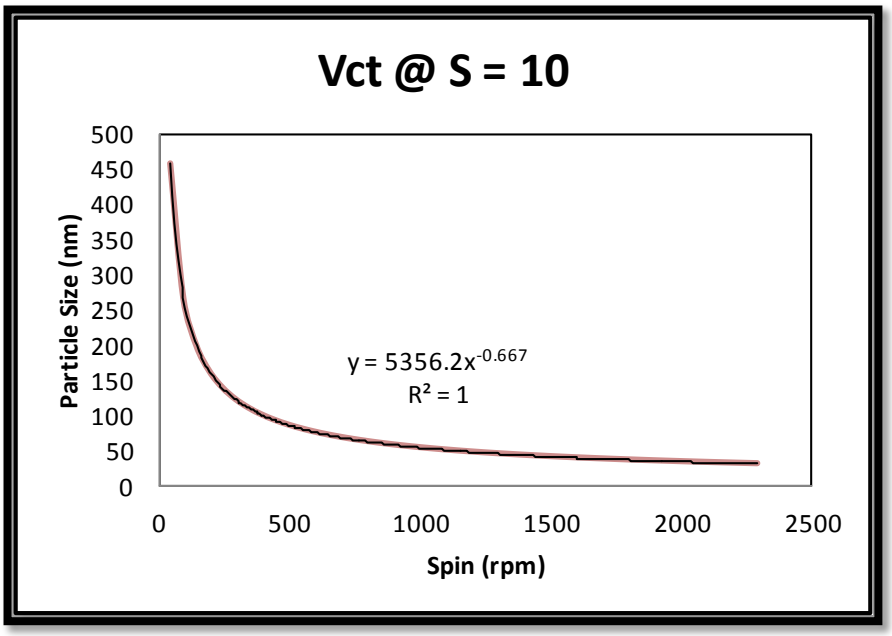

Figure 6-3: Effect of Spin on Particle Size at Degree at Supersaturation of 10

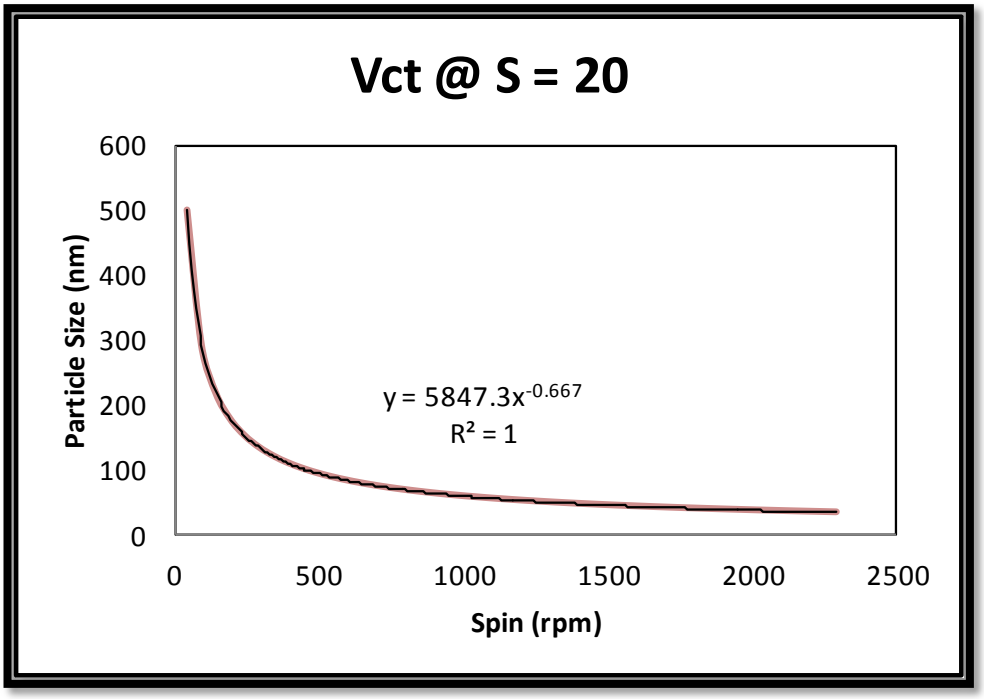

Figure 6-4: Effect of Spin on Particle Size at Degree at Supersaturation of 20

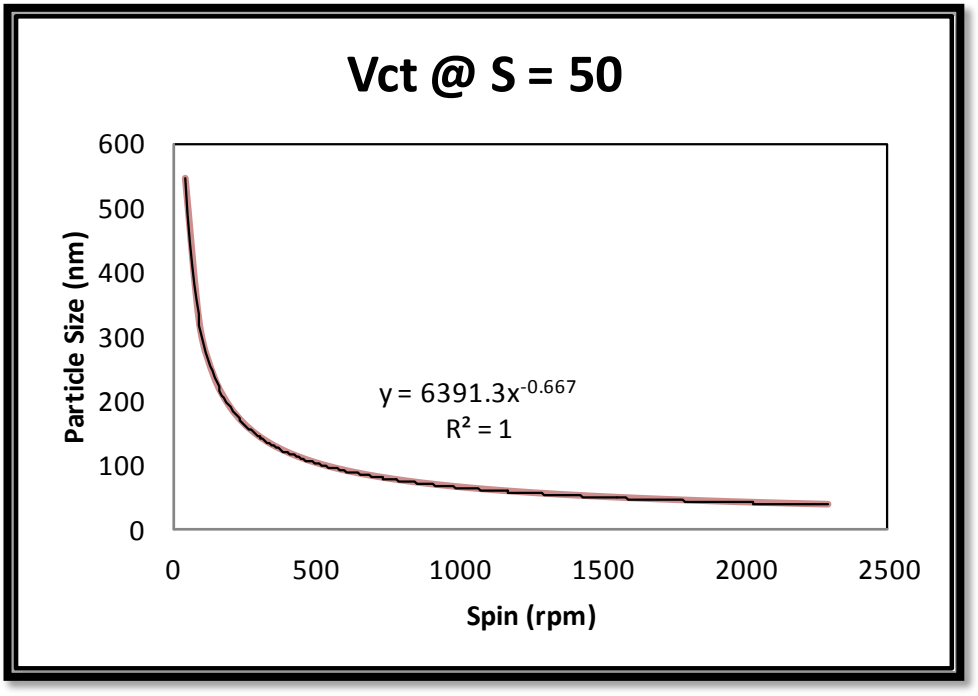

Figure 6-5: Effect of Spin on Particle Size at Degree at Supersaturation of 50

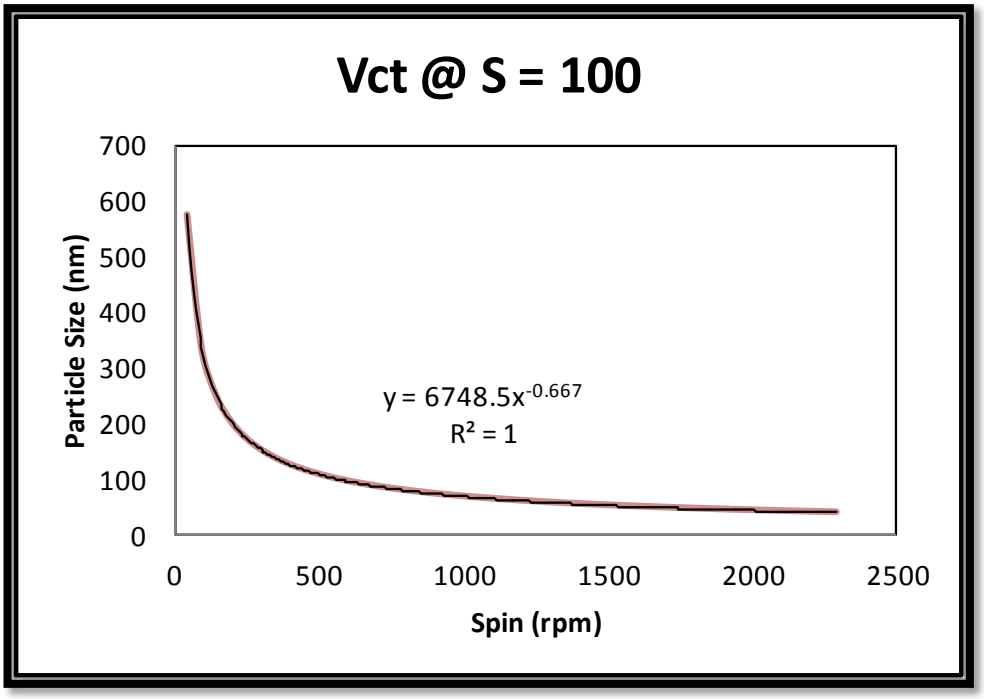

Figure 6-6: Effect of Spin on Particle Size at Degree at Supersaturation of 100

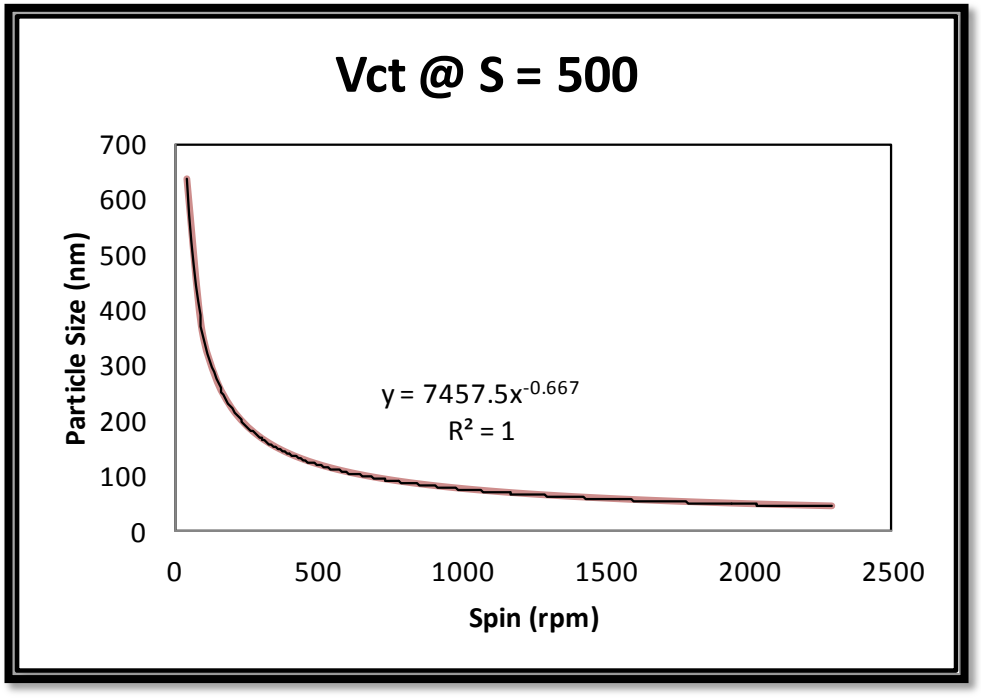

Figure 6-7: Effect of Spin on Particle Size at Degree at Supersaturation of 500

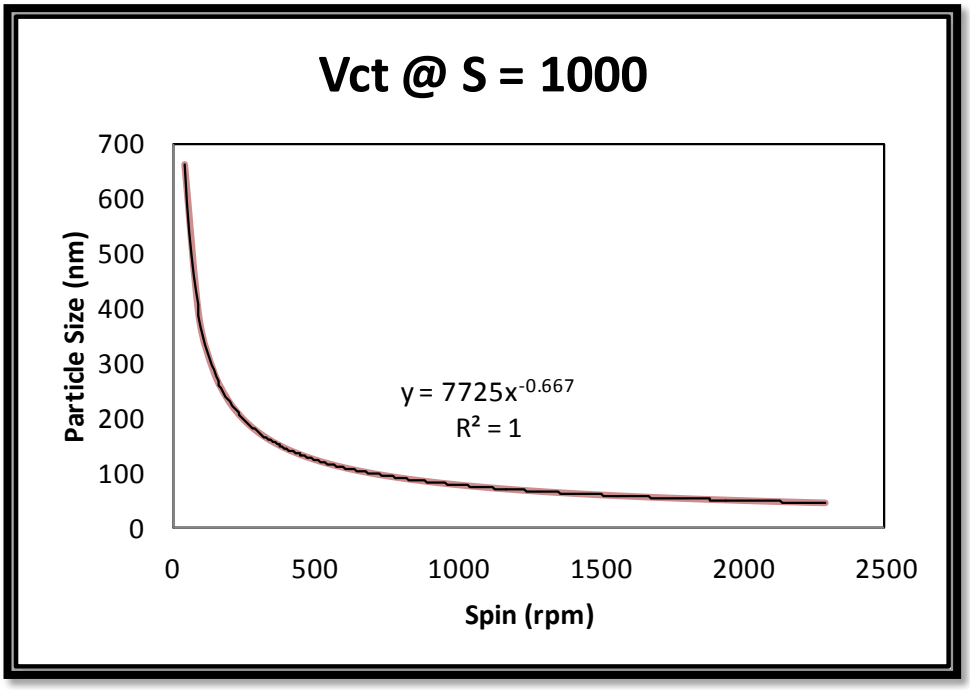

Figure 6-8: Effect of Spin on Particle Size at Degree at Supersaturation of 1000

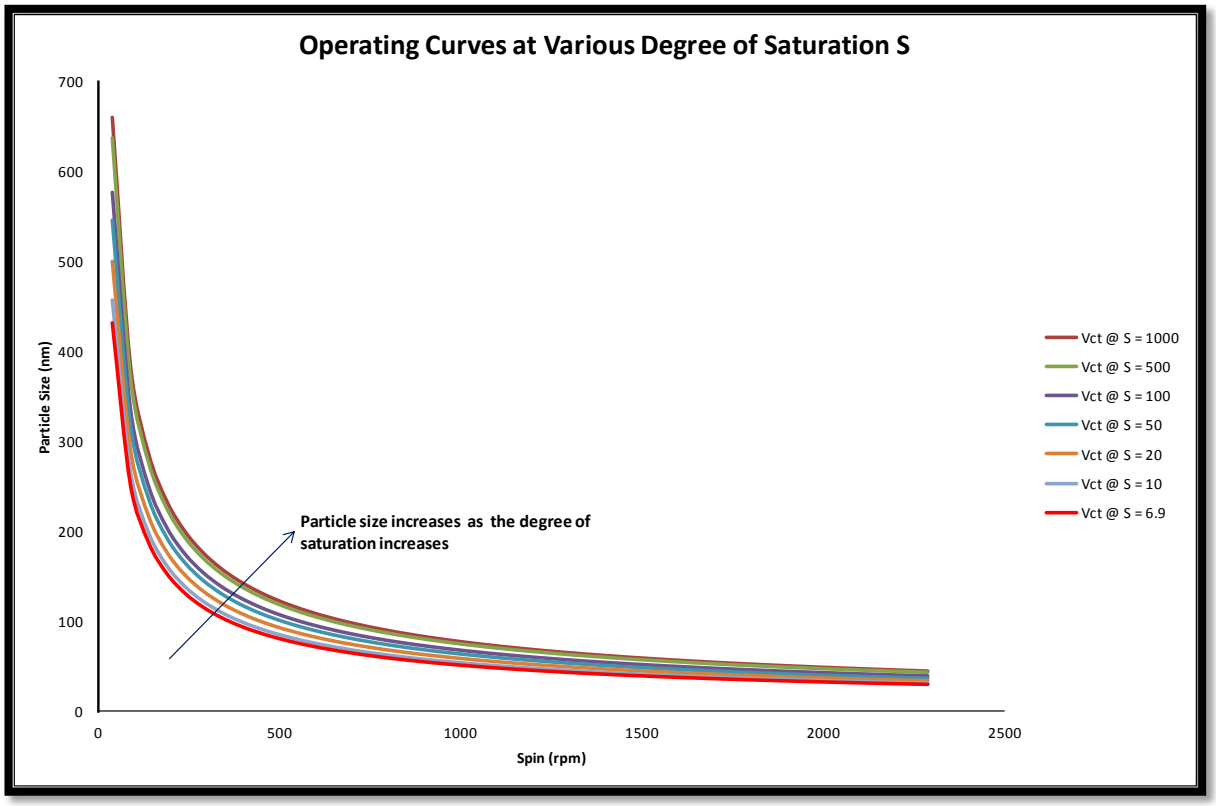

Figure 6-9: Effect of Spin on Particle Size at Various Degrees of Supersaturation

Upon using Ms Excel inbuilt power regression sub-routine for line of best fits, all the curves resulted in a general form given by equation 6-5 below.

$$\boldsymbol{Y = AX^{-0.667}} \qquad 6\text{-}5$$

where “Y” is the modal particle size, “X” is the spin (rpm) and “A” is the initial particle size from the precipitating crystallization reaction. The exponent “-0.667” is constant and represents rate at which the particles diminish in size for every spin. Hence, it provides a quick evaluating and predicting tool for estimating the modal particle size for a given set of operating conditions once the initial plausible particle size without shear has been determined using a basic laboratory bench experiment.

6.6 Structural formation

As shown in Table 5-1, operating temperature, TiCl4 molar concentration and the molar ratio of H2O/TiCl4 were the main factors that influenced which formation was produced. Operating at 1.0M, 60°C and molar ratio of 6 produced a mesoporous structure; synthesizing at 0.5M, 40°C and molar ratio 2 produced the tubular structure, whereas operating at 47°C and molar ratio of 2 produced nano-crystalline particles for all molar concentration.

The above trends below are in good agreement with Xia et al (1999) as presented in Figures 3-16, and 6-10 below.

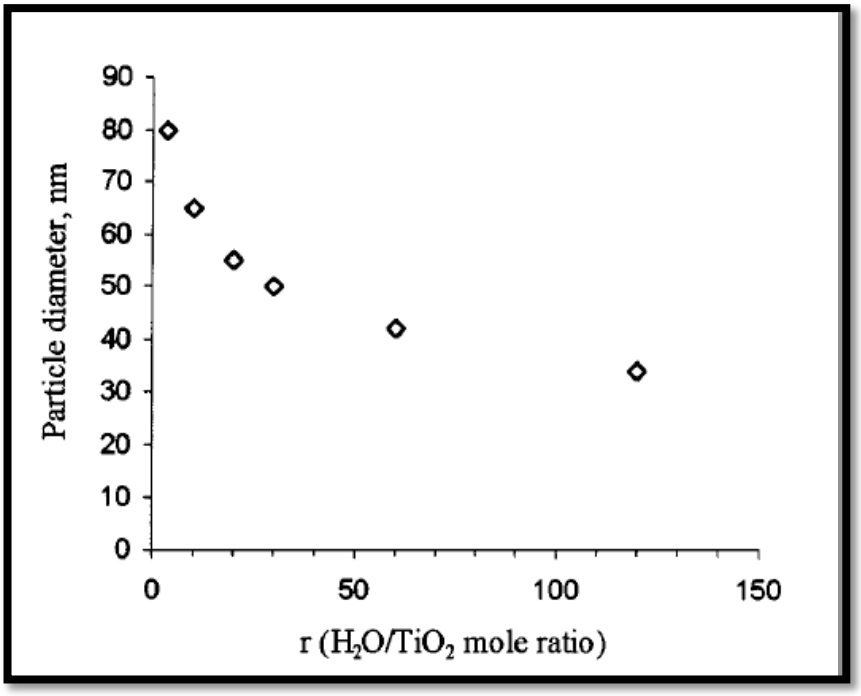

Figure 6-10: Particle Size at different $H_2O/TiCl_4$ ratios (Xia et al, 1999)

6.7 Conclusions

This work presents parametric relationship between the modal particles sizes and critical operating conditions for the new SDCSTRS process route for continuously synthesizing Titania nanoparticles using $TiCl_4/H_2O$ molar ratio, $TiCl_4$ concentration, spinning disc and CSTR impeller rotation speeds as parameters. The results show a good correlation between experimental and theoretical values with narrow particle size distribution; where for a given the nominated 900rpm impeller rotation speed, sample 7 on Table 5-1 with 0.5M $TiCl_4$ and $H_2O/TiCl_4$ molar ratio of 2 operating at 47°C (319K) produced the optimal particles (with 1.29 standard deviation) as theoretically predicted by simulation.

Chapter 7 : CONCLUSIONS AND RECOMMENDATIONS FOR FUTURE WORK

7.1 Conclusions

The overall aim of this work was to develop a tailor-made process for the continuous synthesis of Titania nanoparticles through Multi-scale simulation and experimental investigations. Compared to existing technologies, this work investigated and sought to develop a better scheme with improved energy efficiency, narrow particle size distribution, polymorph selectivity and controllability; and specifically focused on the under-listed objectives:

1. Development of a methodology for designing Titania nanoparticles of desired shape, size and morphology via a theoretical strategy that combines molecular modelling, reactor design and population balance approaches.
2. Investigated the sol-gel and aerosol processes with a view to developing a modelled reactor for the synthesis of Titania nanoparticles under a controlled hydrodynamic regime in a novel spinning disc continuous Stirred Tank Reactor.
3. Production and characterization of Titania nanoparticles through experiments and comparing them with simulation results.

Upon completion, this study investigated and modelled six polymorphs of Titania: Rutile, Anatase, Brookite, high-pressure Brookite, the columbite-type TiO2-II and Corundum-like type CLT, under constant pressure using the General Utility Lattice Program (GULP) with satisfactory results compared to the Classical data on the subject. The simulated thermodynamic, mechanical

and optical properties compare favourably with acceptably known references and results extended to simulate stable optimized nanoparticles except for CLT due to its large compressibility and electronegativity equalization correction. The alternative Buckingham potentials are simpler to implement and the results provide a modern crystallographic compendium for Titania polymorphs. In addition, Randolph and Larson's population balance analytical solution yielded satisfactory results for the number density of Rutile nanoparticles as a base case compared to experimental data (in Chapter 5).

Further, there are indications that hydroxylated TiO2 may present yet unknown but important applications in semiconductors.

The results in Chapter 4 demonstrated the technical feasibility of continuously synthesizing TiO2 nanoparticles at 47.27 °C using a SDCSTR, representing a deviation from the energy intensive CVD and batch sol-gel processes. It also provides the opportunities for algorithms and software to be developed for simulations of a composite spinning-disc Continuous Stirred Tank Reactors; and provides a tool for predicting yield, residence time, and particle size distribution (population density), respectively.

The results of the experiments in Figure 5-1 to Figure 5-6 and Table 5-1 showed that TiO2 nanoparticles were successfully produced at the set conditions with unique sizes and morphologies which provided the required impetus for a larger scale production to examine the impact of spin and impeller speed on size distribution using the 47°C to 55°C reaction

temperature cases. Further and from the numerical results and graphs in Chapter 5, two conclusions were drawn that

a) In general and for all three reactor modes of operations, it is evident that the higher the spin and/or impeller speed the smaller the particle size and the narrower the distribution for the range examined.

b) In contrast, the three modes of operations presented varied results. Whereas the SD-CSTR gave narrower distributions with mostly single peaks, the SD alone and CSTR alone produced multi-peaks and wider size distributions.

Both of the above therefore led to an overall conclusion that the SD-CSTR is a more efficient reactor mode for the continuous synthesis of TiO_2.

And finally Chapter 6 presented parametric relationships between the modal particles sizes and critical operating conditions and hence quick tool for the new SDCSTRS process route for continuously synthesizing Titania nanoparticles using $TiCl_4/H_2O$ molar ratio, $TiCl_4$ concentration, spinning disc and CSTR impeller rotation speeds as parameters. The results show a good correlation between experimental and theoretical values with narrow particle size distribution; where for a given the nominated 900rpm impeller rotation speed, sample 7 in Table 5-1 with 0.5M $TiCl_4$ and $H_2O/TiCl_4$ molar ratio of 2 operating at 47°C (319K) produced the optimal particles (with 1.29 standard deviation) as theoretically predicted by simulation.

Overall,

c) Compared to the Chemical Vapour Deposition (CVD) technology that operates at 900°C – 1100°C, this system operates between 25°C and 100°C depending on target characteristics of the desired nanoparticles. This is a significant saving in energy requirements.

d) This system produces particles within controllable and predictable narrow size distribution unlike the wide particle distribution obtainable from using the SD or CSTR alone in the Sol-Gel process.

e) While other technologies require very high super-saturation levels, typically in 20 –1000 range, our novel system only requires a maximum of 8; hence preventing material wastages.

f) By increasing the degrees of freedom, this system achieves controllability for

    i. Particle size

    ii. Particle size distribution

    iii. Polymorph selectivity

g) This system is suitable for the synthesis of temperature sensitive organic nanoparticles because the optimal operating temperature is well below the temperatures required to denature most organic particles.

h) This device is suitable for both aqua and non-aqua flow processes; adequate for developing target oriented drug delivery nanoparticles.

i) The overall process time for this system is 0.859s compared to the more than 2s for Sol-Gel processes (typically followed by calcination) and more than 5min for CVD. This translates into a gross reduction in the total time required for products to reach the target market.

7.2 Recommendations for Future Works

1. The impact and effect of different reactant entry configurations should be investigated.
2. The effect of spinning disc surface geometry on Micro-structural defects should be investigated.
3. The behavior of the SDCSTR using super-critical steam and on the products should be investigated to provide more insight on the overall applications of this novel reactor.
4. The impacts of using different impellers should be investigated.
5. Computational Fluid Dynamics should be deployed to investigate the boundaries of the settling volume.

References

Akindeju, M; Rohl, A; Carter, D; Pareek, V; and Tade, M.O; 2010, Constant Pressure Molecular Modelling of six Optimised Titanium Oxide polymorphs, International Journal of Chemistry, vol 2. No. 1. Pg 26 – 37.

Allegretti F., O'Brien S., Polcik D., Sayago D.I., and Woodruff D.P.; 2005, Adsorption Bond Length for H_2O on TiO_2 (110): A Key Parameter for Theoretical Understanding; Physical Review Letters, PRL 95, 226104.

Artelt, C;, Schmid, H.-J; and Peukert, W; 2004, On the impact of accessible surface and surface energy on particle formation and growth from the vapour phase, Journal of Aerosol Science, Elsevier Ltd, Vol. 36: 144-142

Banfield, J.F., Welsh, S.A., Zhang, H.Z., Elbert, TT., & Penn, R.L. (2000) Aggregation-Based Crystal Growth and Microstructure Development in Natural Iron Oxyhydroxide Biomineralization Products. Science Vol 289, No 5480, 751-754.

Baldereschi, A.;1973, Mean-value point in the brillouin zone. Phys. Rev. B, 7:5212–5215.

Banerjee, A.; Adams, N.; Simons, J.; and Shepard, R.; 1985, Search for stationary points on surfaces. J. Phys. Chem., 89:52–57.

Bokhimi, X. and Pedraza, F.; 2004: Characterization of brookite and a new corundum-like titania phase synthesis under hydrothermal conditions; Journal of solid state chemistry, vol. 177, pp. 2456 – 2463.

Borissova, A., Khan, S. et. al., 2009; In Situ Measurement of Solution Concentration during the Batch Cooling Crystallization of L-Glutamic Acid using ATR-FTIR Spectroscopy Coupled with Chemometrics. Crystal Growth & Design, Vol. 9, No. 2, 692-706.

Brode, S. and Ahlrichs, R.; 1986: An optimized MD program for the vector computer cyber-205. *Comp. Phys. Commun.*, 42:51–57.

Charlton, G.; Howes, P.B.; Nicklin, C.L.; Steadman, P.; Taylor, J.S.G.; Muryn, C.A.; Harte, S.P.; Mercer, J.; McGrath, R.; Norman, D.; Turner, T.S. and Thornton, G.; 1997, Relaxation of TiO_2 (110)-(1 x 1) using X-Ray Diffraction, Physical Review Letters, Vol. 78, No. 3.

Chew, J. W., Black, S. N., Chow, p. S., Tan, R. B. H., 2007; Comparison between Open- Loop Temperature Control and Closed-Loop Supersaturation Control for Cooling Crystallization of Glycine. Ind. Eng. Chem. Res., 46, 830-838.

Coltrin, ME; Kee, RJ; Evans, GH; Meeks, E; Rupley, FM; and Grcar, JF; 1991, A Fortran program for modelling one-dimensional rotating disc chemical vapour deposition reactors, Sandra Report, Sand91-8003.UC-401.

Crystallization (n.d) http://www.cheresources.com/cryst.shtml

Darby Ronald, Chemical Engineering Fluid Mechanics; 2nd Ed, CRC Press, 2001

Darvey, R. and Garside J, 2000; From molcules to crystallizers, an introduction to crystallization. Oxford: Oxford science publications, chp 2.

David van der Spoel, Erik Lindahl, Berk Hess, Aldert R. van Buuren, Emile Apol, Pieter J. Meulenhoff, D. Peter Tieleman, Alfons L.T.M. Sijbers, K. Anton Feenstra, Rudi van Drunen, and Herman J.C. Berendsen; GROMACS Development Team; Department of Biophysical Chemistry, University of Groningen. Nijenborgh 4, 9747 AG Groningen, The Netherlands.

D. Devakumar, 2008, Study and Design of Impellers for Multiphase Reactors, Modern Applied Science, CCSE, No 2, Vol 5.

De Anda, J.C., Wang, X.Z., Lai, X., Roberts K.J., et al., 2005; Real-time Product Morphology Monitoring in Crystallization Using Imaging Technique. AIChE Journal, 51(5), 1406-1414.

Gale, JD; 2007, General Utility Lattice Program, Version 3.1, Nanochemistry Research Institute, Department of Applied Chemistry, Curtin University of Technology, Perth, W/Australia.

Gilbert, B., Zhang, H., Huang, F., Finnegan, M.P., Waychunasc, G.A., & Banfield, J., 2003; Special phase transformation and crystal growth pathways observed in nanoparticles.

Gutsch, A., Kramer, M., Michael, G., Muhlenweg, H., Pridohl, M., and Zimmermann, G., 2002; Gas-Phase production of nanoparticles, Project House Nanomaterials, Rodenbacher Chausee 4, 63457 Hanau, Germany.

He, G., Bhamidi, V., Tan, R.B.H., Kenis, P.J.A., Zukoski, C.F., 2006; Determination of Critical Supersaturation from Microdroplet Evaporation Experiments. Crystal Growth & Design, Vol. 6, No. 5 1175-1180.

He, G., Bhamidi, V., Wilson, S.R., Tan, R.B.H., Kenis, P.J.A., Zukoski, C.F., 2006; Direct Growth of γ-Glycine from Neutral Aqueous Solutions by Slow, Evaporation-Driven Crystallization. Crystal Growth & Design, Vol. 6, No. 8, 1746-1749.

Hoover, G.W.; Canonical dynamics, 1985: Equilibrium phase-space distribution, Phys. Rev. A , Vol. 31, No. 3, 1695.

Hounslow, MJ; 1990, A discrete population Balance for Continuous systems at steady state, AIChE Journal, Vol. 36, No. 1: 106-116.

Iskander, F., 2009; Nanoparticle processing for optical applications – A review, Advance powder Technology, Vol 20, issue 4, 283-292.

Kees de Weerd, 2004, Application of Microscale Technology in the Chemical Process Industry, Akzo Nobel Research and Technology Chemicals, Arnhem, The Netherlands.

Ken Onda, Bin Li, Jin Zhao, Kenneth D. Jordan, Jinlong Yang andHrvoje Petek; Wet Electrons at the H2O/TiO2(110) Surface; Science 308, 1154, 2005.

Kim, D-W.; Enomoto, N.; and Nakagawa, Z.; 1996: Molecular Dynamic Simulations in Titanium Dioxide polymorphs: Rutile, Brookite, and Anatase; J. American Ceramic Society, Vol. 79 (4), pgs. 1095-99.

Isaac, D.G.; Carnes, J.D.; Anderson, D.L.; Cynn, H.; and Hake, E.; 1997: Phys. Chem. Minerals, vol. 26, pg 31-43.

IUPAC Compendium of Chemical Terminology, 2nd Ed (1997)

Jayaraman, D., Subramanium, C., & Ramasamy, P. (1993) Evaluation of the Gibbs' free energy and nucleation kinetics of YBCO. Journal of Materials Science Letters 10 292-293

Jha A.K., Prasad K. and Kulkarni A.R., 2009; Synthesis of TiO2 nanoparticles using microorganisms, Colloids Surf B Biointerfaces. 2009 Jul 1;41(2):226-9. Epub 2009 Feb 21.

John, AK; Savithri, S; Prasad, KR; Characteristics of TiO_2 nanoparticles synthesis through low temperature aerosol process, Regional Research Laboratory (CSIR), Trivandrum- 695 019 India

John, A.K. and Surender, G.D.; Low temperature process for the synthesis of rutile phase titania through vapour phase hydrolysis, 2009, Journal of Material Science, Vol. 40, 2999 – 3001.

Jone, A; Rigopoulos, S; and Zauner, R; 2005, Crystallisation and Precipitation engineering, Computers and Chemical Engineering, vol. 29, 1159-1166

Joseph John, Deeptangshu Chaudhary, Hazim Haroosh, Paul Guagliardo, Shin-ichi Yusa; Drug release from magnetically aligned bionanocomposites, CHEMECA 2011.

Kirk-Othmer Encyclopedia of Chemical Technology, 1999-2012, John Wiley and Sons, Inc

Li, H.; Duan, X.; Liu, G.; Jia, X.; and Liu, X.; 2008: Morphology controllable synthesis of TiO2 by a facile hydrothermal process; Materials Letters 62, 4035–4037.

Lindan, P.J.D. and Gillan, M.J.; 1993: Shell-model molecular-dynamics simulation of superionic conduction in caf2. *J. Phys. Condens. Matter*, 5:1019–1030.

Li, Y; White, TJ; Lim, SH; 2004, Low temperature synthesis and micro structural control of Titania nanoparticles at temperatures lower than 100^{o}C, ScienceDirect, Journal of Solid State Chem., vol. 144, 1342-1381

Maribel G. Guzman, Jean Dill end Stephan Godet, 2009; Synthesis of silver nanoparticles by chmical reduction method and their antibacterial activity; international journal of Chemical abd Bilogical Engineering 2:3.

Matsui, M and Akaogi M; 1991, Molecular Dynamics Simulation of the Structural and Physical Properties of the Four Polymorphs of TiO_2, Molecular Simulation, Molecular Simulation, vol. 6:4, 239 — 244

McCabe, W. L. “Crystal Growth in Aqueous Solution: II - Experimental.” Industrial & Engineering Chemistry 21, 1929: 112-119.

McCoy, BJ; 2002, A population balance framework for nucleation, growth, and aggregation, Chemical Engineering Science, Vol. 54: 2249-2285

Meagher, E.P. and Lager, G.A; 1979, polyhedral thermal expansion in the TiO2 polymorphs: Refinement of the crystal structure of Rutile and Brookite at High temperature; Canadian Mineralogist, Vol. 17, pp. 77 – 85.

Mendez del Rıo, J. R. and Rousseau, R. W. Batch and Tubular-Batch Crystallization of Paracetamol: Crystal Size Distribution and Polymorph Formation. Crystal Growth & Design, 2006 Vol. 6, No. 6, 1407-1414.

Mersmann, A. Crystallization Technology Handbook. USA: Marcel Dekker, 2001.

Mohammad A. Behnajady, Hamed Eskandarloo, Nasser Modirshahla and Mohammad Shokri, 2011; Sol-Gel Low-temperature Synthesis of Stable Anatase-type TiO2 Nanoparticles Under Different Conditions and its Photocatalytic Activity, Photochemistry and Photobiology, 2011, 84: 1002–1008.

Moody EG and Collin LR; Effects of mixing on the nucleation and growth of titania particles, 2003, Aerosol Science and Technology, American Association for Aerosol Research, Taylor & Francis, vol. 34:403-424

Motoyuki Iijima and Hidehiro Kamiya; Surface Modification for Improving the Stability of Nanoparticles in Liquid Media, KONA Powder and Particle Journal 120 No.24 (2009)

Mowbray, D. J., Martinez, J. I., Garcı´a Lastra, J. M., Thygesen, K. S., and Jacobsen, K. W.; Stability and Electronic Properties of TiO2 Nanostructures With and Without B and N Doping; Center for Atomic-scale Materials Design, Department of Physics, Technical UniVersity of Denmark,DK-2800 Kgs. Lyngby, Denmark

Mullin, J.W. (2001) Crystallization. Butterworth Heinemann.

Mullin, J. W., and Raven, K. D.; Influence of mechanical agitation on the nucleation of aqueous salt solutions; Nature 195, 1962: 35-38.

Muneer M. Ba-Abbad, Abdul Amir H. Kadhum, Abu Bakar Mohamad, Mohd S. Takriff1, and Kamaruzzaman Sopian, 2012; Synthesis and Catalytic Activity of TiO2 Nanoparticles for Photochemical Oxidation of Concentrated Chlorophenols under Direct Solar Radiation; Int. J. Electrochem. Sci., 4 (2012) 4841 – 4888.

Njo, S.L.; Fan, J.F. and Van de Graaf, B.; 1998: Extending and simplifying the electronegativity equalization method. *J. Mol. Catal. A*, 134:79–88.

Nolas, G.S. and Goldsmid, H.J., 2006: Thermal Conductivity- Theory, Principles, and Applications, Sprinklink Books, Chapter 4.

Nose, S.; 1984; A unified formulation of the constant temperature molecular dynamics methods, J. Chem. Phys. 81, 511; Mol. Phys. 52, 255.

Nye, J.F.;1957, Physical properties of crystals, Oxford University Press.

Okyama kikuo and Lenggoro Wuled, Nanoparticle precipitation and its applications- A Nanotechnology particle project in Japan; Proceedings

of the 2004 International Conference on MEMS, NANO and Smart systems (ICMENS'04)

Pearlman, D.A.; Case, D.A.; Caldwell, J.W.; Ross, W.S.; Cheatham III, T.E.; DeBolt, S.; Ferguson, D.; Seibel, G.; and Kollman, P.; 1995; Amber, a package of computer programs for applying molecular mechanics, normal mode analysis, molecular dynamics and free energy calculations to simulate the structural and energetic properties of molecules. *Comput. Phys. Commun.*, 91:1–41.

Perry, RH; 1994, Perry's Chemical Engineers' Handbook, 4th Edition, McGraw-Hill International Edition, New York

Pratsinis, SE; Bai, H; and Biwas, P; 1990, Kinetics of Titanium (IV) chloride oxidation, Journal of American Ceramics Society, vol. 43 (4), 2158-2162.

Pratsinis, SE and Spicer, PT; 1998, Competition between gas phase and surface oxidation of $TiCl_4$ during synthesis of TiO_2 particles, Chemical Engineering Science, vol. 53 (10): 1861-1868

Press, W.H.; Teukolsky, S.A.; Vetterling, W.T.; and Flanner, B.P.; 1986, Numerical recipes in FORTRAN: The art of scientific computing, Cambridge University Press.

Quigley D and Rodger, PM; 2008, Free energy and structure of calcium carbonate nanoparticles during early stages of crystallization, The journal of Chemical Physics vol. 128, 221101

Quigley D and Rodger, PM; 2008, Metadynamics simulations of ice nucleation and growth, The journal of Chemical Physics vol. 128, 154518

Rajesh R Naik, Sarah J. Stringer, Gunjan Agarwal, Sharon E. Jones and Morley O. Stone, 2002; Biomimetic synthesis and patterning of silver nanoparticles, Nature Materials,1, 169-172.

Ramirez, R. and Boehm, M.C.: 1988, The use of symmetry in reciprocal space integrations- asymmetric units and weighting factors for numerical-integration procedures in any crystal symmetry. Int. J. Quantum Chem., 34:571–594.

Randolph, AD and Larson MA; Theory of Particulate Processes: 2nd ed., Academic Press, New York; Gelbart & J. Seinfeld, Computational Physics, Vol. 28: 357 (1978).

Rene Overney, Nanoparticle Synthesis, 2010, Nanothermodynamics and Nanopartilce Synthesis, NME 498 A/A.

Rivallin, M; Benamami, AK; and Gaunad, A; 2005, Sol-Gel reactor with rapid micro mixing modelling and measurements of Titanium Oxide nanoparticle growth, IChemE Chemical Engineering Research and Design, vol. 83(A1): 67-74

Rohani, S., Horne, S., Murthy, K, 2005; Control of Product Quality in Batch Crystallization of Pharmaceuticals and Fine Chemicals. Part 2: External Control. Organic Process Research & Development, 9, 873-883.

Royal Society of London, July 2004.

Sanderson, R.T.; 1951: An interpretation of bond lengths and a classification of bonds. Science, 114:670–672.

Sebastien Kerisit, N. Aaron Deskins, Kevin M. Rosso, and Michel Dupuis; 2008, A Shell model for atomistic Simulation of Charge Transfer in Titania, Journal of Physical Cehmistry, 112, 7678-7688.

Shanno, D.F.; 1970: Conditioning of quasi-newton methods for function minimization, Math. Comput., 24:647–656.

Somiya Shigeyuki and Roy Rustum, 2000; Hydrothermal synthesis of fine oxide powders, Indian Academy of Sciences, Bull Mater. Sci., Vol 23, No. 6, Dec 2000 pp 453-460.

Swaminathan, K; Raston, CL; and Saunders, M; 2004, Continuous flow nano-technology: manipulating the size, shape, agglomeration, defects and phase of silver nano-particles, Lab on chip, vol. 4, 1800-1805

Swamy, V.; Gale, J.D.; Dubovinsky, L.S.: 2001, Atomistic simulation of the crystal structures and bulk moduli of TiO2 polymorphs, J. of Phys. and Chem., vol 62, pg 887-895.

Thomas M. Christensen, 2000, PES 449 / PHYS 549 Lecture notes , Department of Physics and Energy Science, university of Colorado, 1420 Austin Bluffs Parkway, Colorado Springs, CO 80918

Tsuji Masaharu, Hashimoto Masayuki, Nishizaqa Yuki, Kubokawa Masatoshi and Tsuji Takeshi, 2005; Rapid synthesis of metallic nanostructures in solution under microwave dieletic heating, European Journal of Chemistry, 11, 440-452.

Usman Mustafa, Elfaki A.M. Faiz and Daoud I. Jamal; 2008 Experimental Design for Scientists and Engineers.

Van Laarhoven, P.J.M.; and Aarts, E.H.L.; 1987, Simulated annealing: Theory and applications, Reidel.

Vogtenhunger Doris, Raimund podloucky and J. Redinger; 1997, ab initio studies of H2O adsorption on the TiO_2 (110) rutile surface, surface Science 402-404, 798-801.

Wang, G; and Garrick, SC; Modeling and simulation of Titania formation and growth in temporal mixing layers, 2006, Journal of Aerosol Science, Vol. 37: 431-451.

Wauqier, J.P. (1998) Separation Process. Editions TECHNIP, Paris

Weiwei Yu, Sujun Yuan, Yaogang Li, Qinghong Zhang, and Hongzhi Wang, 2011; Preparation of TiO2 Nanoparticle/Nanotube Composites via a Vapor Hydrolysis Method and Their Photocatalytic Activities, ISRN Nanotechnology, Volume 2011 (2011), Article ID 582534

Xia, B; Li, W; Zhang, B; and Xie, Y; 1999, low temperature vapour phase preparation of TiO_2 powders, Jr. of material science, vol. 34: 3505-3511

Yang, X. F. , Konish, H., Xu, H. F., Wu, M. M., 2006; Comparative sol-hydro(solvo)thermal synthesis of TiO2 nanocrystals, European Journal of Inorganic Chemistry, [11] 2229-2235.

Yu, C. Jimmy, 2009; Nanoparticle Synthesis, Department of Chemistry (Environmnetal Scicence Program), The Chinnese university of Hong kong.

Zhang Lianfeng, William A Anderson and Zisheng (Jason) Zhang; 2006, Development and Modelling of a Rotating Disch photocatalytic Reactor for Wastewater Treatment, Elsevier's Chemical Engineering Journal, 121, 125-134.

Zhang Liu, Zicong Jian, jianzhang Fang, Xiaoxin Xu, Ximiao Zhu and Shxing Wu, 2012; Low-Temperature Reverse microemulsion sysnthesis, Characterization, and Photocatalytic Performance of nanocrystalline Titanium Dioxide; international Journal of photoenergy, Article ID 702503.

Every reasonable effort has been made to acknowledge the owners of copyright material. I would be pleased to hear from any copyright owner who has been omitted or incorrectly acknowledged.

APPENDIX 3a: Starter input file for Rutile

```
opti conp efg pot bond

# Created by GDIS version 0.90.0
#

switch rfo gnorm 0.100000

name Rutile


dump Rutile.res

output movie arc Rutile.arc

cell
4.492683 4.492683 3.008396  90.000000 90.000000 90.000000
fractional
Ti   core     0.000000    0.000000    0.000000    2.1960000
1.0000000
O    core     0.303283    0.303283    0.000000   -1.0980000
1.0000000

space
P 42/M N M

species
Ti     core    2.196000
O      core   -1.098000
end

buck
O     core Ti    core  16957.6560     0.194000  12.59259
0.00 15.00
buck
O     core O     core  11782.8466     0.234000  30.22222
0.00 15.00
buck
Ti    core Ti    core  31120.4285     0.154000  5.246913
0.00 15.00

print 1
```

APPENDIX 3b: Optimised Rutile molecule (Starter File)

```
*******************************************************************
***************
*                        GENERAL UTILITY LATTICE PROGRAM
*
*                                    Julian Gale
*
*                       Nanochemistry Research Institute
*
*              Curtin University of Technology, Western Australia
*
*******************************************************************
***************
* Version = 3.1   * Last modified = 23rd May 2010
*
*******************************************************************
***************
*  optimise     - perform optimisation run
*
*  conp         - constant pressure calculation
*
*  potential    - calculate electrostatic site potentials
*
*  efg          - calculate electrostatic electric field gradient
*
*  bond         - calculate bond lengths
*
*******************************************************************
***************

  Job Started  at 10:29.44  23rd May  2010

  Number of CPUs =     1


  Total number of configurations input =   1

*******************************************************************
***************
*  Input for Configuration =   1 : Rutile
*
*******************************************************************
***************

  Formula = Ti2O4

  Number of irreducible atoms/shells =       2


  Total number atoms/shells =       6

  Dimensionality = 3               :  Bulk
```

Symmetry :

Crystal family : Tetragonal
Crystal class (Groth - 1921) : Ditetragonal Dipyramidal

Space group (centrosymmetric) : P 42/M N M

Patterson group : P 4/m m m

Cartesian lattice vectors (Angstroms) :

4.492683	0.000000	0.000000
0.000000	4.492683	0.000000
0.000000	0.000000	3.008396

Cell parameters (Angstroms/Degrees):

a = 4.4927 alpha = 90.0000
b = 4.4927 beta = 90.0000
c = 3.0084 gamma = 90.0000

Initial cell volume = 60.722068 Angs**3

Temperature of configuration = 0.000 K

Pressure of configuration = 0.000 GPa

Fractional coordinates of asymmetric unit :

No.	Atomic Label	x (Frac)	y (Frac)	z (Frac)	Charge (e)	Occupancy (Frac)
1	Ti c	0.000000	0.000000	0.000000	2.1960	1.000000
2	O c	0.303283 *	0.303283	0.000000	-1.0980	1.000000

Constraints :

Constraint no.	Unconstrained Variable	Constrained Variable	Coefficient	Offset
1	Strain 1	Strain 2	1.00000	0.0000
2	2 x	2 y	1.00000	0.0000

```
  Bond calculation :

-------------------------------------------------------------------
---------------
  Asymmetric unit site  Full lattice sites    No.  Distance
No.  Distance
                                                      (Angs)
(Angs)
-------------------------------------------------------------------
---------------
  No bonds found for any atoms in the system
-------------------------------------------------------------------
---------------



*******************************************************************
***************
*  General input information
*
*******************************************************************
***************

  Species output for all configurations :

-------------------------------------------------------------------
---------------
  Species    Type    Atomic    Atomic    Charge       Radii
(Angs)     Library
                     Number     Mass       (e)     Cova   Ionic
VDW   Symbol
-------------------------------------------------------------------
---------------
    Ti       Core       22      47.88     2.1960   1.470  0.000
2.190
    O        Core        8      16.00    -1.0980   0.730  0.000
1.360
-------------------------------------------------------------------
---------------


  Lattice summation method              =    Ewald
  Accuracy factor for lattice sums      =    8.000


  Time limit = Infinity
```

```
General interatomic potentials :

-------------------------------------------------------------------
---------------
Atom  Types   Potential         A         B         C         D
Cutoffs(Ang)
  1     2
Min    Max
-------------------------------------------------------------------
---------------
O    c Ti   c Buckingham    0.170E+05 0.194     12.6     0.00
0.000 15.000
O    c O    c Buckingham    0.118E+05 0.234     30.2     0.00
0.000 15.000
Ti   c Ti   c Buckingham    0.311E+05 0.154     5.25     0.00
0.000 15.000
-------------------------------------------------------------------
---------------

*******************************************************************
***************
*  Output for configuration   1 : Rutile
*
*******************************************************************
***************


  Components of energy :

-------------------------------------------------------------------
---------------
  Interatomic potentials     =           6.19028013 eV
  Monopole - monopole (real) =         -25.17073329 eV
  Monopole - monopole (recip)=         -60.62511546 eV
  Monopole - monopole (total)=         -85.79584875 eV
-------------------------------------------------------------------
---------------
  Total lattice energy       =         -79.60556862 eV
-------------------------------------------------------------------
---------------
  Total lattice energy       =          -7680.7205 kJ/(mole unit
cells)
-------------------------------------------------------------------
---------------

  MSI Archive (version 3) open for Movie as Rutile_3D.arc



  Number of variables =      3

  Maximum number of calculations  =          1000
  Maximum Hessian update interval =            10
  Maximum step size               =   1.000000000
  Maximum parameter tolerance     =   0.000010000
  Maximum function  tolerance     =   0.000010000
  Maximum gradient  tolerance     =   0.001000000
  Maximum gradient  component     =   0.010000000
```

```
  Symmetry constrained optimisation

  Symmetry used for second derivatives

  Cell parameters to be optimised using strains

  Newton-Raphson optimiser to be used

  BFGS hessian update to be used

  Minimiser to switch to RFO
  When gradient norm is less than     0.100000

  Start of bulk optimisation :

  Cycle:      0 Energy:       -79.605569  Gnorm:      0.000473
CPU:    0.016


  **** Optimisation achieved ****


  Final energy =     -79.60556862 eV
  Final Gnorm  =       0.00047256

  Components of energy :

------------------------------------------------------------------
---------------
  Interatomic potentials     =           6.19028013 eV
  Monopole - monopole (real) =         -25.17073329 eV
  Monopole - monopole (recip)=         -60.62511546 eV
  Monopole - monopole (total)=         -85.79584875 eV
------------------------------------------------------------------
---------------
  Total lattice energy       =         -79.60556862 eV
------------------------------------------------------------------
---------------
  Total lattice energy       =           -7680.7205 kJ/(mole unit
cells)
------------------------------------------------------------------
---------------

  Final asymmetric unit coordinates :

------------------------------------------------------------------
---------------
   No.  Atomic        x           y           z         Radius
        Label       (Frac)      (Frac)      (Frac)       (Angs)
------------------------------------------------------------------
---------------
     1  Ti    c     0.000000    0.000000    0.000000    0.000000
     2  O     c     0.303283    0.303283    0.000000    0.000000
------------------------------------------------------------------
---------------
```

```
  Final Cartesian lattice vectors (Angstroms) :

        4.492683    0.000000    0.000000
        0.000000    4.492683    0.000000
        0.000000    0.000000    3.008396


  Final cell parameters and derivatives :

------------------------------------------------------------------
---------------
       a            4.492683 Angstrom     dE/de1(xx)     0.000014
eV/strain
       b            4.492683 Angstrom     dE/de2(yy)     0.000000
eV/strain
       c            3.008396 Angstrom     dE/de3(zz)    -0.000039
eV/strain
       alpha       90.000000 Degrees      dE/de4(yz)     0.000000
eV/strain
       beta        90.000000 Degrees      dE/de5(xz)     0.000000
eV/strain
       gamma       90.000000 Degrees      dE/de6(xy)     0.000000
eV/strain
------------------------------------------------------------------
---------------

  Primitive cell volume =            60.722068 Angs**3

  Density of cell =      4.368954 g/cm**3

  Non-primitive cell volume =            60.722068 Angs**3


  Final internal derivatives :

------------------------------------------------------------------
---------------
   No.  Atomic          x             y             z
Radius
        Label          (eV)          (eV)          (eV)
(eV/Angs)
------------------------------------------------------------------
---------------
      1 Ti    c       0.000000      0.000000      0.000000
0.000000
      2 O     c       0.001417      0.000000      0.000000
0.000000
------------------------------------------------------------------
---------------
```

Bond calculation :

Asymmetric unit site	Full lattice sites	No.	Distance (Angs)

No. Distance (Angs)

No bonds found for any atoms in the system

Time to end of optimisation = 0.0160 seconds

Electrostatic potential at atomic positions :

Site No.	Atomic Label		Potential (V)	Derivatives (V/Angs) x	y	z
1	Ti	c	-24.810042	0.000000	0.000000	0.000000
2	O	c	14.259106	0.598140	0.598140	0.000000

Electric Field Gradients at atomic positions :

Site no.	EFGs (V/Angs**2) xx	xy	yy	xz	yz	zz
1	-0.0085	-1.0651	-0.0085	0.0000	0.0000	0.0171
2	-0.9695	9.4124	-0.9695	0.0000	0.0000	1.9389

```
  EFG Tensor properties :

------------------------------------------------------------------------
--------------
   Site no.    Diagonalised EFGs (V/Angs**2)          eVzz/h
Asymmetry
                 xx        yy        zz              (MHz/barn)
Parameter
------------------------------------------------------------------------
--------------
       1        0.0171    1.0565   -1.0736             2.5959
0.9682
       2        1.9389    8.4429  -10.3818            25.1030
0.6265
------------------------------------------------------------------------
--------------

  Total time to end of lattice properties =       0.0160 s


  Peak dynamic memory used =       0.45 MB


  Timing analysis for GULP :

------------------------------------------------------------------------
---------------
  Task / Subroutine                                                  Time
(Seconds)
------------------------------------------------------------------------
---------------
  Calculation of real space energy using symmetry
0.0080
------------------------------------------------------------------------
---------------
  Total CPU time
0.0160
------------------------------------------------------------------------
---------------


  Dump file written as Rutile.res


  Job Finished at 10:29.44  23rd May   2010
```

APPENDIX 3c: Rutile_MD4_298K

```
opti conp conjugate prop distance bond pot efg

# Created by GDIS version 0.90.0
#

switch rfo gnorm 0.100000

name Optimised_Rutile_MD2_298K


dump Optimised_Rutile_MD_phon.res

temperature 298.000

cartesian
O    core    -3.996057   -1.017877   -4.410175   -1.0980000
1.0000000
O    core    -5.533671   -0.712236    1.213252   -1.0980000
1.0000000
O    core    -3.987066   -1.252000    4.156693   -1.0980000
1.0000000
O    core    -4.076434    1.385362   -4.723667   -1.0980000
1.0000000
O    core    -5.213882    0.792325   -1.671573   -1.0980000
1.0000000
O    core    -4.492634    1.457151    1.637137   -1.0980000
1.0000000
O    core    -5.371959    0.717806    4.463831   -1.0980000
1.0000000
O    core    -0.032985   -5.065467   -3.901502   -1.0980000
1.0000000
O    core    -0.966819   -5.494387    1.545334   -1.0980000
1.0000000
O    core    -0.470863   -5.128959    4.608690   -1.0980000
1.0000000
Ti   core    -1.744943   -2.328801   -7.178962    2.1960000
1.0000000
O    core    -3.530398   -2.567656   -6.423862   -1.0980000
1.0000000
O    core    -1.182537   -1.587049   -8.756125   -1.0980000
1.0000000
Ti   core    -2.950870   -2.653096   -4.521746    2.1960000
1.0000000
O    core    -1.442703   -3.353470   -5.599807   -1.0980000
1.0000000
O    core    -2.107108   -0.699016   -6.327321   -1.0980000
1.0000000
O    core    -3.483041   -3.442551   -2.953674   -1.0980000
1.0000000
O    core    -1.629298   -1.907551   -3.162609   -1.0980000
1.0000000
Ti   core    -2.543910   -2.640554   -1.509974    2.1960000
1.0000000
O    core    -0.964920   -3.800651   -1.369848   -1.0980000
1.0000000
O    core    -3.519687   -0.894771   -1.584334   -1.0980000
1.0000000
```

```
O    core    -3.157564   -2.988948    0.216675   -1.0980000
1.0000000
O    core    -1.378381   -1.281709   -0.213247   -1.0980000
1.0000000
Ti   core    -2.120435   -2.095214    1.440256    2.1960000
1.0000000
O    core    -0.541475   -3.110461    1.329252   -1.0980000
1.0000000
O    core    -3.115190   -0.513513    1.713348   -1.0980000
1.0000000
O    core    -2.064145   -3.034472    3.195460   -1.0980000
1.0000000
O    core    -0.508677   -0.438129    4.142268   -1.0980000
1.0000000
Ti   core    -2.755580   -2.536938    4.853167    2.1960000
1.0000000
O    core    -1.031100   -2.776318    5.711813   -1.0980000
1.0000000
O    core    -2.332817   -0.765316    5.870563   -1.0980000
1.0000000
O    core    -3.567296   -2.737127    6.555947   -1.0980000
1.0000000
O    core    -1.109896   -1.279403    8.046450   -1.0980000
1.0000000
Ti   core    -2.904606   -1.472359    7.705364    2.1960000
1.0000000
Ti   core    -2.182757    2.493199   -7.604380    2.1960000
1.0000000
O    core    -1.399609    1.254312   -8.767924   -1.0980000
1.0000000
Ti   core    -3.798498    0.022151   -6.021846    2.1960000
1.0000000
O    core    -3.651935    1.391237   -7.268316   -1.0980000
1.0000000
O    core    -0.809481    3.772321   -7.589040   -1.0980000
1.0000000
Ti   core    -2.456989    2.380680   -4.411049    2.1960000
1.0000000
O    core    -1.284389    1.726540   -6.029386   -1.0980000
1.0000000
O    core    -2.433096    3.718262   -5.782855   -1.0980000
1.0000000
Ti   core    -3.936951    0.425622   -2.975018    2.1960000
1.0000000
O    core    -2.065664    0.533036   -3.725340   -1.0980000
1.0000000
O    core    -0.817016    3.201428   -3.922157   -1.0980000
1.0000000
Ti   core    -1.810459    2.589438   -1.222826    2.1960000
1.0000000
O    core    -0.785124    0.962951   -1.501630   -1.0980000
1.0000000
O    core    -3.066135    2.344037   -2.606969   -1.0980000
1.0000000
Ti   core    -4.473539    0.159401   -0.075784    2.1960000
1.0000000
O    core    -2.921631    1.361167   -0.180383   -1.0980000
1.0000000
```

```
O    core    -1.302704    3.122285    0.551630   -1.0980000
1.0000000
Ti   core    -2.567998    1.713169    1.685496    2.1960000
1.0000000
O    core    -0.835071    0.859107    1.672942   -1.0980000
1.0000000
O    core    -2.498861    3.444418    2.631428   -1.0980000
1.0000000
Ti   core    -4.802492   -0.049181    2.806791    2.1960000
1.0000000
O    core    -3.108658    1.257930    3.715341   -1.0980000
1.0000000
O    core    -0.841778    2.786231    4.201554   -1.0980000
1.0000000
Ti   core    -2.760840    3.016492    4.421173    2.1960000
1.0000000
O    core    -0.441036    0.745423    6.923367   -1.0980000
1.0000000
O    core    -2.942693    2.034042    6.053905   -1.0980000
1.0000000
Ti   core    -3.830077    0.390515    5.446167    2.1960000
1.0000000
O    core    -3.809157    0.119430    7.434105   -1.0980000
1.0000000
O    core    -0.511057    3.282605    7.152371   -1.0980000
1.0000000
Ti   core    -1.802255    1.975134    7.551844    2.1960000
1.0000000
O    core    -1.502756    1.037121    9.118724   -1.0980000
1.0000000
O    core    -1.315216    4.395761   -1.677470   -1.0980000
1.0000000
O    core    -0.837708    5.546343    1.190937   -1.0980000
1.0000000
O    core    -2.152075    4.453212    5.414238   -1.0980000
1.0000000
O    core     2.152075   -4.453212   -5.414237   -1.0980000
1.0000000
O    core     0.837708   -5.546343   -1.190936   -1.0980000
1.0000000
O    core     1.315216   -4.395760    1.677471   -1.0980000
1.0000000
Ti   core     1.802256   -1.975133   -7.551843    2.1960000
1.0000000
O    core     1.502757   -1.037120   -9.118723   -1.0980000
1.0000000
Ti   core     0.273787   -4.177904   -5.467887    2.1960000
1.0000000
O    core     0.511058   -3.282604   -7.152370   -1.0980000
1.0000000
O    core     3.809157   -0.119429   -7.434104   -1.0980000
1.0000000
Ti   core     2.760841   -3.016491   -4.421172    2.1960000
1.0000000
O    core     2.942694   -2.034041   -6.053904   -1.0980000
1.0000000
O    core     0.441036   -0.745423   -6.923366   -1.0980000
1.0000000
```

```
Ti   core     0.655699   -4.175480   -2.416375    2.1960000
1.0000000
O    core     0.841778   -2.786229   -4.201553   -1.0980000
1.0000000
O    core     3.108659   -1.257929   -3.715341   -1.0980000
1.0000000
Ti   core     2.567999   -1.713168   -1.685496    2.1960000
1.0000000
O    core     2.498862   -3.444417   -2.631427   -1.0980000
1.0000000
O    core     0.835071   -0.859106   -1.672942   -1.0980000
1.0000000
Ti   core    -0.014267   -4.666538    0.176418    2.1960000
1.0000000
O    core     1.302704   -3.122284   -0.551629   -1.0980000
1.0000000
O    core     2.921632   -1.361166    0.180383   -1.0980000
1.0000000
Ti   core     1.810460   -2.589438    1.222827    2.1960000
1.0000000
O    core     3.066136   -2.344036    2.606969   -1.0980000
1.0000000
O    core     0.785125   -0.962950    1.501631   -1.0980000
1.0000000
Ti   core    -0.398321   -4.351875    2.898619    2.1960000
1.0000000
O    core     0.817017   -3.201427    3.922158   -1.0980000
1.0000000
O    core     2.065664   -0.533035    3.725340   -1.0980000
1.0000000
Ti   core     2.456990   -2.380679    4.411050    2.1960000
1.0000000
O    core     2.433097   -3.718261    5.782856   -1.0980000
1.0000000
O    core     1.284390   -1.726539    6.029387   -1.0980000
1.0000000
Ti   core     0.450736   -4.032363    5.778584    2.1960000
1.0000000
O    core     0.809482   -3.772320    7.589041   -1.0980000
1.0000000
O    core     3.651936   -1.391236    7.268316   -1.0980000
1.0000000
Ti   core     2.182758   -2.493199    7.604381    2.1960000
1.0000000
O    core     1.399609   -1.254311    8.767924   -1.0980000
1.0000000
Ti   core    -0.105093   -0.053606   -8.838008    2.1960000
1.0000000
Ti   core     2.904607    1.472360   -7.705363    2.1960000
1.0000000
Ti   core     0.384251    0.884409   -5.925669    2.1960000
1.0000000
O    core     1.109897    1.279404   -8.046449   -1.0980000
1.0000000
O    core     3.567297    2.737128   -6.555946   -1.0980000
1.0000000
Ti   core     2.755580    2.536939   -4.853166    2.1960000
1.0000000
```

```
O    core     2.332818    0.765317   -5.870562   -1.0980000
1.0000000
O    core     1.031101    2.776319   -5.711812   -1.0980000
1.0000000
Ti   core    -0.582769   -0.365627   -2.905004    2.1960000
1.0000000
O    core     0.508678    0.438130   -4.142267   -1.0980000
1.0000000
O    core     2.064145    3.034473   -3.195460   -1.0980000
1.0000000
Ti   core     2.120436    2.095214   -1.440255    2.1960000
1.0000000
O    core     3.115190    0.513514   -1.713347   -1.0980000
1.0000000
O    core     0.541476    3.110462   -1.329251   -1.0980000
1.0000000
Ti   core     0.000000    0.000000    0.000000    2.1960000
1.0000000
O    core     1.378381    1.281709    0.213248   -1.0980000
1.0000000
O    core     3.157564    2.988949   -0.216674   -1.0980000
1.0000000
Ti   core     2.543910    2.640555    1.509975    2.1960000
1.0000000
O    core     3.519688    0.894772    1.584335   -1.0980000
1.0000000
O    core     0.964921    3.800651    1.369848   -1.0980000
1.0000000
Ti   core     0.582770    0.365627    2.905004    2.1960000
1.0000000
O    core     1.629298    1.907552    3.162609   -1.0980000
1.0000000
O    core     3.483041    3.442552    2.953675   -1.0980000
1.0000000
Ti   core     2.950871    2.653096    4.521747    2.1960000
1.0000000
O    core     2.107109    0.699017    6.327322   -1.0980000
1.0000000
O    core     1.442704    3.353471    5.599807   -1.0980000
1.0000000
Ti   core    -0.384250   -0.884408    5.925670    2.1960000
1.0000000
O    core     1.182538    1.587049    8.756126   -1.0980000
1.0000000
O    core     3.530399    2.567656    6.423863   -1.0980000
1.0000000
Ti   core     1.744943    2.328802    7.178963    2.1960000
1.0000000
Ti   core     0.105094    0.053607    8.838009    2.1960000
1.0000000
Ti   core    -0.450735    4.032364   -5.778583    2.1960000
1.0000000
Ti   core     0.398322    4.351876   -2.898618    2.1960000
1.0000000
O    core     0.470864    5.128960   -4.608689   -1.0980000
1.0000000
Ti   core     0.014268    4.666539   -0.176417    2.1960000
1.0000000
```

```
O    core     0.966819    5.494387   -1.545333   -1.0980000
1.0000000
Ti   core    -0.655698    4.175481    2.416376    2.1960000
1.0000000
O    core     0.032985    5.065468    3.901503   -1.0980000
1.0000000
Ti   core    -0.273786    4.177905    5.467888    2.1960000
1.0000000
O    core     5.371960   -0.717805   -4.463830   -1.0980000
1.0000000
O    core     4.492635   -1.457150   -1.637136   -1.0980000
1.0000000
O    core     5.213883   -0.792324    1.671574   -1.0980000
1.0000000
O    core     4.076435   -1.385361    4.723668   -1.0980000
1.0000000
Ti   core     3.830078   -0.390514   -5.446167    2.1960000
1.0000000
Ti   core     4.802493    0.049182   -2.806790    2.1960000
1.0000000
O    core     3.987067    1.252001   -4.156692   -1.0980000
1.0000000
Ti   core     4.473540   -0.159400    0.075784    2.1960000
1.0000000
O    core     5.533672    0.712237   -1.213251   -1.0980000
1.0000000
Ti   core     3.936952   -0.425621    2.975019    2.1960000
1.0000000
O    core     3.996058    1.017877    4.410176   -1.0980000
1.0000000
Ti   core     3.798499   -0.022150    6.021847    2.1960000
1.0000000

species
Ti     core    2.196000
O      core   -1.098000
end

buck
O     core Ti    core  16957.6560     0.194000  12.59259
0.00 15.00
buck
O     core O     core  11782.8466     0.234000  30.22222
0.00 15.00
buck
Ti    core Ti    core  31120.4285     0.154000  5.246913
0.00 15.00

print 1
```

APPENDIX 3d: Optimised Rutile Nanoparticles (MD)

```
*****************************************************************
***************
*                        GENERAL UTILITY LATTICE PROGRAM
*
*                                  Julian Gale
*
*                       Nanochemistry Research Institute
*
*             Curtin University of Technology, Western Australia
*
*****************************************************************
***************
* Version = 3.1   * Last modified = 23rd June 2010
*
*****************************************************************
***************
*  optimise     - perform optimisation run
*
*  conp         - constant pressure calculation
*
*  property     - calculate properties for final geometry
*
*  potential    - calculate electrostatic site potentials
*
*  efg          - calculate electrostatic electric field gradient
*
*  bond         - calculate bond lengths
*
*  distance     - calculate distances
*
*  conjugate    - use conjugate gradients minimiser
*
*****************************************************************
***************

  Job Started  at 13:01.28 23rd June 2010

  Number of CPUs =     1


  Total number of configurations input =   1

*****************************************************************
***************
*  Input for Configuration =   1 : Rutile_MD4_298K
*
*****************************************************************
***************

  Formula = O918Ti459

  Number of irreducible atoms/shells =    1377


  Total number atoms/shells =    1377
```

Dimensionality = 0 : Cluster

Charge on cluster = 0.00

Initial cluster dipoles : x = 0.000109 e.Angs
y = -0.000030 e.Angs
z = 0.000020 e.Angs

Temperature of configuration = 298.0 K

Cartesian coordinates of cluster :

No.	Atomic Label		x (Angs)		y (Angs)		z (Angs)		Charge (e)	Occupancy (Frac)
1	O	c	-3.9961	*	-1.0179	*	-4.4102	*	-1.0980	1.000000
2	O	c	-5.5337	*	-0.7122	*	1.2133	*	-1.0980	1.000000
3	O	c	-3.9871	*	-1.2520	*	4.1567	*	-1.0980	1.000000
4	O	c	-4.0764	*	1.3854	*	-4.7237	*	-1.0980	1.000000
5	O	c	-5.2139	*	0.7923	*	-1.6716	*	-1.0980	1.000000
6	O	c	-4.4926	*	1.4572	*	1.6371	*	-1.0980	1.000000
7	O	c	-5.3720	*	0.7178	*	4.4638	*	-1.0980	1.000000
8	O	c	-0.0330	*	-5.0655	*	-3.9015	*	-1.0980	1.000000
9	O	c	-0.9668	*	-5.4944	*	1.5453	*	-1.0980	1.000000
10	O	c	-0.4709	*	-5.1290	*	4.6087	*	-1.0980	1.000000
11	Ti	c	-1.7449	*	-2.3288	*	-7.1790	*	2.1960	1.000000
12	O	c	-3.5304	*	-2.5677	*	-6.4239	*	-1.0980	1.000000
13	O	c	-1.1825	*	-1.5870	*	-8.7561	*	-1.0980	1.000000
14	Ti	c	-2.9509	*	-2.6531	*	-4.5217	*	2.1960	1.000000
15	O	c	-1.4427	*	-3.3535	*	-5.5998	*	-1.0980	1.000000
16	O	c	-2.1071	*	-0.6990	*	-6.3273	*	-1.0980	1.000000
17	O	c	-3.4830	*	-3.4426	*	-2.9537	*	-1.0980	1.000000
18	O	c	-1.6293	*	-1.9076	*	-3.1626	*	-1.0980	1.000000

```
     19 Ti    c     -2.5439 *   -2.6406 *   -1.5100 *    2.1960
1.000000
     20 O     c     -0.9649 *   -3.8007 *   -1.3698 *   -1.0980
1.000000
     21 O     c     -3.5197 *   -0.8948 *   -1.5843 *   -1.0980
1.000000
     22 O     c     -3.1576 *   -2.9889 *    0.2167 *   -1.0980
1.000000
     23 O     c     -1.3784 *   -1.2817 *   -0.2132 *   -1.0980
1.000000
     24 Ti    c     -2.1204 *   -2.0952 *    1.4403 *    2.1960
1.000000
     25 O     c     -0.5415 *   -3.1105 *    1.3293 *   -1.0980
1.000000
     26 O     c     -3.1152 *   -0.5135 *    1.7133 *   -1.0980
1.000000
     27 O     c     -2.0641 *   -3.0345 *    3.1955 *   -1.0980
1.000000
     28 O     c     -0.5087 *   -0.4381 *    4.1423 *   -1.0980
1.000000
     29 Ti    c     -2.7556 *   -2.5369 *    4.8532 *    2.1960
1.000000
     30 O     c     -1.0311 *   -2.7763 *    5.7118 *   -1.0980
1.000000
     31 O     c     -2.3328 *   -0.7653 *    5.8706 *   -1.0980
1.000000
     32 O     c     -3.5673 *   -2.7371 *    6.5559 *   -1.0980
1.000000
     33 O     c     -1.1099 *   -1.2794 *    8.0465 *   -1.0980
1.000000
     34 Ti    c     -2.9046 *   -1.4724 *    7.7054 *    2.1960
1.000000
     35 Ti    c     -2.1828 *    2.4932 *   -7.6044 *    2.1960
1.000000
     36 O     c     -1.3996 *    1.2543 *   -8.7679 *   -1.0980
1.000000
     37 Ti    c     -3.7985 *    0.0222 *   -6.0218 *    2.1960
1.000000
     38 O     c     -3.6519 *    1.3912 *   -7.2683 *   -1.0980
1.000000
     39 O     c     -0.8095 *    3.7723 *   -7.5890 *   -1.0980
1.000000
     40 Ti    c     -2.4570 *    2.3807 *   -4.4110 *    2.1960
1.000000
     41 O     c     -1.2844 *    1.7265 *   -6.0294 *   -1.0980
1.000000
     42 O     c     -2.4331 *    3.7183 *   -5.7829 *   -1.0980
1.000000
     43 Ti    c     -3.9370 *    0.4256 *   -2.9750 *    2.1960
1.000000
     44 O     c     -2.0657 *    0.5330 *   -3.7253 *   -1.0980
1.000000
     45 O     c     -0.8170 *    3.2014 *   -3.9222 *   -1.0980
1.000000
     46 Ti    c     -1.8105 *    2.5894 *   -1.2228 *    2.1960
1.000000
     47 O     c     -0.7851 *    0.9630 *   -1.5016 *   -1.0980
1.000000
```

```
     48 O     c     -3.0661 *    2.3440 *   -2.6070 *   -1.0980
1.000000
     49 Ti    c     -4.4735 *    0.1594 *   -0.0758 *    2.1960
1.000000
     50 O     c     -2.9216 *    1.3612 *   -0.1804 *   -1.0980
1.000000
     51 O     c     -1.3027 *    3.1223 *    0.5516 *   -1.0980
1.000000
     52 Ti    c     -2.5680 *    1.7132 *    1.6855 *    2.1960
1.000000
     53 O     c     -0.8351 *    0.8591 *    1.6729 *   -1.0980
1.000000
     54 O     c     -2.4989 *    3.4444 *    2.6314 *   -1.0980
1.000000
     55 Ti    c     -4.8025 *   -0.0492 *    2.8068 *    2.1960
1.000000
     56 O     c     -3.1087 *    1.2579 *    3.7153 *   -1.0980
1.000000
     57 O     c     -0.8418 *    2.7862 *    4.2016 *   -1.0980
1.000000
     58 Ti    c     -2.7608 *    3.0165 *    4.4212 *    2.1960
1.000000
     59 O     c     -0.4410 *    0.7454 *    6.9234 *   -1.0980
1.000000
     60 O     c     -2.9427 *    2.0340 *    6.0539 *   -1.0980
1.000000
     61 Ti    c     -3.8301 *    0.3905 *    5.4462 *    2.1960
1.000000
     62 O     c     -3.8092 *    0.1194 *    7.4341 *   -1.0980
1.000000
     63 O     c     -0.5111 *    3.2826 *    7.1524 *   -1.0980
1.000000
     64 Ti    c     -1.8023 *    1.9751 *    7.5518 *    2.1960
1.000000
     65 O     c     -1.5028 *    1.0371 *    9.1187 *   -1.0980
1.000000
     66 O     c     -1.3152 *    4.3958 *   -1.6775 *   -1.0980
1.000000
     67 O     c     -0.8377 *    5.5463 *    1.1909 *   -1.0980
1.000000
     68 O     c     -2.1521 *    4.4532 *    5.4142 *   -1.0980
1.000000
     69 O     c      2.1521 *   -4.4532 *   -5.4142 *   -1.0980
1.000000
     70 O     c      0.8377 *   -5.5463 *   -1.1909 *   -1.0980
1.000000
     71 O     c      1.3152 *   -4.3958 *    1.6775 *   -1.0980
1.000000
     72 Ti    c      1.8023 *   -1.9751 *   -7.5518 *    2.1960
1.000000
     73 O     c      1.5028 *   -1.0371 *   -9.1187 *   -1.0980
1.000000
     74 Ti    c      0.2738 *   -4.1779 *   -5.4679 *    2.1960
1.000000
     75 O     c      0.5111 *   -3.2826 *   -7.1524 *   -1.0980
1.000000
     76 O     c      3.8092 *   -0.1194 *   -7.4341 *   -1.0980
1.000000
```

```
     77 Ti    c      2.7608 *   -3.0165 *   -4.4212 *    2.1960
1.000000
     78 O     c      2.9427 *   -2.0340 *   -6.0539 *   -1.0980
1.000000
     79 O     c      0.4410 *   -0.7454 *   -6.9234 *   -1.0980
1.000000
     80 Ti    c      0.6557 *   -4.1755 *   -2.4164 *    2.1960
1.000000
     81 O     c      0.8418 *   -2.7862 *   -4.2016 *   -1.0980
1.000000
     82 O     c      3.1087 *   -1.2579 *   -3.7153 *   -1.0980
1.000000
     83 Ti    c      2.5680 *   -1.7132 *   -1.6855 *    2.1960
1.000000
     84 O     c      2.4989 *   -3.4444 *   -2.6314 *   -1.0980
1.000000
     85 O     c      0.8351 *   -0.8591 *   -1.6729 *   -1.0980
1.000000
     86 Ti    c     -0.0143 *   -4.6665 *    0.1764 *    2.1960
1.000000
     87 O     c      1.3027 *   -3.1223 *   -0.5516 *   -1.0980
1.000000
     88 O     c      2.9216 *   -1.3612 *    0.1804 *   -1.0980
1.000000
     89 Ti    c      1.8105 *   -2.5894 *    1.2228 *    2.1960
1.000000
     90 O     c      3.0661 *   -2.3440 *    2.6070 *   -1.0980
1.000000
     91 O     c      0.7851 *   -0.9630 *    1.5016 *   -1.0980
1.000000
     92 Ti    c     -0.3983 *   -4.3519 *    2.8986 *    2.1960
1.000000
     93 O     c      0.8170 *   -3.2014 *    3.9222 *   -1.0980
1.000000
     94 O     c      2.0657 *   -0.5330 *    3.7253 *   -1.0980
1.000000
     95 Ti    c      2.4570 *   -2.3807 *    4.4111 *    2.1960
1.000000
     96 O     c      2.4331 *   -3.7183 *    5.7829 *   -1.0980
1.000000
     97 O     c      1.2844 *   -1.7265 *    6.0294 *   -1.0980
1.000000
     98 Ti    c      0.4507 *   -4.0324 *    5.7786 *    2.1960
1.000000
     99 O     c      0.8095 *   -3.7723 *    7.5890 *   -1.0980
1.000000
    100 O     c      3.6519 *   -1.3912 *    7.2683 *   -1.0980
1.000000
    101 Ti    c      2.1828 *   -2.4932 *    7.6044 *    2.1960
1.000000
    102 O     c      1.3996 *   -1.2543 *    8.7679 *   -1.0980
1.000000
    103 Ti    c     -0.1051 *   -0.0536 *   -8.8380 *    2.1960
1.000000
    104 Ti    c      2.9046 *    1.4724 *   -7.7054 *    2.1960
1.000000
    105 Ti    c      0.3843 *    0.8844 *   -5.9257 *    2.1960
1.000000
```

```
    106 O     c      1.1099 *    1.2794 *   -8.0464 *   -1.0980
1.000000
    107 O     c      3.5673 *    2.7371 *   -6.5559 *   -1.0980
1.000000
    108 Ti    c      2.7556 *    2.5369 *   -4.8532 *    2.1960
1.000000
    109 O     c      2.3328 *    0.7653 *   -5.8706 *   -1.0980
1.000000
    110 O     c      1.0311 *    2.7763 *   -5.7118 *   -1.0980
1.000000
    111 Ti    c     -0.5828 *   -0.3656 *   -2.9050 *    2.1960
1.000000
    112 O     c      0.5087 *    0.4381 *   -4.1423 *   -1.0980
1.000000
    113 O     c      2.0641 *    3.0345 *   -3.1955 *   -1.0980
1.000000
    114 Ti    c      2.1204 *    2.0952 *   -1.4403 *    2.1960
1.000000
    115 O     c      3.1152 *    0.5135 *   -1.7133 *   -1.0980
1.000000
    116 O     c      0.5415 *    3.1105 *   -1.3293 *   -1.0980
1.000000
    117 Ti    c      0.0000 *    0.0000 *    0.0000 *    2.1960
1.000000
    118 O     c      1.3784 *    1.2817 *    0.2132 *   -1.0980
1.000000
    119 O     c      3.1576 *    2.9889 *   -0.2167 *   -1.0980
1.000000
    120 Ti    c      2.5439 *    2.6406 *    1.5100 *    2.1960
1.000000
    121 O     c      3.5197 *    0.8948 *    1.5843 *   -1.0980
1.000000
    122 O     c      0.9649 *    3.8007 *    1.3698 *   -1.0980
1.000000
    123 Ti    c      0.5828 *    0.3656 *    2.9050 *    2.1960
1.000000
    124 O     c      1.6293 *    1.9076 *    3.1626 *   -1.0980
1.000000
    125 O     c      3.4830 *    3.4426 *    2.9537 *   -1.0980
1.000000
    126 Ti    c      2.9509 *    2.6531 *    4.5217 *    2.1960
1.000000
    127 O     c      2.1071 *    0.6990 *    6.3273 *   -1.0980
1.000000
    128 O     c      1.4427 *    3.3535 *    5.5998 *   -1.0980
1.000000
    129 Ti    c     -0.3843 *   -0.8844 *    5.9257 *    2.1960
1.000000
    130 O     c      1.1825 *    1.5870 *    8.7561 *   -1.0980
1.000000
    131 O     c      3.5304 *    2.5677 *    6.4239 *   -1.0980
1.000000
    132 Ti    c      1.7449 *    2.3288 *    7.1790 *    2.1960
1.000000
    133 Ti    c      0.1051 *    0.0536 *    8.8380 *    2.1960
1.000000
    134 Ti    c     -0.4507 *    4.0324 *   -5.7786 *    2.1960
1.000000
```

```
    135 Ti    c      0.3983 *    4.3519 *   -2.8986 *    2.1960
1.000000
    136 O     c      0.4709 *    5.1290 *   -4.6087 *   -1.0980
1.000000
    137 Ti    c      0.0143 *    4.6665 *   -0.1764 *    2.1960
1.000000
    138 O     c      0.9668 *    5.4944 *   -1.5453 *   -1.0980
1.000000
    139 Ti    c     -0.6557 *    4.1755 *    2.4164 *    2.1960
1.000000
    140 O     c      0.0330 *    5.0655 *    3.9015 *   -1.0980
1.000000
    141 Ti    c     -0.2738 *    4.1779 *    5.4679 *    2.1960
1.000000
    142 O     c      5.3720 *   -0.7178 *   -4.4638 *   -1.0980
1.000000
    143 O     c      4.4926 *   -1.4571 *   -1.6371 *   -1.0980
1.000000
    144 O     c      5.2139 *   -0.7923 *    1.6716 *   -1.0980
1.000000
    145 O     c      4.0764 *   -1.3854 *    4.7237 *   -1.0980
1.000000
    146 Ti    c      3.8301 *   -0.3905 *   -5.4462 *    2.1960
1.000000
    147 Ti    c      4.8025 *    0.0492 *   -2.8068 *    2.1960
1.000000
    148 O     c      3.9871 *    1.2520 *   -4.1567 *   -1.0980
1.000000
    149 Ti    c      4.4735 *   -0.1594 *    0.0758 *    2.1960
1.000000
    150 O     c      5.5337 *    0.7122 *   -1.2133 *   -1.0980
1.000000
    151 Ti    c      3.9370 *   -0.4256 *    2.9750 *    2.1960
1.000000
    152 O     c      3.9961 *    1.0179 *    4.4102 *   -1.0980
1.000000
    153 Ti    c      3.7985 *   -0.0222 *    6.0218 *    2.1960
1.000000
    154 Ti    c      3.7985     -0.0222      6.0218      2.1960
1.000000
    155 O     c      3.9961      1.0179      4.4102     -1.0980
1.000000
    156 Ti    c      3.9370     -0.4256      2.9750      2.1960
1.000000
    157 O     c      5.5337      0.7122     -1.2133     -1.0980
1.000000
    158 Ti    c      4.4735     -0.1594      0.0758      2.1960
1.000000
    159 O     c      3.9871      1.2520     -4.1567     -1.0980
1.000000
    160 Ti    c      4.8025      0.0492     -2.8068      2.1960
1.000000
    161 Ti    c      3.8301     -0.3905     -5.4462      2.1960
1.000000
    162 O     c      4.0764     -1.3854      4.7237     -1.0980
1.000000
    163 O     c      5.2139     -0.7923      1.6716     -1.0980
1.000000
```

```
    164 O     c      4.4926     -1.4571     -1.6371     -1.0980
1.000000
    165 O     c      5.3720     -0.7178     -4.4638     -1.0980
1.000000
    166 Ti    c     -0.2738      4.1779      5.4679      2.1960
1.000000
    167 O     c      0.0330      5.0655      3.9015     -1.0980
1.000000
    168 Ti    c     -0.6557      4.1755      2.4164      2.1960
1.000000
    169 O     c      0.9668      5.4944     -1.5453     -1.0980
1.000000
    170 Ti    c      0.0143      4.6665     -0.1764      2.1960
1.000000
    171 O     c      0.4709      5.1290     -4.6087     -1.0980
1.000000
    172 Ti    c      0.3983      4.3519     -2.8986      2.1960
1.000000
    173 Ti    c     -0.4507      4.0324     -5.7786      2.1960
1.000000
    174 Ti    c      0.1051      0.0536      8.8380      2.1960
1.000000
    175 Ti    c      1.7449      2.3288      7.1790      2.1960
1.000000
    176 O     c      3.5304      2.5677      6.4239     -1.0980
1.000000
    177 O     c      1.1825      1.5870      8.7561     -1.0980
1.000000
    178 Ti    c     -0.3843     -0.8844      5.9257      2.1960
1.000000
    179 O     c      1.4427      3.3535      5.5998     -1.0980
1.000000
    180 O     c      2.1071      0.6990      6.3273     -1.0980
1.000000
    181 Ti    c      2.9509      2.6531      4.5217      2.1960
1.000000
    182 O     c      3.4830      3.4426      2.9537     -1.0980
1.000000
    183 O     c      1.6293      1.9076      3.1626     -1.0980
1.000000
    184 Ti    c      0.5828      0.3656      2.9050      2.1960
1.000000
    185 O     c      0.9649      3.8007      1.3698     -1.0980
1.000000
    186 O     c      3.5197      0.8948      1.5843     -1.0980
1.000000
    187 Ti    c      2.5439      2.6406      1.5100      2.1960
1.000000
    188 O     c      3.1576      2.9889     -0.2167     -1.0980
1.000000
    189 O     c      1.3784      1.2817      0.2132     -1.0980
1.000000
    190 Ti    c      0.0000      0.0000      0.0000      2.1960
1.000000
    191 O     c      0.5415      3.1105     -1.3293     -1.0980
1.000000
    192 O     c      3.1152      0.5135     -1.7133     -1.0980
1.000000
```

```
    193 Ti    c      2.1204      2.0952     -1.4403      2.1960
1.000000
    194 O     c      2.0641      3.0345     -3.1955     -1.0980
1.000000
    195 O     c      0.5087      0.4381     -4.1423     -1.0980
1.000000
    196 Ti    c     -0.5828     -0.3656     -2.9050      2.1960
1.000000
    197 O     c      1.0311      2.7763     -5.7118     -1.0980
1.000000
    198 O     c      2.3328      0.7653     -5.8706     -1.0980
1.000000
    199 Ti    c      2.7556      2.5369     -4.8532      2.1960
1.000000
    200 O     c      3.5673      2.7371     -6.5559     -1.0980
1.000000
    201 O     c      1.1099      1.2794     -8.0464     -1.0980
1.000000
    202 Ti    c      0.3843      0.8844     -5.9257      2.1960
1.000000
    203 Ti    c      2.9046      1.4724     -7.7054      2.1960
1.000000
    204 Ti    c     -0.1051     -0.0536     -8.8380      2.1960
1.000000
    205 O     c      1.3996     -1.2543      8.7679     -1.0980
1.000000
    206 Ti    c      2.1828     -2.4932      7.6044      2.1960
1.000000
    207 O     c      3.6519     -1.3912      7.2683     -1.0980
1.000000
    208 O     c      0.8095     -3.7723      7.5890     -1.0980
1.000000
    209 Ti    c      0.4507     -4.0324      5.7786      2.1960
1.000000
    210 O     c      1.2844     -1.7265      6.0294     -1.0980
1.000000
    211 O     c      2.4331     -3.7183      5.7829     -1.0980
1.000000
    212 Ti    c      2.4570     -2.3807      4.4111      2.1960
1.000000
    213 O     c      2.0657     -0.5330      3.7253     -1.0980
1.000000
    214 O     c      0.8170     -3.2014      3.9222     -1.0980
1.000000
    215 Ti    c     -0.3983     -4.3519      2.8986      2.1960
1.000000
    216 O     c      0.7851     -0.9630      1.5016     -1.0980
1.000000
    217 O     c      3.0661     -2.3440      2.6070     -1.0980
1.000000
    218 Ti    c      1.8105     -2.5894      1.2228      2.1960
1.000000
    219 O     c      2.9216     -1.3612      0.1804     -1.0980
1.000000
    220 O     c      1.3027     -3.1223     -0.5516     -1.0980
1.000000
    221 Ti    c     -0.0143     -4.6665      0.1764      2.1960
1.000000
```

```
    222 O     c      0.8351     -0.8591     -1.6729     -1.0980
1.000000
    223 O     c      2.4989     -3.4444     -2.6314     -1.0980
1.000000
    224 Ti    c      2.5680     -1.7132     -1.6855      2.1960
1.000000
    225 O     c      3.1087     -1.2579     -3.7153     -1.0980
1.000000
    226 O     c      0.8418     -2.7862     -4.2016     -1.0980
1.000000
    227 Ti    c      0.6557     -4.1755     -2.4164      2.1960
1.000000
    228 O     c      0.4410     -0.7454     -6.9234     -1.0980
1.000000
    229 O     c      2.9427     -2.0340     -6.0539     -1.0980
1.000000
    230 Ti    c      2.7608     -3.0165     -4.4212      2.1960
1.000000
    231 O     c      3.8092     -0.1194     -7.4341     -1.0980
1.000000
    232 O     c      0.5111     -3.2826     -7.1524     -1.0980
1.000000
    233 Ti    c      0.2738     -4.1779     -5.4679      2.1960
1.000000
    234 O     c      1.5028     -1.0371     -9.1187     -1.0980
1.000000
    235 Ti    c      1.8023     -1.9751     -7.5518      2.1960
1.000000
    236 O     c      1.3152     -4.3958      1.6775     -1.0980
1.000000
    237 O     c      0.8377     -5.5463     -1.1909     -1.0980
1.000000
    238 O     c      2.1521     -4.4532     -5.4142     -1.0980
1.000000
    239 O     c     -2.1521      4.4532      5.4142     -1.0980
1.000000
    240 O     c     -0.8377      5.5463      1.1909     -1.0980
1.000000
    241 O     c     -1.3152      4.3958     -1.6775     -1.0980
1.000000
    242 O     c     -1.5028      1.0371      9.1187     -1.0980
1.000000
    243 Ti    c     -1.8023      1.9751      7.5518      2.1960
1.000000
    244 O     c     -0.5111      3.2826      7.1524     -1.0980
1.000000
    245 O     c     -3.8092      0.1194      7.4341     -1.0980
1.000000
    246 Ti    c     -3.8301      0.3905      5.4462      2.1960
1.000000
    247 O     c     -2.9427      2.0340      6.0539     -1.0980
1.000000
    248 O     c     -0.4410      0.7454      6.9234     -1.0980
1.000000
    249 Ti    c     -2.7608      3.0165      4.4212      2.1960
1.000000
    250 O     c     -0.8418      2.7862      4.2016     -1.0980
1.000000
```

```
    251 O     c     -3.1087      1.2579      3.7153     -1.0980
1.000000
    252 Ti    c     -4.8025     -0.0492      2.8068      2.1960
1.000000
    253 O     c     -2.4989      3.4444      2.6314     -1.0980
1.000000
    254 O     c     -0.8351      0.8591      1.6729     -1.0980
1.000000
    255 Ti    c     -2.5680      1.7132      1.6855      2.1960
1.000000
    256 O     c     -1.3027      3.1223      0.5516     -1.0980
1.000000
    257 O     c     -2.9216      1.3612     -0.1804     -1.0980
1.000000
    258 Ti    c     -4.4735      0.1594     -0.0758      2.1960
1.000000
    259 O     c     -3.0661      2.3440     -2.6070     -1.0980
1.000000
    260 O     c     -0.7851      0.9630     -1.5016     -1.0980
1.000000
    261 Ti    c     -1.8105      2.5894     -1.2228      2.1960
1.000000
    262 O     c     -0.8170      3.2014     -3.9222     -1.0980
1.000000
    263 O     c     -2.0657      0.5330     -3.7253     -1.0980
1.000000
    264 Ti    c     -3.9370      0.4256     -2.9750      2.1960
1.000000
    265 O     c     -2.4331      3.7183     -5.7829     -1.0980
1.000000
    266 O     c     -1.2844      1.7265     -6.0294     -1.0980
1.000000
    267 Ti    c     -2.4570      2.3807     -4.4110      2.1960
1.000000
    268 O     c     -0.8095      3.7723     -7.5890     -1.0980
1.000000
    269 O     c     -3.6519      1.3912     -7.2683     -1.0980
1.000000
    270 Ti    c     -3.7985      0.0222     -6.0218      2.1960
1.000000
    271 O     c     -1.3996      1.2543     -8.7679     -1.0980
1.000000
    272 Ti    c     -2.1828      2.4932     -7.6044      2.1960
1.000000
    273 Ti    c     -2.9046     -1.4724      7.7054      2.1960
1.000000
    274 O     c     -1.1099     -1.2794      8.0465     -1.0980
1.000000
    275 O     c     -3.5673     -2.7371      6.5559     -1.0980
1.000000
    276 O     c     -2.3328     -0.7653      5.8706     -1.0980
1.000000
    277 O     c     -1.0311     -2.7763      5.7118     -1.0980
1.000000
    278 Ti    c     -2.7556     -2.5369      4.8532      2.1960
1.000000
    279 O     c     -0.5087     -0.4381      4.1423     -1.0980
1.000000
```

```
    280 O     c     -2.0641     -3.0345      3.1955     -1.0980
1.000000
    281 O     c     -3.1152     -0.5135      1.7133     -1.0980
1.000000
    282 O     c     -0.5415     -3.1105      1.3293     -1.0980
1.000000
    283 Ti    c     -2.1204     -2.0952      1.4403      2.1960
1.000000
    284 O     c     -1.3784     -1.2817     -0.2132     -1.0980
1.000000
    285 O     c     -3.1576     -2.9889      0.2167     -1.0980
1.000000
    286 O     c     -3.5197     -0.8948     -1.5843     -1.0980
1.000000
    287 O     c     -0.9649     -3.8007     -1.3698     -1.0980
1.000000
    288 Ti    c     -2.5439     -2.6406     -1.5100      2.1960
1.000000
    289 O     c     -1.6293     -1.9076     -3.1626     -1.0980
1.000000
    290 O     c     -3.4830     -3.4426     -2.9537     -1.0980
1.000000
    291 O     c     -2.1071     -0.6990     -6.3273     -1.0980
1.000000
    292 O     c     -1.4427     -3.3535     -5.5998     -1.0980
1.000000
    293 Ti    c     -2.9509     -2.6531     -4.5217      2.1960
1.000000
    294 O     c     -1.1825     -1.5870     -8.7561     -1.0980
1.000000
    295 O     c     -3.5304     -2.5677     -6.4239     -1.0980
1.000000
    296 Ti    c     -1.7449     -2.3288     -7.1790      2.1960
1.000000
    297 O     c     -0.4709     -5.1290      4.6087     -1.0980
1.000000
    298 O     c     -0.9668     -5.4944      1.5453     -1.0980
1.000000
    299 O     c     -0.0330     -5.0655     -3.9015     -1.0980
1.000000
    300 O     c     -5.3720      0.7178      4.4638     -1.0980
1.000000
    301 O     c     -4.4926      1.4572      1.6371     -1.0980
1.000000
    302 O     c     -5.2139      0.7923     -1.6716     -1.0980
1.000000
    303 O     c     -4.0764      1.3854     -4.7237     -1.0980
1.000000
    304 O     c     -3.9871     -1.2520      4.1567     -1.0980
1.000000
    305 O     c     -5.5337     -0.7122      1.2133     -1.0980
1.000000
    306 O     c     -3.9961     -1.0179     -4.4102     -1.0980
1.000000
    307 Ti    c      3.7985     -0.0222      6.0218      2.1960
1.000000
    308 O     c      3.9961      1.0179      4.4102     -1.0980
1.000000
```

```
    309 Ti    c      3.9370     -0.4256      2.9750      2.1960
1.000000
    310 O     c      5.5337      0.7122     -1.2133     -1.0980
1.000000
    311 Ti    c      4.4735     -0.1594      0.0758      2.1960
1.000000
    312 O     c      3.9871      1.2520     -4.1567     -1.0980
1.000000
    313 Ti    c      4.8025      0.0492     -2.8068      2.1960
1.000000
    314 Ti    c      3.8301     -0.3905     -5.4462      2.1960
1.000000
    315 O     c      4.0764     -1.3854      4.7237     -1.0980
1.000000
    316 O     c      5.2139     -0.7923      1.6716     -1.0980
1.000000
    317 O     c      4.4926     -1.4571     -1.6371     -1.0980
1.000000
    318 O     c      5.3720     -0.7178     -4.4638     -1.0980
1.000000
    319 Ti    c     -0.2738      4.1779      5.4679      2.1960
1.000000
    320 O     c      0.0330      5.0655      3.9015     -1.0980
1.000000
    321 Ti    c     -0.6557      4.1755      2.4164      2.1960
1.000000
    322 O     c      0.9668      5.4944     -1.5453     -1.0980
1.000000
    323 Ti    c      0.0143      4.6665     -0.1764      2.1960
1.000000
    324 O     c      0.4709      5.1290     -4.6087     -1.0980
1.000000
    325 Ti    c      0.3983      4.3519     -2.8986      2.1960
1.000000
    326 Ti    c     -0.4507      4.0324     -5.7786      2.1960
1.000000
    327 Ti    c      0.1051      0.0536      8.8380      2.1960
1.000000
    328 Ti    c      1.7449      2.3288      7.1790      2.1960
1.000000
    329 O     c      3.5304      2.5677      6.4239     -1.0980
1.000000
    330 O     c      1.1825      1.5870      8.7561     -1.0980
1.000000
    331 Ti    c     -0.3843     -0.8844      5.9257      2.1960
1.000000
    332 O     c      1.4427      3.3535      5.5998     -1.0980
1.000000
    333 O     c      2.1071      0.6990      6.3273     -1.0980
1.000000
    334 Ti    c      2.9509      2.6531      4.5217      2.1960
1.000000
    335 O     c      3.4830      3.4426      2.9537     -1.0980
1.000000
    336 O     c      1.6293      1.9076      3.1626     -1.0980
1.000000
    337 Ti    c      0.5828      0.3656      2.9050      2.1960
1.000000
```

```
    338 O     c      0.9649      3.8007      1.3698     -1.0980
1.000000
    339 O     c      3.5197      0.8948      1.5843     -1.0980
1.000000
    340 Ti    c      2.5439      2.6406      1.5100      2.1960
1.000000
    341 O     c      3.1576      2.9889     -0.2167     -1.0980
1.000000
    342 O     c      1.3784      1.2817      0.2132     -1.0980
1.000000
    343 Ti    c      0.0000      0.0000      0.0000      2.1960
1.000000
    344 O     c      0.5415      3.1105     -1.3293     -1.0980
1.000000
    345 O     c      3.1152      0.5135     -1.7133     -1.0980
1.000000
    346 Ti    c      2.1204      2.0952     -1.4403      2.1960
1.000000
    347 O     c      2.0641      3.0345     -3.1955     -1.0980
1.000000
    348 O     c      0.5087      0.4381     -4.1423     -1.0980
1.000000
    349 Ti    c     -0.5828     -0.3656     -2.9050      2.1960
1.000000
    350 O     c      1.0311      2.7763     -5.7118     -1.0980
1.000000
    351 O     c      2.3328      0.7653     -5.8706     -1.0980
1.000000
    352 Ti    c      2.7556      2.5369     -4.8532      2.1960
1.000000
    353 O     c      3.5673      2.7371     -6.5559     -1.0980
1.000000
    354 O     c      1.1099      1.2794     -8.0464     -1.0980
1.000000
    355 Ti    c      0.3843      0.8844     -5.9257      2.1960
1.000000
    356 Ti    c      2.9046      1.4724     -7.7054      2.1960
1.000000
    357 Ti    c     -0.1051     -0.0536     -8.8380      2.1960
1.000000
    358 O     c      1.3996     -1.2543      8.7679     -1.0980
1.000000
    359 Ti    c      2.1828     -2.4932      7.6044      2.1960
1.000000
    360 O     c      3.6519     -1.3912      7.2683     -1.0980
1.000000
    361 O     c      0.8095     -3.7723      7.5890     -1.0980
1.000000
    362 Ti    c      0.4507     -4.0324      5.7786      2.1960
1.000000
    363 O     c      1.2844     -1.7265      6.0294     -1.0980
1.000000
    364 O     c      2.4331     -3.7183      5.7829     -1.0980
1.000000
    365 Ti    c      2.4570     -2.3807      4.4111      2.1960
1.000000
    366 O     c      2.0657     -0.5330      3.7253     -1.0980
1.000000
```

```
    367 O     c      0.8170     -3.2014      3.9222     -1.0980
1.000000
    368 Ti    c     -0.3983     -4.3519      2.8986      2.1960
1.000000
    369 O     c      0.7851     -0.9630      1.5016     -1.0980
1.000000
    370 O     c      3.0661     -2.3440      2.6070     -1.0980
1.000000
    371 Ti    c      1.8105     -2.5894      1.2228      2.1960
1.000000
    372 O     c      2.9216     -1.3612      0.1804     -1.0980
1.000000
    373 O     c      1.3027     -3.1223     -0.5516     -1.0980
1.000000
    374 Ti    c     -0.0143     -4.6665      0.1764      2.1960
1.000000
    375 O     c      0.8351     -0.8591     -1.6729     -1.0980
1.000000
    376 O     c      2.4989     -3.4444     -2.6314     -1.0980
1.000000
    377 Ti    c      2.5680     -1.7132     -1.6855      2.1960
1.000000
    378 O     c      3.1087     -1.2579     -3.7153     -1.0980
1.000000
    379 O     c      0.8418     -2.7862     -4.2016     -1.0980
1.000000
    380 Ti    c      0.6557     -4.1755     -2.4164      2.1960
1.000000
    381 O     c      0.4410     -0.7454     -6.9234     -1.0980
1.000000
    382 O     c      2.9427     -2.0340     -6.0539     -1.0980
1.000000
    383 Ti    c      2.7608     -3.0165     -4.4212      2.1960
1.000000
    384 O     c      3.8092     -0.1194     -7.4341     -1.0980
1.000000
    385 O     c      0.5111     -3.2826     -7.1524     -1.0980
1.000000
    386 Ti    c      0.2738     -4.1779     -5.4679      2.1960
1.000000
    387 O     c      1.5028     -1.0371     -9.1187     -1.0980
1.000000
    388 Ti    c      1.8023     -1.9751     -7.5518      2.1960
1.000000
    389 O     c      1.3152     -4.3958      1.6775     -1.0980
1.000000
    390 O     c      0.8377     -5.5463     -1.1909     -1.0980
1.000000
    391 O     c      2.1521     -4.4532     -5.4142     -1.0980
1.000000
    392 O     c     -2.1521      4.4532      5.4142     -1.0980
1.000000
    393 O     c     -0.8377      5.5463      1.1909     -1.0980
1.000000
    394 O     c     -1.3152      4.3958     -1.6775     -1.0980
1.000000
    395 O     c     -1.5028      1.0371      9.1187     -1.0980
1.000000
```

```
    396 Ti    c     -1.8023      1.9751      7.5518      2.1960
1.000000
    397 O     c     -0.5111      3.2826      7.1524     -1.0980
1.000000
    398 O     c     -3.8092      0.1194      7.4341     -1.0980
1.000000
    399 Ti    c     -3.8301      0.3905      5.4462      2.1960
1.000000
    400 O     c     -2.9427      2.0340      6.0539     -1.0980
1.000000
    401 O     c     -0.4410      0.7454      6.9234     -1.0980
1.000000
    402 Ti    c     -2.7608      3.0165      4.4212      2.1960
1.000000
    403 O     c     -0.8418      2.7862      4.2016     -1.0980
1.000000
    404 O     c     -3.1087      1.2579      3.7153     -1.0980
1.000000
    405 Ti    c     -4.8025     -0.0492      2.8068      2.1960
1.000000
    406 O     c     -2.4989      3.4444      2.6314     -1.0980
1.000000
    407 O     c     -0.8351      0.8591      1.6729     -1.0980
1.000000
    408 Ti    c     -2.5680      1.7132      1.6855      2.1960
1.000000
    409 O     c     -1.3027      3.1223      0.5516     -1.0980
1.000000
    410 O     c     -2.9216      1.3612     -0.1804     -1.0980
1.000000
    411 Ti    c     -4.4735      0.1594     -0.0758      2.1960
1.000000
    412 O     c     -3.0661      2.3440     -2.6070     -1.0980
1.000000
    413 O     c     -0.7851      0.9630     -1.5016     -1.0980
1.000000
    414 Ti    c     -1.8105      2.5894     -1.2228      2.1960
1.000000
    415 O     c     -0.8170      3.2014     -3.9222     -1.0980
1.000000
    416 O     c     -2.0657      0.5330     -3.7253     -1.0980
1.000000
    417 Ti    c     -3.9370      0.4256     -2.9750      2.1960
1.000000
    418 O     c     -2.4331      3.7183     -5.7829     -1.0980
1.000000
    419 O     c     -1.2844      1.7265     -6.0294     -1.0980
1.000000
    420 Ti    c     -2.4570      2.3807     -4.4110      2.1960
1.000000
    421 O     c     -0.8095      3.7723     -7.5890     -1.0980
1.000000
    422 O     c     -3.6519      1.3912     -7.2683     -1.0980
1.000000
    423 Ti    c     -3.7985      0.0222     -6.0218      2.1960
1.000000
    424 O     c     -1.3996      1.2543     -8.7679     -1.0980
1.000000
```

```
    425 Ti    c     -2.1828      2.4932     -7.6044      2.1960
1.000000
    426 Ti    c     -2.9046     -1.4724      7.7054      2.1960
1.000000
    427 O     c     -1.1099     -1.2794      8.0465     -1.0980
1.000000
    428 O     c     -3.5673     -2.7371      6.5559     -1.0980
1.000000
    429 O     c     -2.3328     -0.7653      5.8706     -1.0980
1.000000
    430 O     c     -1.0311     -2.7763      5.7118     -1.0980
1.000000
    431 Ti    c     -2.7556     -2.5369      4.8532      2.1960
1.000000
    432 O     c     -0.5087     -0.4381      4.1423     -1.0980
1.000000
    433 O     c     -2.0641     -3.0345      3.1955     -1.0980
1.000000
    434 O     c     -3.1152     -0.5135      1.7133     -1.0980
1.000000
    435 O     c     -0.5415     -3.1105      1.3293     -1.0980
1.000000
    436 Ti    c     -2.1204     -2.0952      1.4403      2.1960
1.000000
    437 O     c     -1.3784     -1.2817     -0.2132     -1.0980
1.000000
    438 O     c     -3.1576     -2.9889      0.2167     -1.0980
1.000000
    439 O     c     -3.5197     -0.8948     -1.5843     -1.0980
1.000000
    440 O     c     -0.9649     -3.8007     -1.3698     -1.0980
1.000000
    441 Ti    c     -2.5439     -2.6406     -1.5100      2.1960
1.000000
    442 O     c     -1.6293     -1.9076     -3.1626     -1.0980
1.000000
    443 O     c     -3.4830     -3.4426     -2.9537     -1.0980
1.000000
    444 O     c     -2.1071     -0.6990     -6.3273     -1.0980
1.000000
    445 O     c     -1.4427     -3.3535     -5.5998     -1.0980
1.000000
    446 Ti    c     -2.9509     -2.6531     -4.5217      2.1960
1.000000
    447 O     c     -1.1825     -1.5870     -8.7561     -1.0980
1.000000
    448 O     c     -3.5304     -2.5677     -6.4239     -1.0980
1.000000
    449 Ti    c     -1.7449     -2.3288     -7.1790      2.1960
1.000000
    450 O     c     -0.4709     -5.1290      4.6087     -1.0980
1.000000
    451 O     c     -0.9668     -5.4944      1.5453     -1.0980
1.000000
    452 O     c     -0.0330     -5.0655     -3.9015     -1.0980
1.000000
    453 O     c     -5.3720      0.7178      4.4638     -1.0980
1.000000
```

```
    454 O     c     -4.4926      1.4572      1.6371     -1.0980
1.000000
    455 O     c     -5.2139      0.7923     -1.6716     -1.0980
1.000000
    456 O     c     -4.0764      1.3854     -4.7237     -1.0980
1.000000
    457 O     c     -3.9871     -1.2520      4.1567     -1.0980
1.000000
    458 O     c     -5.5337     -0.7122      1.2133     -1.0980
1.000000
    459 O     c     -3.9961     -1.0179     -4.4102     -1.0980
1.000000
    460 O     c     -3.9961     -1.0179     -4.4102     -1.0980
1.000000
    461 O     c     -5.5337     -0.7122      1.2133     -1.0980
1.000000
    462 O     c     -3.9871     -1.2520      4.1567     -1.0980
1.000000
    463 O     c     -4.0764      1.3854     -4.7237     -1.0980
1.000000
    464 O     c     -5.2139      0.7923     -1.6716     -1.0980
1.000000
    465 O     c     -4.4926      1.4572      1.6371     -1.0980
1.000000
    466 O     c     -5.3720      0.7178      4.4638     -1.0980
1.000000
    467 O     c     -0.0330     -5.0655     -3.9015     -1.0980
1.000000
    468 O     c     -0.9668     -5.4944      1.5453     -1.0980
1.000000
    469 O     c     -0.4709     -5.1290      4.6087     -1.0980
1.000000
    470 Ti    c     -1.7449     -2.3288     -7.1790      2.1960
1.000000
    471 O     c     -3.5304     -2.5677     -6.4239     -1.0980
1.000000
    472 O     c     -1.1825     -1.5870     -8.7561     -1.0980
1.000000
    473 Ti    c     -2.9509     -2.6531     -4.5217      2.1960
1.000000
    474 O     c     -1.4427     -3.3535     -5.5998     -1.0980
1.000000
    475 O     c     -2.1071     -0.6990     -6.3273     -1.0980
1.000000
    476 O     c     -3.4830     -3.4426     -2.9537     -1.0980
1.000000
    477 O     c     -1.6293     -1.9076     -3.1626     -1.0980
1.000000
    478 Ti    c     -2.5439     -2.6406     -1.5100      2.1960
1.000000
    479 O     c     -0.9649     -3.8007     -1.3698     -1.0980
1.000000
    480 O     c     -3.5197     -0.8948     -1.5843     -1.0980
1.000000
    481 O     c     -3.1576     -2.9889      0.2167     -1.0980
1.000000
    482 O     c     -1.3784     -1.2817     -0.2132     -1.0980
1.000000
```

```
    483 Ti    c     -2.1204     -2.0952      1.4403      2.1960
1.000000
    484 O     c     -0.5415     -3.1105      1.3293     -1.0980
1.000000
    485 O     c     -3.1152     -0.5135      1.7133     -1.0980
1.000000
    486 O     c     -2.0641     -3.0345      3.1955     -1.0980
1.000000
    487 O     c     -0.5087     -0.4381      4.1423     -1.0980
1.000000
    488 Ti    c     -2.7556     -2.5369      4.8532      2.1960
1.000000
    489 O     c     -1.0311     -2.7763      5.7118     -1.0980
1.000000
```

********This section has been cut off**

```
   1367 Ti    c       0.000000      0.000000      0.000000
0.000000
   1368 O     c       0.000000      0.000000      0.000000
0.000000
   1369 O     c       0.000000      0.000000      0.000000
0.000000
   1370 O     c       0.000000      0.000000      0.000000
0.000000
   1371 O     c       0.000000      0.000000      0.000000
0.000000
   1372 O     c       0.000000      0.000000      0.000000
0.000000
   1373 O     c       0.000000      0.000000      0.000000
0.000000
   1374 O     c       0.000000      0.000000      0.000000
0.000000
   1375 O     c       0.000000      0.000000      0.000000
0.000000
   1376 O     c       0.000000      0.000000      0.000000
0.000000
   1377 O     c       0.000000      0.000000      0.000000
0.000000
------------------------------------------------------------------
---------------


  Bond calculation :

------------------------------------------------------------------
---------------
  Asymmetric unit site  Full lattice sites    No.  Distance
No.  Distance
                                                        (Angs)
(Angs)
------------------------------------------------------------------
---------------
  No bonds found for any atoms in the system
------------------------------------------------------------------
---------------
```

Distance calculation :

Cutoff for distances = 2.000000 Angstroms

Asymmetric unit site No.	At.No.		Full lattice sites At.No.		No.	Distance (Angs)	No.	Distance (Angs)
1	O	core	Ti	core	9	1.8877	9	1.9914
					9	1.9944		
2	O	core	Ti	core	9	1.8726	9	1.8949
3	O	core	Ti	core	9	1.8791		
4	O	core	Ti	core	9	1.9052	9	1.9669
					9	1.9751		
5	O	core	Ti	core	9	1.8582	9	1.8672
6	O	core	Ti	core	9	1.8548	9	1.9157
7	O	core	Ti	core	9	1.8601	9	1.8992
8	O	core	Ti	core	9	1.8316	9	1.8782
9	O	core	Ti	core	9	1.8498	9	1.8572
10	O	core	Ti	core	9	1.8553	9	1.8810
11	Ti	core	O	core	9	1.8419	9	1.8846

```
                                                    9    1.9382
9    1.9561
-------------------------------------------------------------------
---------------
      12   O     core        Ti    core         9    1.8846
9    1.8931
-------------------------------------------------------------------
---------------
      13   O     core        Ti    core         9    1.8419
9    1.9162
-------------------------------------------------------------------
---------------
      14   Ti    core        O     core         9    1.8597
9    1.8867
                                                    9    1.8877
9    1.9191
-------------------------------------------------------------------
---------------
      15   O     core        Ti    core         9    1.8867
9    1.8925
-------------------------------------------------------------------
---------------
      16   O     core        Ti    core         9    1.9561
-------------------------------------------------------------------
---------------
      17   O     core        Ti    core         9    1.8597
9    1.8834
-------------------------------------------------------------------
---------------
      18   O     core        Ti    core         9    1.8596
9    1.9191
-------------------------------------------------------------------
---------------
      19   Ti    core        O     core         9    1.8834
9    1.9327
                                                    9    1.9683
-------------------------------------------------------------------
---------------
      20   O     core        Ti    core         9    1.9277
9    1.9327
                                                    9    1.9849
-------------------------------------------------------------------
---------------
      21   O     core        Ti    core         9    1.9286
9    1.9683
-------------------------------------------------------------------
---------------
      22   O     core        Ti    core         9    1.9286
9    1.9400
-------------------------------------------------------------------
---------------
      23   O     core        Ti    core         9    1.9261
-------------------------------------------------------------------
---------------
      24   Ti    core        O     core         9    1.8738
9    1.8816
                                                    9    1.9286
9    1.9704
```

25	O	core	Ti	core	9	1.8738	9 1.8967
26	O	core	Ti	core	9	1.8816	
27	O	core	Ti	core	9	1.9255	9 1.9704
					9	1.9790	
28	O	core	Ti	core	9	1.8382	9 1.8493
29	Ti	core	O	core	9	1.8791	9 1.8867
					9	1.9203	9 1.9255
30	O	core	Ti	core	9	1.9203	9 1.9207
32	O	core	Ti	core	9	1.8505	9 1.8867
33	O	core	Ti	core	9	1.8176	9 1.9356
34	Ti	core	O	core	9	1.8176	9 1.8345
					9	1.8505	
35	Ti	core	O	core	9	1.8479	9 1.8605
					9	1.8887	9 1.9906
36	O	core	Ti	core	9	1.8479	9 1.8674
37	Ti	core	O	core	9	1.8549	9 1.8931
					9	1.9669	9 1.9914

38	O	core	Ti	core	9	1.8549	9 1.8605
39	O	core	Ti	core	9	1.8437	9 1.8887
40	Ti	core	O	core	9	1.8891	9 1.9052
					9	1.9280	9 1.9688
41	O	core	Ti	core	9	1.9005	9 1.9906
42	O	core	Ti	core	9	1.9280	
43	Ti	core	O	core	9	1.8582	9 1.9286
					9	1.9751	9 1.9944
44	O	core	Ti	core	9	1.8862	9 1.9688
45	O	core	Ti	core	9	1.8891	9 1.9363
46	Ti	core	O	core	9	1.9010	9 1.9116
					9	1.9128	9 1.9372
					9	1.9982	
47	O	core	Ti	core	9	1.9116	9 1.9270
					9	1.9366	
48	O	core	Ti	core	9	1.9010	
49	Ti	core	O	core	9	1.8672	9 1.8726
					9	1.9400	9 1.9692
50	O	core	Ti	core	9	1.9609	9 1.9692

					9	1.9982
51	O	core	Ti	core	9	1.9128
52	Ti	core	O	core	9	1.8548
					9	1.9609
53	O	core	Ti	core	9	1.9369
					9	1.9669
54	O	core	Ti	core	9	1.8633
					9	1.9783
55	Ti	core	O	core	9	1.8949
					9	1.9157
56	O	core	Ti	core	9	1.8466
57	O	core	Ti	core	9	1.9114
58	Ti	core	O	core	9	1.8466
					9	1.9114
					9	1.9664
59	O	core	Ti	core	9	1.8596
					9	1.9911
60	O	core	Ti	core	9	1.9352
61	Ti	core	O	core	9	1.8601
					9	1.9735
62	O	core	Ti	core	9	1.8345

```
---------------------------------------------------------------------
---------------
      63   O     core        Ti    core         9    1.9365
9    1.9382
                                                 9    1.9410
---------------------------------------------------------------------
---------------
      64   Ti    core        O     core         9    1.8391
9    1.9352
                                                 9    1.9410
9    1.9804
---------------------------------------------------------------------
---------------
      65   O     core        Ti    core         9    1.8391
9    1.9215
---------------------------------------------------------------------
---------------
      66   O     core        Ti    core         9    1.9372
---------------------------------------------------------------------
---------------
      67   O     core        Ti    core         9    1.8549
9    1.8681
---------------------------------------------------------------------
---------------
      68   O     core        Ti    core         9    1.9357
9    1.9650
---------------------------------------------------------------------
---------------
      69   O     core        Ti    core         9    1.9357
9    1.9650
---------------------------------------------------------------------
---------------
      70   O     core        Ti    core         9    1.8549
9    1.8681
---------------------------------------------------------------------
---------------
      71   O     core        Ti    core         9    1.9372
---------------------------------------------------------------------
---------------
      72   Ti    core        O     core         9    1.8391
9    1.9352
                                                 9    1.9410
9    1.9804
---------------------------------------------------------------------
---------------
      73   O     core        Ti    core         9    1.8391
9    1.9215
---------------------------------------------------------------------
---------------
      74   Ti    core        O     core         9    1.8316
9    1.8925
                                                 9    1.9365
9    1.9650
                                                 9    1.9695
---------------------------------------------------------------------
---------------
      75   O     core        Ti    core         9    1.9365
9    1.9382
```

```
                                                    9    1.9410
-------------------------------------------------------------------
---------------
      76   O     core        Ti    core         9    1.8345
9    1.8612
-------------------------------------------------------------------
---------------
      77   Ti    core        O     core         9    1.8466
9    1.8633
                                                    9    1.9114
9    1.9357
                                                    9    1.9664
-------------------------------------------------------------------
---------------
      78   O     core        Ti    core         9    1.9352
9    1.9664
-------------------------------------------------------------------
---------------
      79   O     core        Ti    core         9    1.8596
9    1.9804
                                                    9    1.9911
-------------------------------------------------------------------
---------------
      80   Ti    core        O     core         9    1.8681
9    1.8782
                                                    9    1.9277
9    1.9306
-------------------------------------------------------------------
---------------
      81   O     core        Ti    core         9    1.9114
9    1.9695
-------------------------------------------------------------------
---------------
      82   O     core        Ti    core         9    1.8466
9    1.9735
-------------------------------------------------------------------
---------------
      83   Ti    core        O     core         9    1.8548
9    1.9539
                                                    9    1.9609
9    1.9783
-------------------------------------------------------------------
---------------
      84   O     core        Ti    core         9    1.8633
9    1.9306
                                                    9    1.9783
-------------------------------------------------------------------
---------------
      85   O     core        Ti    core         9    1.9369
9    1.9539
                                                    9    1.9669
-------------------------------------------------------------------
---------------
      86   Ti    core        O     core         9    1.8549
9    1.8572
                                                    9    1.8967
9    1.9849
```

```
------------------------------------------------------------------------
---------------
      87   O     core        Ti    core         9    1.9128
------------------------------------------------------------------------
---------------
      88   O     core        Ti    core         9    1.9609
9    1.9692
                                                9    1.9982
------------------------------------------------------------------------
---------------
      89   Ti    core        O     core         9    1.9010
9    1.9116
                                                9    1.9128
9    1.9372
                                                9    1.9982
------------------------------------------------------------------------
---------------
      90   O     core        Ti    core         9    1.9010
------------------------------------------------------------------------
---------------
      91   O     core        Ti    core         9    1.9116
9    1.9270
                                                9    1.9366
------------------------------------------------------------------------
---------------
      92   Ti    core        O     core         9    1.8498
9    1.8810
                                                9    1.9363
9    1.9790
------------------------------------------------------------------------
---------------
      93   O     core        Ti    core         9    1.8891
9    1.9363
------------------------------------------------------------------------
---------------
      94   O     core        Ti    core         9    1.8862
9    1.9688
------------------------------------------------------------------------
---------------
      95   Ti    core        O     core         9    1.8891
9    1.9052
                                                9    1.9280
9    1.9688
------------------------------------------------------------------------
---------------
```

********** This section has been cut off

```
1349   Ti    core        O     core         9    1.8791        9
1.8867
                                                9    1.9203
9    1.9255
------------------------------------------------------------------------
---------------
    1350   O     core        Ti    core         9    1.8382
9    1.8493
```

1351	O	core	Ti	core	9	1.9255	9 1.9704
					9	1.9790	
1352	O	core	Ti	core	9	1.8816	
1353	O	core	Ti	core	9	1.8738	9 1.8967
1354	Ti	core	O	core	9	1.8738	9 1.8816
					9	1.9286	9 1.9704
1355	O	core	Ti	core	9	1.9261	
1356	O	core	Ti	core	9	1.9286	9 1.9400
1357	O	core	Ti	core	9	1.9286	9 1.9683
1358	O	core	Ti	core	9	1.9277	9 1.9327
					9	1.9849	
1359	Ti	core	O	core	9	1.8834	9 1.9327
					9	1.9683	
1360	O	core	Ti	core	9	1.8596	9 1.9191
1361	O	core	Ti	core	9	1.8597	9 1.8834
1362	O	core	Ti	core	9	1.9561	
1363	O	core	Ti	core	9	1.8867	9 1.8925
1364	Ti	core	O	core	9	1.8597	9 1.8867

```
                                                    9    1.8877
9    1.9191
-------------------------------------------------------------------
---------------
    1365   O     core        Ti    core         9    1.8419
9    1.9162
-------------------------------------------------------------------
---------------
    1366   O     core        Ti    core         9    1.8846
9    1.8931
-------------------------------------------------------------------
---------------
    1367   Ti    core        O     core         9    1.8419
9    1.8846
                                                    9    1.9382
9    1.9561
-------------------------------------------------------------------
---------------
    1368   O     core        Ti    core         9    1.8553
9    1.8810
-------------------------------------------------------------------
---------------
    1369   O     core        Ti    core         9    1.8498
9    1.8572
-------------------------------------------------------------------
---------------
    1370   O     core        Ti    core         9    1.8316
9    1.8782
-------------------------------------------------------------------
---------------
    1371   O     core        Ti    core         9    1.8601
9    1.8992
-------------------------------------------------------------------
---------------
    1372   O     core        Ti    core         9    1.8548
9    1.9157
-------------------------------------------------------------------
---------------
    1373   O     core        Ti    core         9    1.8582
9    1.8672
-------------------------------------------------------------------
---------------
    1374   O     core        Ti    core         9    1.9052
9    1.9669
                                                    9    1.9751
-------------------------------------------------------------------
---------------
    1375   O     core        Ti    core         9    1.8791
-------------------------------------------------------------------
---------------
    1376   O     core        Ti    core         9    1.8726
9    1.8949
-------------------------------------------------------------------
---------------
    1377   O     core        Ti    core         9    1.8877
9    1.9914
                                                    9    1.9944
```

Born effective charge tensors :

Atom		x	y	z
1 O	x	-1.0980	0.0000	0.0000
	y	0.0000	-1.0980	0.0000
	z	0.0000	0.0000	-1.0980
2 O	x	-1.0980	0.0000	0.0000
	y	0.0000	-1.0980	0.0000
	z	0.0000	0.0000	-1.0980
3 O	x	-1.0980	0.0000	0.0000
	y	0.0000	-1.0980	0.0000
	z	0.0000	0.0000	-1.0980
4 O	x	-1.0980	0.0000	0.0000
	y	0.0000	-1.0980	0.0000
	z	0.0000	0.0000	-1.0980
5 O	x	-1.0980	0.0000	0.0000
	y	0.0000	-1.0980	0.0000
	z	0.0000	0.0000	-1.0980
6 O	x	-1.0980	0.0000	0.0000
	y	0.0000	-1.0980	0.0000
	z	0.0000	0.0000	-1.0980
7 O	x	-1.0980	0.0000	0.0000
	y	0.0000	-1.0980	0.0000
	z	0.0000	0.0000	-1.0980
8 O	x	-1.0980	0.0000	0.0000
	y	0.0000	-1.0980	0.0000
	z	0.0000	0.0000	-1.0980
9 O	x	-1.0980	0.0000	0.0000
	y	0.0000	-1.0980	0.0000
	z	0.0000	0.0000	-1.0980
10 O	x	-1.0980	0.0000	0.0000

```
           y       0.0000     -1.0980      0.0000
           z       0.0000      0.0000     -1.0980
-------------------------------------------------------------------
--------------
  11 Ti    x       2.1960      0.0000      0.0000
           y       0.0000      2.1960      0.0000
           z       0.0000      0.0000      2.1960
-------------------------------------------------------------------
--------------
  12 O     x      -1.0980      0.0000      0.0000
           y       0.0000     -1.0980      0.0000
           z       0.0000      0.0000     -1.0980
-------------------------------------------------------------------
--------------
  13 O     x      -1.0980      0.0000      0.0000
           y       0.0000     -1.0980      0.0000
           z       0.0000      0.0000     -1.0980
-------------------------------------------------------------------
--------------
  14 Ti    x       2.1960      0.0000      0.0000
           y       0.0000      2.1960      0.0000
           z       0.0000      0.0000      2.1960
-------------------------------------------------------------------
--------------
  15 O     x      -1.0980      0.0000      0.0000
           y       0.0000     -1.0980      0.0000
           z       0.0000      0.0000     -1.0980
-------------------------------------------------------------------
--------------
  16 O     x      -1.0980      0.0000      0.0000
           y       0.0000     -1.0980      0.0000
           z       0.0000      0.0000     -1.0980
-------------------------------------------------------------------
--------------
  17 O     x      -1.0980      0.0000      0.0000
           y       0.0000     -1.0980      0.0000
           z       0.0000      0.0000     -1.0980
-------------------------------------------------------------------
--------------
```

********* This section has been cutoff**

```
-------------------------------------------------------------------
--------------
1364 Ti    x       2.1960      0.0000      0.0000
           y       0.0000      2.1960      0.0000
           z       0.0000      0.0000      2.1960
-------------------------------------------------------------------
--------------
1365 O     x      -1.0980      0.0000      0.0000
           y       0.0000     -1.0980      0.0000
           z       0.0000      0.0000     -1.0980
-------------------------------------------------------------------
--------------
1366 O     x      -1.0980      0.0000      0.0000
           y       0.0000     -1.0980      0.0000
           z       0.0000      0.0000     -1.0980
```

1367 Ti	x	2.1960	0.0000	0.0000
	y	0.0000	2.1960	0.0000
	z	0.0000	0.0000	2.1960
1368 O	x	-1.0980	0.0000	0.0000
	y	0.0000	-1.0980	0.0000
	z	0.0000	0.0000	-1.0980
1369 O	x	-1.0980	0.0000	0.0000
	y	0.0000	-1.0980	0.0000
	z	0.0000	0.0000	-1.0980
1370 O	x	-1.0980	0.0000	0.0000
	y	0.0000	-1.0980	0.0000
	z	0.0000	0.0000	-1.0980
1371 O	x	-1.0980	0.0000	0.0000
	y	0.0000	-1.0980	0.0000
	z	0.0000	0.0000	-1.0980
1372 O	x	-1.0980	0.0000	0.0000
	y	0.0000	-1.0980	0.0000
	z	0.0000	0.0000	-1.0980
1373 O	x	-1.0980	0.0000	0.0000
	y	0.0000	-1.0980	0.0000
	z	0.0000	0.0000	-1.0980
1374 O	x	-1.0980	0.0000	0.0000
	y	0.0000	-1.0980	0.0000
	z	0.0000	0.0000	-1.0980
1375 O	x	-1.0980	0.0000	0.0000
	y	0.0000	-1.0980	0.0000
	z	0.0000	0.0000	-1.0980
1376 O	x	-1.0980	0.0000	0.0000
	y	0.0000	-1.0980	0.0000
	z	0.0000	0.0000	-1.0980
1377 O	x	-1.0980	0.0000	0.0000
	y	0.0000	-1.0980	0.0000
	z	0.0000	0.0000	-1.0980

Moment of inertia tensor (10^-46 x kgm^2):

	x	y	z	Principle axis system
x	190112.81	-805.82	3369.99	76813.689976
y	-805.82	191707.23	1013.92	189884.904948
z	3369.99	1013.92	76923.30	192044.742642

Centre of mass (Ang) = 0.000001 0.000000 0.000000

Time to end of optimisation = 647.8645 seconds

Electrostatic potential at atomic positions :

Site No.	Atomic Label		Potential (V)	Derivatives (V/Angs) x	y	z
1	O	c	162.500261	38.111781	11.332113	-6.678067
2	O	c	135.623511	40.485011	17.610652	-1.636391
3	O	c	148.449584	25.381653	5.195225	10.631821
4	O	c	162.233928	41.479585	-20.987995	15.895832
5	O	c	140.818119	54.288724	-16.318036	3.336249
6	O	c	133.150452	43.330985	-40.247179	6.406712
7	O	c	133.904303	60.330743	-15.733753	-7.689742
8	O	c	152.565234	6.588675	31.604631	-8.974142
9	O	c	140.412449	6.921225	64.596644	-12.688390
10	O	c	145.781905	34.555417	47.851638	-11.661647

```
   11  Ti    c   -181.787428         -1.601282  -13.880146
4.294351
   12  O     c    142.430830         45.827279   24.743172
24.293891
   13  O     c    137.985119         15.217196    1.066981
38.488928
   14  Ti    c   -183.253629         -1.249186    1.937385   -
8.734198
   15  O     c    164.089136         26.038012   30.458747
14.127158
   16  O     c    153.272732        -31.567314  -23.558675  -
16.167122
   17  O     c    138.343969         37.480518   43.757135   -
6.961798
   18  O     c    160.258846        -21.082857   26.993788   -
1.654113
   19  Ti    c   -188.601365          3.541438   -0.563991
7.711042
   20  O     c    159.934041          9.855663   -3.979809
9.862996
   21  O     c    152.140341         -9.377656   -2.851746   -
5.790150
   22  O     c    156.163249         32.574997   26.838184
1.578169
   23  O     c    159.129608         -5.391327    2.792670
3.158950
   24  Ti    c   -180.780302          1.385760    1.348411
10.545179
   25  O     c    151.406827         24.487900   21.765886
1.681901
   26  O     c    158.019320         -2.421880   -7.026837   -
9.843576
   27  O     c    169.652948          0.203759    1.767802
1.879882
   28  O     c    154.336602         36.751501   18.123929
16.044377
   29  Ti    c   -180.634830          0.947049   -5.413908   -
5.895695
   30  O     c    163.081576         -4.053901    2.579244  -
10.464251
```

******* This section has been cutoff**

```
1258  Ti    c   -188.601015         -3.541621    0.563991   -
7.711103
 1259  O     c    156.164116        -32.574294  -26.838127   -
1.578466
 1260  O     c    159.129504          5.391692   -2.792766   -
3.159159
 1261  Ti    c   -184.576317          0.000268   -0.000064
0.000010
 1262  O     c    151.407309        -24.487441  -21.765879   -
1.682046
 1263  O     c    158.019759          2.422021    7.026854
9.843241
 1264  Ti    c   -180.779739         -1.385396   -1.348034  -
10.545243
```

```
 1265  O     c    169.653318          -0.203935   -1.767605   -
1.879377
 1266  O     c    154.337192         -36.750467  -18.124568  -
16.045343
 1267  Ti    c   -186.097153           1.207352   -2.732417
6.073355
 1268  O     c    163.082725           4.052841   -2.581706
10.464699
 1269  O     c    169.342184           5.398599   17.359874   -
0.000010
 1270  Ti    c   -180.633809          -0.947339    5.414519
5.895056
 1271  O     c    147.116433         -23.840428  -51.994007
5.572863
 1272  O     c    146.581050          12.830440   -0.914517
28.663359
 1273  Ti    c   -183.944050          -0.235412   -1.565483   -
3.415455
 1274  Ti    c   -177.526047          -0.791783   11.129380  -
10.918742
 1275  Ti    c   -194.942104           2.711267   -0.390686  -
15.653263
 1276  O     c    139.639876          -3.266232    5.606131  -
22.532055
 1277  Ti    c   -188.763948          10.925420  -14.216551
1.900985
 1278  O     c    144.486462         -30.005344    4.178516  -
27.768548
 1279  O     c    141.837535          24.469542   21.217986  -
53.053967
 1280  Ti    c   -181.484830           8.520658   -7.792847   -
1.778722
 1281  O     c    161.446205         -10.946103  -12.219403
2.096463
 1282  O     c    151.543300         -37.888311   31.268368  -
14.172733
 1283  Ti    c   -182.628817           3.439496   -1.703469   -
1.213614
 1284  O     c    161.215480           1.788985  -10.902357  -
13.407849
 1285  O     c    164.418116           0.017449   -2.232192
17.466738
 1286  Ti    c   -184.534729          -2.900511    6.689047   -
3.535969
 1287  O     c    169.407850          -2.491499   10.731826   -
5.652528
 1288  O     c    158.322210         -26.321163   19.531926   -
0.269861
 1289  Ti    c   -181.985072           6.835584   -6.040223
0.468424
 1290  O     c    158.363763          -7.969749   -2.775972  -
12.787909
 1291  O     c    159.725262           0.944398   19.981893   -
0.031662
 1292  Ti    c   -186.919386          -2.353383   -2.963665   -
6.516244
 1293  O     c    166.561953          -5.435206   14.673786   -
0.113852
```

```
 1294  O     c    170.214140          -7.195485    8.239196   -
5.065034
 1295  Ti    c   -188.586039          -8.013275    0.189998   -
2.568610
 1296  O     c    158.716669          10.335838  -22.802865  -
26.451575
 1297  O     c    151.974502          29.318831  -39.924058   -
9.988296
 1298  Ti    c   -186.647406           6.322129    3.342731   -
1.816312
 1299  O     c    163.918274           8.108309    7.596525
0.334422
 1300  O     c    164.649440         -24.527951   -4.411020
23.268538
 1301  Ti    c   -176.063074          11.491516  -13.792031   -
4.643376
 1302  O     c    146.318957         -51.589017   11.007466
31.070503
 1303  O     c    168.305772           3.700513   19.788764
31.764939
 1304  Ti    c   -176.687829          -1.473836   -8.972440   -
6.798819
 1305  O     c    138.774709         -21.393758   12.941877
52.848579
 1306  Ti    c   -177.046313           6.795456  -11.324598
7.771003
 1307  O     c    159.649484          -3.208190   -5.012674   -
0.765022
 1308  O     c    141.893040         -32.145608   54.443453
0.575671
 1309  O     c    161.576213         -25.597090   45.474791
19.746548
 1310  O     c    161.574878          25.598165  -45.474145  -
19.747782
 1311  O     c    141.892909          32.145575  -54.443543   -
0.575801
 1312  O     c    159.649706           3.208540    5.012974
0.765232
 1313  O     c    138.773501          21.393800  -12.941900  -
52.848254
 1314  Ti    c   -177.047001          -6.795604   11.324393   -
7.771610
 1315  O     c    168.305238          -3.700306  -19.789420  -
31.766248
 1316  O     c    146.317835          51.589241  -11.006356  -
31.070171
 1317  Ti    c   -186.606754           2.701984    0.234528
0.250399
 1318  O     c    164.648172          24.529378    4.412013  -
23.268298
 1319  O     c    163.917663          -8.108013   -7.595347   -
0.335502
 1320  Ti    c   -176.063787         -11.491627   13.792605
4.642816
 1321  O     c    151.974396         -29.318936   39.923665
9.988302
 1322  O     c    158.716201         -10.336478   22.802309
26.451158
```

```
 1323  Ti    c   -195.908275          -0.194383   -7.690917
3.210853
 1324  O     c    170.213657           7.194722   -8.237877
5.064550
 1325  O     c    166.561917           5.435705  -14.673845
0.114310
 1326  Ti    c   -188.586475           8.013364   -0.190076
2.568940
 1327  O     c    159.724787          -0.943972  -19.981946
0.031455
 1328  O     c    158.363166           7.969868    2.776812
12.787198
 1329  Ti    c   -189.093445           2.795979   -1.216451   -
0.930193
 1330  O     c    158.322419          26.320852  -19.532644
0.269557
 1331  O     c    169.407396           2.492006  -10.731514
5.653644
 1332  Ti    c   -181.985289          -6.835115    6.040018   -
0.468265
 1333  O     c    164.418532          -0.017833    2.233381  -
17.467006
 1334  O     c    161.215171          -1.788206   10.903171
13.406991
 1335  Ti    c   -184.576320           0.632536    6.508124   -
6.997883
 1336  O     c    151.543505          37.888314  -31.268911
14.171690
 1337  O     c    161.447019          10.947027   12.219992   -
2.096559
 1338  Ti    c   -182.628692          -3.439326    1.703372
1.213537
 1339  O     c    141.837926         -24.469089  -21.218570
53.054301
 1340  O     c    144.487270          30.003610   -4.178221
27.768137
 1341  Ti    c   -182.509056          -6.879200   -1.156421
6.072586
 1342  O     c    139.640763           3.266007   -5.606932
22.531870
 1343  Ti    c   -188.763519         -10.925448   14.216378   -
1.901062
 1344  Ti    c   -177.527351           0.792016  -11.128878
10.918300
 1345  O     c    146.579995         -12.829743    0.914991  -
28.664612
 1346  O     c    147.115277          23.839367   51.994764   -
5.572800
 1347  O     c    169.340312          -5.399477  -17.361390   -
0.000682
 1348  O     c    163.081576          -4.053901    2.579244  -
10.464251
 1349  Ti    c   -180.634830           0.947049   -5.413908   -
5.895695
 1350  O     c    154.336602          36.751501   18.123929
16.044377
 1351  O     c    169.652948           0.203759    1.767802
1.879882
```

```
 1352  O     c    158.019320          -2.421880   -7.026837   -
9.843576
 1353  O     c    151.406827          24.487900   21.765886
1.681901
 1354  Ti    c   -180.780302           1.385760    1.348411
10.545179
 1355  O     c    159.129608          -5.391327    2.792670
3.158950
 1356  O     c    156.163249          32.574997   26.838184
1.578169
 1357  O     c    152.140341          -9.377656   -2.851746   -
5.790150
 1358  O     c    159.934041           9.855663   -3.979809
9.862996
 1359  Ti    c   -188.601365           3.541438   -0.563991
7.711042
 1360  O     c    160.258846         -21.082857   26.993788   -
1.654113
 1361  O     c    138.343969          37.480518   43.757135   -
6.961798
 1362  O     c    153.272732         -31.567314  -23.558675  -
16.167122
 1363  O     c    164.089136          26.038012   30.458747
14.127158
 1364  Ti    c   -183.253629          -1.249186    1.937385   -
8.734198
 1365  O     c    137.985119          15.217196    1.066981
38.488928
 1366  O     c    142.430830          45.827279   24.743172
24.293891
 1367  Ti    c   -181.787428          -1.601282  -13.880146
4.294351
 1368  O     c    145.781905          34.555417   47.851638  -
11.661647
 1369  O     c    140.412449           6.921225   64.596644  -
12.688390
 1370  O     c    152.565234           6.588675   31.604631   -
8.974142
 1371  O     c    133.904303          60.330743  -15.733753   -
7.689742
 1372  O     c    133.150452          43.330985  -40.247179
6.406712
 1373  O     c    140.818119          54.288724  -16.318036
3.336249
 1374  O     c    162.233928          41.479585  -20.987995
15.895832
 1375  O     c    148.449584          25.381653    5.195225
10.631821
 1376  O     c    135.623511          40.485011   17.610652   -
1.636391
 1377  O     c    162.500261          38.111781   11.332113   -
6.678067
-------------------------------------------------------------------
--------------
```

Electric Field Gradients at atomic positions :

Site no.	EFGs (V/Angs**2)					
	xx	xy	yy	xz	yz	zz
1	-36.8505	-50.4424	22.4451	1.9241	5.4317	14.4053
2	-38.0553	14.9056	-65.8962	-16.7249	14.2405	103.9515
3	-7.5138	-70.6731	12.9659	45.9176	-26.7742	-5.4521
4	-21.5615	40.8654	2.0075	4.7646	22.7655	19.5539
5	-13.6277	-8.8845	-60.0669	-20.7225	-40.4883	73.6947
6	36.2898	9.9162	3.2791	-39.6088	-34.5490	-39.5689
7	9.1684	-18.9025	-64.9261	21.1339	13.8371	55.7576
8	-59.3749	-0.4788	-58.9669	56.2598	-16.3954	118.3418
9	-75.5848	8.5120	10.6834	1.0238	15.6885	64.9014
10	-29.4162	31.2659	-34.1491	34.9755	0.6685	63.5653
11	-15.6202	14.9804	24.7718	16.5506	11.6930	-9.1516
12	25.2027	-36.6868	14.1675	-17.5493	51.5325	-39.3702
13	-3.6379	70.5393	-10.3251	-48.2498	-56.6214	13.9630
14	3.7131	7.3797	4.5248	11.2031	9.9344	-8.2379
15	34.3310	-49.6484	-35.2089	-21.9605	21.3103	0.8779
16	-12.2268	-19.1677	-7.4161	-9.3782	5.0450	19.6429
17	-44.8141	33.6901	-32.5207	14.2827	-11.4478	77.3348
18	-6.3489	62.5125	14.5443	32.7895	19.4220	-8.1954
19	-5.5724	15.1551	2.4888	-9.5219	-15.8953	3.0836
20	45.4183	-67.6579	-23.6643	-25.0293	-33.9645	-21.7540
21	-20.7048	-61.4732	23.0355	12.1323	-50.9923	-2.3307
22	-1.4765	-53.6639	-12.6992	18.1585	-0.5570	14.1757
23	-5.5008	84.5889	0.1332	-14.3356	-0.2289	5.3676
24	28.2702	17.9235	-25.0278	-6.6226	-5.1738	-3.2424
25	-9.3802	-73.2209	41.7079	-24.3659	47.6387	-32.3277

```
      26     -30.0635  -27.3086   88.3220  -31.4528   15.5131  -
58.2585
      27     -20.8755  -64.3977  -32.6827  -19.5639  -11.6185
53.5583
      28     -31.6306   39.7608  -53.8397  -31.7717  -34.7624
85.4703
      29      -7.8287   15.9825   27.8365   -1.8250   10.6762  -
20.0078
      30      37.0557  -37.5818   32.5899   45.8006   -0.4754  -
69.6457
      31      43.4377   -7.8450  -23.8283  -12.5898   -1.6141  -
19.6093
      32     -66.0500   19.1530  -11.3115  -19.8409   33.0061
77.3615
      33      46.4886   89.5364  -17.2152   59.8698   37.4756  -
29.2733
      34      -8.3460   -1.1932    0.3919  -31.7027  -26.9831
7.9541
      35      -6.0533  -21.9842   -9.4154   24.9700  -11.7148
15.4687
      36       2.5649  -98.6826   20.2603  -48.2924   55.1641  -
22.8252
      37      38.0701    4.6866  -23.9339    5.8535    3.4195  -
14.1362
      38     -11.0356   68.7289   31.6222  -26.7671  -74.5305  -
20.5865
      39     -20.8023   58.9531  -11.8359   24.5586   23.9289
32.6383
      40       2.5277  -13.3111   -1.2914   -5.3149    8.0630   -
1.2362
      41      29.2533  -61.9994  -34.7428    4.7660  -10.4611
5.4895
      42      -4.3943   20.8547  -15.5248   -5.1678  -16.5779
19.9191
      43       4.9694    3.8059    7.0742   12.1921    5.8149  -
12.0435
      44      45.8625  -42.8620    0.9812   27.9996  -53.1172  -
46.8437
      45      22.2715   84.6903  -21.5526   37.8308   17.9019   -
0.7190
      46       0.1955  -16.4071    6.1098   -4.2606   -5.7747   -
6.3052
      47     -38.0077  -82.9441   21.4210    6.6476   21.5338
16.5867
      48     -34.9423   33.8493  -26.7895   31.4586   18.4955
61.7318
      49      11.7512    2.9892    2.3721    9.0285   21.0838  -
14.1233
      50     -16.7741   80.7567    4.1383    5.8641  -12.6050
12.6358
      51     -54.9983   45.9820  -10.5130   23.8203   30.1897
65.5113
      52     -17.2809    2.1928    1.2219    5.9876   -6.6311
16.0590
      53      41.9491  -65.0073  -55.9254    8.7664   15.9762
13.9763
      54     -54.4099   50.7242  -10.1596  -42.5439   -7.3461
64.5695
```

```
      55      18.7003    2.2987    3.8947   -1.0928   -0.0737  -
22.5949
      56     -30.0542   75.7294   22.2574    1.0787   15.9784
7.7968
      57      33.0358    7.1460   17.7007   12.7378   12.0158  -
50.7365
      58      16.7885  -15.2140    0.6752    1.5940   -9.5120  -
17.4638
      59     -64.8053  -44.5766   29.0886    2.5385   50.2249
35.7167
      60       4.8124   66.6532  -19.3799   37.7966    2.5898
14.5675
      61      -8.8074   -5.4048   26.2999   -9.2763   14.1162  -
17.4925
      62      -7.7420  -48.9212  -13.9013   11.6267  -64.2066
21.6433
      63      57.7106   -3.3208  -42.6803    0.7436  -37.8800  -
15.0303
      64      -3.5133   -7.5735    8.0540  -11.8268   13.6242   -
4.5408
      65     -35.0510  -54.7376    1.8727   12.0264  -42.5558
33.1783
      66      15.2664   79.3894  -12.9639  -25.5192   -4.1116   -
2.3024
      67     -21.5812  -16.9113   -7.2070  -59.2814  -29.1882
28.7882
      68      10.4011   23.5920  -14.5577    6.4547    6.6567
4.1566
      69      10.3989   23.5918  -14.5581    6.4548    6.6546
4.1592
      70     -21.5813  -16.9112   -7.2071  -59.2814  -29.1886
28.7884
      71      15.2670   79.3891  -12.9647  -25.5192   -4.1115   -
2.3022
      72      -3.5127   -7.5734    8.0530  -11.8262   13.6256   -
4.5403
      73     -35.0528  -54.7376    1.8756   12.0250  -42.5563
33.1771
      74      -7.3103    4.0133   23.1291   -5.5888   21.0080  -
15.8187
      75      57.7119   -3.3223  -42.6820    0.7429  -37.8800  -
15.0300
      76      -7.7446  -48.9217  -13.8974   11.6246  -64.2071
21.6420
      77      16.7875  -15.2144    0.6758    1.5938   -9.5113  -
17.4633
      78       4.8140   66.6545  -19.3803   37.7959    2.5904
14.5662
      79     -64.8080  -44.5753   29.0953    2.5404   50.2265
35.7127
      80       9.8542  -16.6459   10.7553   -3.4084    6.9704  -
20.6095
      81      33.0384    7.1467   17.6995   12.7363   12.0195  -
50.7379
      82     -30.0525   75.7298   22.2559    1.0779   15.9776
7.7966
      83     -17.2811    2.1921    1.2218    5.9875   -6.6309
16.0593
```

```
      84     -54.4109   50.7242  -10.1597  -42.5416   -7.3473
64.5705
      85      41.9487  -65.0070  -55.9253    8.7675   15.9756
13.9766
      86       4.2543   25.6277    9.3335   18.7370    8.6125  -
13.5877
      87     -54.9976   45.9825  -10.5135   23.8208   30.1892
65.5112
      88     -16.7742   80.7568    4.1388    5.8640  -12.6052
12.6354
      89       0.1948  -16.4072    6.1102   -4.2613   -5.7744   -
6.3050
      90     -34.9433   33.8488  -26.7884   31.4587   18.4962
61.7317
      91     -38.0074  -82.9448   21.4210    6.6485   21.5333
16.5864
      92      16.0965  -11.0809   -6.8336    4.9413   -7.8457   -
9.2629
      93      22.2724   84.6905  -21.5525   37.8313   17.9032   -
0.7198
      94      45.8609  -42.8617    0.9798   28.0015  -53.1182  -
46.8407
      95       2.5284  -13.3116   -1.2917   -5.3156    8.0626   -
1.2367
      96      -4.3931   20.8553  -15.5256   -5.1679  -16.5786
19.9187
      97      29.2496  -61.9987  -34.7407    4.7675  -10.4618
5.4911
      98      -3.2113   -2.9170   23.1334  -19.3183  -14.5342  -
19.9221
      99     -20.8020   58.9532  -11.8357   24.5581   23.9301
32.6377
     100     -11.0364   68.7259   31.6216  -26.7650  -74.5311  -
20.5852
     101      -6.0533  -21.9844   -9.4150   24.9697  -11.7148
15.4683
     102       2.5648  -98.6821   20.2600  -48.2925   55.1643  -
22.8248
     103     -23.9887    2.4026  -21.5898    5.8046   -4.8267
45.5786
     104      -8.3463   -1.1935    0.3908  -31.7024  -26.9829
7.9556
     105      -0.4789   10.4346    5.7364   -6.1475  -20.5586   -
5.2575
     106      46.4917   89.5370  -17.2159   59.8684   37.4747  -
29.2758
     107     -66.0492   19.1537  -11.3128  -19.8408   33.0074
77.3620
     108      -7.8279   15.9833   27.8369   -1.8249   10.6773  -
20.0089
     109      43.4400   -7.8485  -23.8280  -12.5902   -1.6142  -
19.6120
     110      37.0568  -37.5809   32.5894   45.7998   -0.4735  -
69.6461
     111      -4.5788   -2.0484   -5.8247   -6.0952    6.7591
10.4034
     112     -31.6321   39.7616  -53.8379  -31.7733  -34.7657
85.4701
```

113	-20.8743	-64.3973	-32.6831	-19.5661	-11.6204	53.5575
114	28.2703	17.9232	-25.0279	-6.6218	-5.1732	-3.2424
115	-30.0644	-27.3079	88.3225	-31.4515	15.5122	-58.2580
116	-9.3807	-73.2206	41.7065	-24.3655	47.6383	-32.3258
117	6.9941	-12.4519	-7.9795	1.4006	7.0632	0.9855
118	-5.5011	84.5886	0.1342	-14.3363	-0.2288	5.3669
119	-1.4766	-53.6658	-12.6981	18.1572	-0.5564	14.1747
120	-5.5714	15.1562	2.4876	-9.5225	-15.8957	3.0839
121	-20.7026	-61.4716	23.0370	12.1363	-50.9947	-2.3344
122	45.4179	-67.6589	-23.6638	-25.0304	-33.9644	-21.7541
123	-4.5776	-2.0468	-5.8245	-6.0957	6.7575	10.4021
124	-6.3504	62.5095	14.5483	32.7931	19.4280	-8.1979
125	-44.8151	33.6896	-32.5224	14.2811	-11.4457	77.3375
126	3.7125	7.3793	4.5260	11.2029	9.9335	-8.2384
127	-12.2255	-19.1647	-7.4155	-9.3775	5.0455	19.6409
128	34.3293	-49.6484	-35.2090	-21.9608	21.3094	0.8797
129	-0.4782	10.4346	5.7372	-6.1486	-20.5585	-5.2590
130	-3.6409	70.5382	-10.3246	-48.2485	-56.6216	13.9655
131	25.2024	-36.6867	14.1686	-17.5501	51.5324	-39.3710
132	-15.6195	14.9806	24.7720	16.5505	11.6932	-9.1525
133	-23.9887	2.4023	-21.5895	5.8044	-4.8263	45.5781
134	-3.2114	-2.9172	23.1341	-19.3179	-14.5339	-19.9227
135	16.0968	-11.0808	-6.8344	4.9413	-7.8457	-9.2624
136	-29.4166	31.2661	-34.1480	34.9759	0.6676	63.5646
137	4.2547	25.6273	9.3329	18.7371	8.6127	-13.5877
138	-75.5850	8.5122	10.6837	1.0231	15.6886	64.9013
139	9.8548	-16.6459	10.7547	-3.4080	6.9703	-20.6095
140	-59.3762	-0.4779	-58.9676	56.2573	-16.3941	118.3437
141	-7.3103	4.0134	23.1297	-5.5878	21.0084	-15.8194

```
     142       9.1683  -18.9010  -64.9269   21.1355   13.8380
55.7586
     143      36.2892    9.9169    3.2790  -39.6095  -34.5489  -
39.5682
     144     -13.6290   -8.8824  -60.0695  -20.7227  -40.4875
73.6985
     145     -21.5625   40.8647    2.0090    4.7638   22.7653
19.5535
     146      -8.8090   -5.4050   26.3012   -9.2766   14.1173  -
17.4922
     147      18.7008    2.2992    3.8934   -1.0933   -0.0725  -
22.5942
     148      -7.5153  -70.6738   12.9680   45.9199  -26.7826   -
5.4527
     149      11.7518    2.9880    2.3721    9.0275   21.0841  -
14.1239
     150     -38.0547   14.9059  -65.8962  -16.7247   14.2393
103.9509
     151       4.9689    3.8061    7.0748   12.1917    5.8148  -
12.0438
     152     -36.8506  -50.4434   22.4454    1.9231    5.4323
14.4052
     153      38.0701    4.6879  -23.9340    5.8527    3.4200  -
14.1361
     154      38.0701    4.6879  -23.9340    5.8527    3.4200  -
14.1361
     155     -36.8506  -50.4434   22.4454    1.9231    5.4323
14.4052
     156       4.9689    3.8061    7.0748   12.1917    5.8148  -
12.0438
     157     -38.0547   14.9059  -65.8962  -16.7247   14.2393
103.9509
     158      11.7518    2.9880    2.3721    9.0275   21.0841  -
14.1239
     159      -7.5153  -70.6738   12.9680   45.9199  -26.7826   -
5.4527
     160      18.7008    2.2992    3.8934   -1.0933   -0.0725  -
22.5942
     161      -8.8090   -5.4050   26.3012   -9.2766   14.1173  -
17.4922
     162     -21.5625   40.8647    2.0090    4.7638   22.7653
19.5535
     163     -13.6290   -8.8824  -60.0695  -20.7227  -40.4875
73.6985
     164      36.2892    9.9169    3.2790  -39.6095  -34.5489  -
39.5682
```

******** This section has been cuttoff**

```
    1259      -1.4766  -53.6658  -12.6981   18.1572   -0.5564
14.1747
    1260      -5.5011   84.5886    0.1342  -14.3363   -0.2288
5.3669
    1261       6.9941  -12.4519   -7.9795    1.4006    7.0632
0.9855
    1262      -9.3807  -73.2206   41.7065  -24.3655   47.6383  -
32.3258
```

1263	-30.0644	-27.3079	88.3225	-31.4515	15.5122	-58.2580
1264	28.2703	17.9232	-25.0279	-6.6218	-5.1732	-3.2424
1265	-20.8743	-64.3973	-32.6831	-19.5661	-11.6204	53.5575
1266	-31.6321	39.7616	-53.8379	-31.7733	-34.7657	85.4701
1267	-4.5788	-2.0484	-5.8247	-6.0952	6.7591	10.4034
1268	37.0568	-37.5809	32.5894	45.7998	-0.4735	-69.6461
1269	43.4400	-7.8485	-23.8280	-12.5902	-1.6142	-19.6120
1270	-7.8279	15.9833	27.8369	-1.8249	10.6773	-20.0089
1271	-66.0492	19.1537	-11.3128	-19.8408	33.0074	77.3620
1272	46.4917	89.5370	-17.2159	59.8684	37.4747	-29.2758
1273	-0.4789	10.4346	5.7364	-6.1475	-20.5586	-5.2575
1274	-8.3463	-1.1935	0.3908	-31.7024	-26.9829	7.9556
1275	-23.9887	2.4026	-21.5898	5.8046	-4.8267	45.5786
1276	2.5648	-98.6821	20.2600	-48.2925	55.1643	-22.8248
1277	-6.0533	-21.9844	-9.4150	24.9697	-11.7148	15.4683
1278	-11.0364	68.7259	31.6216	-26.7650	-74.5311	-20.5852
1279	-20.8020	58.9532	-11.8357	24.5581	23.9301	32.6377
1280	-3.2113	-2.9170	23.1334	-19.3183	-14.5342	-19.9221
1281	29.2496	-61.9987	-34.7407	4.7675	-10.4618	5.4911
1282	-4.3931	20.8553	-15.5256	-5.1679	-16.5786	19.9187
1283	2.5284	-13.3116	-1.2917	-5.3156	8.0626	-1.2367
1284	45.8609	-42.8617	0.9798	28.0015	-53.1182	-46.8407
1285	22.2724	84.6905	-21.5525	37.8313	17.9032	-0.7198
1286	16.0965	-11.0809	-6.8336	4.9413	-7.8457	-9.2629
1287	-38.0074	-82.9448	21.4210	6.6485	21.5333	16.5864
1288	-34.9433	33.8488	-26.7884	31.4587	18.4962	61.7317
1289	0.1948	-16.4072	6.1102	-4.2613	-5.7744	-6.3050
1290	-16.7742	80.7568	4.1388	5.8640	-12.6052	12.6354
1291	-54.9976	45.9825	-10.5135	23.8208	30.1892	65.5112

1292	4.2543	25.6277	9.3335	18.7370	8.6125	-13.5877
1293	41.9487	-65.0070	-55.9253	8.7675	15.9756	13.9766
1294	-54.4109	50.7242	-10.1597	-42.5416	-7.3473	64.5705
1295	-17.2811	2.1921	1.2218	5.9875	-6.6309	16.0593
1296	-30.0525	75.7298	22.2559	1.0779	15.9776	7.7966
1297	33.0384	7.1467	17.6995	12.7363	12.0195	-50.7379
1298	9.8542	-16.6459	10.7553	-3.4084	6.9704	-20.6095
1299	-64.8080	-44.5753	29.0953	2.5404	50.2265	35.7127
1300	4.8140	66.6545	-19.3803	37.7959	2.5904	14.5662
1301	16.7875	-15.2144	0.6758	1.5938	-9.5113	-17.4633
1302	-7.7446	-48.9217	-13.8974	11.6246	-64.2071	21.6420
1303	57.7119	-3.3223	-42.6820	0.7429	-37.8800	-15.0300
1304	-7.3103	4.0133	23.1291	-5.5888	21.0080	-15.8187
1305	-35.0528	-54.7376	1.8756	12.0250	-42.5563	33.1771
1306	-3.5127	-7.5734	8.0530	-11.8262	13.6256	-4.5403
1307	15.2670	79.3891	-12.9647	-25.5192	-4.1115	-2.3022
1308	-21.5813	-16.9112	-7.2071	-59.2814	-29.1886	28.7884
1309	10.3989	23.5918	-14.5581	6.4548	6.6546	4.1592
1310	10.4011	23.5920	-14.5577	6.4547	6.6567	4.1566
1311	-21.5812	-16.9113	-7.2070	-59.2814	-29.1882	28.7882
1312	15.2664	79.3894	-12.9639	-25.5192	-4.1116	-2.3024
1313	-35.0510	-54.7376	1.8727	12.0264	-42.5558	33.1783
1314	-3.5133	-7.5735	8.0540	-11.8268	13.6242	-4.5408
1315	57.7106	-3.3208	-42.6803	0.7436	-37.8800	-15.0303
1316	-7.7420	-48.9212	-13.9013	11.6267	-64.2066	21.6433
1317	-8.8074	-5.4048	26.2999	-9.2763	14.1162	-17.4925
1318	4.8124	66.6532	-19.3799	37.7966	2.5898	14.5675
1319	-64.8053	-44.5766	29.0886	2.5385	50.2249	35.7167
1320	16.7885	-15.2140	0.6752	1.5940	-9.5120	-17.4638

```
    1321      33.0358    7.1460   17.7007   12.7378   12.0158  -
50.7365
    1322     -30.0542   75.7294   22.2574    1.0787   15.9784
7.7968
    1323      18.7003    2.2987    3.8947   -1.0928   -0.0737  -
22.5949
    1324     -54.4099   50.7242  -10.1596  -42.5439   -7.3461
64.5695
    1325      41.9491  -65.0073  -55.9254    8.7664   15.9762
13.9763
    1326     -17.2809    2.1928    1.2219    5.9876   -6.6311
16.0590
    1327     -54.9983   45.9820  -10.5130   23.8203   30.1897
65.5113
    1328     -16.7741   80.7567    4.1383    5.8641  -12.6050
12.6358
    1329      11.7512    2.9892    2.3721    9.0285   21.0838  -
14.1233
    1330     -34.9423   33.8493  -26.7895   31.4586   18.4955
61.7318
    1331     -38.0077  -82.9441   21.4210    6.6476   21.5338
16.5867
    1332       0.1955  -16.4071    6.1098   -4.2606   -5.7747   -
6.3052
    1333      22.2715   84.6903  -21.5526   37.8308   17.9019   -
0.7190
    1334      45.8625  -42.8620    0.9812   27.9996  -53.1172  -
46.8437
    1335       4.9694    3.8059    7.0742   12.1921    5.8149  -
12.0435
    1336      -4.3943   20.8547  -15.5248   -5.1678  -16.5779
19.9191
    1337      29.2533  -61.9994  -34.7428    4.7660  -10.4611
5.4895
    1338       2.5277  -13.3111   -1.2914   -5.3149    8.0630   -
1.2362
    1339     -20.8023   58.9531  -11.8359   24.5586   23.9289
32.6383
    1340     -11.0356   68.7289   31.6222  -26.7671  -74.5305  -
20.5865
    1341      38.0701    4.6866  -23.9339    5.8535    3.4195  -
14.1362
    1342       2.5649  -98.6826   20.2603  -48.2924   55.1641  -
22.8252
    1343      -6.0533  -21.9842   -9.4154   24.9700  -11.7148
15.4687
    1344      -8.3460   -1.1932    0.3919  -31.7027  -26.9831
7.9541
    1345      46.4886   89.5364  -17.2152   59.8698   37.4756  -
29.2733
    1346     -66.0500   19.1530  -11.3115  -19.8409   33.0061
77.3615
    1347      43.4377   -7.8450  -23.8283  -12.5898   -1.6141  -
19.6093
    1348      37.0557  -37.5818   32.5899   45.8006   -0.4754  -
69.6457
    1349      -7.8287   15.9825   27.8365   -1.8250   10.6762  -
20.0078
```

```
    1350     -31.6306   39.7608  -53.8397  -31.7717  -34.7624
85.4703
    1351     -20.8755  -64.3977  -32.6827  -19.5639  -11.6185
53.5583
    1352     -30.0635  -27.3086   88.3220  -31.4528   15.5131  -
58.2585
    1353      -9.3802  -73.2209   41.7079  -24.3659   47.6387  -
32.3277
    1354      28.2702   17.9235  -25.0278   -6.6226   -5.1738   -
3.2424
    1355      -5.5008   84.5889    0.1332  -14.3356   -0.2289
5.3676
    1356      -1.4765  -53.6639  -12.6992   18.1585   -0.5570
14.1757
    1357     -20.7048  -61.4732   23.0355   12.1323  -50.9923   -
2.3307
    1358      45.4183  -67.6579  -23.6643  -25.0293  -33.9645  -
21.7540
    1359      -5.5724   15.1551    2.4888   -9.5219  -15.8953
3.0836
    1360      -6.3489   62.5125   14.5443   32.7895   19.4220   -
8.1954
    1361     -44.8141   33.6901  -32.5207   14.2827  -11.4478
77.3348
    1362     -12.2268  -19.1677   -7.4161   -9.3782    5.0450
19.6429
    1363      34.3310  -49.6484  -35.2089  -21.9605   21.3103
0.8779
    1364       3.7131    7.3797    4.5248   11.2031    9.9344   -
8.2379
    1365      -3.6379   70.5393  -10.3251  -48.2498  -56.6214
13.9630
    1366      25.2027  -36.6868   14.1675  -17.5493   51.5325  -
39.3702
    1367     -15.6202   14.9804   24.7718   16.5506   11.6930   -
9.1516
    1368     -29.4162   31.2659  -34.1491   34.9755    0.6685
63.5653
    1369     -75.5848    8.5120   10.6834    1.0238   15.6885
64.9014
    1370     -59.3749   -0.4788  -58.9669   56.2598  -16.3954
118.3418
    1371       9.1684  -18.9025  -64.9261   21.1339   13.8371
55.7576
    1372      36.2898    9.9162    3.2791  -39.6088  -34.5490  -
39.5689
    1373     -13.6277   -8.8845  -60.0669  -20.7225  -40.4883
73.6947
    1374     -21.5615   40.8654    2.0075    4.7646   22.7655
19.5539
    1375      -7.5138  -70.6731   12.9659   45.9176  -26.7742   -
5.4521
    1376     -38.0553   14.9056  -65.8962  -16.7249   14.2405
103.9515
    1377     -36.8505  -50.4424   22.4451    1.9241    5.4317
14.4053
-------------------------------------------------------------------
--------------
```

EFG Tensor properties :

Site no.	Diagonalised EFGs (V/Angs**2)			eVzz/h (MHz/barn)	Asymmetry Parameter
	xx	yy	zz		
1	14.2624	51.6880	-65.9504	159.4660	0.5675
2	-32.2214	-74.5769	106.7983	258.2348	0.3966
3	-24.4325	-74.3829	98.8154	238.9325	0.5055
4	5.1754	48.5640	-53.7394	129.9402	0.8074
5	-13.3286	-74.7405	88.0691	212.9483	0.6973
6	5.1719	62.8928	-68.0646	164.5781	0.8480
7	7.9646	64.2234	-72.1880	174.5483	0.7793
8	-59.2423	-76.7066	135.9489	328.7201	0.1285
9	7.2337	69.1848	-76.4185	184.7775	0.8107
10	-8.7116	-67.6191	76.3307	184.5652	0.7717
11	-6.3274	-29.6345	35.9619	86.9548	0.6481
12	-6.2221	-70.8714	77.0936	186.4098	0.8386
13	-38.2677	-78.6870	116.9547	282.7926	0.3456
14	-3.1872	-16.3537	19.5409	47.2493	0.6738
15	-9.8898	-62.4163	72.3061	174.8338	0.7264
16	3.4803	25.9526	-29.4329	71.1677	0.7635
17	-4.4226	-75.1106	79.5333	192.3089	0.8888
18	-19.2592	-62.7686	82.0278	198.3406	0.5304
19	-10.1893	-17.6763	27.8656	67.3780	0.2687
20	3.7560	86.9763	-90.7323	219.3878	0.9172
21	-20.7377	-71.4003	92.1380	222.7868	0.5499
22	10.7703	52.1044	-62.8747	152.0291	0.6574
23	5.1443	83.2797	-88.4240	213.8064	0.8836

24	-4.5013	-30.8361	35.3374	85.4448	0.7452
25	-47.7670	-65.2764	113.0434	273.3353	0.1549
26	-18.8607	-78.6504	97.5111	235.7786	0.6132
27	35.8444	58.8073	-94.6517	228.8647	0.2426
28	-21.3317	-84.5166	105.8483	255.9378	0.5969
29	-11.1249	-24.4070	35.5319	85.9149	0.3738
30	7.3925	80.6376	-88.0301	212.8539	0.8320
31	-20.0086	-26.6286	46.6372	112.7672	0.1419
32	-11.6130	-77.7784	89.3914	216.1455	0.7402
33	-58.2136	-80.9895	139.2031	336.5887	0.1636
34	-2.0054	-41.4012	43.4066	104.9557	0.9076
35	-9.7399	-31.9428	41.6827	100.7875	0.5327
36	-55.1784	-87.7322	142.9106	345.5532	0.2278
37	-13.9874	-25.1339	39.1213	94.5941	0.2849
38	-41.5620	-81.5526	123.1146	297.6871	0.3248
39	3.1240	72.3494	-75.4735	182.4924	0.9172
40	-4.9250	-13.5701	18.4952	44.7207	0.4674
41	4.5806	68.4685	-73.0492	176.6306	0.8746
42	1.9874	31.5952	-33.5826	81.2016	0.8816
43	3.1269	15.7428	-18.8696	45.6262	0.6686
44	-10.8752	-81.1833	92.0586	222.5946	0.7637
45	-15.7161	-88.1595	103.8756	251.1679	0.6974
46	-2.1574	-17.7830	19.9404	48.2152	0.7836
47	16.4097	82.7619	-99.1716	239.7937	0.6691
48	-12.4920	-66.1086	78.6006	190.0538	0.6821
49	6.8995	22.4514	-29.3509	70.9695	0.5299
50	13.7216	75.6182	-89.3398	216.0207	0.6928
51	-2.9584	-83.9616	86.9201	210.1699	0.9319
52	-0.3456	-18.8941	19.2398	46.5211	0.9641

```
      53       17.1114   74.3888  -91.5002          221.2445
0.6260
      54        9.7265   84.4809  -94.2074          227.7905
0.7935
      55        3.5463   19.0775  -22.6238           54.7037
0.6865
      56        5.9336   78.8545  -84.7881          205.0150
0.8600
      57       15.4234   38.8578  -54.2813          131.2503
0.4317
      58       -4.6702  -22.1960   26.8662           64.9615
0.6523
      59       -1.7748  -86.7167   88.4914          213.9695
0.9599
      60        4.1149   76.4964  -80.6113          194.9156
0.8979
      61       -6.7861  -25.2009   31.9869           77.3433
0.5757
      62       -8.2620  -79.2990   87.5610          211.7196
0.8113
      63       11.3328   57.8881  -69.2208          167.3737
0.6726
      64       -5.9402  -17.1619   23.1021           55.8602
0.4857
      65       -2.8885  -76.7352   79.6237          192.5275
0.9274
      66       -5.5735  -81.7753   87.3488          211.2065
0.8724
      67        3.4942   71.1659  -74.6601          180.5257
0.9064
      68        0.9501   27.9955  -28.9456           69.9895
0.9344
      69        0.9524   27.9936  -28.9460           69.9905
0.9342
      70        3.4941   71.1661  -74.6602          180.5259
0.9064
      71       -5.5733  -81.7752   87.3485          211.2059
0.8724
      72       -5.9409  -17.1617   23.1027           55.8615
0.4857
      73       -2.8882  -76.7355   79.6237          192.5276
0.9275
      74       -5.0914  -27.2629   32.3543           78.2315
0.6853
      75       11.3324   57.8895  -69.2219          167.3764
0.6726
      76       -8.2619  -79.2990   87.5610          211.7196
0.8113
      77       -4.6708  -22.1950   26.8658           64.9607
0.6523
      78        4.1140   76.4977  -80.6117          194.9164
0.8979
      79       -1.7759  -86.7177   88.4936          213.9747
0.9599
      80       -5.9876  -22.0894   28.0770           67.8892
0.5735
      81       15.4231   38.8602  -54.2832          131.2551
0.4318
```

82	5.9339	78.8540	-84.7880	205.0146	0.8600
83	-0.3458	-18.8941	19.2399	46.5214	0.9641
84	9.7263	84.4807	-94.2070	227.7894	0.7935
85	17.1116	74.3883	-91.5000	221.2440	0.6260
86	-12.0860	-27.3845	39.4705	95.4383	0.3876
87	-2.9582	-83.9617	86.9199	210.1695	0.9319
88	13.7212	75.6186	-89.3398	216.0207	0.6928
89	-2.1570	-17.7834	19.9404	48.2152	0.7837
90	-12.4926	-66.1082	78.6009	190.0543	0.6821
91	16.4100	82.7622	-99.1721	239.7950	0.6691
92	-5.9333	-16.4795	22.4128	54.1934	0.4705
93	-15.7177	-88.1593	103.8769	251.1711	0.6974
94	-10.8763	-81.1826	92.0588	222.5953	0.7637
95	-4.9257	-13.5702	18.4959	44.7226	0.4674
96	1.9878	31.5958	-33.5835	81.2039	0.8816
97	4.5815	68.4664	-73.0479	176.6275	0.8746
98	7.9342	27.9220	-35.8562	86.6992	0.5574
99	3.1233	72.3500	-75.4733	182.4920	0.9172
100	-41.5595	-81.5523	123.1118	297.6803	0.3248
101	-9.7397	-31.9428	41.6825	100.7869	0.5327
102	-55.1783	-87.7319	142.9102	345.5523	0.2278
103	-20.1184	-26.2546	46.3730	112.1285	0.1323
104	-2.0060	-41.4008	43.4068	104.9561	0.9076
105	-5.6540	-21.1676	26.8216	64.8538	0.5784
106	-58.2143	-80.9893	139.2036	336.5899	0.1636
107	-11.6140	-77.7784	89.3924	216.1479	0.7402
108	-11.1246	-24.4084	35.5331	85.9178	0.3738
109	-20.0099	-26.6303	46.6402	112.7744	0.1419
110	7.3937	80.6364	-88.0301	212.8540	0.8320

111	-6.6808	-8.2836	14.9645	36.1836	0.1071
112	-21.3339	-84.5168	105.8507	255.9436	0.5969
113	35.8442	58.8076	-94.6518	228.8649	0.2426
114	-4.5010	-30.8360	35.3370	85.4438	0.7453
115	-18.8616	-78.6492	97.5108	235.7780	0.6131
116	-47.7655	-65.2766	113.0420	273.3320	0.1549
117	3.0992	14.4653	-17.5645	42.4703	0.6471
118	5.1437	83.2799	-88.4236	213.8053	0.8837
119	10.7706	52.1054	-62.8760	152.0322	0.6574
120	-10.1893	-17.6774	27.8667	67.3807	0.2687
121	-20.7440	-71.3968	92.1408	222.7936	0.5497
122	3.7560	86.9772	-90.7332	219.3900	0.9172
123	-6.6797	-8.2829	14.9626	36.1790	0.1071
124	-19.2654	-62.7655	82.0309	198.3482	0.5303
125	-4.4245	-75.1108	79.5353	192.3138	0.8887
126	-3.1865	-16.3536	19.5400	47.2471	0.6739
127	3.4783	25.9504	-29.4288	71.1578	0.7636
128	-9.8888	-62.4163	72.3051	174.8313	0.7265
129	-5.6541	-21.1680	26.8221	64.8549	0.5784
130	-38.2662	-78.6870	116.9533	282.7892	0.3456
131	-6.2226	-70.8715	77.0941	186.4110	0.8386
132	-6.3279	-29.6344	35.9623	86.9558	0.6481
133	-20.1184	-26.2541	46.3725	112.1272	0.1323
134	7.9339	27.9223	-35.8562	86.6991	0.5575
135	-5.9331	-16.4797	22.4129	54.1936	0.4706
136	-8.7108	-67.6193	76.3301	184.5637	0.7718
137	-12.0861	-27.3841	39.4702	95.4377	0.3876
138	7.2340	69.1847	-76.4187	184.7781	0.8107
139	-5.9875	-22.0895	28.0769	67.8891	0.5735

140	-59.2426	-76.7065	135.9490	328.7204	0.1285
141	-5.0920	-27.2630	32.3550	78.2333	0.6852
142	7.9631	64.2254	-72.1885	174.5494	0.7794
143	5.1709	62.8934	-68.0643	164.5772	0.8481
144	-13.3311	-74.7412	88.0723	212.9560	0.6973
145	5.1756	48.5634	-53.7390	129.9391	0.8074
146	-6.7873	-25.2015	31.9888	77.3479	0.5756
147	3.5450	19.0782	-22.6232	54.7021	0.6866
148	-24.4401	-74.3821	98.8222	238.9490	0.5054
149	6.9014	22.4500	-29.3515	70.9709	0.5297
150	-32.2207	-74.5768	106.7975	258.2330	0.3966
151	3.1269	15.7426	-18.8695	45.6259	0.6686
152	14.2621	51.6893	-65.9514	159.4683	0.5675
153	-13.9870	-25.1344	39.1214	94.5942	0.2849
154	-13.9870	-25.1344	39.1214	94.5942	0.2849
155	14.2621	51.6893	-65.9514	159.4683	0.5675
156	3.1269	15.7426	-18.8695	45.6259	0.6686
157	-32.2207	-74.5768	106.7975	258.2330	0.3966
158	6.9014	22.4500	-29.3515	70.9709	0.5297
159	-24.4401	-74.3821	98.8222	238.9490	0.5054
160	3.5450	19.0782	-22.6232	54.7021	0.6866
161	-6.7873	-25.2015	31.9888	77.3479	0.5756
162	5.1756	48.5634	-53.7390	129.9391	0.8074
163	-13.3311	-74.7412	88.0723	212.9560	0.6973
164	5.1709	62.8934	-68.0643	164.5772	0.8481
165	7.9631	64.2254	-72.1885	174.5494	0.7794
166	-5.0920	-27.2630	32.3550	78.2333	0.6852
167	-59.2426	-76.7065	135.9490	328.7204	0.1285
168	-5.9875	-22.0895	28.0769	67.8891	0.5735

169	7.2340	69.1847	-76.4187	184.7781	0.8107
170	-12.0861	-27.3841	39.4702	95.4377	0.3876
171	-8.7108	-67.6193	76.3301	184.5637	0.7718
172	-5.9331	-16.4797	22.4129	54.1936	0.4706
173	7.9339	27.9223	-35.8562	86.6991	0.5575
174	-20.1184	-26.2541	46.3725	112.1272	0.1323
175	-6.3279	-29.6344	35.9623	86.9558	0.6481
176	-6.2226	-70.8715	77.0941	186.4110	0.8386
177	-38.2662	-78.6870	116.9533	282.7892	0.3456
178	-5.6541	-21.1680	26.8221	64.8549	0.5784
179	-9.8888	-62.4163	72.3051	174.8313	0.7265
180	3.4783	25.9504	-29.4288	71.1578	0.7636
181	-3.1865	-16.3536	19.5400	47.2471	0.6739
182	-4.4245	-75.1108	79.5353	192.3138	0.8887
183	-19.2654	-62.7655	82.0309	198.3482	0.5303
184	-6.6797	-8.2829	14.9626	36.1790	0.1071
185	3.7560	86.9772	-90.7332	219.3900	0.9172
186	-20.7440	-71.3968	92.1408	222.7936	0.5497
187	-10.1893	-17.6774	27.8667	67.3807	0.2687
188	10.7706	52.1054	-62.8760	152.0322	0.6574
189	5.1437	83.2799	-88.4236	213.8053	0.8837
190	3.0992	14.4653	-17.5645	42.4703	0.6471
191	-47.7655	-65.2766	113.0420	273.3320	0.1549
192	-18.8616	-78.6492	97.5108	235.7780	0.6131
193	-4.5010	-30.8360	35.3370	85.4438	0.7453
194	35.8442	58.8076	-94.6518	228.8649	0.2426
195	-21.3339	-84.5168	105.8507	255.9436	0.5969
196	-6.6808	-8.2836	14.9645	36.1836	0.1071
197	7.3937	80.6364	-88.0301	212.8540	0.8320

198	-20.0099	-26.6303	46.6402	112.7744	0.1419
199	-11.1246	-24.4084	35.5331	85.9178	0.3738
200	-11.6140	-77.7784	89.3924	216.1479	0.7402
201	-58.2143	-80.9893	139.2036	336.5899	0.1636
202	-5.6540	-21.1676	26.8216	64.8538	0.5784
203	-2.0060	-41.4008	43.4068	104.9561	0.9076
204	-20.1184	-26.2546	46.3730	112.1285	0.1323
205	-55.1783	-87.7319	142.9102	345.5523	0.2278
206	-9.7397	-31.9428	41.6825	100.7869	0.5327
207	-41.5595	-81.5523	123.1118	297.6803	0.3248
208	3.1233	72.3500	-75.4733	182.4920	0.9172
209	7.9342	27.9220	-35.8562	86.6992	0.5574
210	4.5815	68.4664	-73.0479	176.6275	0.8746
211	1.9878	31.5958	-33.5835	81.2039	0.8816
212	-4.9257	-13.5702	18.4959	44.7226	0.4674
213	-10.8763	-81.1826	92.0588	222.5953	0.7637
214	-15.7177	-88.1593	103.8769	251.1711	0.6974
215	-5.9333	-16.4795	22.4128	54.1934	0.4705
216	16.4100	82.7622	-99.1721	239.7950	0.6691
217	-12.4926	-66.1082	78.6009	190.0543	0.6821
218	-2.1570	-17.7834	19.9404	48.2152	0.7837
219	13.7212	75.6186	-89.3398	216.0207	0.6928
220	-2.9582	-83.9617	86.9199	210.1695	0.9319
221	-12.0860	-27.3845	39.4705	95.4383	0.3876
222	17.1116	74.3883	-91.5000	221.2440	0.6260
223	9.7263	84.4807	-94.2070	227.7894	0.7935
224	-0.3458	-18.8941	19.2399	46.5214	0.9641
225	5.9339	78.8540	-84.7880	205.0146	0.8600
226	15.4231	38.8602	-54.2832	131.2551	0.4318

227	-5.9876	-22.0894	28.0770	67.8892	0.5735
228	-1.7759	-86.7177	88.4936	213.9747	0.9599
229	4.1140	76.4977	-80.6117	194.9164	0.8979
230	-4.6708	-22.1950	26.8658	64.9607	0.6523
231	-8.2619	-79.2990	87.5610	211.7196	0.8113
232	11.3324	57.8895	-69.2219	167.3764	0.6726
233	-5.0914	-27.2629	32.3543	78.2315	0.6853
234	-2.8882	-76.7355	79.6237	192.5276	0.9275
235	-5.9409	-17.1617	23.1027	55.8615	0.4857
236	-5.5733	-81.7752	87.3485	211.2059	0.8724
237	3.4941	71.1661	-74.6602	180.5259	0.9064
238	0.9524	27.9936	-28.9460	69.9905	0.9342
239	0.9501	27.9955	-28.9456	69.9895	0.9344
240	3.4942	71.1659	-74.6601	180.5257	0.9064
241	-5.5735	-81.7753	87.3488	211.2065	0.8724
242	-2.8885	-76.7352	79.6237	192.5275	0.9274
243	-5.9402	-17.1619	23.1021	55.8602	0.4857
244	11.3328	57.8881	-69.2208	167.3737	0.6726
245	-8.2620	-79.2990	87.5610	211.7196	0.8113
246	-6.7861	-25.2009	31.9869	77.3433	0.5757
247	4.1149	76.4964	-80.6113	194.9156	0.8979
248	-1.7748	-86.7167	88.4914	213.9695	0.9599
249	-4.6702	-22.1960	26.8662	64.9615	0.6523
250	15.4234	38.8578	-54.2813	131.2503	0.4317
251	5.9336	78.8545	-84.7881	205.0150	0.8600
252	3.5463	19.0775	-22.6238	54.7037	0.6865
253	9.7265	84.4809	-94.2074	227.7905	0.7935
254	17.1114	74.3888	-91.5002	221.2445	0.6260
255	-0.3456	-18.8941	19.2398	46.5211	0.9641

256	-2.9584	-83.9616	86.9201	210.1699	0.9319
257	13.7216	75.6182	-89.3398	216.0207	0.6928
258	6.8995	22.4514	-29.3509	70.9695	0.5299
259	-12.4920	-66.1086	78.6006	190.0538	0.6821
260	16.4097	82.7619	-99.1716	239.7937	0.6691
261	-2.1574	-17.7830	19.9404	48.2152	0.7836
262	-15.7161	-88.1595	103.8756	251.1679	0.6974
263	-10.8752	-81.1833	92.0586	222.5946	0.7637
264	3.1269	15.7428	-18.8696	45.6262	0.6686
265	1.9874	31.5952	-33.5826	81.2016	0.8816
266	4.5806	68.4685	-73.0492	176.6306	0.8746
267	-4.9250	-13.5701	18.4952	44.7207	0.4674
268	3.1240	72.3494	-75.4735	182.4924	0.9172
269	-41.5620	-81.5526	123.1146	297.6871	0.3248
270	-13.9874	-25.1339	39.1213	94.5941	0.2849
271	-55.1784	-87.7322	142.9106	345.5532	0.2278
272	-9.7399	-31.9428	41.6827	100.7875	0.5327
273	-2.0054	-41.4012	43.4066	104.9557	0.9076
274	-58.2136	-80.9895	139.2031	336.5887	0.1636
275	-11.6130	-77.7784	89.3914	216.1455	0.7402
276	-20.0086	-26.6286	46.6372	112.7672	0.1419
277	7.3925	80.6376	-88.0301	212.8539	0.8320
278	-11.1249	-24.4070	35.5319	85.9149	0.3738
279	-21.3317	-84.5166	105.8483	255.9378	0.5969
280	35.8444	58.8073	-94.6517	228.8647	0.2426
281	-18.8607	-78.6504	97.5111	235.7786	0.6132
282	-47.7670	-65.2764	113.0434	273.3353	0.1549
283	-4.5013	-30.8361	35.3374	85.4448	0.7452
284	5.1443	83.2797	-88.4240	213.8064	0.8836

285	10.7703	52.1044	-62.8747	152.0291	0.6574
286	-20.7377	-71.4003	92.1380	222.7868	0.5499
287	3.7560	86.9763	-90.7323	219.3878	0.9172
288	-10.1893	-17.6763	27.8656	67.3780	0.2687
289	-19.2592	-62.7686	82.0278	198.3406	0.5304
290	-4.4226	-75.1106	79.5333	192.3089	0.8888
291	3.4803	25.9526	-29.4329	71.1677	0.7635
292	-9.8898	-62.4163	72.3061	174.8338	0.7264
293	-3.1872	-16.3537	19.5409	47.2493	0.6738
294	-38.2677	-78.6870	116.9547	282.7926	0.3456
295	-6.2221	-70.8714	77.0936	186.4098	0.8386
296	-6.3274	-29.6345	35.9619	86.9548	0.6481
297	-8.7116	-67.6191	76.3307	184.5652	0.7717
298	7.2337	69.1848	-76.4185	184.7775	0.8107
299	-59.2423	-76.7066	135.9489	328.7201	0.1285
300	7.9646	64.2234	-72.1880	174.5483	0.7793
301	5.1719	62.8928	-68.0646	164.5781	0.8480
302	-13.3286	-74.7405	88.0691	212.9483	0.6973
303	5.1754	48.5640	-53.7394	129.9402	0.8074
304	-24.4325	-74.3829	98.8154	238.9325	0.5055
305	-32.2214	-74.5769	106.7983	258.2348	0.3966
306	14.2624	51.6880	-65.9504	159.4660	0.5675
307	-13.9870	-25.1344	39.1214	94.5942	0.2849
308	14.2621	51.6893	-65.9514	159.4683	0.5675
309	3.1269	15.7426	-18.8695	45.6259	0.6686
310	-32.2207	-74.5768	106.7975	258.2330	0.3966
311	6.9014	22.4500	-29.3515	70.9709	0.5297
312	-24.4401	-74.3821	98.8222	238.9490	0.5054
313	3.5450	19.0782	-22.6232	54.7021	0.6866

314	-6.7873	-25.2015	31.9888	77.3479	0.5756
315	5.1756	48.5634	-53.7390	129.9391	0.8074
316	-13.3311	-74.7412	88.0723	212.9560	0.6973
317	5.1709	62.8934	-68.0643	164.5772	0.8481
318	7.9631	64.2254	-72.1885	174.5494	0.7794
319	-5.0920	-27.2630	32.3550	78.2333	0.6852
320	-59.2426	-76.7065	135.9490	328.7204	0.1285
321	-5.9875	-22.0895	28.0769	67.8891	0.5735
322	7.2340	69.1847	-76.4187	184.7781	0.8107
323	-12.0861	-27.3841	39.4702	95.4377	0.3876
324	-8.7108	-67.6193	76.3301	184.5637	0.7718
325	-5.9331	-16.4797	22.4129	54.1936	0.4706
326	7.9339	27.9223	-35.8562	86.6991	0.5575
327	-20.1184	-26.2541	46.3725	112.1272	0.1323
328	-6.3279	-29.6344	35.9623	86.9558	0.6481
329	-6.2226	-70.8715	77.0941	186.4110	0.8386
330	-38.2662	-78.6870	116.9533	282.7892	0.3456
331	-5.6541	-21.1680	26.8221	64.8549	0.5784
332	-9.8888	-62.4163	72.3051	174.8313	0.7265
333	3.4783	25.9504	-29.4288	71.1578	0.7636
334	-3.1865	-16.3536	19.5400	47.2471	0.6739
335	-4.4245	-75.1108	79.5353	192.3138	0.8887
336	-19.2654	-62.7655	82.0309	198.3482	0.5303
337	-6.6797	-8.2829	14.9626	36.1790	0.1071
338	3.7560	86.9772	-90.7332	219.3900	0.9172
339	-20.7440	-71.3968	92.1408	222.7936	0.5497
340	-10.1893	-17.6774	27.8667	67.3807	0.2687
341	10.7706	52.1054	-62.8760	152.0322	0.6574
342	5.1437	83.2799	-88.4236	213.8053	0.8837

343	3.0992	14.4653	-17.5645	42.4703	0.6471
344	-47.7655	-65.2766	113.0420	273.3320	0.1549
345	-18.8616	-78.6492	97.5108	235.7780	0.6131
346	-4.5010	-30.8360	35.3370	85.4438	0.7453
347	35.8442	58.8076	-94.6518	228.8649	0.2426
348	-21.3339	-84.5168	105.8507	255.9436	0.5969
349	-6.6808	-8.2836	14.9645	36.1836	0.1071
350	7.3937	80.6364	-88.0301	212.8540	0.8320
351	-20.0099	-26.6303	46.6402	112.7744	0.1419
352	-11.1246	-24.4084	35.5331	85.9178	0.3738
353	-11.6140	-77.7784	89.3924	216.1479	0.7402
354	-58.2143	-80.9893	139.2036	336.5899	0.1636
355	-5.6540	-21.1676	26.8216	64.8538	0.5784
356	-2.0060	-41.4008	43.4068	104.9561	0.9076
357	-20.1184	-26.2546	46.3730	112.1285	0.1323
358	-55.1783	-87.7319	142.9102	345.5523	0.2278
359	-9.7397	-31.9428	41.6825	100.7869	0.5327
360	-41.5595	-81.5523	123.1118	297.6803	0.3248
361	3.1233	72.3500	-75.4733	182.4920	0.9172
362	7.9342	27.9220	-35.8562	86.6992	0.5574
363	4.5815	68.4664	-73.0479	176.6275	0.8746
364	1.9878	31.5958	-33.5835	81.2039	0.8816
365	-4.9257	-13.5702	18.4959	44.7226	0.4674
366	-10.8763	-81.1826	92.0588	222.5953	0.7637
367	-15.7177	-88.1593	103.8769	251.1711	0.6974
368	-5.9333	-16.4795	22.4128	54.1934	0.4705
369	16.4100	82.7622	-99.1721	239.7950	0.6691
370	-12.4926	-66.1082	78.6009	190.0543	0.6821
371	-2.1570	-17.7834	19.9404	48.2152	0.7837

372	13.7212	75.6186	-89.3398	216.0207	0.6928
373	-2.9582	-83.9617	86.9199	210.1695	0.9319
374	-12.0860	-27.3845	39.4705	95.4383	0.3876
375	17.1116	74.3883	-91.5000	221.2440	0.6260
376	9.7263	84.4807	-94.2070	227.7894	0.7935
377	-0.3458	-18.8941	19.2399	46.5214	0.9641
378	5.9339	78.8540	-84.7880	205.0146	0.8600
379	15.4231	38.8602	-54.2832	131.2551	0.4318
380	-5.9876	-22.0894	28.0770	67.8892	0.5735
381	-1.7759	-86.7177	88.4936	213.9747	0.9599
382	4.1140	76.4977	-80.6117	194.9164	0.8979
383	-4.6708	-22.1950	26.8658	64.9607	0.6523
384	-8.2619	-79.2990	87.5610	211.7196	0.8113
385	11.3324	57.8895	-69.2219	167.3764	0.6726
386	-5.0914	-27.2629	32.3543	78.2315	0.6853
387	-2.8882	-76.7355	79.6237	192.5276	0.9275
388	-5.9409	-17.1617	23.1027	55.8615	0.4857
389	-5.5733	-81.7752	87.3485	211.2059	0.8724
390	3.4941	71.1661	-74.6602	180.5259	0.9064
391	0.9524	27.9936	-28.9460	69.9905	0.9342
392	0.9501	27.9955	-28.9456	69.9895	0.9344
393	3.4942	71.1659	-74.6601	180.5257	0.9064
394	-5.5735	-81.7753	87.3488	211.2065	0.8724
395	-2.8885	-76.7352	79.6237	192.5275	0.9274
396	-5.9402	-17.1619	23.1021	55.8602	0.4857
397	11.3328	57.8881	-69.2208	167.3737	0.6726
398	-8.2620	-79.2990	87.5610	211.7196	0.8113
399	-6.7861	-25.2009	31.9869	77.3433	0.5757
400	4.1149	76.4964	-80.6113	194.9156	0.8979

401	-1.7748	-86.7167	88.4914	213.9695	0.9599
402	-4.6702	-22.1960	26.8662	64.9615	0.6523
403	15.4234	38.8578	-54.2813	131.2503	0.4317
404	5.9336	78.8545	-84.7881	205.0150	0.8600
405	3.5463	19.0775	-22.6238	54.7037	0.6865
406	9.7265	84.4809	-94.2074	227.7905	0.7935
407	17.1114	74.3888	-91.5002	221.2445	0.6260
408	-0.3456	-18.8941	19.2398	46.5211	0.9641
409	-2.9584	-83.9616	86.9201	210.1699	0.9319
410	13.7216	75.6182	-89.3398	216.0207	0.6928
411	6.8995	22.4514	-29.3509	70.9695	0.5299
412	-12.4920	-66.1086	78.6006	190.0538	0.6821
413	16.4097	82.7619	-99.1716	239.7937	0.6691
414	-2.1574	-17.7830	19.9404	48.2152	0.7836
415	-15.7161	-88.1595	103.8756	251.1679	0.6974
416	-10.8752	-81.1833	92.0586	222.5946	0.7637
417	3.1269	15.7428	-18.8696	45.6262	0.6686
418	1.9874	31.5952	-33.5826	81.2016	0.8816
419	4.5806	68.4685	-73.0492	176.6306	0.8746
420	-4.9250	-13.5701	18.4952	44.7207	0.4674
421	3.1240	72.3494	-75.4735	182.4924	0.9172
422	-41.5620	-81.5526	123.1146	297.6871	0.3248
423	-13.9874	-25.1339	39.1213	94.5941	0.2849
424	-55.1784	-87.7322	142.9106	345.5532	0.2278
425	-9.7399	-31.9428	41.6827	100.7875	0.5327
426	-2.0054	-41.4012	43.4066	104.9557	0.9076
427	-58.2136	-80.9895	139.2031	336.5887	0.1636
428	-11.6130	-77.7784	89.3914	216.1455	0.7402
429	-20.0086	-26.6286	46.6372	112.7672	0.1419

430	7.3925	80.6376	-88.0301	212.8539	0.8320
431	-11.1249	-24.4070	35.5319	85.9149	0.3738
432	-21.3317	-84.5166	105.8483	255.9378	0.5969
433	35.8444	58.8073	-94.6517	228.8647	0.2426
434	-18.8607	-78.6504	97.5111	235.7786	0.6132
435	-47.7670	-65.2764	113.0434	273.3353	0.1549
436	-4.5013	-30.8361	35.3374	85.4448	0.7452
437	5.1443	83.2797	-88.4240	213.8064	0.8836
438	10.7703	52.1044	-62.8747	152.0291	0.6574
439	-20.7377	-71.4003	92.1380	222.7868	0.5499
440	3.7560	86.9763	-90.7323	219.3878	0.9172
441	-10.1893	-17.6763	27.8656	67.3780	0.2687
442	-19.2592	-62.7686	82.0278	198.3406	0.5304
443	-4.4226	-75.1106	79.5333	192.3089	0.8888
444	3.4803	25.9526	-29.4329	71.1677	0.7635
445	-9.8898	-62.4163	72.3061	174.8338	0.7264
446	-3.1872	-16.3537	19.5409	47.2493	0.6738
447	-38.2677	-78.6870	116.9547	282.7926	0.3456
448	-6.2221	-70.8714	77.0936	186.4098	0.8386
449	-6.3274	-29.6345	35.9619	86.9548	0.6481
450	-8.7116	-67.6191	76.3307	184.5652	0.7717
451	7.2337	69.1848	-76.4185	184.7775	0.8107
452	-59.2423	-76.7066	135.9489	328.7201	0.1285
453	7.9646	64.2234	-72.1880	174.5483	0.7793
454	5.1719	62.8928	-68.0646	164.5781	0.8480
455	-13.3286	-74.7405	88.0691	212.9483	0.6973
456	5.1754	48.5640	-53.7394	129.9402	0.8074
457	-24.4325	-74.3829	98.8154	238.9325	0.5055
458	-32.2214	-74.5769	106.7983	258.2348	0.3966

459	14.2624	51.6880	-65.9504	159.4660	0.5675
460	14.2624	51.6880	-65.9504	159.4660	0.5675
461	-32.2214	-74.5769	106.7983	258.2348	0.3966
462	-24.4325	-74.3829	98.8154	238.9325	0.5055
463	5.1754	48.5640	-53.7394	129.9402	0.8074
464	-13.3286	-74.7405	88.0691	212.9483	0.6973
465	5.1719	62.8928	-68.0646	164.5781	0.8480
466	7.9646	64.2234	-72.1880	174.5483	0.7793
467	-59.2423	-76.7066	135.9489	328.7201	0.1285
468	7.2337	69.1848	-76.4185	184.7775	0.8107
469	-8.7116	-67.6191	76.3307	184.5652	0.7717
470	-6.3274	-29.6345	35.9619	86.9548	0.6481
471	-6.2221	-70.8714	77.0936	186.4098	0.8386
472	-38.2677	-78.6870	116.9547	282.7926	0.3456
473	-3.1872	-16.3537	19.5409	47.2493	0.6738
474	-9.8898	-62.4163	72.3061	174.8338	0.7264
475	3.4803	25.9526	-29.4329	71.1677	0.7635
476	-4.4226	-75.1106	79.5333	192.3089	0.8888
477	-19.2592	-62.7686	82.0278	198.3406	0.5304
478	-10.1893	-17.6763	27.8656	67.3780	0.2687
479	3.7560	86.9763	-90.7323	219.3878	0.9172
480	-20.7377	-71.4003	92.1380	222.7868	0.5499
481	10.7703	52.1044	-62.8747	152.0291	0.6574
482	5.1443	83.2797	-88.4240	213.8064	0.8836
483	-4.5013	-30.8361	35.3374	85.4448	0.7452
484	-47.7670	-65.2764	113.0434	273.3353	0.1549
485	-18.8607	-78.6504	97.5111	235.7786	0.6132
486	35.8444	58.8073	-94.6517	228.8647	0.2426
487	-21.3317	-84.5166	105.8483	255.9378	0.5969

488	-11.1249	-24.4070	35.5319	85.9149	0.3738
489	7.3925	80.6376	-88.0301	212.8539	0.8320
490	-20.0086	-26.6286	46.6372	112.7672	0.1419
491	-11.6130	-77.7784	89.3914	216.1455	0.7402
492	-58.2136	-80.9895	139.2031	336.5887	0.1636
493	-2.0054	-41.4012	43.4066	104.9557	0.9076
494	-9.7399	-31.9428	41.6827	100.7875	0.5327
495	-55.1784	-87.7322	142.9106	345.5532	0.2278
496	-13.9874	-25.1339	39.1213	94.5941	0.2849
497	-41.5620	-81.5526	123.1146	297.6871	0.3248
498	3.1240	72.3494	-75.4735	182.4924	0.9172
499	-4.9250	-13.5701	18.4952	44.7207	0.4674
500	4.5806	68.4685	-73.0492	176.6306	0.8746
501	1.9874	31.5952	-33.5826	81.2016	0.8816
502	3.1269	15.7428	-18.8696	45.6262	0.6686
503	-10.8752	-81.1833	92.0586	222.5946	0.7637
504	-15.7161	-88.1595	103.8756	251.1679	0.6974
505	-2.1574	-17.7830	19.9404	48.2152	0.7836
506	16.4097	82.7619	-99.1716	239.7937	0.6691
507	-12.4920	-66.1086	78.6006	190.0538	0.6821
508	6.8995	22.4514	-29.3509	70.9695	0.5299
509	13.7216	75.6182	-89.3398	216.0207	0.6928
510	-2.9584	-83.9616	86.9201	210.1699	0.9319
511	-0.3456	-18.8941	19.2398	46.5211	0.9641
512	17.1114	74.3888	-91.5002	221.2445	0.6260
513	9.7265	84.4809	-94.2074	227.7905	0.7935
514	3.5463	19.0775	-22.6238	54.7037	0.6865
515	5.9336	78.8545	-84.7881	205.0150	0.8600
516	15.4234	38.8578	-54.2813	131.2503	0.4317

517	-4.6702	-22.1960	26.8662	64.9615	0.6523
518	-1.7748	-86.7167	88.4914	213.9695	0.9599
519	4.1149	76.4964	-80.6113	194.9156	0.8979
520	-6.7861	-25.2009	31.9869	77.3433	0.5757
521	-8.2620	-79.2990	87.5610	211.7196	0.8113
522	11.3328	57.8881	-69.2208	167.3737	0.6726
523	-5.9402	-17.1619	23.1021	55.8602	0.4857
524	-2.8885	-76.7352	79.6237	192.5275	0.9274
525	-5.5735	-81.7753	87.3488	211.2065	0.8724
526	3.4942	71.1659	-74.6601	180.5257	0.9064
527	0.9501	27.9955	-28.9456	69.9895	0.9344
528	0.9524	27.9936	-28.9460	69.9905	0.9342
529	3.4941	71.1661	-74.6602	180.5259	0.9064
530	-5.5733	-81.7752	87.3485	211.2059	0.8724
531	-5.9409	-17.1617	23.1027	55.8615	0.4857
532	-2.8882	-76.7355	79.6237	192.5276	0.9275
533	-5.0914	-27.2629	32.3543	78.2315	0.6853
534	11.3324	57.8895	-69.2219	167.3764	0.6726
535	-8.2619	-79.2990	87.5610	211.7196	0.8113
536	-4.6708	-22.1950	26.8658	64.9607	0.6523
537	4.1140	76.4977	-80.6117	194.9164	0.8979
538	-1.7759	-86.7177	88.4936	213.9747	0.9599
539	-5.9876	-22.0894	28.0770	67.8892	0.5735
540	15.4231	38.8602	-54.2832	131.2551	0.4318
541	5.9339	78.8540	-84.7880	205.0146	0.8600
542	-0.3458	-18.8941	19.2399	46.5214	0.9641
543	9.7263	84.4807	-94.2070	227.7894	0.7935
544	17.1116	74.3883	-91.5000	221.2440	0.6260
545	-12.0860	-27.3845	39.4705	95.4383	0.3876

546	-2.9582	-83.9617	86.9199	210.1695	0.9319
547	13.7212	75.6186	-89.3398	216.0207	0.6928
548	-2.1570	-17.7834	19.9404	48.2152	0.7837
549	-12.4926	-66.1082	78.6009	190.0543	0.6821
550	16.4100	82.7622	-99.1721	239.7950	0.6691
551	-5.9333	-16.4795	22.4128	54.1934	0.4705
552	-15.7177	-88.1593	103.8769	251.1711	0.6974
553	-10.8763	-81.1826	92.0588	222.5953	0.7637
554	-4.9257	-13.5702	18.4959	44.7226	0.4674
555	1.9878	31.5958	-33.5835	81.2039	0.8816
556	4.5815	68.4664	-73.0479	176.6275	0.8746
557	7.9342	27.9220	-35.8562	86.6992	0.5574
558	3.1233	72.3500	-75.4733	182.4920	0.9172
559	-41.5595	-81.5523	123.1118	297.6803	0.3248
560	-9.7397	-31.9428	41.6825	100.7869	0.5327
561	-55.1783	-87.7319	142.9102	345.5523	0.2278
562	-20.1184	-26.2546	46.3730	112.1285	0.1323
563	-2.0060	-41.4008	43.4068	104.9561	0.9076
564	-5.6540	-21.1676	26.8216	64.8538	0.5784
565	-58.2143	-80.9893	139.2036	336.5899	0.1636
566	-11.6140	-77.7784	89.3924	216.1479	0.7402
567	-11.1246	-24.4084	35.5331	85.9178	0.3738
568	-20.0099	-26.6303	46.6402	112.7744	0.1419
569	7.3937	80.6364	-88.0301	212.8540	0.8320
570	-6.6808	-8.2836	14.9645	36.1836	0.1071
571	-21.3339	-84.5168	105.8507	255.9436	0.5969
572	35.8442	58.8076	-94.6518	228.8649	0.2426
573	-4.5010	-30.8360	35.3370	85.4438	0.7453
574	-18.8616	-78.6492	97.5108	235.7780	0.6131

575	-47.7655	-65.2766	113.0420	273.3320	0.1549
576	3.0992	14.4653	-17.5645	42.4703	0.6471
577	5.1437	83.2799	-88.4236	213.8053	0.8837
578	10.7706	52.1054	-62.8760	152.0322	0.6574
579	-10.1893	-17.6774	27.8667	67.3807	0.2687
580	-20.7440	-71.3968	92.1408	222.7936	0.5497
581	3.7560	86.9772	-90.7332	219.3900	0.9172
582	-6.6797	-8.2829	14.9626	36.1790	0.1071
583	-19.2654	-62.7655	82.0309	198.3482	0.5303
584	-4.4245	-75.1108	79.5353	192.3138	0.8887
585	-3.1865	-16.3536	19.5400	47.2471	0.6739
586	3.4783	25.9504	-29.4288	71.1578	0.7636
587	-9.8888	-62.4163	72.3051	174.8313	0.7265
588	-5.6541	-21.1680	26.8221	64.8549	0.5784
589	-38.2662	-78.6870	116.9533	282.7892	0.3456
590	-6.2226	-70.8715	77.0941	186.4110	0.8386
591	-6.3279	-29.6344	35.9623	86.9558	0.6481
592	-20.1184	-26.2541	46.3725	112.1272	0.1323
593	7.9339	27.9223	-35.8562	86.6991	0.5575
594	-5.9331	-16.4797	22.4129	54.1936	0.4706
595	-8.7108	-67.6193	76.3301	184.5637	0.7718
596	-12.0861	-27.3841	39.4702	95.4377	0.3876
597	7.2340	69.1847	-76.4187	184.7781	0.8107
598	-5.9875	-22.0895	28.0769	67.8891	0.5735
599	-59.2426	-76.7065	135.9490	328.7204	0.1285
600	-5.0920	-27.2630	32.3550	78.2333	0.6852
601	7.9631	64.2254	-72.1885	174.5494	0.7794
602	5.1709	62.8934	-68.0643	164.5772	0.8481
603	-13.3311	-74.7412	88.0723	212.9560	0.6973

604	5.1756	48.5634	-53.7390	129.9391	0.8074
605	-6.7873	-25.2015	31.9888	77.3479	0.5756
606	3.5450	19.0782	-22.6232	54.7021	0.6866
607	-24.4401	-74.3821	98.8222	238.9490	0.5054
608	6.9014	22.4500	-29.3515	70.9709	0.5297
609	-32.2207	-74.5768	106.7975	258.2330	0.3966
610	3.1269	15.7426	-18.8695	45.6259	0.6686
611	14.2621	51.6893	-65.9514	159.4683	0.5675
612	-13.9870	-25.1344	39.1214	94.5942	0.2849
613	-13.9870	-25.1344	39.1214	94.5942	0.2849
614	14.2621	51.6893	-65.9514	159.4683	0.5675
615	3.1269	15.7426	-18.8695	45.6259	0.6686
616	-32.2207	-74.5768	106.7975	258.2330	0.3966
617	6.9014	22.4500	-29.3515	70.9709	0.5297
618	-24.4401	-74.3821	98.8222	238.9490	0.5054
619	3.5450	19.0782	-22.6232	54.7021	0.6866
620	-6.7873	-25.2015	31.9888	77.3479	0.5756
621	5.1756	48.5634	-53.7390	129.9391	0.8074
622	-13.3311	-74.7412	88.0723	212.9560	0.6973
623	5.1709	62.8934	-68.0643	164.5772	0.8481
624	7.9631	64.2254	-72.1885	174.5494	0.7794
625	-5.0920	-27.2630	32.3550	78.2333	0.6852
626	-59.2426	-76.7065	135.9490	328.7204	0.1285
627	-5.9875	-22.0895	28.0769	67.8891	0.5735
628	7.2340	69.1847	-76.4187	184.7781	0.8107
629	-12.0861	-27.3841	39.4702	95.4377	0.3876
630	-8.7108	-67.6193	76.3301	184.5637	0.7718
631	-5.9331	-16.4797	22.4129	54.1936	0.4706
632	7.9339	27.9223	-35.8562	86.6991	0.5575

633	-20.1184	-26.2541	46.3725	112.1272	0.1323
634	-6.3279	-29.6344	35.9623	86.9558	0.6481
635	-6.2226	-70.8715	77.0941	186.4110	0.8386
636	-38.2662	-78.6870	116.9533	282.7892	0.3456
637	-5.6541	-21.1680	26.8221	64.8549	0.5784
638	-9.8888	-62.4163	72.3051	174.8313	0.7265
639	3.4783	25.9504	-29.4288	71.1578	0.7636
640	-3.1865	-16.3536	19.5400	47.2471	0.6739
641	-4.4245	-75.1108	79.5353	192.3138	0.8887
642	-19.2654	-62.7655	82.0309	198.3482	0.5303
643	-6.6797	-8.2829	14.9626	36.1790	0.1071
644	3.7560	86.9772	-90.7332	219.3900	0.9172
645	-20.7440	-71.3968	92.1408	222.7936	0.5497
646	-10.1893	-17.6774	27.8667	67.3807	0.2687
647	10.7706	52.1054	-62.8760	152.0322	0.6574
648	5.1437	83.2799	-88.4236	213.8053	0.8837
649	3.0992	14.4653	-17.5645	42.4703	0.6471
650	-47.7655	-65.2766	113.0420	273.3320	0.1549
651	-18.8616	-78.6492	97.5108	235.7780	0.6131
652	-4.5010	-30.8360	35.3370	85.4438	0.7453
653	35.8442	58.8076	-94.6518	228.8649	0.2426
654	-21.3339	-84.5168	105.8507	255.9436	0.5969
655	-6.6808	-8.2836	14.9645	36.1836	0.1071
656	7.3937	80.6364	-88.0301	212.8540	0.8320
657	-20.0099	-26.6303	46.6402	112.7744	0.1419
658	-11.1246	-24.4084	35.5331	85.9178	0.3738
659	-11.6140	-77.7784	89.3924	216.1479	0.7402
660	-58.2143	-80.9893	139.2036	336.5899	0.1636
661	-5.6540	-21.1676	26.8216	64.8538	0.5784

662	-2.0060	-41.4008	43.4068	104.9561	0.9076
663	-20.1184	-26.2546	46.3730	112.1285	0.1323
664	-55.1783	-87.7319	142.9102	345.5523	0.2278
665	-9.7397	-31.9428	41.6825	100.7869	0.5327
666	-41.5595	-81.5523	123.1118	297.6803	0.3248
667	3.1233	72.3500	-75.4733	182.4920	0.9172
668	7.9342	27.9220	-35.8562	86.6992	0.5574
669	4.5815	68.4664	-73.0479	176.6275	0.8746
670	1.9878	31.5958	-33.5835	81.2039	0.8816
671	-4.9257	-13.5702	18.4959	44.7226	0.4674
672	-10.8763	-81.1826	92.0588	222.5953	0.7637
673	-15.7177	-88.1593	103.8769	251.1711	0.6974
674	-5.9333	-16.4795	22.4128	54.1934	0.4705
675	16.4100	82.7622	-99.1721	239.7950	0.6691
676	-12.4926	-66.1082	78.6009	190.0543	0.6821
677	-2.1570	-17.7834	19.9404	48.2152	0.7837
678	13.7212	75.6186	-89.3398	216.0207	0.6928
679	-2.9582	-83.9617	86.9199	210.1695	0.9319
680	-12.0860	-27.3845	39.4705	95.4383	0.3876
681	17.1116	74.3883	-91.5000	221.2440	0.6260
682	9.7263	84.4807	-94.2070	227.7894	0.7935
683	-0.3458	-18.8941	19.2399	46.5214	0.9641
684	5.9339	78.8540	-84.7880	205.0146	0.8600
685	15.4231	38.8602	-54.2832	131.2551	0.4318
686	-5.9876	-22.0894	28.0770	67.8892	0.5735
687	-1.7759	-86.7177	88.4936	213.9747	0.9599
688	4.1140	76.4977	-80.6117	194.9164	0.8979
689	-4.6708	-22.1950	26.8658	64.9607	0.6523
690	-8.2619	-79.2990	87.5610	211.7196	0.8113

691	11.3324	57.8895	-69.2219	167.3764	0.6726
692	-5.0914	-27.2629	32.3543	78.2315	0.6853
693	-2.8882	-76.7355	79.6237	192.5276	0.9275
694	-5.9409	-17.1617	23.1027	55.8615	0.4857
695	-5.5733	-81.7752	87.3485	211.2059	0.8724
696	3.4941	71.1661	-74.6602	180.5259	0.9064
697	0.9524	27.9936	-28.9460	69.9905	0.9342
698	0.9501	27.9955	-28.9456	69.9895	0.9344
699	3.4942	71.1659	-74.6601	180.5257	0.9064
700	-5.5735	-81.7753	87.3488	211.2065	0.8724
701	-2.8885	-76.7352	79.6237	192.5275	0.9274
702	-5.9402	-17.1619	23.1021	55.8602	0.4857
703	11.3328	57.8881	-69.2208	167.3737	0.6726
704	-8.2620	-79.2990	87.5610	211.7196	0.8113
705	-6.7861	-25.2009	31.9869	77.3433	0.5757
706	4.1149	76.4964	-80.6113	194.9156	0.8979
707	-1.7748	-86.7167	88.4914	213.9695	0.9599
708	-4.6702	-22.1960	26.8662	64.9615	0.6523
709	15.4234	38.8578	-54.2813	131.2503	0.4317
710	5.9336	78.8545	-84.7881	205.0150	0.8600
711	3.5463	19.0775	-22.6238	54.7037	0.6865
712	9.7265	84.4809	-94.2074	227.7905	0.7935
713	17.1114	74.3888	-91.5002	221.2445	0.6260
714	-0.3456	-18.8941	19.2398	46.5211	0.9641
715	-2.9584	-83.9616	86.9201	210.1699	0.9319
716	13.7216	75.6182	-89.3398	216.0207	0.6928
717	6.8995	22.4514	-29.3509	70.9695	0.5299
718	-12.4920	-66.1086	78.6006	190.0538	0.6821
719	16.4097	82.7619	-99.1716	239.7937	0.6691

720	-2.1574	-17.7830	19.9404	48.2152	0.7836
721	-15.7161	-88.1595	103.8756	251.1679	0.6974
722	-10.8752	-81.1833	92.0586	222.5946	0.7637
723	3.1269	15.7428	-18.8696	45.6262	0.6686
724	1.9874	31.5952	-33.5826	81.2016	0.8816
725	4.5806	68.4685	-73.0492	176.6306	0.8746
726	-4.9250	-13.5701	18.4952	44.7207	0.4674
727	3.1240	72.3494	-75.4735	182.4924	0.9172
728	-41.5620	-81.5526	123.1146	297.6871	0.3248
729	-13.9874	-25.1339	39.1213	94.5941	0.2849
730	-55.1784	-87.7322	142.9106	345.5532	0.2278
731	-9.7399	-31.9428	41.6827	100.7875	0.5327
732	-2.0054	-41.4012	43.4066	104.9557	0.9076
733	-58.2136	-80.9895	139.2031	336.5887	0.1636
734	-11.6130	-77.7784	89.3914	216.1455	0.7402
735	-20.0086	-26.6286	46.6372	112.7672	0.1419
736	7.3925	80.6376	-88.0301	212.8539	0.8320
737	-11.1249	-24.4070	35.5319	85.9149	0.3738
738	-21.3317	-84.5166	105.8483	255.9378	0.5969
739	35.8444	58.8073	-94.6517	228.8647	0.2426
740	-18.8607	-78.6504	97.5111	235.7786	0.6132
741	-47.7670	-65.2764	113.0434	273.3353	0.1549
742	-4.5013	-30.8361	35.3374	85.4448	0.7452
743	5.1443	83.2797	-88.4240	213.8064	0.8836
744	10.7703	52.1044	-62.8747	152.0291	0.6574
745	-20.7377	-71.4003	92.1380	222.7868	0.5499
746	3.7560	86.9763	-90.7323	219.3878	0.9172
747	-10.1893	-17.6763	27.8656	67.3780	0.2687
748	-19.2592	-62.7686	82.0278	198.3406	0.5304

749	-4.4226	-75.1106	79.5333	192.3089	0.8888
750	3.4803	25.9526	-29.4329	71.1677	0.7635
751	-9.8898	-62.4163	72.3061	174.8338	0.7264
752	-3.1872	-16.3537	19.5409	47.2493	0.6738
753	-38.2677	-78.6870	116.9547	282.7926	0.3456
754	-6.2221	-70.8714	77.0936	186.4098	0.8386
755	-6.3274	-29.6345	35.9619	86.9548	0.6481
756	-8.7116	-67.6191	76.3307	184.5652	0.7717
757	7.2337	69.1848	-76.4185	184.7775	0.8107
758	-59.2423	-76.7066	135.9489	328.7201	0.1285
759	7.9646	64.2234	-72.1880	174.5483	0.7793
760	5.1719	62.8928	-68.0646	164.5781	0.8480
761	-13.3286	-74.7405	88.0691	212.9483	0.6973
762	5.1754	48.5640	-53.7394	129.9402	0.8074
763	-24.4325	-74.3829	98.8154	238.9325	0.5055
764	-32.2214	-74.5769	106.7983	258.2348	0.3966
765	14.2624	51.6880	-65.9504	159.4660	0.5675
766	-13.9870	-25.1344	39.1214	94.5942	0.2849
767	14.2621	51.6893	-65.9514	159.4683	0.5675
768	3.1269	15.7426	-18.8695	45.6259	0.6686
769	-32.2207	-74.5768	106.7975	258.2330	0.3966
770	6.9014	22.4500	-29.3515	70.9709	0.5297
771	-24.4401	-74.3821	98.8222	238.9490	0.5054
772	3.5450	19.0782	-22.6232	54.7021	0.6866
773	-6.7873	-25.2015	31.9888	77.3479	0.5756
774	5.1756	48.5634	-53.7390	129.9391	0.8074
775	-13.3311	-74.7412	88.0723	212.9560	0.6973
776	5.1709	62.8934	-68.0643	164.5772	0.8481
777	7.9631	64.2254	-72.1885	174.5494	0.7794

778	-5.0920	-27.2630	32.3550	78.2333	0.6852
779	-59.2426	-76.7065	135.9490	328.7204	0.1285
780	-5.9875	-22.0895	28.0769	67.8891	0.5735
781	7.2340	69.1847	-76.4187	184.7781	0.8107
782	-12.0861	-27.3841	39.4702	95.4377	0.3876
783	-8.7108	-67.6193	76.3301	184.5637	0.7718
784	-5.9331	-16.4797	22.4129	54.1936	0.4706
785	7.9339	27.9223	-35.8562	86.6991	0.5575
786	-20.1184	-26.2541	46.3725	112.1272	0.1323
787	-6.3279	-29.6344	35.9623	86.9558	0.6481
788	-6.2226	-70.8715	77.0941	186.4110	0.8386
789	-38.2662	-78.6870	116.9533	282.7892	0.3456
790	-5.6541	-21.1680	26.8221	64.8549	0.5784
791	-9.8888	-62.4163	72.3051	174.8313	0.7265
792	3.4783	25.9504	-29.4288	71.1578	0.7636
793	-3.1865	-16.3536	19.5400	47.2471	0.6739
794	-4.4245	-75.1108	79.5353	192.3138	0.8887
795	-19.2654	-62.7655	82.0309	198.3482	0.5303
796	-6.6797	-8.2829	14.9626	36.1790	0.1071
797	3.7560	86.9772	-90.7332	219.3900	0.9172
798	-20.7440	-71.3968	92.1408	222.7936	0.5497
799	-10.1893	-17.6774	27.8667	67.3807	0.2687
800	10.7706	52.1054	-62.8760	152.0322	0.6574
801	5.1437	83.2799	-88.4236	213.8053	0.8837
802	3.0992	14.4653	-17.5645	42.4703	0.6471
803	-47.7655	-65.2766	113.0420	273.3320	0.1549
804	-18.8616	-78.6492	97.5108	235.7780	0.6131
805	-4.5010	-30.8360	35.3370	85.4438	0.7453
806	35.8442	58.8076	-94.6518	228.8649	0.2426

807	-21.3339	-84.5168	105.8507	255.9436	0.5969
808	-6.6808	-8.2836	14.9645	36.1836	0.1071
809	7.3937	80.6364	-88.0301	212.8540	0.8320
810	-20.0099	-26.6303	46.6402	112.7744	0.1419
811	-11.1246	-24.4084	35.5331	85.9178	0.3738
812	-11.6140	-77.7784	89.3924	216.1479	0.7402
813	-58.2143	-80.9893	139.2036	336.5899	0.1636
814	-5.6540	-21.1676	26.8216	64.8538	0.5784
815	-2.0060	-41.4008	43.4068	104.9561	0.9076
816	-20.1184	-26.2546	46.3730	112.1285	0.1323
817	-55.1783	-87.7319	142.9102	345.5523	0.2278
818	-9.7397	-31.9428	41.6825	100.7869	0.5327
819	-41.5595	-81.5523	123.1118	297.6803	0.3248
820	3.1233	72.3500	-75.4733	182.4920	0.9172
821	7.9342	27.9220	-35.8562	86.6992	0.5574
822	4.5815	68.4664	-73.0479	176.6275	0.8746
823	1.9878	31.5958	-33.5835	81.2039	0.8816
824	-4.9257	-13.5702	18.4959	44.7226	0.4674
825	-10.8763	-81.1826	92.0588	222.5953	0.7637
826	-15.7177	-88.1593	103.8769	251.1711	0.6974
827	-5.9333	-16.4795	22.4128	54.1934	0.4705
828	16.4100	82.7622	-99.1721	239.7950	0.6691
829	-12.4926	-66.1082	78.6009	190.0543	0.6821
830	-2.1570	-17.7834	19.9404	48.2152	0.7837
831	13.7212	75.6186	-89.3398	216.0207	0.6928
832	-2.9582	-83.9617	86.9199	210.1695	0.9319
833	-12.0860	-27.3845	39.4705	95.4383	0.3876
834	17.1116	74.3883	-91.5000	221.2440	0.6260
835	9.7263	84.4807	-94.2070	227.7894	0.7935

836	-0.3458	-18.8941	19.2399	46.5214	0.9641
837	5.9339	78.8540	-84.7880	205.0146	0.8600
838	15.4231	38.8602	-54.2832	131.2551	0.4318
839	-5.9876	-22.0894	28.0770	67.8892	0.5735
840	-1.7759	-86.7177	88.4936	213.9747	0.9599
841	4.1140	76.4977	-80.6117	194.9164	0.8979
842	-4.6708	-22.1950	26.8658	64.9607	0.6523
843	-8.2619	-79.2990	87.5610	211.7196	0.8113
844	11.3324	57.8895	-69.2219	167.3764	0.6726
845	-5.0914	-27.2629	32.3543	78.2315	0.6853
846	-2.8882	-76.7355	79.6237	192.5276	0.9275
847	-5.9409	-17.1617	23.1027	55.8615	0.4857
848	-5.5733	-81.7752	87.3485	211.2059	0.8724
849	3.4941	71.1661	-74.6602	180.5259	0.9064
850	0.9524	27.9936	-28.9460	69.9905	0.9342
851	0.9501	27.9955	-28.9456	69.9895	0.9344
852	3.4942	71.1659	-74.6601	180.5257	0.9064
853	-5.5735	-81.7753	87.3488	211.2065	0.8724
854	-2.8885	-76.7352	79.6237	192.5275	0.9274
855	-5.9402	-17.1619	23.1021	55.8602	0.4857
856	11.3328	57.8881	-69.2208	167.3737	0.6726
857	-8.2620	-79.2990	87.5610	211.7196	0.8113
858	-6.7861	-25.2009	31.9869	77.3433	0.5757
859	4.1149	76.4964	-80.6113	194.9156	0.8979
860	-1.7748	-86.7167	88.4914	213.9695	0.9599
861	-4.6702	-22.1960	26.8662	64.9615	0.6523
862	15.4234	38.8578	-54.2813	131.2503	0.4317
863	5.9336	78.8545	-84.7881	205.0150	0.8600
864	3.5463	19.0775	-22.6238	54.7037	0.6865

865	9.7265	84.4809	-94.2074	227.7905	0.7935
866	17.1114	74.3888	-91.5002	221.2445	0.6260
867	-0.3456	-18.8941	19.2398	46.5211	0.9641
868	-2.9584	-83.9616	86.9201	210.1699	0.9319
869	13.7216	75.6182	-89.3398	216.0207	0.6928
870	6.8995	22.4514	-29.3509	70.9695	0.5299
871	-12.4920	-66.1086	78.6006	190.0538	0.6821
872	16.4097	82.7619	-99.1716	239.7937	0.6691
873	-2.1574	-17.7830	19.9404	48.2152	0.7836
874	-15.7161	-88.1595	103.8756	251.1679	0.6974
875	-10.8752	-81.1833	92.0586	222.5946	0.7637
876	3.1269	15.7428	-18.8696	45.6262	0.6686
877	1.9874	31.5952	-33.5826	81.2016	0.8816
878	4.5806	68.4685	-73.0492	176.6306	0.8746
879	-4.9250	-13.5701	18.4952	44.7207	0.4674
880	3.1240	72.3494	-75.4735	182.4924	0.9172
881	-41.5620	-81.5526	123.1146	297.6871	0.3248
882	-13.9874	-25.1339	39.1213	94.5941	0.2849
883	-55.1784	-87.7322	142.9106	345.5532	0.2278
884	-9.7399	-31.9428	41.6827	100.7875	0.5327
885	-2.0054	-41.4012	43.4066	104.9557	0.9076
886	-58.2136	-80.9895	139.2031	336.5887	0.1636
887	-11.6130	-77.7784	89.3914	216.1455	0.7402
888	-20.0086	-26.6286	46.6372	112.7672	0.1419
889	7.3925	80.6376	-88.0301	212.8539	0.8320
890	-11.1249	-24.4070	35.5319	85.9149	0.3738
891	-21.3317	-84.5166	105.8483	255.9378	0.5969
892	35.8444	58.8073	-94.6517	228.8647	0.2426
893	-18.8607	-78.6504	97.5111	235.7786	0.6132

894	-47.7670	-65.2764	113.0434	273.3353	0.1549
895	-4.5013	-30.8361	35.3374	85.4448	0.7452
896	5.1443	83.2797	-88.4240	213.8064	0.8836
897	10.7703	52.1044	-62.8747	152.0291	0.6574
898	-20.7377	-71.4003	92.1380	222.7868	0.5499
899	3.7560	86.9763	-90.7323	219.3878	0.9172
900	-10.1893	-17.6763	27.8656	67.3780	0.2687
901	-19.2592	-62.7686	82.0278	198.3406	0.5304
902	-4.4226	-75.1106	79.5333	192.3089	0.8888
903	3.4803	25.9526	-29.4329	71.1677	0.7635
904	-9.8898	-62.4163	72.3061	174.8338	0.7264
905	-3.1872	-16.3537	19.5409	47.2493	0.6738
906	-38.2677	-78.6870	116.9547	282.7926	0.3456
907	-6.2221	-70.8714	77.0936	186.4098	0.8386
908	-6.3274	-29.6345	35.9619	86.9548	0.6481
909	-8.7116	-67.6191	76.3307	184.5652	0.7717
910	7.2337	69.1848	-76.4185	184.7775	0.8107
911	-59.2423	-76.7066	135.9489	328.7201	0.1285
912	7.9646	64.2234	-72.1880	174.5483	0.7793
913	5.1719	62.8928	-68.0646	164.5781	0.8480
914	-13.3286	-74.7405	88.0691	212.9483	0.6973
915	5.1754	48.5640	-53.7394	129.9402	0.8074
916	-24.4325	-74.3829	98.8154	238.9325	0.5055
917	-32.2214	-74.5769	106.7983	258.2348	0.3966
918	14.2624	51.6880	-65.9504	159.4660	0.5675
919	14.2624	51.6880	-65.9504	159.4660	0.5675
920	-32.2214	-74.5769	106.7983	258.2348	0.3966
921	-24.4325	-74.3829	98.8154	238.9325	0.5055
922	5.1754	48.5640	-53.7394	129.9402	0.8074

923	-13.3286	-74.7405	88.0691	212.9483	0.6973
924	5.1719	62.8928	-68.0646	164.5781	0.8480
925	7.9646	64.2234	-72.1880	174.5483	0.7793
926	-59.2423	-76.7066	135.9489	328.7201	0.1285
927	7.2337	69.1848	-76.4185	184.7775	0.8107
928	-8.7116	-67.6191	76.3307	184.5652	0.7717
929	-6.3274	-29.6345	35.9619	86.9548	0.6481
930	-6.2221	-70.8714	77.0936	186.4098	0.8386
931	-38.2677	-78.6870	116.9547	282.7926	0.3456
932	-3.1872	-16.3537	19.5409	47.2493	0.6738
933	-9.8898	-62.4163	72.3061	174.8338	0.7264
934	3.4803	25.9526	-29.4329	71.1677	0.7635
935	-4.4226	-75.1106	79.5333	192.3089	0.8888
936	-19.2592	-62.7686	82.0278	198.3406	0.5304
937	-10.1893	-17.6763	27.8656	67.3780	0.2687
938	3.7560	86.9763	-90.7323	219.3878	0.9172
939	-20.7377	-71.4003	92.1380	222.7868	0.5499
940	10.7703	52.1044	-62.8747	152.0291	0.6574
941	5.1443	83.2797	-88.4240	213.8064	0.8836
942	-4.5013	-30.8361	35.3374	85.4448	0.7452
943	-47.7670	-65.2764	113.0434	273.3353	0.1549
944	-18.8607	-78.6504	97.5111	235.7786	0.6132
945	35.8444	58.8073	-94.6517	228.8647	0.2426
946	-21.3317	-84.5166	105.8483	255.9378	0.5969
947	-11.1249	-24.4070	35.5319	85.9149	0.3738
948	7.3925	80.6376	-88.0301	212.8539	0.8320
949	-20.0086	-26.6286	46.6372	112.7672	0.1419
950	-11.6130	-77.7784	89.3914	216.1455	0.7402
951	-58.2136	-80.9895	139.2031	336.5887	0.1636

952	-2.0054	-41.4012	43.4066	104.9557	0.9076
953	-9.7399	-31.9428	41.6827	100.7875	0.5327
954	-55.1784	-87.7322	142.9106	345.5532	0.2278
955	-13.9874	-25.1339	39.1213	94.5941	0.2849
956	-41.5620	-81.5526	123.1146	297.6871	0.3248
957	3.1240	72.3494	-75.4735	182.4924	0.9172
958	-4.9250	-13.5701	18.4952	44.7207	0.4674
959	4.5806	68.4685	-73.0492	176.6306	0.8746
960	1.9874	31.5952	-33.5826	81.2016	0.8816
961	3.1269	15.7428	-18.8696	45.6262	0.6686
962	-10.8752	-81.1833	92.0586	222.5946	0.7637
963	-15.7161	-88.1595	103.8756	251.1679	0.6974
964	-2.1574	-17.7830	19.9404	48.2152	0.7836
965	16.4097	82.7619	-99.1716	239.7937	0.6691
966	-12.4920	-66.1086	78.6006	190.0538	0.6821
967	6.8995	22.4514	-29.3509	70.9695	0.5299
968	13.7216	75.6182	-89.3398	216.0207	0.6928
969	-2.9584	-83.9616	86.9201	210.1699	0.9319
970	-0.3456	-18.8941	19.2398	46.5211	0.9641
971	17.1114	74.3888	-91.5002	221.2445	0.6260
972	9.7265	84.4809	-94.2074	227.7905	0.7935
973	3.5463	19.0775	-22.6238	54.7037	0.6865
974	5.9336	78.8545	-84.7881	205.0150	0.8600
975	15.4234	38.8578	-54.2813	131.2503	0.4317
976	-4.6702	-22.1960	26.8662	64.9615	0.6523
977	-1.7748	-86.7167	88.4914	213.9695	0.9599
978	4.1149	76.4964	-80.6113	194.9156	0.8979
979	-6.7861	-25.2009	31.9869	77.3433	0.5757
980	-8.2620	-79.2990	87.5610	211.7196	0.8113

981	11.3328	57.8881	-69.2208	167.3737	0.6726
982	-5.9402	-17.1619	23.1021	55.8602	0.4857
983	-2.8885	-76.7352	79.6237	192.5275	0.9274
984	-5.5735	-81.7753	87.3488	211.2065	0.8724
985	3.4942	71.1659	-74.6601	180.5257	0.9064
986	0.9501	27.9955	-28.9456	69.9895	0.9344
987	0.9524	27.9936	-28.9460	69.9905	0.9342
988	3.4941	71.1661	-74.6602	180.5259	0.9064
989	-5.5733	-81.7752	87.3485	211.2059	0.8724
990	-5.9409	-17.1617	23.1027	55.8615	0.4857
991	-2.8882	-76.7355	79.6237	192.5276	0.9275
992	-5.0914	-27.2629	32.3543	78.2315	0.6853
993	11.3324	57.8895	-69.2219	167.3764	0.6726
994	-8.2619	-79.2990	87.5610	211.7196	0.8113
995	-4.6708	-22.1950	26.8658	64.9607	0.6523
996	4.1140	76.4977	-80.6117	194.9164	0.8979
997	-1.7759	-86.7177	88.4936	213.9747	0.9599
998	-5.9876	-22.0894	28.0770	67.8892	0.5735
999	15.4231	38.8602	-54.2832	131.2551	0.4318
1000	5.9339	78.8540	-84.7880	205.0146	0.8600
1001	-0.3458	-18.8941	19.2399	46.5214	0.9641
1002	9.7263	84.4807	-94.2070	227.7894	0.7935
1003	17.1116	74.3883	-91.5000	221.2440	0.6260
1004	-12.0860	-27.3845	39.4705	95.4383	0.3876
1005	-2.9582	-83.9617	86.9199	210.1695	0.9319
1006	13.7212	75.6186	-89.3398	216.0207	0.6928
1007	-2.1570	-17.7834	19.9404	48.2152	0.7837
1008	-12.4926	-66.1082	78.6009	190.0543	0.6821
1009	16.4100	82.7622	-99.1721	239.7950	0.6691

1010	-5.9333	-16.4795	22.4128	54.1934	0.4705
1011	-15.7177	-88.1593	103.8769	251.1711	0.6974
1012	-10.8763	-81.1826	92.0588	222.5953	0.7637
1013	-4.9257	-13.5702	18.4959	44.7226	0.4674
1014	1.9878	31.5958	-33.5835	81.2039	0.8816
1015	4.5815	68.4664	-73.0479	176.6275	0.8746
1016	7.9342	27.9220	-35.8562	86.6992	0.5574
1017	3.1233	72.3500	-75.4733	182.4920	0.9172
1018	-41.5595	-81.5523	123.1118	297.6803	0.3248
1019	-9.7397	-31.9428	41.6825	100.7869	0.5327
1020	-55.1783	-87.7319	142.9102	345.5523	0.2278
1021	-20.1184	-26.2546	46.3730	112.1285	0.1323
1022	-2.0060	-41.4008	43.4068	104.9561	0.9076
1023	-5.6540	-21.1676	26.8216	64.8538	0.5784
1024	-58.2143	-80.9893	139.2036	336.5899	0.1636
1025	-11.6140	-77.7784	89.3924	216.1479	0.7402
1026	-11.1246	-24.4084	35.5331	85.9178	0.3738
1027	-20.0099	-26.6303	46.6402	112.7744	0.1419
1028	7.3937	80.6364	-88.0301	212.8540	0.8320
1029	-6.6808	-8.2836	14.9645	36.1836	0.1071
1030	-21.3339	-84.5168	105.8507	255.9436	0.5969
1031	35.8442	58.8076	-94.6518	228.8649	0.2426
1032	-4.5010	-30.8360	35.3370	85.4438	0.7453
1033	-18.8616	-78.6492	97.5108	235.7780	0.6131
1034	-47.7655	-65.2766	113.0420	273.3320	0.1549
1035	3.0992	14.4653	-17.5645	42.4703	0.6471
1036	5.1437	83.2799	-88.4236	213.8053	0.8837
1037	10.7706	52.1054	-62.8760	152.0322	0.6574
1038	-10.1893	-17.6774	27.8667	67.3807	0.2687

1039	-20.7440	-71.3968	92.1408	222.7936	0.5497
1040	3.7560	86.9772	-90.7332	219.3900	0.9172
1041	-6.6797	-8.2829	14.9626	36.1790	0.1071
1042	-19.2654	-62.7655	82.0309	198.3482	0.5303
1043	-4.4245	-75.1108	79.5353	192.3138	0.8887
1044	-3.1865	-16.3536	19.5400	47.2471	0.6739
1045	3.4783	25.9504	-29.4288	71.1578	0.7636
1046	-9.8888	-62.4163	72.3051	174.8313	0.7265
1047	-5.6541	-21.1680	26.8221	64.8549	0.5784
1048	-38.2662	-78.6870	116.9533	282.7892	0.3456
1049	-6.2226	-70.8715	77.0941	186.4110	0.8386
1050	-6.3279	-29.6344	35.9623	86.9558	0.6481
1051	-20.1184	-26.2541	46.3725	112.1272	0.1323
1052	7.9339	27.9223	-35.8562	86.6991	0.5575
1053	-5.9331	-16.4797	22.4129	54.1936	0.4706
1054	-8.7108	-67.6193	76.3301	184.5637	0.7718
1055	-12.0861	-27.3841	39.4702	95.4377	0.3876
1056	7.2340	69.1847	-76.4187	184.7781	0.8107
1057	-5.9875	-22.0895	28.0769	67.8891	0.5735
1058	-59.2426	-76.7065	135.9490	328.7204	0.1285
1059	-5.0920	-27.2630	32.3550	78.2333	0.6852
1060	7.9631	64.2254	-72.1885	174.5494	0.7794
1061	5.1709	62.8934	-68.0643	164.5772	0.8481
1062	-13.3311	-74.7412	88.0723	212.9560	0.6973
1063	5.1756	48.5634	-53.7390	129.9391	0.8074
1064	-6.7873	-25.2015	31.9888	77.3479	0.5756
1065	3.5450	19.0782	-22.6232	54.7021	0.6866
1066	-24.4401	-74.3821	98.8222	238.9490	0.5054
1067	6.9014	22.4500	-29.3515	70.9709	0.5297

1068	-32.2207	-74.5768	106.7975	258.2330	0.3966
1069	3.1269	15.7426	-18.8695	45.6259	0.6686
1070	14.2621	51.6893	-65.9514	159.4683	0.5675
1071	-13.9870	-25.1344	39.1214	94.5942	0.2849
1072	14.2624	51.6880	-65.9504	159.4660	0.5675
1073	-32.2214	-74.5769	106.7983	258.2348	0.3966
1074	-24.4325	-74.3829	98.8154	238.9325	0.5055
1075	5.1754	48.5640	-53.7394	129.9402	0.8074
1076	-13.3286	-74.7405	88.0691	212.9483	0.6973
1077	5.1719	62.8928	-68.0646	164.5781	0.8480
1078	7.9646	64.2234	-72.1880	174.5483	0.7793
1079	-59.2423	-76.7066	135.9489	328.7201	0.1285
1080	7.2337	69.1848	-76.4185	184.7775	0.8107
1081	-8.7116	-67.6191	76.3307	184.5652	0.7717
1082	-6.3274	-29.6345	35.9619	86.9548	0.6481
1083	-6.2221	-70.8714	77.0936	186.4098	0.8386
1084	-38.2677	-78.6870	116.9547	282.7926	0.3456
1085	-3.1872	-16.3537	19.5409	47.2493	0.6738
1086	-9.8898	-62.4163	72.3061	174.8338	0.7264
1087	3.4803	25.9526	-29.4329	71.1677	0.7635
1088	-4.4226	-75.1106	79.5333	192.3089	0.8888
1089	-19.2592	-62.7686	82.0278	198.3406	0.5304
1090	-10.1893	-17.6763	27.8656	67.3780	0.2687
1091	3.7560	86.9763	-90.7323	219.3878	0.9172
1092	-20.7377	-71.4003	92.1380	222.7868	0.5499
1093	10.7703	52.1044	-62.8747	152.0291	0.6574
1094	5.1443	83.2797	-88.4240	213.8064	0.8836
1095	-4.5013	-30.8361	35.3374	85.4448	0.7452
1096	-47.7670	-65.2764	113.0434	273.3353	0.1549

1097	-18.8607	-78.6504	97.5111	235.7786	0.6132
1098	35.8444	58.8073	-94.6517	228.8647	0.2426
1099	-21.3317	-84.5166	105.8483	255.9378	0.5969
1100	-11.1249	-24.4070	35.5319	85.9149	0.3738
1101	7.3925	80.6376	-88.0301	212.8539	0.8320
1102	-20.0086	-26.6286	46.6372	112.7672	0.1419
1103	-11.6130	-77.7784	89.3914	216.1455	0.7402
1104	-58.2136	-80.9895	139.2031	336.5887	0.1636
1105	-2.0054	-41.4012	43.4066	104.9557	0.9076
1106	-9.7399	-31.9428	41.6827	100.7875	0.5327
1107	-55.1784	-87.7322	142.9106	345.5532	0.2278
1108	-13.9874	-25.1339	39.1213	94.5941	0.2849
1109	-41.5620	-81.5526	123.1146	297.6871	0.3248
1110	3.1240	72.3494	-75.4735	182.4924	0.9172
1111	-4.9250	-13.5701	18.4952	44.7207	0.4674
1112	4.5806	68.4685	-73.0492	176.6306	0.8746
1113	1.9874	31.5952	-33.5826	81.2016	0.8816
1114	3.1269	15.7428	-18.8696	45.6262	0.6686
1115	-10.8752	-81.1833	92.0586	222.5946	0.7637
1116	-15.7161	-88.1595	103.8756	251.1679	0.6974
1117	-2.1574	-17.7830	19.9404	48.2152	0.7836
1118	16.4097	82.7619	-99.1716	239.7937	0.6691
1119	-12.4920	-66.1086	78.6006	190.0538	0.6821
1120	6.8995	22.4514	-29.3509	70.9695	0.5299
1121	13.7216	75.6182	-89.3398	216.0207	0.6928
1122	-2.9584	-83.9616	86.9201	210.1699	0.9319
1123	-0.3456	-18.8941	19.2398	46.5211	0.9641
1124	17.1114	74.3888	-91.5002	221.2445	0.6260
1125	9.7265	84.4809	-94.2074	227.7905	0.7935

1126	3.5463	19.0775	-22.6238	54.7037	0.6865
1127	5.9336	78.8545	-84.7881	205.0150	0.8600
1128	15.4234	38.8578	-54.2813	131.2503	0.4317
1129	-4.6702	-22.1960	26.8662	64.9615	0.6523
1130	-1.7748	-86.7167	88.4914	213.9695	0.9599
1131	4.1149	76.4964	-80.6113	194.9156	0.8979
1132	-6.7861	-25.2009	31.9869	77.3433	0.5757
1133	-8.2620	-79.2990	87.5610	211.7196	0.8113
1134	11.3328	57.8881	-69.2208	167.3737	0.6726
1135	-5.9402	-17.1619	23.1021	55.8602	0.4857
1136	-2.8885	-76.7352	79.6237	192.5275	0.9274
1137	-5.5735	-81.7753	87.3488	211.2065	0.8724
1138	3.4942	71.1659	-74.6601	180.5257	0.9064
1139	0.9501	27.9955	-28.9456	69.9895	0.9344
1140	0.9524	27.9936	-28.9460	69.9905	0.9342
1141	3.4941	71.1661	-74.6602	180.5259	0.9064
1142	-5.5733	-81.7752	87.3485	211.2059	0.8724
1143	-5.9409	-17.1617	23.1027	55.8615	0.4857
1144	-2.8882	-76.7355	79.6237	192.5276	0.9275
1145	-5.0914	-27.2629	32.3543	78.2315	0.6853
1146	11.3324	57.8895	-69.2219	167.3764	0.6726
1147	-8.2619	-79.2990	87.5610	211.7196	0.8113
1148	-4.6708	-22.1950	26.8658	64.9607	0.6523
1149	4.1140	76.4977	-80.6117	194.9164	0.8979
1150	-1.7759	-86.7177	88.4936	213.9747	0.9599
1151	-5.9876	-22.0894	28.0770	67.8892	0.5735
1152	15.4231	38.8602	-54.2832	131.2551	0.4318
1153	5.9339	78.8540	-84.7880	205.0146	0.8600
1154	-0.3458	-18.8941	19.2399	46.5214	0.9641

1155	9.7263	84.4807	-94.2070	227.7894	0.7935
1156	17.1116	74.3883	-91.5000	221.2440	0.6260
1157	-12.0860	-27.3845	39.4705	95.4383	0.3876
1158	-2.9582	-83.9617	86.9199	210.1695	0.9319
1159	13.7212	75.6186	-89.3398	216.0207	0.6928
1160	-2.1570	-17.7834	19.9404	48.2152	0.7837
1161	-12.4926	-66.1082	78.6009	190.0543	0.6821
1162	16.4100	82.7622	-99.1721	239.7950	0.6691
1163	-5.9333	-16.4795	22.4128	54.1934	0.4705
1164	-15.7177	-88.1593	103.8769	251.1711	0.6974
1165	-10.8763	-81.1826	92.0588	222.5953	0.7637
1166	-4.9257	-13.5702	18.4959	44.7226	0.4674
1167	1.9878	31.5958	-33.5835	81.2039	0.8816
1168	4.5815	68.4664	-73.0479	176.6275	0.8746
1169	7.9342	27.9220	-35.8562	86.6992	0.5574
1170	3.1233	72.3500	-75.4733	182.4920	0.9172
1171	-41.5595	-81.5523	123.1118	297.6803	0.3248
1172	-9.7397	-31.9428	41.6825	100.7869	0.5327
1173	-55.1783	-87.7319	142.9102	345.5523	0.2278
1174	-20.1184	-26.2546	46.3730	112.1285	0.1323
1175	-2.0060	-41.4008	43.4068	104.9561	0.9076
1176	-5.6540	-21.1676	26.8216	64.8538	0.5784
1177	-58.2143	-80.9893	139.2036	336.5899	0.1636
1178	-11.6140	-77.7784	89.3924	216.1479	0.7402
1179	-11.1246	-24.4084	35.5331	85.9178	0.3738
1180	-20.0099	-26.6303	46.6402	112.7744	0.1419
1181	7.3937	80.6364	-88.0301	212.8540	0.8320
1182	-6.6808	-8.2836	14.9645	36.1836	0.1071
1183	-21.3339	-84.5168	105.8507	255.9436	0.5969

1184	35.8442	58.8076	-94.6518	228.8649	0.2426
1185	-4.5010	-30.8360	35.3370	85.4438	0.7453
1186	-18.8616	-78.6492	97.5108	235.7780	0.6131
1187	-47.7655	-65.2766	113.0420	273.3320	0.1549
1188	3.0992	14.4653	-17.5645	42.4703	0.6471
1189	5.1437	83.2799	-88.4236	213.8053	0.8837
1190	10.7706	52.1054	-62.8760	152.0322	0.6574
1191	-10.1893	-17.6774	27.8667	67.3807	0.2687
1192	-20.7440	-71.3968	92.1408	222.7936	0.5497
1193	3.7560	86.9772	-90.7332	219.3900	0.9172
1194	-6.6797	-8.2829	14.9626	36.1790	0.1071
1195	-19.2654	-62.7655	82.0309	198.3482	0.5303
1196	-4.4245	-75.1108	79.5353	192.3138	0.8887
1197	-3.1865	-16.3536	19.5400	47.2471	0.6739
1198	3.4783	25.9504	-29.4288	71.1578	0.7636
1199	-9.8888	-62.4163	72.3051	174.8313	0.7265
1200	-5.6541	-21.1680	26.8221	64.8549	0.5784
1201	-38.2662	-78.6870	116.9533	282.7892	0.3456
1202	-6.2226	-70.8715	77.0941	186.4110	0.8386
1203	-6.3279	-29.6344	35.9623	86.9558	0.6481
1204	-20.1184	-26.2541	46.3725	112.1272	0.1323
1205	7.9339	27.9223	-35.8562	86.6991	0.5575
1206	-5.9331	-16.4797	22.4129	54.1936	0.4706
1207	-8.7108	-67.6193	76.3301	184.5637	0.7718
1208	-12.0861	-27.3841	39.4702	95.4377	0.3876
1209	7.2340	69.1847	-76.4187	184.7781	0.8107
1210	-5.9875	-22.0895	28.0769	67.8891	0.5735
1211	-59.2426	-76.7065	135.9490	328.7204	0.1285
1212	-5.0920	-27.2630	32.3550	78.2333	0.6852

1213	7.9631	64.2254	-72.1885	174.5494	0.7794
1214	5.1709	62.8934	-68.0643	164.5772	0.8481
1215	-13.3311	-74.7412	88.0723	212.9560	0.6973
1216	5.1756	48.5634	-53.7390	129.9391	0.8074
1217	-6.7873	-25.2015	31.9888	77.3479	0.5756
1218	3.5450	19.0782	-22.6232	54.7021	0.6866
1219	-24.4401	-74.3821	98.8222	238.9490	0.5054
1220	6.9014	22.4500	-29.3515	70.9709	0.5297
1221	-32.2207	-74.5768	106.7975	258.2330	0.3966
1222	3.1269	15.7426	-18.8695	45.6259	0.6686
1223	14.2621	51.6893	-65.9514	159.4683	0.5675
1224	-13.9870	-25.1344	39.1214	94.5942	0.2849
1225	-13.9870	-25.1344	39.1214	94.5942	0.2849
1226	14.2621	51.6893	-65.9514	159.4683	0.5675
1227	3.1269	15.7426	-18.8695	45.6259	0.6686
1228	-32.2207	-74.5768	106.7975	258.2330	0.3966
1229	6.9014	22.4500	-29.3515	70.9709	0.5297
1230	-24.4401	-74.3821	98.8222	238.9490	0.5054
1231	3.5450	19.0782	-22.6232	54.7021	0.6866
1232	-6.7873	-25.2015	31.9888	77.3479	0.5756
1233	5.1756	48.5634	-53.7390	129.9391	0.8074
1234	-13.3311	-74.7412	88.0723	212.9560	0.6973
1235	5.1709	62.8934	-68.0643	164.5772	0.8481
1236	7.9631	64.2254	-72.1885	174.5494	0.7794
1237	-5.0920	-27.2630	32.3550	78.2333	0.6852
1238	-59.2426	-76.7065	135.9490	328.7204	0.1285
1239	-5.9875	-22.0895	28.0769	67.8891	0.5735
1240	7.2340	69.1847	-76.4187	184.7781	0.8107
1241	-12.0861	-27.3841	39.4702	95.4377	0.3876

1242	-8.7108	-67.6193	76.3301	184.5637	0.7718
1243	-5.9331	-16.4797	22.4129	54.1936	0.4706
1244	7.9339	27.9223	-35.8562	86.6991	0.5575
1245	-20.1184	-26.2541	46.3725	112.1272	0.1323
1246	-6.3279	-29.6344	35.9623	86.9558	0.6481
1247	-6.2226	-70.8715	77.0941	186.4110	0.8386
1248	-38.2662	-78.6870	116.9533	282.7892	0.3456
1249	-5.6541	-21.1680	26.8221	64.8549	0.5784
1250	-9.8888	-62.4163	72.3051	174.8313	0.7265
1251	3.4783	25.9504	-29.4288	71.1578	0.7636
1252	-3.1865	-16.3536	19.5400	47.2471	0.6739
1253	-4.4245	-75.1108	79.5353	192.3138	0.8887
1254	-19.2654	-62.7655	82.0309	198.3482	0.5303
1255	-6.6797	-8.2829	14.9626	36.1790	0.1071
1256	3.7560	86.9772	-90.7332	219.3900	0.9172
1257	-20.7440	-71.3968	92.1408	222.7936	0.5497
1258	-10.1893	-17.6774	27.8667	67.3807	0.2687
1259	10.7706	52.1054	-62.8760	152.0322	0.6574
1260	5.1437	83.2799	-88.4236	213.8053	0.8837
1261	3.0992	14.4653	-17.5645	42.4703	0.6471
1262	-47.7655	-65.2766	113.0420	273.3320	0.1549
1263	-18.8616	-78.6492	97.5108	235.7780	0.6131
1264	-4.5010	-30.8360	35.3370	85.4438	0.7453
1265	35.8442	58.8076	-94.6518	228.8649	0.2426
1266	-21.3339	-84.5168	105.8507	255.9436	0.5969
1267	-6.6808	-8.2836	14.9645	36.1836	0.1071
1268	7.3937	80.6364	-88.0301	212.8540	0.8320
1269	-20.0099	-26.6303	46.6402	112.7744	0.1419
1270	-11.1246	-24.4084	35.5331	85.9178	0.3738

1271	-11.6140	-77.7784	89.3924	216.1479	0.7402
1272	-58.2143	-80.9893	139.2036	336.5899	0.1636
1273	-5.6540	-21.1676	26.8216	64.8538	0.5784
1274	-2.0060	-41.4008	43.4068	104.9561	0.9076
1275	-20.1184	-26.2546	46.3730	112.1285	0.1323
1276	-55.1783	-87.7319	142.9102	345.5523	0.2278
1277	-9.7397	-31.9428	41.6825	100.7869	0.5327
1278	-41.5595	-81.5523	123.1118	297.6803	0.3248
1279	3.1233	72.3500	-75.4733	182.4920	0.9172
1280	7.9342	27.9220	-35.8562	86.6992	0.5574
1281	4.5815	68.4664	-73.0479	176.6275	0.8746
1282	1.9878	31.5958	-33.5835	81.2039	0.8816
1283	-4.9257	-13.5702	18.4959	44.7226	0.4674
1284	-10.8763	-81.1826	92.0588	222.5953	0.7637
1285	-15.7177	-88.1593	103.8769	251.1711	0.6974
1286	-5.9333	-16.4795	22.4128	54.1934	0.4705
1287	16.4100	82.7622	-99.1721	239.7950	0.6691
1288	-12.4926	-66.1082	78.6009	190.0543	0.6821
1289	-2.1570	-17.7834	19.9404	48.2152	0.7837
1290	13.7212	75.6186	-89.3398	216.0207	0.6928
1291	-2.9582	-83.9617	86.9199	210.1695	0.9319
1292	-12.0860	-27.3845	39.4705	95.4383	0.3876
1293	17.1116	74.3883	-91.5000	221.2440	0.6260
1294	9.7263	84.4807	-94.2070	227.7894	0.7935
1295	-0.3458	-18.8941	19.2399	46.5214	0.9641
1296	5.9339	78.8540	-84.7880	205.0146	0.8600
1297	15.4231	38.8602	-54.2832	131.2551	0.4318
1298	-5.9876	-22.0894	28.0770	67.8892	0.5735
1299	-1.7759	-86.7177	88.4936	213.9747	0.9599

1300	4.1140	76.4977	-80.6117	194.9164	0.8979
1301	-4.6708	-22.1950	26.8658	64.9607	0.6523
1302	-8.2619	-79.2990	87.5610	211.7196	0.8113
1303	11.3324	57.8895	-69.2219	167.3764	0.6726
1304	-5.0914	-27.2629	32.3543	78.2315	0.6853
1305	-2.8882	-76.7355	79.6237	192.5276	0.9275
1306	-5.9409	-17.1617	23.1027	55.8615	0.4857
1307	-5.5733	-81.7752	87.3485	211.2059	0.8724
1308	3.4941	71.1661	-74.6602	180.5259	0.9064
1309	0.9524	27.9936	-28.9460	69.9905	0.9342
1310	0.9501	27.9955	-28.9456	69.9895	0.9344
1311	3.4942	71.1659	-74.6601	180.5257	0.9064
1312	-5.5735	-81.7753	87.3488	211.2065	0.8724
1313	-2.8885	-76.7352	79.6237	192.5275	0.9274
1314	-5.9402	-17.1619	23.1021	55.8602	0.4857
1315	11.3328	57.8881	-69.2208	167.3737	0.6726
1316	-8.2620	-79.2990	87.5610	211.7196	0.8113
1317	-6.7861	-25.2009	31.9869	77.3433	0.5757
1318	4.1149	76.4964	-80.6113	194.9156	0.8979
1319	-1.7748	-86.7167	88.4914	213.9695	0.9599
1320	-4.6702	-22.1960	26.8662	64.9615	0.6523
1321	15.4234	38.8578	-54.2813	131.2503	0.4317
1322	5.9336	78.8545	-84.7881	205.0150	0.8600
1323	3.5463	19.0775	-22.6238	54.7037	0.6865
1324	9.7265	84.4809	-94.2074	227.7905	0.7935
1325	17.1114	74.3888	-91.5002	221.2445	0.6260
1326	-0.3456	-18.8941	19.2398	46.5211	0.9641
1327	-2.9584	-83.9616	86.9201	210.1699	0.9319
1328	13.7216	75.6182	-89.3398	216.0207	0.6928

1329	6.8995	22.4514	-29.3509	70.9695	0.5299
1330	-12.4920	-66.1086	78.6006	190.0538	0.6821
1331	16.4097	82.7619	-99.1716	239.7937	0.6691
1332	-2.1574	-17.7830	19.9404	48.2152	0.7836
1333	-15.7161	-88.1595	103.8756	251.1679	0.6974
1334	-10.8752	-81.1833	92.0586	222.5946	0.7637
1335	3.1269	15.7428	-18.8696	45.6262	0.6686
1336	1.9874	31.5952	-33.5826	81.2016	0.8816
1337	4.5806	68.4685	-73.0492	176.6306	0.8746
1338	-4.9250	-13.5701	18.4952	44.7207	0.4674
1339	3.1240	72.3494	-75.4735	182.4924	0.9172
1340	-41.5620	-81.5526	123.1146	297.6871	0.3248
1341	-13.9874	-25.1339	39.1213	94.5941	0.2849
1342	-55.1784	-87.7322	142.9106	345.5532	0.2278
1343	-9.7399	-31.9428	41.6827	100.7875	0.5327
1344	-2.0054	-41.4012	43.4066	104.9557	0.9076
1345	-58.2136	-80.9895	139.2031	336.5887	0.1636
1346	-11.6130	-77.7784	89.3914	216.1455	0.7402
1347	-20.0086	-26.6286	46.6372	112.7672	0.1419
1348	7.3925	80.6376	-88.0301	212.8539	0.8320
1349	-11.1249	-24.4070	35.5319	85.9149	0.3738
1350	-21.3317	-84.5166	105.8483	255.9378	0.5969
1351	35.8444	58.8073	-94.6517	228.8647	0.2426
1352	-18.8607	-78.6504	97.5111	235.7786	0.6132
1353	-47.7670	-65.2764	113.0434	273.3353	0.1549
1354	-4.5013	-30.8361	35.3374	85.4448	0.7452
1355	5.1443	83.2797	-88.4240	213.8064	0.8836
1356	10.7703	52.1044	-62.8747	152.0291	0.6574
1357	-20.7377	-71.4003	92.1380	222.7868	0.5499

```
    1358        3.7560   86.9763  -90.7323           219.3878
0.9172
    1359      -10.1893  -17.6763   27.8656            67.3780
0.2687
    1360      -19.2592  -62.7686   82.0278           198.3406
0.5304
    1361       -4.4226  -75.1106   79.5333           192.3089
0.8888
    1362        3.4803   25.9526  -29.4329            71.1677
0.7635
    1363       -9.8898  -62.4163   72.3061           174.8338
0.7264
    1364       -3.1872  -16.3537   19.5409            47.2493
0.6738
    1365      -38.2677  -78.6870  116.9547           282.7926
0.3456
    1366       -6.2221  -70.8714   77.0936           186.4098
0.8386
    1367       -6.3274  -29.6345   35.9619            86.9548
0.6481
    1368       -8.7116  -67.6191   76.3307           184.5652
0.7717
    1369        7.2337   69.1848  -76.4185           184.7775
0.8107
    1370      -59.2423  -76.7066  135.9489           328.7201
0.1285
    1371        7.9646   64.2234  -72.1880           174.5483
0.7793
    1372        5.1719   62.8928  -68.0646           164.5781
0.8480
    1373      -13.3286  -74.7405   88.0691           212.9483
0.6973
    1374        5.1754   48.5640  -53.7394           129.9402
0.8074
    1375      -24.4325  -74.3829   98.8154           238.9325
0.5055
    1376      -32.2214  -74.5769  106.7983           258.2348
0.3966
    1377       14.2624   51.6880  -65.9504           159.4660
0.5675
------------------------------------------------------------------
--------------

  Total time to end of lattice properties =     648.0725 s


  Peak dynamic memory used =     429.09 MB


  Timing analysis for GULP :

------------------------------------------------------------------
--------------
  Task / Subroutine                                          Time
(Seconds)
------------------------------------------------------------------
--------------
```

```
  Calculation of reciprocal space energy and derivatives
0.1720
  Calculation of real space energy and derivatives
93.0218
  Global summation overhead
0.0080
---------------------------------------------------------------
---------------
  Total CPU time
648.0725
---------------------------------------------------------------
---------------


  Dump file written as Optimised_Rutile_MD_phon.res


  Job Finished at 13:12.34 23rd June 2010
```

APPENDIX 3e: Results Data Sheet

Supersaturation	Critical radius (nm)	Residence Time (ms)	Number Density (x10^{26})
1.1	694	2	2
1.3	252	16	37
1.5	163	38	136
1.7	125	65	304
1.9	103	95	535
2.1	89	127	821
2.3	79	160	1,150
2.5	72	194	1,513
2.7	67	228	1,900
2.9	62	262	2,302
3.1	58	296	2,711
3.3	55	329	3,119
3.5	53	362	3,522
3.7	51	395	3,913
3.9	49	428	4,289
4.1	47	460	4,646
4.3	45	491	4,981
4.5	44	522	5,293
4.7	43	553	5,579
4.9	42	583	5,840
5.1	41	612	6,073
5.3	40	641	6,280
5.5	39	670	6,460
5.7	38	698	6,613
5.9	37	726	6,741
6.1	37	754	6,845
6.3	36	781	6,924
6.5	35	807	6,981
6.7	35	834	7,017
6.9	34	859	7,033
7.1	34	885	7,029
7.3	33	910	7,009
7.5	33	935	6,972
7.7	32	959	6,920
7.9	32	984	6,854
8.1	32	1,007	6,777
8.3	31	1,031	6,688
8.5	31	1,054	6,589
8.7	31	1,077	6,481
8.9	30	1,100	6,366
9.1	30	1,122	6,243
9.3	30	1,144	6,115
9.5	29	1,166	5,982
9.7	29	1,188	5,845
9.9	29	1,209	5,705
10.1	29	1,230	5,561
10.3	28	1,251	5,416
10.5	28	1,272	5,270
10.7	28	1,292	5,123

Supersaturation	Critical radius (nm)	Residence Time (ms)	Number Density (x10^{26})
10.9	28	1,312	4,975
11.1	27	1,332	4,828
11.3	27	1,352	4,681
11.5	27	1,372	4,536
11.7	27	1,391	4,391
11.9	27	1,410	4,249
12.1	27	1,429	4,108
12.3	26	1,448	3,969
12.5	26	1,466	3,833
12.7	26	1,485	3,699
12.9	26	1,503	3,568
13.1	26	1,521	3,440
13.3	26	1,539	3,315
13.5	25	1,557	3,193
13.7	25	1,574	3,073
13.9	25	1,592	2,957
14.1	25	1,609	2,844
14.3	25	1,626	2,735
14.5	25	1,643	2,628
14.7	25	1,660	2,525
14.9	24	1,676	2,424
15.1	24	1,693	2,327
15.3	24	1,709	2,234
15.5	24	1,725	2,143
15.7	24	1,741	2,055
15.9	24	1,757	1,970